DEVELOPMENT OF NEW ANTICANCER AGENTS BASED ON α - MANNOSIDASE INHIBITION

THÈSE N^{O} 3793 (2007)

PRÉSENTÉE LE 1ER JUIN 2007

À LA FACULTÉ DES SCIENCES DE BASE

Laboratoire de glycochimie et de synthèse asymétrique
PROGRAMME DOCTORAL EN CHIMIE ET GÉNIE CHIMIQUE

ÉCOLE POLYTECHNIQUE FÉDÉRALE DE LAUSANNE

POUR L'OBTENTION DU GRADE DE DOCTEUR ÈS SCIENCES

PAR

Hélène FIAUX

biologiste diplômée de l'Université de Lausanne
de nationalité suisse et originaire de Hermenches (VD)

acceptée sur proposition du jury:

Prof. P. Vogel, président du jury
Dr S. Gerber, directrice de thèse
Dr B. Faller, rapporteur
Prof. C. Friedli, rapporteur
Dr L. Juillerat-Jeanneret, rapporteur

ÉCOLE POLYTECHNIQUE
FÉDÉRALE DE LAUSANNE

Suisse
2007

Cette thèse n'aurait jamais vu le jour sans les conseils, le soutien, l'aide technique et l'amitié des personnes de mon entourage. Je tiens aujourd'hui à les remercier pour leur contribution indirecte mais très importante pour la réalisation de ce travail.

Je remercie le Professeur Pierre Vogel de m'avoir accueilli dans son laboratoire, en 2002, pour effectuer un travail pratique dans le cadre de ma licence ès Sciences, ce qui m'a permis de rencontrer ma future directrice de thèse. Je le remercie également pour les moyens qu'il a mis à ma disposition, pour sa supervision et pour la place de travail qui m'a été attribuée avec une magnifique vue sur le lac.

Je remercie infiniment le Docteur Sandrine Gerber-Lemaire, ma directrice de thèse, pour son encadrement, son ouverture d'esprit qui m'a permis de m'épanouir en initiant de nouvelles collaborations afin de donner à cette thèse son caractère si pluridisciplinaire. Je la remercie également pour la rigueur qu'elle a su me transmettre, son écoute et son soutien indispensables pour faire face aux nombreux moments de doutes, sa très grande disponibilité et son investissement durant ces 4 années ainsi que dans la correction de ce manuscrit.

Je remercie également le Docteur Lucienne Juillerat-Jeanneret pour son accueil chaleureux dans son groupe de recherche à l'Institut de Pathologie de l'Université de Lausanne, ce qui m'a permis d'effectuer tous les tests biologiques. Sa supervision et son regard expérimenté lors de la rédaction de ce manuscrit m'ont été d'une aide précieuse.

Un grand « Merci » au Professeur Nicolas Moitessier de l'Université de McGill pour m'avoir prêté une station de travail durant 4 mois dans ses locaux à Montréal (Canada). Cette collaboration m'a permis de reprendre confiance en moi et nous a ouvert l'esprit pour la suite du travail de recherche.

Je tiens à remercier le Professeur David Rose de l'Université de Toronto et tout particulièrement le Docteur Douglas Kuntz pour l'énorme travail effectué sur les structures aux rayons-x, sans qui cette thèse n'aurait tout simplement pas été réalisable.

Je remercie également le Docteur Bernard Faller de Novartis pour m'avoir guidée vers le chemin de la thèse, m'avoir suivie durant ces années et pour avoir accepté d'évaluer les paramètres physicochimiques de mes composés.

Je remercie encore une fois les Docteurs Lucienne Juillerat-Jeanneret et Bernard Faller, ainsi que le Professeur Claude Friedli pour s'être plongé dans ce manuscrit et avoir accepté d'examiner ce travail de thèse. Je remercie également le Professeur Pierre Vogel pour avoir accepté la présidence de mon jury de thèse.

Je remercie très sincèrement et en vrac tous les membres des différents instituts avec lesquels j'ai pu travailler et partager des points de vue scientifiques. Un Merci tout particulier à Pablo pour son aide lors du docking, Catherine et Christelle pour leur aide précieuse lors des tests biologiques, Lucienne L., Yann, Feride et Frédéric ainsi que Xavier et Frédérique pour les mesures effectuées et pour leur aide lors de la préparation de l'examen final. Je remercie Anne-Sophie, Wee Han, Marie, Jeremy et Sonia des différents laboratoires du BCH ainsi que tous les (ex)-collaborateurs du groupe Vogel dont Florence, Robert, Claudia et Catherine pour ses précieux produits de départ ainsi que mes étudiants de master Carine et Sylvain. Finalement, un Enorme « Merci » à Gérald avec qui j'ai pu partager le quotidien de ces années de thèse. Je le remercie vivement pour son soutien, ses idées et sur le fait que j'ai toujours pu compter sur lui.

Un tout grand Merci à Christine Kupper et Anne Lene Odegaard pour leur aide dans la résolution de tous les problèmes administratifs que j'ai pu rencontrer durant ces années.

Je remercie également l'équipe du magasin constituée de Gladys Pasche, Giovanni Petrucci, Jacky Grémaud et Annelise Carrupt qui s'est toujours montrée incroyablement disponible, souriante et diaboliquement efficace.

Je remercie le personnel de l'Institut pour leur support technique, Alain Razaname et Francisco Sepulveda pour les spectres de masses, Martial Rey pour les nombreuses fois où il est venu débloquer la RMN, Patrick Favre, Alain Borel et Donald Zbinden pour le support informatique et toute l'équipe de l'atelier.

Quelques lignes encore pour remercier mes amis et amies, Anja et Javier, Alexandra, Evalie, Marie-Claude et Madeline, Sabine, Katia, Sarah, David et Caroline, Sébastien, Pipo et Marie, Corina, Christopher, Simone et Samuele.

Enfin, je voudrais remercier mes parents qui m’ont soutenue durant toutes mes années d’étude et sans qui je ne serai jamais arrivée jusqu’ici. Je remercie également Sylvain qui a partagé ma vie durant ces années ainsi que sa famille pour leur écoute et les nombreux moments partagés.

This work has been carried out under the supervision of Dr. MER Sandrine Gerber from October 2003 at the Laboratory of Glycochemistry and Asymmetric Synthesis (LGSA) headed by Prof. P. Vogel at the Institute of Chemical Sciences and Engineering (ISIC) of the Swiss Federal Institute of Technology (EPFL), at the Department of Chemistry of the University of McGill, Montreal, (Canada) between May and September 2005 and at the Institute of Pathology of the University of Lausanne, CHUV.

Publications:

- De Carlo, S.; Fiaux, H.; Marca-Martinet, C. *J. Liposomes Res.* **2004**, *14*, 61-76. Electron cryo-microscopy reveals mechanism of action of propranolol on artificial membranes.
- Fiaux, H.; Popowycz, F.; Favre, S.; Schütz, C.; Vogel, P. ; Gerber-Lemaire, S. ; Juillerat-Jeanneret, L. *J. Med. Chem*. **2005**, *48*, 4237-4246. Functionalized pyrrolidines inhibit α-mannosidase activity and growth of human glioblastoma and melanoma cells.
- Fiaux, H.; Schütz, C.; Vogel, P.; Juillerat-Jeanneret, L.; Gerber-Lemaire, S. *Chimia* **2006**, *60*, 185-189. Pyrrolidine derivatives as new inhibitors of α-mannosidases and growth inhibitors of human cancer cells.
- Favre, S.; Fiaux, H.; Schütz, C.; Vogel, P.; Juillerat-Jeanneret, L.; Gerber-Lemaire, S. *Heterocycles*, **2006**, *69*, 179-192. Synthesis of new pyrrolidine derivatives as inhibitors of α-mannosidase and of the growth of human glioblastoma cells.
- Englebienne, P.; Fiaux, H.; Kuntz, D. A.; Corbeil, C. R.; Gerber-Lemaire, S.; Rose, D. R.; Moitessier, N. *Proteins*, **2007**, in press. Evaluation of docking programs for predicting binding of Golgi α-mannosidase II inhibitors: a comparison with crystallography.
- Fiaux, H.; Kuntz, D. A.; Hoffman, D.; Janzer, R. C.; Gerber-Lemaire, S.; Rose, D. R.; Juillerat-Jeanneret, L., in preparation. Functionalized pyrrolidine inhibitors of human α-mannosidases II in cancer: optimizing the fit to the active site.

Oral communications:

- Fiaux H., Pyrrolidine derivatives as new inhibitors of α-mannosidases and growth inhibitors of human cancer cells. *Fall Meeting of the Swiss Chemical Society (SCS)*, EPFL, **2005**.
- Fiaux H., Pyrrolidinone based α-mannosidases inhibitors act as growth inhibitors of human glioblastoma cells. *Fall Meeting of the Swiss Chemical Society (SCS)*, Univeristiy of Zürich, **2006**.

Posters:

- Fiaux, H.; Gerber-Lemaire, S.; Vogel, P. *Fall Meeting of the Swiss Chemical Society (SCS)*, **2004**.
- Fiaux, H.; Juillerat-Jeanneret, L.; Kuntz, D. A.; Vogel, P.; Gerber-Lemaire, S. « *Journée de la recherche* », EPFL, **2005**.
- Vogel, P.; Gerber-Lemaire, S.; Fiaux, H.; Popowycz, F.; Favre, S.; Juillerat-Jeanneret, L. 230th ACS National Meeting, Washington, DC, **2005**.

- Fiaux, H.; Juillerat-Jeanneret, L.; Kuntz, D. A.; Vogel, P.; Gerber-Lemaire, S. *MipTec,* Basel, **2006**.
- Fiaux, H.; Juillerat-Jeanneret, L.; Kuntz, D. A.; Vogel, P.; Gerber-Lemaire, S. *1st Euchems*, Budapest, **2006**.
- Kuntz, D. A.; Englebienne, P.; Fiaux, H.; Gerber-Lemaire, S.; Moitessier, N.; Rose, D. R. *Gordon Conference on Diffraction Methods in Structural Biology*, Lewiston ME USA, **2006**.

Abstract

Enzymes that are involved in the synthesis and processing of oligosaccharides, such as glycosidases, are important catalysts for the specific assembly of oligosaccharide structures on proteins. Design and preparation of selective inhibitors of these enzymes are of high interest as these molecules can be used to modulate cellular functions. Moreover, they may provide potential drugs in new therapeutic strategies. In particular, swainsonine (Swa), a natural inhibitor of Golgi α-mannosidase II, reduces certain tumors and hematological dysfunctions. Nevertheless, some side effects resulted in limitations for the development of this compound in medicinal treatments.

Recently, our laboratory has developed a new combinatorial methodology for the disclosure of glycosidase inhibitors based on the dihydroxypyrrolidine scaffold found in Swa. This method allowed the preparation of a new family of selective and competitive α-mannosidase inhibitors with inhibitory activities (K_i values) ranging from 3 μM to 135 nM for the best congeners toward α-mannosidase from jack bean, a reliable model enzyme for mammalian Golgi α-mannosidase II.

The aim of the present work was to design and synthesise optimized inhibitors of α-mannosidases II based on a 2-aminomethyl-3,4-dihydroxypyrrolidine scaffold and to assess their potential as new anti cancer leads.

In a first time, a structural study was carried out through the analysis of x-ray structures of the best inhibitors previously developed in our laboratory complexed to Golgi α-mannosidase II from *Drosophila melanogaster* (dGMII), which presents a high sequence identity with the human enzyme. The binding mode of these inhibitors could be thus established. This study combined with docking experiments allowed us to design inhibitors of α-mannosidase II, with improved efficacy. The best congener (3*R*,4*R*,5*R*)-3,4-dihydroxy-5-({[(1*R*)-2-hydroxy-1-phenylethyl]amino}methyl)-1-methylpyrrolidin-2-one displayed an enhanced inhibitory potency against dGMII (IC_{50} = 0.5 μM vs 80 μM for the first generation inhibitor). Introduction of a polar substituent on the C(5) position of the pyrrolidine ring accounted for this improved activity as revealed by the x-ray structure of this new derivative complexed to dGMII which displayed additional interactions with active site residues.

In a second time, these new α-mannosidase inhibitors have been evaluated as anti cancer agents and their effects were determined on human cancer cells from glioblastoma and melanoma, two tumors associated with a high proliferative and invasive potential, multiple resistance toward conventional chemotherapeutic agents, and poor prognosis. As these compounds were not able to inhibit cellular growth, probably due to a poor cellular uptake, derivatization of our inhibitors into more lipophilic esters, ethers and amides derivatives was envisaged. In particular, introduction of a 4-bromobenzoate moiety resulted in an improvement of cellular uptake, leading to a complete inhibition of cellular growth at 300 μM with inhibitors (2*R*)-2-({[(2*R*,3*R*,4*S*)-3,4-dihydroxypyrrolidin-2-yl]methyl}amino)-2-phenylethyl 4-bromobenzoate and (2*R*)-2-({[(2*R*,3*R*,4*R*)-3,4-dihydroxy-1-methyl-5-oxopyrrolidin-2-yl]methyl}amino)-2-phenylethyl 4-bromobenzoate. Under the same conditions, Swa didn't provide any significant growth inhibition. Moreover, exposure of human fibroblasts, as model of healthy cells, to our lead derivatives revealed some selectivity toward tumoral cells. It was hypothesized that cellular esterases were able to hydrolyse the ester moiety and thus release the more hydrophilic parent inhibitors within the tumoral cells.

Finally, in order to get more insights into the mode of action of our derivatives, their inhibitory activity on α-mannosidases from human glioblastoma extracts was determined and compared to the activity of Swa. The first generation inhibitor presented a moderate inhibitory potency on α-mannosidases whereas the optimized derivative displayed potent inhibitory activity on human α-mannosidases (IC_{50} = 50 μM decreased to 0.5 μM). Nevertheless, Swa presented higher potency than our new lead (IC_{50} = 10-50 nM). It was also determined by gel filtration that the cellular α-mannosidases targeted by our pyrrolidine based inhibitors displayed apparent molecular weight of about 120 kD.

Keywords

Anti-cancer therapy

α-mannosidase inhibitors

Crystal structure (x-ray)

Dihydroxypyrrolidine

Docking (Glide)

Golgi α-mannosidase II from *Drosophila melanogaster* (dGMII)

Jack bean α-mannosidase

Swainsonine

Résumé

Les enzymes impliquées dans la synthèse des oligosaccharides, telles que les glycosidases, sont des catalyseurs biologiques essentiels pour l'assemblage spécifique des structures oligosaccharidiques sur les protéines. L'élaboration et la préparation d'inhibiteurs sélectifs de ces enzymes présentent un grand intérêt dans la mesure où ces produits peuvent être utilisés pour moduler les fonctions cellulaires. De plus, ils pourraient être utilisés dans de nouvelles stratégies thérapeutiques. En particulier, la swainsonine (Swa), un inhibiteur naturel de l'α-mannosidase II de l'appareil de Golgi, a révélé une aptitude à diminuer certaines tumeurs et des dysfonctions hématologiques. Malheureusement, les effets secondaires engendrés ont limité le développement de la Swa comme agent thérapeutique.

Récemment, notre laboratoire a développé une nouvelle méthode combinatoire pour la découverte d'inhibiteurs de glycosidases dont le motif de base est une dihydroxypyrrolidine présente dans la Swa. Cette méthode a permis la préparation d'une nouvelle famille d'inhibiteurs, sélectifs et compétitifs, d'α-mannosidase avec des constantes d'inhibitions (mesure de K_i) qui s'échelonnent de 3 μM à 135 nM pour les meilleurs composés. L'enzyme utilisée pour ces mesures est l'α-mannosidase de jack bean, un modèle valable de l'α-mannosidase de Golgi chez les mammifères.

L'objectif de ce travail a consisté à élaborer et synthétiser de meilleurs inhibiteurs d'α-mannosidases II basés sur un motif 2-aminomethyl-3,4-dihydroxypyrrolidine. Leur potentiel thérapeutique en tant qu'agents anti cancer a aussi été évalué.

Dans un premier temps, une analyse structurale a été effectuée à partir de rayons-x obtenus avec les meilleurs inhibiteurs développés précédemment dans nos laboratoires complexés dans le site actif de l'α-mannosidase II, golgienne, de *Drosophila melanogaster* (dGMII) qui présente une séquence d'acide-aminés comparable à celle de l'enzyme humaine. Le mode de reconnaissance de ces inhibiteurs a ainsi pu être déterminé. Cette étude, combinée à des expériences de « docking », nous ont permis d'élaborer de nouveaux inhibiteurs d'α-mannosidase II. Le meilleur composé, soit la (3*R*,4*R*,5*R*)-3,4-dihydroxy-5-({[(1*R*)-2-hydroxy-1-phenylethyl]amino} methyl)-1-methyl pyrrolidin-2-one a montré une activité inhibitrice supérieure à celle obtenue avec le composé de la première génération (IC_{50} = 0.5 μM *vs* 80

μM pour l'inhibiteur de la première génération sur la dGMII). L'introduction d'un groupement polaire sur la position C(5) de la pyrrolidine a contribué à l'amélioration de l'activité inhibitrice et a été démontrée par les rayons-x du nouvel inhibiteur dans le site actif de la dGMII qui ont ainsi révélés de nouvelles interactions avec les acide aminés de l'enzyme.

Dans un deuxième temps, ces nouveaux inhibiteurs d'α-mannosidases ont été évalués en tant qu'agents anti cancéreux. Leurs effets ont été déterminés sur des cellules cancéreuses de glioblastome et de mélanome, deux tumeurs hautement invasives et présentant de multiples résistances aux agents thérapeutiques conventionnels ainsi qu'à un mauvais pronostic vital. Comme ces composés n'étaient pas capables de diminuer la croissance cellulaire de ces tumeurs, probablement à cause d'une mauvaise internalisation dans les cellules, il a été envisagé de dérivatiser ces composés en esters, éthers et amides qui présentent une plus grande lipophilie. L'introduction d'un motif 4-bromobenzyle a particulièrement amélioré l'internalisation des composés dans les cellules et a engendré une inhibition complète de la croissance cellulaire à 300 μM pour les composés (2*R*)-2-({[(2*R*,3*R*,4*S*)-3,4-di-hydroxypyrrolidin-2-yl]methyl}amino)-2-phenylethyl 4-bromobenzoate et (2*R*)-2-({[(2*R*,3*R*,4*R*)-3,4-dihydroxy-1-methyl-5-oxopyrrolidin-2-yl]methyl}amino)-2-phenylethyl 4-bromo benzoate. Dans les mêmes conditions, la Swa n'a montré aucune diminution de la croissance cellulaire. De plus, des fibroblastes humains utilisés comme modèles de cellules saines ont été moins sensibles que les cellules tumorales révélant ainsi une certaine sélectivité de nos inhibiteurs pour les cellules cancéreuses. L'hypothèse a été proposée que des estérases cellulaires puissent hydrolyser l'ester et libérer les inhibiteurs hydrophiles correspondants dans les cellules tumorales.

Finalement, pour obtenir de plus amples informations sur le mode d'action de nos dérivés, leur activité inhibitrice a été évaluée sur des α-mannosidases humaines d'extraits cellulaires de glioblastomes, puis comparée à celle de la Swa. L'inhibiteur de première génération a présenté une activité inhibitrice modeste alors que le dérivé optimisé a révélé une excellente inhibition des α-mannosidases humaines (IC_{50} = 50 μM améliorée à 0.5 μM). Cependant, la Swa demeure plus active que notre meilleur inhibiteur (IC_{50} = 10-50 nM). De plus, le poids moléculaire apparent des α-mannosidases cellulaires ciblées par nos inhibiteurs a été évalué, par filtration sur gel, à 120 kD.

Mots clés

α-mannosidase II de l'appareil de Golgi de *Drosophila melanogaster* (dGMII)

α-mannosidase de Jack bean

Dihydroxypyrrolidine

Docking (Glide)

Inhibiteurs d'α-mannosidases

Structures cristallographiques (rayons-x)

Swainsonine

Thérapie contre le cancer

Abbreviations

AIDS	acquired immune deficiency syndrome
Arg	arginine
Asn	asparagine
Asp	aspartic acid
AZT	zidovudine
Bn	benzyl
Boc	*tert*-butoxycarbonyl
Bu-DNJ	*N*-butyl-deoxynojirimycin
Bu-Cast	6-*O*-butanoylcastanospermine
BuLi	butyl lithium
CNX/CRT	calnexin/calreticulin
CST	castanospermine
DAST	diethylaminosulphur trifluoride
DFT	density functional theory
dGMII	golgi α-mannosidase II from *Drosophila melanogaster*
DIBAL-H	diisobutylaluminium hydride
DMAP	4-dimethylalaminopyridine
DMF	dimethylformamide
DMJ	1-deoxymannonojirimycin
DMSO	dimethylsulfoxide
DNA, cDNA	deoxyribonucleic acid, complementary DNA
DNJ	deoxynojirimycin
ECM	extracellular matrix
ER	endoplasmic reticulum
ERMI	endoplasmic reticulum α-mannosidase I
FDA	food and drug administration
Gal	galactose
Glc	glucose
GlcI	α-glucosidase I
GlcII	α-glucosidase II
GlcNAc	*N*-acethylglucosamine
GlcNAcTI	*N*-acetylglucosamine transferase I

GlcNAcTV	*N*-acetylglucosamine transferase V
GMI	golgi α-mannosidase I
GMII	golgi α-mannosidase II
GMIII	golgi α-mannosidase III
GMX	golgi α-mannosidase IIx
HCEC	human cerebral endothelial cells
hGMII	human golgi α-mannosidase II
His	histidine
HIV	human immunodeficiency virus
^{3}H-Leu	^{3}H-leucine
HNJ	homonojirimycin
HPLC	high pressure liquid chromatography
^{3}HT	^{3}H-thymidine
IC_{50}	concentration of an inhibitor required for 50% inhibition of the enzyme
IUPAC	international union of pure and applied chemistry
K_i	inhibition constant
K_M	Michaelis-Menten constant
K-selectride	potassium tri-*sec*-butylborohydride
$LiAlH_4$	lithium aluminium hydride
$LiBH_4$	lithium borohydride
LN18, LNZ308	glioblastoma cells
LogPo/w	octanol-water partition coefficient
Man	mannose
Me237, Me275	melanoma cells
Me-DNJ	*N*-methyl 1-deoxynojirimycin
Me-HNJ	*N*-methyl homonojirimycin
MJ	mannonojirimycin
MOM	methoxymethyl
mRNA	messenger ribonucleic acid
Ms	methanesulfonyl (mesyl)
MTT	dimethyl thiazol tetrazolium salt
$NaBH_4$	sodium borohydride
$NaBH(OAc)_3$	sodium triacetoxyborohydride

NADH	nicotinamide adenine dinucleotide
NEt_3	triethylamine
NJ	nojirimycin
NMO	*N*-methyl-morpholine-*N*-oxide
PDB	protein data bank
Ph	phenyl
PG98/5, PO08	fibroblasts cells
pKa	acid dissociation constant
Pyr	pyridine
RMSD, SD	root mean square deviation, standard deviation
S	substrate
SA	sialic acid
Ser	serine
STZ	Streptozotocin
Swa	swainsonine
TBAF	tetrabutylammonium fluoride
TBS	*tert*-butyldimethylsilyl
Thr	threonine
Tlc	thin layer chromatography
TM	tunicamycin
TPAP	tetrapropylammonium perruthenate
Tr	trityl
Trp	triptophan
Tyr	tyrosine
UDP-Glc	uracil diphosphate glucosyltransferase
V, Vmax	rate of an enzyme-catalyzed reaction, maximum reaction rate

Table of Contents

1. Introduction

1.1. Biological function of sugars

Carbohydrates or saccharides (Greek *sakcharon*: "sugar") are simple molecules present in all living species and display numerous properties such as the storage and transport of energy or act as structural components (cellulose in plants or chitin in insects). Additionally, carbohydrates and their derivatives play major roles in the activity of the immune system, fertilization, cell growth, pathogenesis, blood clotting, inflammation and interactions, adhesions.[1]

Carbohydrates can be found as monosaccharides (monomeric units), oligosaccharides (composed of two or more monomeric units) and polysaccharides (composed of several hundreds or thousands of monomeric units). Monosaccharides are the simplest carbohydrates with a general formula $(CH_2O)_n$, with n = 3 to 7, called respectively trioses, tetroses, pentoses, hexoses or heptoses. Glucose (Glc, $C_6H_{12}O_6$), an example of hexose, is one of the most common monosaccharide and as polysaccharide is used to store energy in plant cells (starch) or in animal cells (glycogen).

Carbohydrates differ from proteins and nucleic acids in two important characteristics. They can be highly branched molecules and their monomeric units may be connected to one another by many different linkage types whereas proteins and nucleic acids are almost exclusively linear and they only display a single type of linkage. This complexity allows carbohydrates to provide almost unlimited variations in their structures. Although carbohydrates can be present without being attached to other molecules, the majority of them are attached to proteins, lipids or nucleosides. The terminology glycoproteins and glycolipids is used to reflect this conjugaison. Lectins are carbohydrate-binding proteins able to recognize glycoproteins and/or glycolipids and can consequently mediate many specific biological functions such as immune defense (mannose binding protein) and cell-cell adhesion (selectins).[2]

---

[1] a) Alberts, B.; Bray, D.; Lewis, J.; Raff, M.; Roberts, K.; Watson, J. D. *Molecular Biology of the Cell* , 3rd edition, Garland Publishing, **1994.** b) Rudd, P. M.; Elliott, T.; Cresswell, P.; Wilson, I. A.; Dwek, R. A. *Carbohydrate and Glycobiology* **2001**, *291*, 2370-2376.

[2] a) Dwek, R. A *Chem Rev.* **1996**, 96, 683-720. b) Drickamer, K.; Taylor, M. E. *Annu. Rev. Cell Biol.* **1993**, *9*, 237-264. c) Hart, G. W. *Curr. Opin. Cell. Biol.* **1992**, *4*, 1017-1023.

1.2. Biosynthesis of glycoproteins

The cell is the smallest functional unity that all living organisms have in common. Delimited by a membrane, they contain as major constituents: a nucleus,[3] where the genetic information is stored, mitochondria,[4] to produce energy, the endoplasmic reticulum (ER), where proteins are synthesised and the Golgi apparatus for maturation of proteins. Cells are principally made of proteins, which constitute more than half of their dry weight. Proteins determine the shape and structure of the cell and serve as the main instruments of molecular recognition. They also ensure the capacity of cells to effect many kinds of chemical reactions that are needed for their growth and survival.

To synthesize a protein, the DNA (deoxyribonucleic acid) strand, contained in the nucleus, is transformed into mRNA (messenger ribonucleic acid) through a process called transcription. The mRNA is then translocated to the cytosol where ribosomes can read it and bind the specific amino acids together to synthesize the protein (Scheme 1). Depending on the destination of the protein, the ribosomes are floating in the cytosol (for proteins intended to stay in the cell) or attached to the ER (for secreted and membrane proteins). In the first case, the protein is directly available in the cytosol after folding through hydrogen and disulphur bonds to obtain a functional three-dimensional protein. In the second case, the protein is synthesized in the ER and then carried out of the cell. In contrast to cytosolic proteins which are rarely glycosylated, most of the soluble and membrane-bound proteins that are synthesised in the ER are glycosylated.

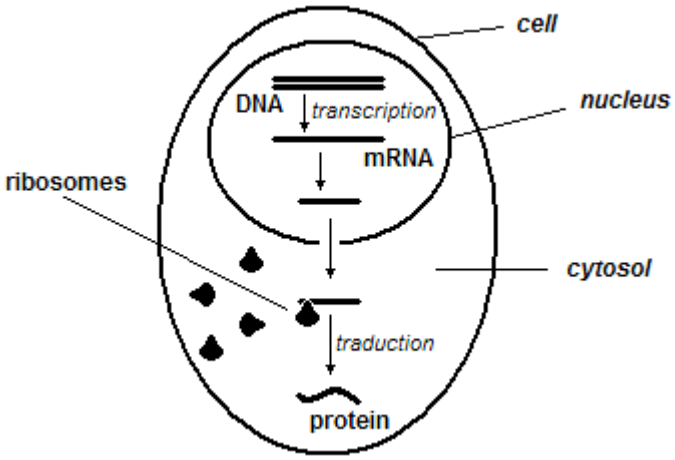

Scheme 1: Protein synthesis.

[3] Felsenfeld, G. *Sci. Am*. **1985**, *253*, 58-67.
[4] Bereiter-Hahn, J. *Int. Rev. Cytol*. **1990**, *122*, 1-63.

1.2.1. Structure and diversity of N-linked and O-linked glycans

The majority of cell surface and secreted proteins are glycosylated with carbohydrates covalently attached through either a nitrogen atom (*via* the amino group of an asparagine residue) or an oxygen atom (*via* the hydroxyl group of serine or threonine). Glycoproteins are thus classified as *N*-linked or *O*-linked depending on the nature of the glycosidic bond between the protein and the polysaccharide. With a molecular weight up to 3 kDa, the oligosaccharide groups in mammalian glycoproteins cover a large fraction of its surface and form flexible and hydrated branches that can extend 3 nm or further into the extracellular medium. This carbohydrate moiety may thus participate directly in recognition events but it may also modify the conformation[5] and the stability[6] of the protein.

N-linked glycoproteins are widespread due to the importance of their role in biological functions. The advances in techniques for oligosaccharide structural analysis have made it possible to deduce the complete structure of hundreds of asparagine-linked oligosaccharides from a variety of plant and animal sources. When these structures are examined, they fall into three main categories[7] termed high mannose, hybrid and complex (Scheme 2). They share the common structure: Manα1,3(Manα1,6) Manβ1,4 GlcNAcβ1,4 GlcNAc-Asn (boxed area in Scheme 2, Man (mannose), GlcNAc (*N*-acethylglucosamine), Asn (asparagine)). The high mannose-type oligosaccharide has typically two to six additional mannose residues linked to the pentasaccharide core. The complex-type glycans contain no other mannose residues except those of the core but are often multibranched with GlcNac, galactose (Gal) and sialic acid residues (SA). The hybrid-type molecules display features of both high-mannose and complex-type oligosaccharides: one or two mannose residues are linked to the Manα1,6 arm of the core (as in high mannose-type glycans) and usually one or two branches (as found in complex-type glycans) are linked to Manα1,3 of the core.

[5] Varki, A. *Glycobiology* **1993**, *3*, 97-130.
[6] Opdenakker, G.; Rudd, P.M.; Ponting, C.P.; Dwek, R.A. *FASEB J.* **1993**, *7*, 1330-1337.
[7] Kornfeld, R.; Kornfeld, S. *Annu. Rev. Biochem.* **1985,** *54*, 631-664.

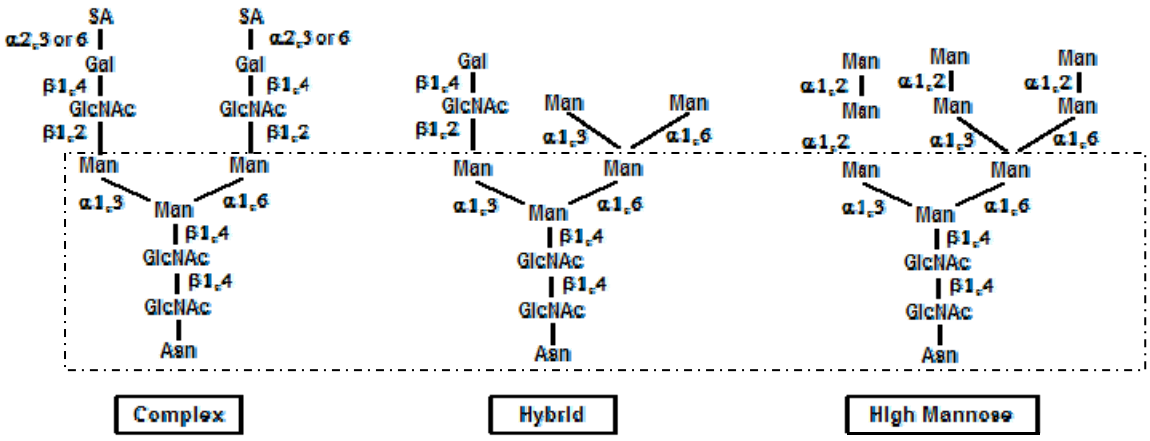

Scheme 2: Structures of the major types of asparagine-linked oligosaccharides. The boxed area encloses the pentasaccharide core common to all *N*-linked structures.

1.2.2. Biosynthesis of N-linked oligosaccharides

The biosynthesis of glycoproteins is a process shared by the ER and the Golgi apparatus. The sugars are added to the nascent protein, synthesized in the ER, as a core oligosaccharide unit, which is then extensively modified by removal and addition of sugar residues in the ER and the Golgi complex.

The core oligosaccharides have a clearly defined structure composed of a branched unit made of three glucoses, nine mannoses and two *N*-acetyl-glucosamines ($Glc_3Man_9GlcNAc_2$) (Scheme 3)**.**[8] This "14-saccharide core" unit is assembled as a membrane-bound dolicholpyrophosphate precursor by enzymes located on both sides of the ER membrane.[9] The completed core oligosaccharide is transferred by a flipping mechanism from the dolichylpyrophosphate carrier to a growing nascent polypeptide chain, and is coupled through a *N*-glycosidic bond to the side chain of an asparagine residue. The oligosaccharyltransferase recognizes a specific conformation of the glycosylation sequence (Asn-X-Ser/Thr) formed when the polypeptide chain emerges, where X can be any amino acid except proline.[10] At this stage all glycoproteins bear the same carbohydrate structure in the ER.

[8] a) Gahmberg, C. G.; Tolvanen, M. *Trends Biochem. Sci.* **1996**, *21*, 308-311. b) Helenius, A.; Aebi, M. *Ann. Rev. Biochem.* **2004**, *73*, 1019-1049.
[9] Burda, P.; Aebi, M. *Biochim. Biophys. Acta* **1999**, *1426*, 239-257.
[10] Knauer, R.; Lehle, L. *Biochim. Biophys. Acta* **1999**, 1426, 259-273.

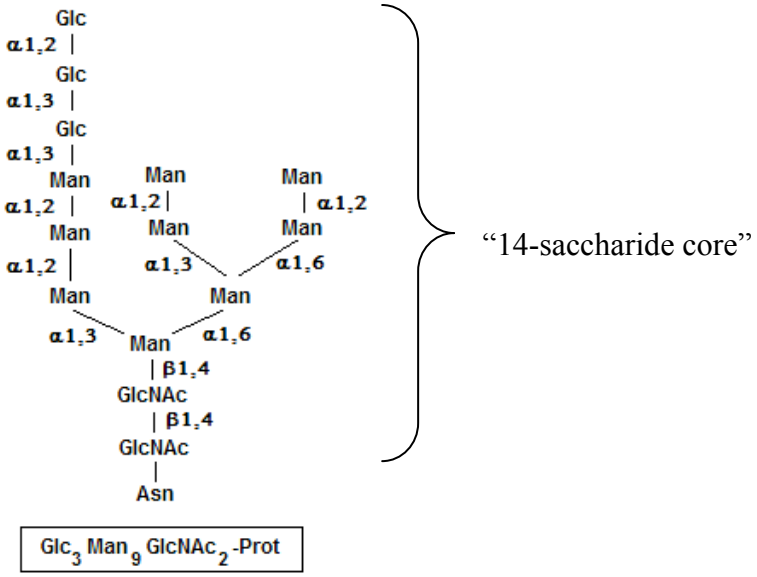

Scheme 3: Structure of the untrimmed *N*-glycosidic oligosaccharide $Glc_3Man_9GlcNAc_2$-protein. This "14-saccharide core" is composed of 14 saccharides: 3 glucoses (Glc), 9 mannoses (Man) and 2 *N*-acetylglucosamines (GlcNac).

Then a second phase of ordered trimming of selected monosaccharides by glycosidases and addition of others by glycosyltransferases begins in the ER and continues in the Golgi apparatus. This enzymatic pathway and the cellular location of the various reactions in that sequence are depicted in Scheme 4 and Scheme 5. This oligosaccharide processing is pre-determined, protein selective and cell-specific, but does not request a template as is necessary for the synthesis of DNA, RNA or proteins.

First, α-Glucosidase I (GlcI) and α-glucosidase II (GlcII) remove the external α1,2-Glc and α1,3-Glc, respectively, to produce the $GlcMan_9GlcNAc_2$-protein, a process associated with the calnexin/calreticulin (CNX/CRT) cycle,[11] that facilitates the folding of newly-formed glycoproteins. Indeed, the monoglucosylated glycoprotein binds two ER-resident lectins: the membrane bound calnexin and its soluble homologue calreticulin. These proteins sequester the newly synthesized glycopeptide chains and serve as molecular chaperones, preventing aggregation and export of the incompletely folded chains from the ER.[12] In many cases, they also protect the folding intermediates against premature degradation.

[11] Parodi, J. *Biochem J.* **2000**, *348*, 1-13.
[12] Helenius, A.; Aebi, M. *Science* **2001**, *291*, 2364-2369.

To release the bound chains from calnexin or calreticulin, GlcII removes the remaining glucosyl residue to form the $Man_9GlcNAc_2$-protein. The free glycoprotein may subsequently be re-glucosylated by the UDP-Glc glycoprotein glucosyltransferase (UDP-Glc, Scheme 4) and thus be recognized once again by the CNX/CRT. Deglucosylation/reglucosylation cycles catalysed by the opposing activities of GlcII and UDP-Glc only stop when proper folding is achieved. Then, still in the ER, the processing enzyme ER α1,2-mannosidase I (ERMI) removes a single α1,2-Man to form the $Man_8GlcNAc_2$-protein (Scheme 4).

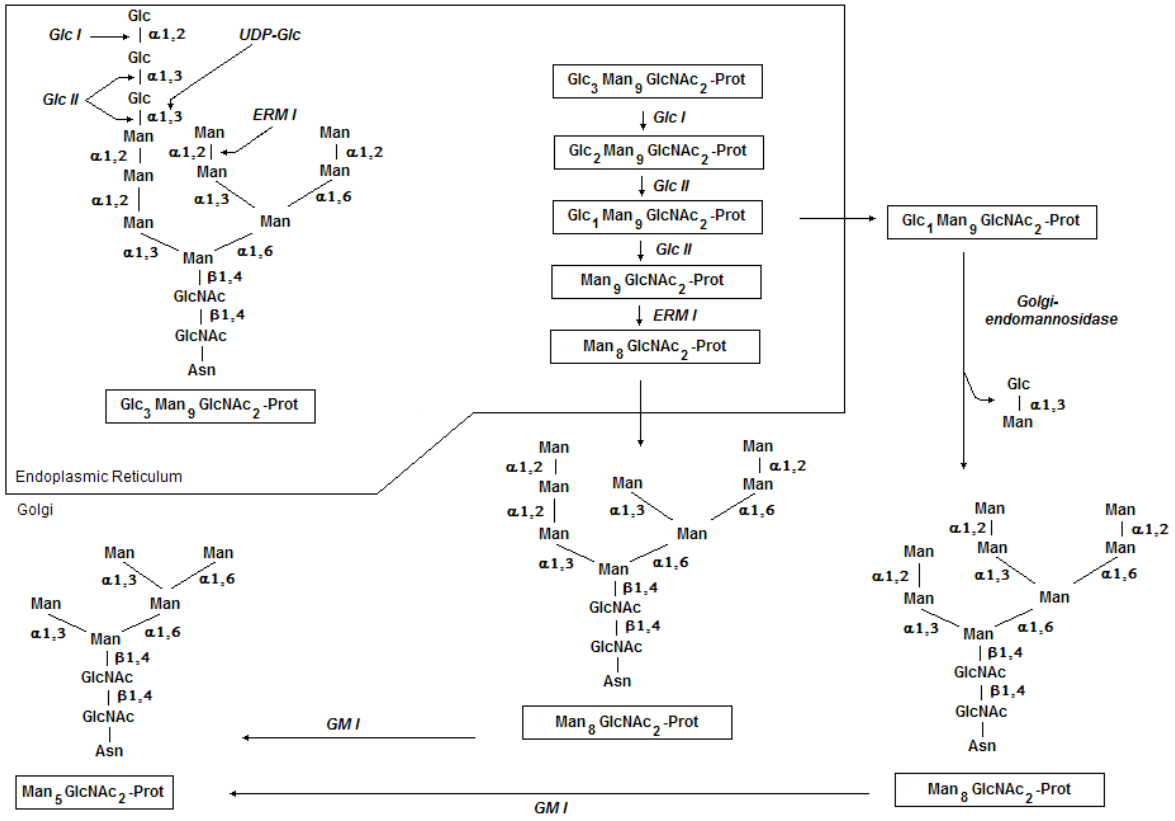

Scheme 4: Detailed glycoprotein processing pathway (first part).

The newly synthesized glycoproteins are next transported to the *cis* Golgi cisternae by vesicles which are believed to bud from the ER and then fuse with the Golgi membrane.[13] This high mannose oligosaccharide can be further trimmed by Class I Golgi α1,2-mannosidase (GMI) to yield a $Man_5GlcNAc_2$-protein.

[13] Rothblatt, J.; Novick, P.; Stevens, T. *Guidebook to the Secretory Pathway*, Oxford University Press, **1994**, 107-109.

The $Man_5GlcNAc_2$-protein chains destined to become complex-type structures are further processed in the medial Golgi where a *N*-acetylglucosamine transferase I (GlcNAcTI) adds a GlcNAc residue from UDP-GlcNAc to the α1,3-Manβ1,4-Man branch (Scheme 5).[14] This addition is a signal for Golgi α-mannosidase II (GMII) to remove two mannosyl residues (α1,3Man and α1,6Man) from the $GlcNAcMan_5GlcNAc_2$-protein to form the $GlcNAcMan_3GlcNAc_2$-protein.[15] The prior addition of the single GlcNAc residue by GlcNAcTI is a prerequisite, since the activity toward $Man_5GlcNAc_2$-protein is reduced by more than 10-fold.[16] During subsequent terminal glycosylation there is addition of new terminal sugars including GlcNAc, galactose, sialic acid and fucose to yield complex or hybrid types glycoproteins.

The hydrolytic steps in the maturation of *N*-glycans had originally been proposed to occur exclusively by the stepwise removal of single sugar residues (called in this introduction "traditional pathway"). But an alternative pathway has been identified due to the discovery of a processing endomannosidase which is able of cleave an oligosaccharide ($Glc_{3\text{-}1}Man$) from the $Glc_{3\text{-}1}Man_{9\text{-}4}GlcNAc_2$-protein to yield $Man_{8\text{-}3}GlcNAc_2$-protein.[17] The $Man_8GlcNAc_2$-protein chain formed by the action of this Golgi endomannosidase on $Glc_1Man_9GlcNAc_2$-protein is distinct from the one detected *in vivo* following digestion of $Man_9GlcNAc_2$-protein by the ERMI (Scheme 4).[18] *In vitro*, the Golgi endomannosidase has been shown to prefer the monoglucosylated oligosaccharides with the release of a α1,3-Glcα1,3-Man disaccharide,[19] but has the capacity to process di- and tri-glucosylated species with the excision of Glc_2Man and Glc_3Man, respectively.[20] Afterwards, the $Man_8GlcNAc_2$-protein chain can further be trimmed by the GMI to yield the conventional $Man_5GlcNAc_2$-protein.

[14] Harpaz, N.; Schachter, H. *J. Biol. Chem.* **1980**, *255*, 4894-4902.
[15] a) Tabas, I.; Kornfeld, S. *J. Biol. Chem.* **1978**, *253*, 7779-7786. b) Tulsiani, D. R. P.; Hubbar, S. C.; Robbins, P. W.; Touster, O. *J. Biol. Chem.* **1982**, *257*, 3660-3668.
[16] Moremen, K. W.; Trimble, R. B.; Herscovics, A. *Glycobiology* **1994**, *4*, 113-125.
[17] Lubas, W. A.; Spiro, R. G. *J. Biol. Chem.* **1988**, *263*, 3990-3998.
[18] Lubas, W. A.; Spiro, R. G. *J. Biol. Chem.* **1987**, *262*, 3775-3781.
[19] Fujimoto, K.; Kornfeld, R. *J. Biol. Chem.* **1991**, *266*, 3571-3578.
[20] Moore, S. E. H.; Spiro, R. G. *J. Biol. Chem.* **1990**, *265*, 13104-13112.

A second alternative route to the traditional pathway was discovered in GMII-*null* mice that developed a dyserythropoietic anemia. Cells from GMII-*null* mice, that lack the GMII activity, were found to accumulate hybrid and complex-type oligosaccharides. This finding indicates that complex oligosaccharides can be synthesized by a GMII-independent pathway, leading to the proposal of an alternative pathway and the prediction of a new α-mannosidase, designated α-mannosidase III (GMIII, Scheme 5). GMIII hydrolyzes two α-mannosyl residues in $Man_5GlcNAc_2$-protein and produces $Man_3GlcNAc_2$-protein which is further converted to the conventional $GlcNAcMan_3GlcNAc_2$-protein by GlcNAcTI.[21] This new mannosidase might be identical to the mannosidase discovered by Bonay and Hughes in rat liver.[22]

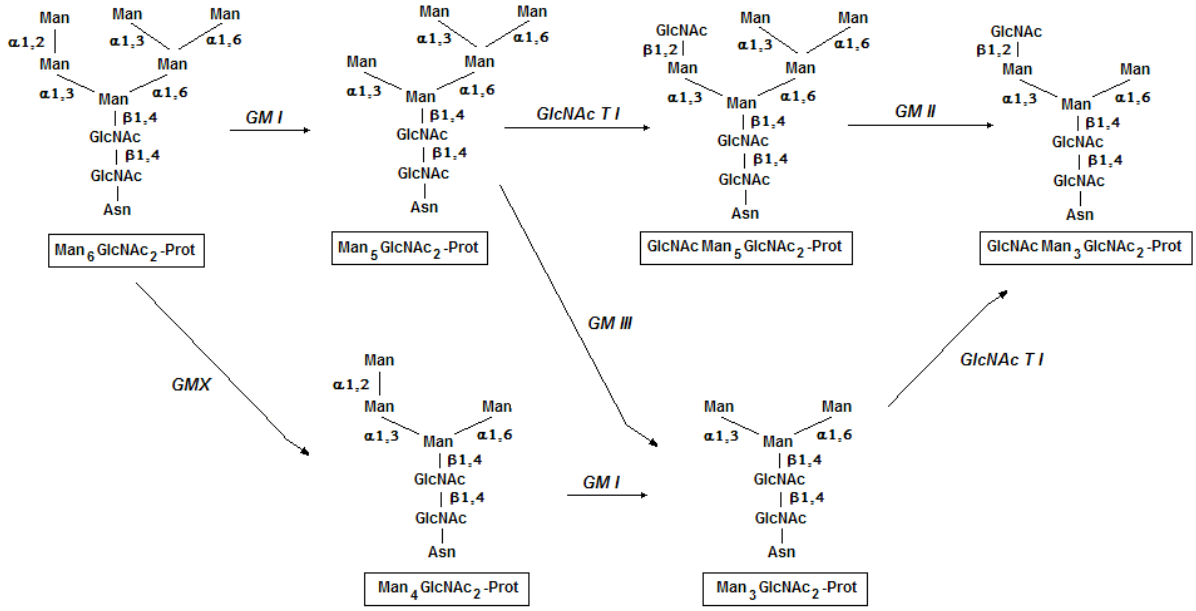

Scheme 5: Detailed glycoprotein processing pathway (second part).

[21] Chui, D.; Oh-Eda, M.; Liao, Y.-F.; Penneerselvam, K.; Lal, A.; Marek, K. W.; Freeze, H. H.; Moremen, K. W.; Fukuda, M. N.; Marth, J. D. *Cell* **1997**, *90*, 157-167.
[22] Bonay, P.; Hughes, C. R.; *Eur. J. Biochem.* **1991**, *197*, 229-238.

A third alternative route to the traditional pathway was discovered when Fukuda et al. screened human-genomic and cDNA libraries by cross-hybridization with human GMII cDNA. They identified an α-mannosidase IIx that they called GMX.[23] This new enzyme composed of 1139 amino-acid residues presents 66% identity with the peptide sequence of GMII.[24] In the presence of GMX, $Man_6GlcNAc_2$-protein was converted to the corresponding $Man_4GlcNAc_2$-protein after removal of α1,6-Man and α1,3-Man residues (Scheme 5).[25] The proposed specificity of GMX is analogous to the action of GMII, which removes α1,6-Man and α1,3-Man residues from $GlcNAcMan_5GlcNAc_2$-protein. After removal of the two mannosyl residues by GMX, the substrate $Man_4GlcNAc_2$-protein was further converted to $Man_3GlcNAc_2$-protein by GMI, which is known to be a substrate for GlcNAcTI.[26]

[23] Misago, M.; Liao, Y.-F.; Kudo, S.; Eto, S.; Mattei, M.-G.; Moremen, K. W.; Fukuda, M. N. *Proc. Natl Acad. Sci. USA* **1995**, *92*, 11766-11770.
[24] Ogawa, R.; Misago, M.; Fukuda, M. N.; Kudo, S.; Tsukada, J.; Morimoto, I.; Eto, S. *Eur. J. Biochem.* **1996**, *242*, 446-453.
[25] Oh-eda, M.; Nakagawa, H.; Akama, T. O.; Lowitz, K.; Misago, M.; Moremen, K. W.; Fukuda, M. N. *Eur. J. Biochem.* **2001**, *268*, 1280-1288.
[26] Nilsson, T.; Warren, G. *Curr. Opin. Cell Biol.* **1994**, *6*, 517-521.

1.3. Glycosidases

1.3.1. Introduction to enzymes

Glycosidases play important roles in biological systems ranging from the degradation of polysaccharides to the manipulation of the structures of glycoconjugates at the surface of proteins. They are involved in biological processes such as the digestion, the biosynthesis of glycoproteins and the catabolism of glycoconjugates.[27]

The glycosidic bond, between two glucosyl residues in cellulose or starch is on of the most stable linkage with a half-live for spontaneous hydrolysis being in the range of 5 million years. But hydrolysis carried out by enzyme is accomplished with rate constants up to $1000s^{-1}$, which make these enzymes some of the most efficient catalysts.[28]

1.3.2. Mechanism for enzymatic hydrolysis of glycosides

Basic mechanisms of the hydrolysis of interglycosidic bonds were proposed in 1953 by Kohsland.[29] Indeed, hydrolysis of the glycosidic bond can occur with one of two possible stereochemical outcomes: inversion or retention of anomeric configuration.[30] Both mechanisms involve oxocarbenium-ion like transition states and a pair of carboxylic acids in the active site of the enzyme.

With inverting β-glycosidases, as described by Kohsland, hydrolysis proceeds via a single-step mechanism in which the sugar anomeric centre is attacked by a water molecule that acts as a nucleophile (Scheme 6). This reaction is catalysed by two carboxylic acid moieties both present in the active site. Deprotonation of the water molecule by the carboxylate enhances its nucleophilicity and allow it to attack the anomeric position. The glycosidic bond is cleaved and released the alcohol which results in the inversion of the anomeric centre of the cleaved sugar.

---

[27] de Melo, E. B.; da Silveira Gomes, A.; Carvalho, I. *Tetrahedron* **2006**, *62*, 10277-10302.
[28] Wolfenden, R.; Lu, X.; Young, G. *J. Am. Chem. Soc.* **1998**, *120*, 6814-6815.
[29] Koshland, D. E. *Biol. Rev.* **1953**, *28*, 416-436.
[30] a) Zechel, D. L.; Withers, S. G. *Acc. Chem. Res* **2000**, *33*, 11-18. b) Withers, S. G. *Carb. Polymers* **2001**, *44*, 325-327. c) Sinnott, M. L. *Chem. Rev*. **1990**, 90, 1171-1202.

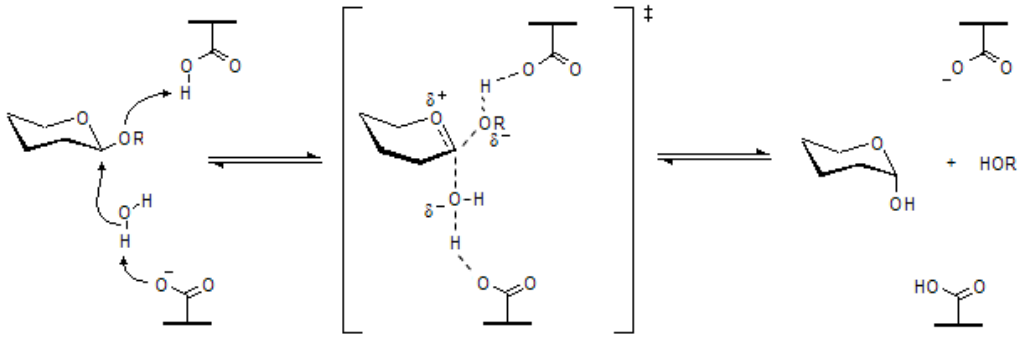

Scheme 6: General mechanism of inverting β-glycosidases.

In contrast, retaining β-glycosidases proceed via a double-step mechanism (Scheme 7). The first carboxylate attacks the anomeric position and cleaves the glycosidic bond with release of an alcohol. A water molecule then attacks the remaining sugar which is bond to the first carboxylic acid. This step is catalysed by the second carboxylic acid which deprotonates the water molecule so enhancing its nucleophilicity. The reaction affords the cleaved sugar without inversion of the anomeric center.[31]

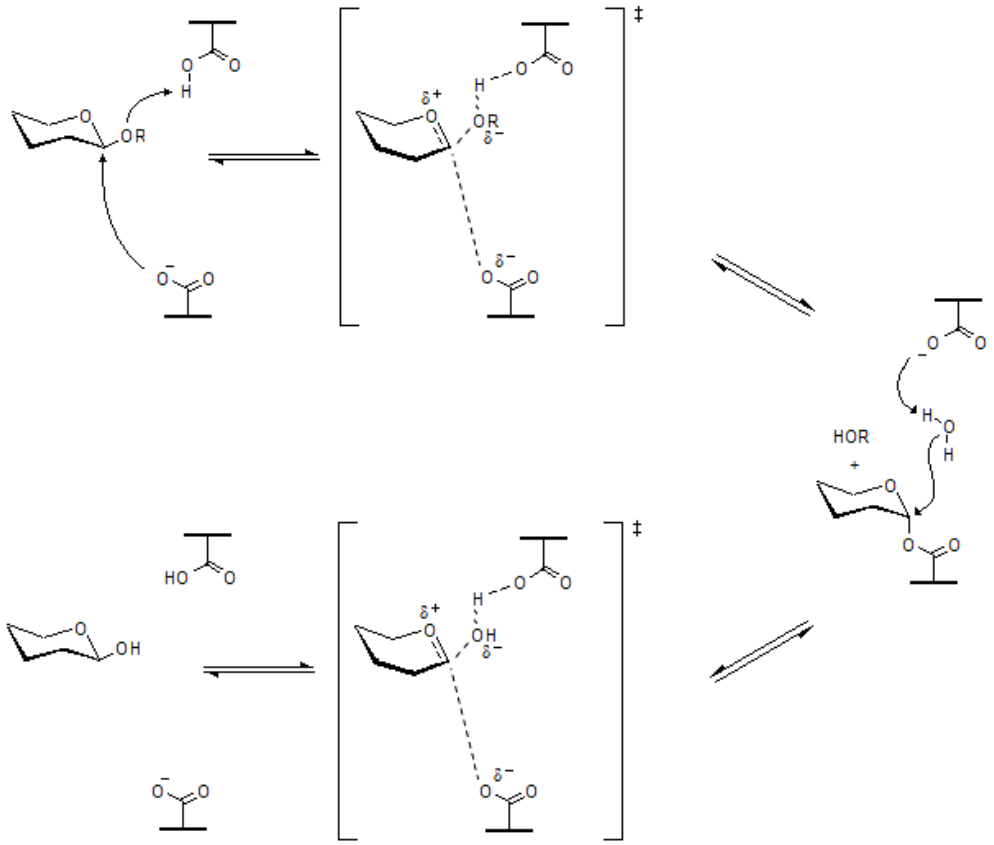

Scheme 7: General mechanism of retaining β-glycosidases.

[31] Vasella, A.; Davies, G. J.; Böhm, M. *Curr. Opin. Chem. Biol*. **2002**, *6*, 619-629.

Retaining and inverting β-glycosidases differ mainly by the distance separating the two carboxylic groups of the active site. This distance is around 5 Å in retaining enzymes and around 10 Å in inverting enzymes. The greater span found in inverters is necessary to accommodate the nucleophilic water molecule.

The hydrolysis processes have been more thoroughly studied for β-glycosidases. Nevertheless, it has been reported that α-glycosidases act through a similar pathway to β-glycosidases.[32] The mechanisms have been evidenced by the isolation of α-linked intermediates.[33]

However, subtle differences, between α- and β-glycosidases seem to exist in the oxocarbenium ion character of the transition state.[30a] For β-glycosidases, the interactions involving the nucleophilic carboxyl oxygens, the anomeric center and the alcohol at C(2) position support delocalization of the positive charge on the anomeric carbon (Scheme 8B). On the other hand, for α-glycosidases, these interactions occur between the carboxyl oxygen, the endocyclic oxygen and the anomeric center resulting in the delocalization of the positive charge on the anomeric oxygen (Scheme 8A).[34]

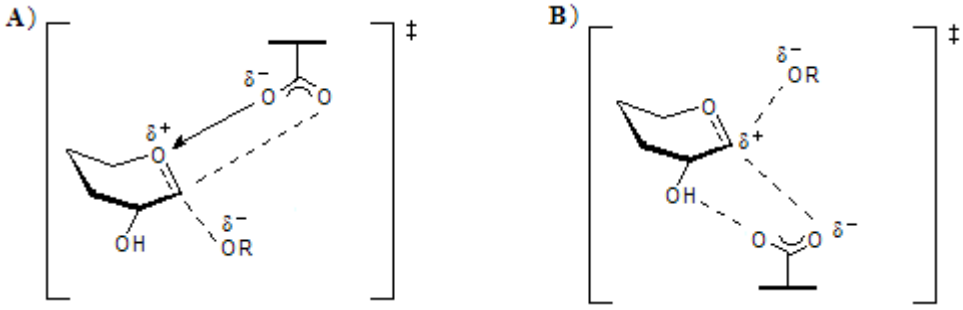

Scheme 8: Comparison of the transition states for **A**) α- and **B**) β- retaining glycosidases.

[32] McCarter, J. D.; Withers, S. G *J. Am. Chem. Soc.* **1996**, *118*, 241-242.
[33] Uitdehaag, J. C. M.; Mosi, R.; Kalk, K. H.; van der Veen, B. A.; Dijkhuisen, L.; Withers, S. G.; Dijkstra, B. W. *Nat. Struct. Biol.* **1999**, *6*, 432-436.
[34] Heightman, T. D.; Vasella, A. T. *Angew. Chem. Int. Ed.* **1999**, *38*, 750-770.

1.3.3. Enzyme kinetics

1.3.3.1. Michaelis-Menten kinetics

Michaelis-Menten equation (Eq.1) describes the kinetics of many enzymes:

$$V = \frac{Vmax \cdot [S]}{(K_M + [S])} \qquad \text{Eq.1}$$

where:
- V = velocity of the reaction
- Vmax = maximum velocity
- [S] = substrate concentration
- K_M = Michaelis-Menten constant

Graphical analysis of the Michaelis-Menten equation presents the reaction rate (V) *vs* substrate concentration [S] and produces an hyperbolic rate plot (Scheme 9).

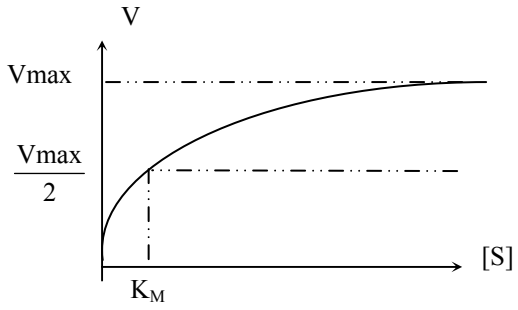

Scheme 9: Plot of substrate concentration *vs* reaction velocity.

At high substrate concentrations, the rate of the reaction reaches Vmax which reflects the fact that at these concentrations almost all of the enzyme molecules are bound to substrate and the rate is virtually independent of substrate. Vmax represents the highest velocity of the enzyme for the catalytic reaction. At lower substrate concentrations, the lower reaction velocities indicate that at any moment only a portion of the enzyme molecules are bound to the substrate. The Michaelis-Menten equation demonstrates that at the substrate concentration that produces exactly half of the maximum reaction rate (Vmax/2) the substrate concentration is numerically equal to K_M. This characteristic value of the enzyme represents its affinity for the substrate.

Lineweaver and Burk introduced an analysis of enzyme kinetics (Eq.2) based on the following rearrangement of the Michaelis-Menten equation:

$$\frac{1}{V} = \frac{K_M}{Vmax} \cdot \frac{1}{[S]} + \frac{1}{Vmax} \qquad \text{Eq. 2}$$

Plots of 1/V *vs* 1/[S] yield straight lines having a slope of K_M/Vmax and intercepts the ordinate at 1/Vmax and the abscise at $-1/K_M$ (Scheme 10).

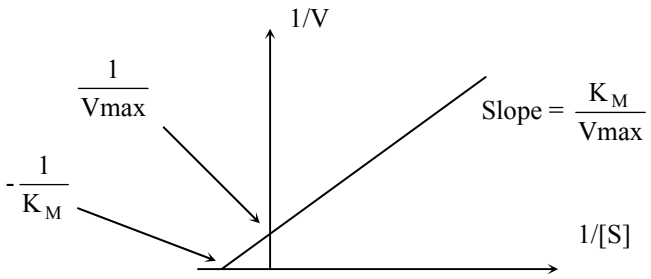

Scheme 10: Lineweaver-Burk Plot.[35]

1.3.3.2. Enzyme inhibitors

Enzyme inhibitors fall into two broad classes: those causing irreversible inactivation of enzymes and those whose inhibitory effects can be reversed.

Inhibitors of the first class usually cause an inactivating, covalent modification of the enzyme structure. The kinetic effect of irreversible inhibitors is to decrease the concentration of active enzyme. Irreversible inhibitors are usually considered to be poisons and are generally unsuitable for therapeutic purposes.

Reversible inhibitors can be divided into three main categories: competitive inhibitors, uncompetitive inhibitors and non competitive inhibitors. Competitive inhibition occurs when both the substrate and the inhibitor compete for binding to the active site of the enzyme. Normally a competitive inhibitor bears some structural similarity to the substrate.

[35] Dowd, J. E.; Riggs, D. S. *J. Biol. Chem.* **1965**, *240*, 863-869.

In the case of a competitive inhibitor, the equation of Michaelis-Menten becomes:

$$V = \frac{Vmax \cdot [S]}{K_M \left(1 + \frac{[I]}{K_i}\right) + [S]} \qquad \text{Eq.3}$$

where: [I] = inhibitor concentration

K_i = inhibition constant = $\frac{[E] \cdot [I]}{[EI]}$

[E]= enzyme concentration

[EI] = complex: enzyme/inhibitor concentration

The velocity equation differs from the usual Michaelis-Menten equation in that the K_M term is multiplied by the factor $\left(1 + \frac{[I]}{K_i}\right)$. As [I] increases, $K_{M_{app}}$ increases. Thus, a competitive inhibitor acts only to increase the apparent K_M for the substrate. The Vmax remains unchanged, but in the presence of a competitive inhibitor a much greater substrate concentration is required to attain any given fraction of Vmax.

An expression for the relative velocity or fractional activity in the presence and absence of a competitive inhibitor can be derived:

With vi = velocity at a given [S] in the presence of inhibitor = $\frac{Vmax \cdot [S]}{K_M \left(1 + \frac{[I]}{K_i}\right) + [S]}$

vo = velocity at the same [S] in the absence of inhibitor = $\frac{Vmax \cdot [S]}{K_M + [S]}$

Then $\frac{vi}{vo}$ = the relative velocity (fractional activity) = $\frac{K_M + [S]}{K_M \left(1 + \frac{[I]}{K_i}\right) + [S]}$

Relative velocity data are frequently expressed in terms of fractional inhibition (i) or percent inhibition ($i_{\%} = 100\ i$):

$$i = \text{fractional inhibition} = 1 - \frac{vi}{vo} = \frac{[I]}{[I] + K_i \left(1 + \frac{[S]}{K_M}\right)} \qquad \text{Eq. 4}$$

As predicted by equation 4, to obtain 50 % inhibition:

$$[I]_{0.5} = IC_{50} = \left(1 + \frac{[S]}{K_M}\right) \cdot K_i \qquad \text{Eq. 5}$$

The degree of inhibition (i) caused by a competitive inhibitor depends on [S], [I], K_M, and K_i. An increase in [S] at constant [I] decreases the degree of inhibition. An increase in [I] at constant [S] increases the degree of inhibition. And the lower the value of K_i, the greater is the degree of inhibition at any given [S] and [I].

IC_{50} is commonly used as a measure of drug effectiveness and represents the concentration of inhibitors required for 50% inhibition of the enzyme (Eq. 5). This value is obtained experimentally when measuring the percentage of the enzyme activity in function of various concentrations of the inhibitor.

The velocity equation for competitive inhibition in reciprocal form is:

$$\frac{1}{v} = \frac{K_M}{Vmax} \cdot \left(1 + \frac{[I]}{K_i}\right) \cdot \frac{1}{[S]} + \frac{1}{Vmax} \qquad \text{Eq. 6}$$

Thus, the slope of the plot increases by the factor $\left(1 + \frac{[I]}{K_i}\right)$ (which multiplied K_M in the original equation), but the 1/V axis intercept remains 1/Vmax. For each inhibitor concentration, a new reciprocal plot can by drawn. As [I] increases, the inhibitor curves increase in slope pivoting counterclockwise about the point of intersection with the control curve (at 1/Vmax on the 1/V axis). As [I] increases, the intercept on the 1/[S] axis moves closer to the origin, that is, $K_{M_{app}}$ continually increases (Scheme 11A).

The inhibition constant (K_i), referring to the dissociation constant between the inhibitor and the enzyme, can be calculated from the slope of any reciprocal plot or from any $K_{M_{app}}$.

$$K_{M_{app}} = \frac{K_M}{Ki}[I] + K_M \qquad \text{Eq. 7}$$

The behaviour of the curves obtained under these conditions will point to the mode of inhibition.[36]

[36] a) Cheng, Y.-C.; Prusoff, W. H. *Biochem. Pharmacol.* **1973**, *22*, 3099-3108. b) Segel, I. H. *Enzyme Kinetics, behavior and analysis of rapid equilibrium and steady-state enzyme systems*, Wiley-Interscience Publication, **1975**.

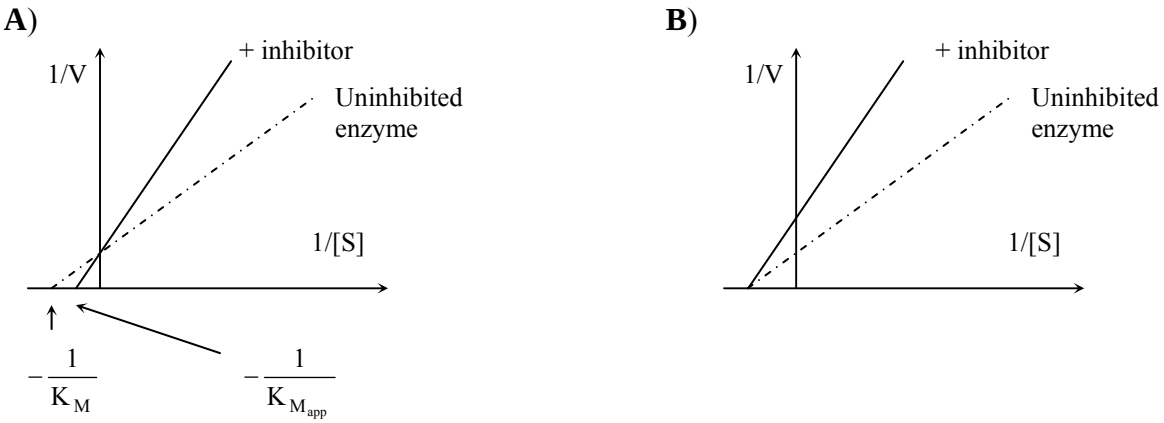

Scheme 11: Lineweaver-Burk plots of inhibited enzymes. **A**) Competitive inhibition. **B**) non competitive inhibition.

Uncompetitive inhibition occurs when the inhibitor binds to a position different than the active site, which becomes available after the substrate has bound the enzyme, and blocks the formation of the products. Apparent Vmax and K_M decrease.

Finally, non competitive inhibition occurs when the inhibitor binds at a different place from the substrate binding site, causing a modification of the active site and such reduction in the catalytic rate. Vmax is decreased proportionally to inhibitor concentration and K_M is unaltered since non competitive inhibitors do not interfere in the equilibration of the enzyme with the substrate (Scheme 11B).[37]

[37] a) www.lsbu.ac.uk/biology/enztech/inhibition.html. b) Cortes, A.; Cascante, M.; Cardenas, M. L.; Cornish-bowden, A. *Biochem. J.* **2001**, *357*, 263-268.

1.4. Glycosidases as therapeutic targets

The post-translational glycosylation patterns of proteins in the various cellular compartments will determine not only the function, structure, physical and biochemical properties, but also the fate of a protein, such as retention in a determined cell compartment, secretion, degradation, insertion in the cell membranes or interactions with other molecules and binding to membrane receptor. Therefore, inhibition of the activity of selected enzymes involved in protein glycosylation, in particular in the latter phases of the biosynthesis process, may alter the function of the target protein and its role in important biological processes. Glycosylation pathways as drug targets have remained relatively little studied until very recently. Nevertheless, the specific inhibition of α-glucosidases and α-mannosidases involved in the trimming of glycoproteins represent promising therapeutic options.

As presented in paragraph 1.2.2, the removal of the outer α1,2 glucose is achieved by glucosidase I and the two remaining α1,3 glucosyl residues are cleaved by glucosidase II. It is such of high interest to find selective inhibitors of these enzymes as they occur at the beginning of the *N*-glycosylation process.

Mannosidases which play key roles in the processing of glycoproteins belong to classes I or II. They are genetically, structurally and functionally distinct and have different subcellular locations.[38] In a general way, α1,2-mannosidases I, localized in the ER or in the Golgi apparatus, are inverting enzymes, belong to the glycosylhydrolase family 47 and require Ca^{2+} for their activity. On the other hand, α-mannosidases II are localized either in the lysosome or in the Golgi apparatus of the cell. The lysosomal α-mannosidases II which catabolizes glycoconjugates and the Golgi α-mannosidases II which hydrolyzes α1,3 and α1,6 linkages, are retaining enzymes and belong to the glycosylhydrolase family 38.[39]

[38] Daniel, P. F.; Winchester, B.; Warren, C. D. *Glycobiology* **1994**, *4*, 551-566.
[39] Rothblatt, J.; Novick, P.; Stevens, T. *Guidebook to the Secretory Pathway*, Oxford University Press, **1994**, 103-104, 185-188

The group of D. Rose has shown that *Drosophila melanogaster* Golgi α-mannosidase II (dGMII) displays 41% sequence identity and 61% similarity, comparable substrate specificity and kinetic properties, and the same inhibitor sensitivity than human GMII (hGMII).[40] The sequence alignment of the human enzyme and its *Drosophila* homologue is shown in Scheme 12. Thus, dGMII can be used as a valid model of the structural and functional features of the mammalian enzymes. Rose and co-workers analyzed a series of crystal structures of dGMII/inhibitor complexes[41] providing insight into the structure and the catalytic mechanism of dGMII. This enzyme presents a protein fold consisting of a *N*-terminal α/β domain, a three-helical bundle and an all-β C-terminal domain forming a single compact entity, connected by five internal disulfide bonds and stabilized by a zinc-binding site. The protein discloses a convex *N*-terminal face and a planar face at its opposite side presenting an extended pocket formed primarily by acidic residues. This pocket is the active site and is conserved in the human GMII sequence. Moreover, detailed binding studies suggest that a putative GlcNAc binding pocket is located near the active site. The hydrolytic process likely starts by the cleavage of the α-1,6-linked Man_6 followed by rotation of the α-1,3-linked Man_7 residue through the active site pocket for its cleavage. Between these two successive hydrolyses, the polypeptide-carbohydrate complex is anchored by the stationary GlcNAc, thus preventing its release. Thus, these data opens the door to the design of specific inhibitors of GMII.

A reliable model of the mammalian lysosomal α-mannosidase II is the α-mannosidase from jack bean which has been shown to be mechanistically similar to the human lysosomal enzyme.[42] Its amino acid sequence surrounding the catalytic nucleophile, identified as aspartic acid, reveals high sequence similarity with the mammalian Golgi α-mannosidase II.

In our study, we will focus on the design of new α-mannosidase II inhibitors for the development of anticancer agents using dGMII and jack bean α-mannosidase as model enzymes for screening purpose.

---

[40] a) Rabouille, C.; Kuntz, D. A.; Lockyer, A.; Watson, R.; Signorelli, T.; Rose, D. R.; van den Heuvel, M.; Roberts, D. B. *J. Cell Sci.* **1999**, *112*, 3319-3330. b) van den Elsen, J. M. H.; Kuntz, D. A.; Rose, D. R. *Embo J.* **2001**, *20*, 3008-3017.

[41] a) Kuntz, D. A.; Ghavami, A.; Johnston, B. D.; Pinto, B. M.; Rose, D. R. *Tetrahedron: Assymetry* **2005**, *16*, 25-32. b) Numao, S.; Kuntz, D. A.; Withers, S, G.; Rose, D. R. *J. Biol. Chem.* **2003**, *278*, 48074-48083. c) Rose, D. R.; Kuntz, D. A.; van den Elsen, J. M. H. *US Pat. Appl. Publ.* **2002**, US 2002172670.

[42] a) Howard S., Braun C., *Biochem. Biophys. Res. Commun*. **1997**, 238, 896-898. b) Howard, S.; He, S.; Withers, S. G. *J. Biol. Chem*. **1998**, *273*, 2067-2072.

```
Human          -MKLSRQFTVFGSAIFCVVIFSLYLMLDRGHLDYPRNPRREGSFPQGQLSMLQEKIDHLE 59
Drosophila     MLRIRRRFALVICSGCLLVFLSLYIILN---FAAPAATQIKPNYEN-----IENKLHELE 52
                ::: *:*::. .:    :*::***::*:   :  *  .: : .: :     :::*:..**
Human          RLLAENNEIISNIRDSVINLSESVEDGPKSSQSNFSQGAGSHLLPSQLSLSVDTADCLFA 119
Drosophila     NGLQEHGEEMRNLRARLAKTSN--RDDPIRP-------------PLKVARSPRPGQCQDV 97
               . * *:.* : *:*  : : *:  .*.*  .              * ::: *  ..:*  .
Human          SQSGSHNSDVQMLDVYSLISFDNPDGGVWKQGFDITYESNEWDTEP-LQVFVVPHSHNDP 178
Drosophila     VQD-VPNVDVQMLELYDRMSFKDIDGGVWKQGWNIKYDPLKYNAHHKLKVFVVPHSHNDP 156
                *.   * *****::*. :**.: ********::*.*:. ::::.  *:***********
Human          GWLKTFNDYFRDKTQYIFNNMVLKLKEDSRRKFIWSEISYLSKWWDIIDIQKKDAVKSLI 238
Drosophila     GWIQTFEEYYQHDTKHILSNALRHLHDNPEMKFIWAEISYFARFYHDLGENKKLQMKSIV 216
               **::**::*::..*::*:.* : :*:::.. ****:****:::::. :. :**  :**::
Human          ENGQLEIVTGGWVMPDEATPHYFALIDQLIEGHQWLENNIGVKPRSGWAIDPFGHSPTMA 298
Drosophila     KNGQLEFVTGGWVMPDEANSHWRNVLLQLTEGQTWLKQFMNVTPTASWAIDPFGHSPTMP 276
               :*****:**********..*:  :: ** **: **:: :.*.* :.************.
Human          YLLNRAGLSHMLIQRVHYAVKKHFALHKTLEFFWRQNWDLGSVTDILCHMMPFYSYDIPH 358
Drosophila     YILQKSGFKNMLIQRTHYSVKKELAQQRQLEFLWRQIWDNKGDTALFTHMMPFYSYDIPH 336
               *:*:::*:.:*****.**:***.:* :: ***:*** **   . * :: ************
Human          TCGPDPKICCQFDFKRLPGGRFGCPWGVPPETIHPGNVQSRARMLLDQYRKKSKLFRTKV 418
Drosophila     TCGPDPKVCCQFDFKRMGSFGLSCPWKVPPRTISDQNVAARSDLLVDQWKKKAELYRTNV 396
               *******:********: .  :.*** ***.**   ** :*: :*:**::**::*:**:*
Human          LLAPLGDDFRYCEYTEWDLQFKNYQQLFDYMNSQSKFKVKIQFGTLSDFFDALDKADETQ 478
Drosophila     LLIPLGDDFRFKQNTEWDVQRVNYERLFEHINSQAHFNVQAQFGTLQEYFDAVHQAER-- 454
               ** *******: : ****:*  **::**:::***::*:*: *****.::***:.:*:.
Human          RDKGQSMFPVLSGDFFTYADRDDHYWSGYFTSRPFYKRMDRIMESHLRAAEILYYFALRQ 538
Drosophila     --AGQAEFPTLSGDFFTYADRSDNYWSGYYTSRPYHKRMDRVLMHYVRAAEMLSAWHSWD 512
                  **: **.***********.*:*****:****::*****::  ::****:*  :   :
Human          AHKYKINKFLSSSLYTALTEARRNLGLFQHHDAITGTAKDWVVVDYGTRLFHSLMVLEKI 598
Drosophila     G---------MARIEERLEQARRELSLFQHHDGITGTAKTHVVVDYEQRMQEALKACQMV 563
               .         : :   * :***:*.******.******  *****  *: .:* . : :
Human          IGNSAFLLILKDKLTYDSYSPDTFLEMDLKQKSQDSLPQKNIIRLSAEPR---YLVVYNP 655
Drosophila     MQQSVYRLLTKPSIYSPDFSFSYFTLDDSRWPGSGVEDSRTTIILGEDILPSKHVVMHNT 623
               : :*.: *: * .:   .:* . *   * :  ...   .:. * *. :     ::*::*.
Human          LEQDRISLVSVYVSSPTVQVFSASGKPVEVQVSAVWDTAN---------TISETAYEISF 706
Drosophila     LPHWREQLVDFYVSSPFVSVTDLANNPVEAQVSPVWSWHHDTLTKTIHPQGSTTKYRIIF 683
               * : * .**..***** *.* . :.:***.***.**.  :           * * *.* *
Human          RAHIPPLGLKVYKILESASS---NSHLADYVLYKN-KVEDSGIFTIKNMINTEEGITLEN 762
Drosophila     KARVPPMGLATYVLTISDSKPEHTSYASNLLLRKNPTSLPLGQYPEDVKFGDPREISLRV 743
               :*::**:** .* :  * *.   .*: :: :* **  .    * :. .  :.  . *:*.
Human          -SFVLLRFDQTGLMKQMMTKEDGKHHEVNVQFSWYGTTIKRDKSGAYLFLPDGNAKPYVY 821
Drosophila     GNGPTLAFSEQGLLKSIQLTQDSPHVPVHFKFLKYGVRSHGDRSGAYLFLPNGPASP-VE 802
                .   * *.: **:*.:  .:*. *  *:.:*  **.  : *:********:* *.* *
Human          TTPPFVRVTHGRIYSEVTCFFDHVTHRVRLYHIQGIEGQSVEVSNIVDIRKVYNREIAMK 881
Drosophila     LGQPVVLVTKGKLESSVSVGLPSVVHQTIMR------GGAPEIRNLVDIGSLDNTEIVMR 856
                  *.* **:*:: *.*:  :  *.*:. :       * : *: *:*** .: * **.*:
Human          ISSDIKSQNRFYTDLNGYQIQPRMTLSKLPLQANVYPMTTMAYIQDAKHRLTLLSAQSLG 941
Drosophila     LETHIDSGDIFYTDLNGLQFIKRRRLDKLPLQANYYPIPSGMFIEDANTRLTLLTGQPLG 916
               :.:.*.* : ******* *:  *  *.****** **:.:  :*:**: *****:.*.**
Human          VSSLNSGQIEVIMDRRLMQDDNRGLEQGIQDNKITANLFRILLEKRSAVNTEEEKKSVSY 1001
Drosophila     GSSLASGELEIMQDRRLASDDERGLGQGVLDNKPVLHIYRLVLEKVNNCVRPSKLHPAGY 976
                *** **::*:: **** .**:*** **: *** . :::*::*** .     .: :...*
Human          PSLLSHITSSLMNHPVIPMANKFSSPTLELQGEFSPLQSSLPCDIHLVNLRTIQSKVGNG 1061
Drosophila     LTSAAHKASQSLLDPLDKFIFAEN-EWIGAQGQFGGDHPSAREDLDVSVMRRLTKSS--A 1033
                :  :* :*. : .*:  :     .   :  **:*.  :.*   *:.:  :* : ..  .
Human          HSNEAALILHRKGFDCRFSSKGTGLFCSTTQGKILVQKLLNKFIVESLTPSSLSLMHSPP 1121
Drosophila     KTQRVGYVLHRT------NLMQCGTPEEHTQKLDVCHLLPN---VARCERTTLTFLQNLE 1084
               :::... :***.      .    *   . **   : : * *   *      ::*::::.
Human          GTQNISEINLSPMEISTFRIQLR- 1144
Drosophila     HLDGMVAPEVCPMETAAYVSSHSS 1108
                 :.:   ::.*** :::  .
```

Scheme 12: Sequence alignment of hGMII (AS: NP 002362) and dGMII (AS: CAA 54732). ClustalW (http://www.ebi.ac.uk/clustalw/) was used to create the above alignment using the default parameters without manual intervention. An alignment score of 2574 was calculated by the software.[43]

[43] Hoffmann, D. Diploma Thesis, Ontario Cancer Institute, **2006**.

1.5. Glycosidase Inhibitors

In addition to natural inhibitors, the disclosure of the function of the active site of glycosidases involved in the biosynthesis of glycoproteins has led to the development of synthetic inhibitors.

The biosynthesis pathway may be interrupted at different stages of the glycosylation process. Representative examples of inhibitors interacting mainly with the α-glucosidases or the α-mannosidases of the glycoprotein biosynthesis pathway will be presented.[44]

1.5.1. Inhibition of the formation of the "14-saccharide core"

One strategy consists in stopping the biosynthesis of the $Glc_3Man_9GlcNAc_2$-protein at the "14-saccharide core" unit stage (Scheme 3). Inhibition of the transfer of GlcNAc-1-P to the lipid carrier by tunicamycin (**1**, TM, Scheme 13**)** is an example of this approach. TM was first identified and isolated from *Streptomyces lysosuperificus* by Takatsuki et al., by virtue of the fact that it inhibited replication of a number of enveloped viruses. This antibiotic is active against animal and plant viruses, Gram-positive bacteria, yeast and fungi.[45] TM are composed of uracil, two linked sugars and fatty acid side chains (I to X).

Five other antibiotics have been reported to inhibit the formation of *N*-acetylglucosaminyl-pyrophosphoryl-dolichol like TM.[46] They are structurally related to tunicamycin and are known as streptovirudin,[47] mycospocidin,[48] antibiotic 24010,[49] antibiotic MM 19290[50] and corynetoxin.[51] All these compounds share the same general structure of TM but differ in the nature of the fatty acid component (Scheme 13).[52]

---

[44] a) Asano, N. *J. Enzyme Inhibition* **2000**, *15*, 215-234. b) Asano, N.; Kato, A.; Watson, A. A. *Mini Rev. Med. Chem.* **2001**, *1*, 145-154.
[45] Takatsuki, A.; Arima, K.; Tamura, G. *J. Antibiot.* **1971**, *24*, 215-223.
[46] a) Elbein, A. D.; Gafford, J.; Kang, M. S. *Arch. Biochem. Biophys.* **1979**, *196*, 311-318. b) James, D. W.; Elbein, A. D. *Plant. Physiol.* **1980**, *65*, 460-464.
[47] Elbein, A. D.; Occolowitz, J. L.; Hamill, R. L.; Eckardt, K. *Biochemistry* **1981**, *20*, 4210-4216.
[48] Nakamura, S.; Arai, M.; Karasawa, K.; Yonehara, H. *J. Antibiot.* **1957**, *10*, 248-253.
[49] a) Mizuno, M.; Shimojima, Y.; Sugawara, T.; Takeda, I. *J. Antibiot.* **1971**, *24*, 896-899. b) Shimojima, Y.; Mizuno, M.; Mizuno, Y.; Ooka, T.; Takeda, I. *J. Antibiot.* **1972**, *25*, 604-606.
[50] Kenig, M.; Reading, C. *J. Antibiot.* **1979**, *32*, 549-554.
[51] Eckardt, K. *Nucleoside Antibiot.* **1983**, *46*, 544-550.
[52] Cockrum, P. A.; Edgar, J. A.; *J. Chromato.* **1983**, *268*, 245-254.

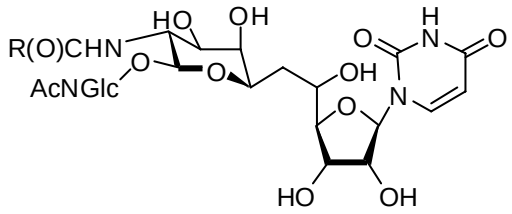

(**1**)

Tunicamycins (TM):

I	R = -CH=CH$(CH_2)_7CH(CH_3)_2$
II	R = -CH=CH$(CH_2)_8CH(CH_3)_2$
III	R = -CH=CH$(CH_2)_{10}CH_3$
IV	R = -CH=CH-$C_{12}H_{25}$
V	R = -CH=CH$(CH_2)_9CH(CH_3)_2$
VI	R = -$(CH_2)_{11}CH(CH_3)_2$
VII	R = -CH=CH$(CH_2)_{10}CH(CH_3)_2$
VIII	R = -CH=CH$(CH_2)_{12}CH_3$
IX	R = -CH=CH-$C_{14}H_{29}$
X	R = -CH=CH$(CH_2)_{11}CH(CH_3)_2$

Streptovirudins

A_2	R = -CH=CH$(CH_2)_6CH(CH_3)_2$
B_2	R = -CH=CH$(CH_2)_6CH(CH_3)(CH_2$-$CH_3)$

Corynetoxins :

H17a	R = -CH_2=CHOH-$(CH_2)_{10}CH(CH_3)(CH_2$-$CH_3)$
U17a	R = -CH=CH$(CH_2)_{10}CH(CH_3)(CH_2$-$CH_3)$

Scheme 13: Structures of Tunicamycin and related antibiotics.

The major drawback associated with inhibitors such as tunicamycin is the complete prevention of glycosylation and therefore result in the synthesis of nonglycosylated proteins. Another approach consists in inhibiting specific enzymes of the trimming process so that glycosylation can occur but the *N*-linked oligosaccharides cannot be modified beyond a specific step. The molecules found in the nature or developed for that purpose are defined as processing inhibitors.

1.5.2. Inhibitors of α-glucosidases and their biological activities

Several families of aza-sugars are inhibitors of glucosidases. These molecules belong to five different structural classes: polyhydroxylated piperidines, pyrrolidines, indolizidines, pyrrolizidines and nortropanes.[53] For instance, polyhydroxylated piperidines such as nojirimycin (**3**, NJ, Scheme 14), 1-deoxynojirimycin (**4**, DNJ, Scheme 15) and *N*-methyl 1-deoxynojirimycin (**5**, Me-DNJ, Scheme 15) are aza-sugar analogues of D-glucose (**2**, Glc, Scheme 14) in which the intracyclic oxygen of the hexose is replaced with a basic nitrogen atom.

[53] Asano, N.; Nash, R. J.; Molyneux, R. J.; Fleet, G. W. J. *Tetrahedron Assymetry* **2000**, *11*, 1645-1680.

In 1966, NJ (**3**), discovered as the first natural glucose mimic, was described as an antibiotic produced by *Streptomyces roseochromogenes* R-468 and *S. lavendulae* SF-425 and was shown to be a potent inhibitor of α- and β-glucosidases of different origins.[54] This non selectivity was explained by the observations of Inouye et al. who reported that NJ exists in aqueous solution in both α- and β- forms in a 6:4 ratio.[55] These two forms are able to inhibit α- and β-glucosidases, respectively.

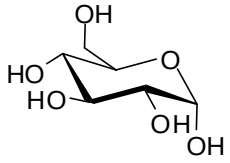

Glucose (**2**, Glc)

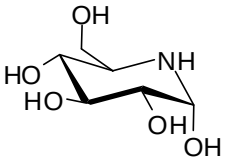

Nojirimycin (**3**, NJ)

IC_{50}	Enzyme [Ref]
0.56 μM	α-glucosidase (rat intestinal sucrase) [27]
0.76 μM	α-glucosidase (rat intestinal glucoamylase) [27]
0.89 μM	β-glucosidase (sweet almond) [27]
0.36 μM	β-glucosidase (Aspergillus wentii) [27]

Scheme 14: Structures of Glucose and Nojirimycin. IC_{50} toward various enzymes.

Moreover, NJ is relatively unstable since the hydroxyl group at C(1) is prone to elimination. The corresponding reduced piperidine, DNJ (**4**, Scheme 15) was isolated from the roots of *Morus bombycis* (mulberry trees) and called moranoline.[56] DNJ, also produced by many strains of the genera *Bacillus* and *Streptomyces*, was found to be a potent inhibitor of α-glucosidase I and II. Saunier et al. reported that the inhibitory ability of DNJ is pH dependent and that DNJ inhibits glucosidase II more strongly than glucosidase I. For instance, IC_{50} values of 2 μM and 20 μM have been reported for α-glucosidase I and α-glucosidase II from *Saccharomyces cerevisiae*, respectively.[57] Nevertheless, DNJ proved to be rather non-specific and inhibits other α-glucosidases, β-glucosidase and reduces the formation of the "14-saccharide core" unit.[58]

[54] Inouye, S.; Tsurouka, T.; Niida, T. *J. Antibiot.* **1966**, *19*, 288-292.
[55] Inouye, S.; Tsurouka, T.; Ito, T.; Niida, T. *Tetrahedron* **1968**, *23*, 2125-2144.
[56] Masahiro, Y.; Tatsuhiko, K.; Yoshiaki, A.; Hiromu, M. *Nippon Nogei Kagaku Kaishi* **1976**, *50*, 571-572.
[57] Saunier, B.; Kilker, R. D.; Tkacz, J. S.; Quaroni, A. Herscovics, A. *J. Biol. Chem.* **1982**, *257*, 14155-14161.
[58] a) Evans, S. V.; Fellows, L. E.; Shing, T. K. M.; Fleet, G. W. J. *Phytochemistry* **1985**, *24*, 1953-1955. b) Li, Y. K.; Byers, L. D. *Biochim. Biophys. Acta* **1989**, *999*, 227-232. c) Ridruejo, J. C.; Munoz, M. D.; Andaluz, E.; Larriba, G. *Biochim. Biophys. Acta* **1989**, *993*, 179-185.

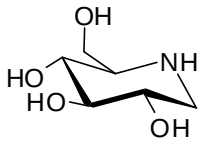

1-Deoxynojirimycin (**4**, DNJ)

IC_{50}	Enzyme [Ref]
20 μM	α-glucosidase I (*S. cerevisiae*) [57]
2 μM	α-glucosidase II (*S. cerevisiae*) [57]
81 μM	β-glucosidase (emulsin) [58a]
560 μM	anti HIV activity [112]

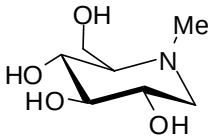

N-methyl 1-deoxynojirimycin
(**5**, Me-DNJ)

0.3 μM	α-glucosidase I (calf liver microsomes) [60]
130 μM	α-glucosidase II (calf liver microsomes) [60]

Scheme 15: Structures of inhibitors of α- and β-glucosidases. IC_{50} toward various enzymes.

The *N*-methyl derivative of 1-deoxynojirimycin (**5**, Scheme 15) isolated from the leaves of mulberry trees demonstrated potent inhibition of ER α-glucosidases I and II.[59] Indeed, *N*-alkylation of compound **4**, induces a shift from α-glucosidase II to α-glucosidase I in the specific inhibition of purified glucosidases.[60] Furthermore, in cell culture, *N*-alkyl derivatives of DNJ are more effective inhibitors of glucosidase I than glucosidase II, since a much larger proportion of the oligosaccharides formed in the presence of these inhibitors contains three glucose residues.[61]

The problem with most of these inhibitors is the lack of specificity leading to the inhibition of both α-glucosidase I and α-glucosidase II, as well as other α-glucosidases. In 1988, homonojirimycin (HNJ, **6**, Scheme 16) was isolated from the tropical liana *Omphalea diandra*.[62] It was the first report of the isolation of the naturally occurring C(1) branched DNJ derivative. Some years later, Zeng et al examined the effect of HNJ and its analogues on the activity of the processing glucosidases. It was found that HNJ was a better inhibitor of glucosidase II than glucosidase I, while its *N*-methyl derivative (Me-HNJ, **7**, Scheme 16) inhibited glucosidase I more effectively than glucosidase II and was also more potent against glucosidase I than DNJ.[63]

[59] Asano. N.; Tomioka, E.; Kizu, H.; Matsui, K. *Carbohydrate Res.* **1994**, *253*, 235-245.
[60] Hettkamp, H.; Legler, G.; Bause, E. *Eur. J. Biochem.* **1984**, *142*, 85-90.
[61] Tan, A.; van den Broek, L.; van Boeckel, S.; Ploegh, H.; Bolscher, J. *J. Biol. Chem.* **1991**, *266*, 14504-14510.
[62] Kite, G. C.; Fellows, L. E.; Fleet, G. W. J.; Liu, P. S.; Scofield, A. M.; Smith, N. G. *Tetraehdron Lett.* **1988**, *29*, 6483-6486.
[63] Zeng, Y.; Pan, Y. T.; Asano, N.; Nash, R .J.; Elbein, A.D. *Glycobiology* **1997**, *7*, 297-304.

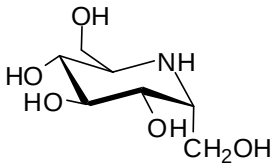

IC_{50}	Enzyme [Ref]
2.5 μg/ml	α-glucosidase I (mung bean seedlings) [63]
1 μg/ml	α-glucosidase II (mung bean seedlings) [63]

Homonojirimycin (**6**, HNJ)

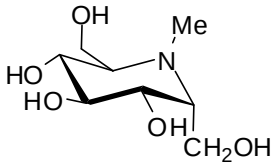

0.25 μg/ml	α-glucosidase I (mung bean seedlings) [63]
10 μg/ml	α-glucosidase II (mung bean seedlings) [63]

N-methyl homonojirimycin (**7**, Me-HNJ)

Scheme 16: Structures of Homonojirimycin and one analogue. IC_{50} toward various enzymes.

Castanospermine (**8**, CST, Scheme 17), another natural glucosidase inhibitor, was isolated in 1981 from the seeds of *Castanospermum australe*,[64] and later from the dried pods of *Alexa leiopetala.*[65] Compound **8** is a polyhydroxylated indolizidine alkaloid which inhibits strongly α- and β-glucosidase as well as intestinal sucrase. Experiments indicate that the extent of castanospermine inhibition is greatly dependent on the pH with better efficiency at pH 6.5 than at lower pH.[66] CST is a more potent inhibitor of α-glucosidase I than α-glucosidase II. Moreover, CST is more active on α-glucosidase I than DNJ.[67] Indeed, conformational comparison between DNJ and castanospermine suggests that the greater activity of CST compared to DNJ may by due to the fixed axial positioning of the O6 atom.[68]

[64] Hohenschutz, L. D.; Bell, E. A.; Jewess, P. J.; Leworthy, D. P.; Pryce, R. J.; Arnold, E.; Clardy, J. *Phytochem.* **1981**, *20*, 811-814.
[65] Nash, R. J.; Fellows, L. E.; Dring, J. V.; Stirton, C. H.; Carter, D.; Hegarty, M. P.; Bell, E. A. *Phytochem.* **1988,** *27*, 1403-1404.
[66] a) Saul, R.; Molyneux, R. J.; Elbein, A. D. *Arch. Biochem. Biophys.* **1984**, *230*, 668-675. b) Trugnan, G.; Roussett, M.; Zweibaum, A. *FEBS Lett.* **1986**, *195*, 28-32.
[67] a) Pan, Y. T.; Hori, H.; Saul, R.; Sanford, B. A.; Molyneux, R. J.; Elbein, A. D. *Biochemistry* **1983**, *22*, 3975-3984. b) Szumilo, T; Kaushak, G. P.; Elbein, A. D. *Arch. Biochem. Biophys.* **1986**, *247*, 261-271.
[68] Hempel, A.; Camerman, N.; Mastropaolo, D.; Camerman, A. *J. Med. Chem.* **1993**, *36*, 4082-4086.

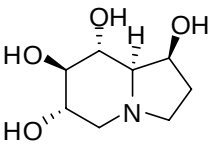

Castanospermine (**8**, CST)

IC_{50}	Enzyme [Ref]
< 1 μg/ml (i.e. 1 μM)	α-glucosidase I (mung bean seedlings) [69]
0.5 – 1 μg/ml	α-glucosidase (amyloglucosidase) [66a]
5 μg/ml	β-glucosidase, pH = 6.5 (almond emulsin) [66a]
20 μg/ml	β-glucosidase, pH = 5.0 (almond emulsin) [66a]
< 1 μM	sucrase [69]
< 1 μM	maltase [69]
29 μM	anti HIV activity [112]

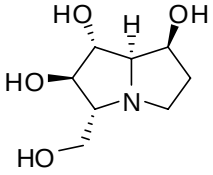

Australine (**9**)

20 μM	α-glucosidase I (mung bean seedlings) [69]
> 500 μM	α-glucosidase II (mung bean seedlings) [69]
5.8 μg/ml	α-glucosidase (amyloglucosidase) [69]
28 μM	sucrase [69]
35 μM	maltase [69]

Scheme 17: Natural inhibitors of glycosidases from *Catanospermum australe*. IC_{50} toward various enzymes.

In addition to indolizidine alkaloids, *C. australe* was reported to produce the polyhydroxylated pyrrolizidine alkaloid australine (**9**, Scheme 17). This compound demonstrated a strong activity and selectivity toward α-glucosidase I as it poorly inhibited α-glucosidase II. Australine was the first example of a compound presenting such selectivity but is nevertheless less active than CST on α-glucosidase I. Australine demonstrated poor inhibitory ability toward β-glucosidase (10 times less active than CST),[69] and was not active toward α- and β- mannosidases, α- and β-galactosidases, sucrase and maltase, which made australine a definitively more selective inhibitor.[70]

[69] Tropea, J. E.; Molyneux, R. J.; Kaushal, G. P.; Pan, Y. T.; Mitchell, M.; Elbein, A. D. *Biochemistry* **1989**, *28*, 2027-2034.
[70] Molyneux, R. J.; Benson, M.; Wong, R. Y *J. Nat. Prod.* **1988**, *51*, 1198-1206.

1.5.3. Inhibitors of α-mannosidases and their biological activities

Several alkaloids isolated from plants and microorganisms display inhibitory ability against α-mannosidases. For instance, 1-deoxymannonojirimycin (**12**, DMJ, Scheme 18) was first isolated from the seeds of the legume *Lonchocarpus sericeus*, a native plant of the West Indies and tropical America[71] and was later isolated from the tropical *Omphalea diandra* and *Angylocalyx pynaertii,*[72] an edible vegetable growing in tropical African forest. In 1979, the discovery of DMJ revealed the second example after NJ of a sugar analogue, containing a nitrogen atom instead of an oxygen atom in the sugar ring. Compound **12** (DMJ) has been found to be a selective inhibitor of rat liver Golgi α-mannosidase I but did not affect ER α-mannosidase or Golgi α-mannosidase II. Nevertheless high concentrations of this compound are necessary for inhibition.[73]

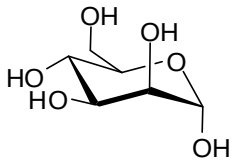

Mannose (**10**, Man)

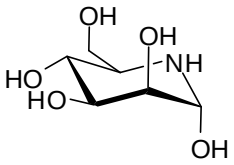

Mannonojirimycin (**11**, MJ)

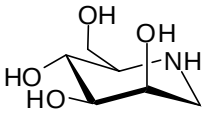

1-Deoxymannonojirimycin (**12**, DMJ)

IC_{50}	Enzyme [Ref]
1-2 μM	Golgi α-mannosidase I (rat liver) [73b]
n.i.	Golgi α-mannosidase II (rat liver) [73b]
n.i.	ER α-mannosidase (rat liver) [73b]

n.i. = no inhibition

Scheme 18: Structures of Mannose, Mannonojirimycin and 1-Deoxymannonojirimycin. IC_{50} toward various enzymes.

[71] Fellows, L. E.; Bell, E. A.; Lynn, D. G.; Pilkiewicz, F.; Miura, I.; Nakanishi, K. *J. Chem. Soc., Chem. Commun.* **1979**, *22*, 977-978.

[72] Molyneux, R. J.; Pan, Y. T.; Tropea, J. E.; Elbein, A. D.; Lawyer, C. H.; Hughes, D. J.; Fleet, G. W. *J. Nat. Prod.* **1993**, *56*, 1356-1364.

[73] a) Fuhrmann, U.; Bause, E.; Legler, G.; Ploegh, H. *Nature* **1984**, *307*, 755-758. b) Bischoff, J.; Kornfeld, R. *Biochim. Biophys. Res. Commun.* **1984**, *125*, 324-331. c) Hardick, D. J.; Hutchinson, D. W.; Trew, S. J.; Wellington, E. M. H. *Tetrahedron* **1992**, *48*, 6285-6296.

Mannostatin A and B (**13** and **14**, Scheme 19) were discovered by Aoyagi and collaborators in 1989 and so named because of their highly potent inhibition of α- and β-mannosidase activities. They were isolated from the soil microorganism *Streptoverticillum verticillus* during screening of culture broths for mannosidase inhibitors.[74] Inhibition by mannostatin A and B of α-mannosidases prepared from epididymes of adult rats has been shown to be competitive. When tested on various glycosidases, Mannostatin A was inactive toward β-glucosidase, α- and β-galactosidase, β-mannosidase but was a potent inhibitor of jack bean α-mannosidase. Mannostatin A also proved to be an effective competitive inhibitor of the glycoprotein-processing enzyme α-mannosidase II but was inactive toward α-mannosidase I.[75]

Kifunensine (15, Scheme 19), initially isolated from the culture broth of the actinomycete *Kitasatosporia kifunensine* 9482,[76] was reported to be a weak inhibitor of jack bean α-mannosidase but was a very potent and selective inhibitor of α-mannosidase I from mung bean seedlings. Studies with rat liver microsomes indicated that kifunensine selectively inhibited Golgi α-mannosidase I but did not inhibit the ER mannosidase. Moreover, introduction of kifunensine in cells culture medium at 1 μg/ml or higher concentration resulted in the production of $Man_9GlcNAc_2$ chains rather than complex structures.[77]

[74] Aoyagi, T.; Yamamoto, T.; Kojiri, K.; Morishima, H.; Nagai, M.; Hamada, M.; Takeuchi, T.; Umezawa, H. *J. Antibiot.* **1989**, *42*, 883-889.

[75] a) Tropea, J. E.; Kaushal, G. P.; Pastuszak, I.; Mitchell, M.; Aoyagi, T.; Molyneux, R. J.; Elbein, A. D. *Biochemistry* **1990**, *29*, 10062-10069. b) Berecibar, A.; Grandjean, C.; Siriwardena, A. *Chem. Rev.* **1999**, *99*, 799-844.

[76] Kayakiri, H.; Takase, S.; Shibata, T.; Okamoto, M.; Terano, H.; Hashimoto, M.; Tada, T.; Koda, S. *J. Org. Chem.* **1989**, *54*, 4015-4016.

[77] Elbein, A. D.; Tropea, J. E.; Mitchell, M.; Kaushal, G. P. *J. Biol. Chem.* **1990**, *265*, 15599-15605.

	IC_{50}	Enzyme [Ref]
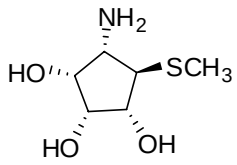 Mannostatin A (**13**)	20 nM	α-mannosidase (rat epididymis) [75a]
	70 nM	α-mannosidase (jack bean) [75a]
	450 nM	α-mannosidase (mung bean) [75a]
	160 nM	α-mannosidase (rat liver lysosomal) [75a]
	15 nM	α-mannosidase II (mung bean seedlings) [75a]
	n.i.	α-mannosidase I (mung bean seedlings) [75a]
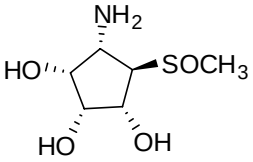 Mannostatin B (**14**)	20 nM	α-mannosidase (rat epididymis) [74]
	30 nM	α-mannosidase (jack bean) [75b]
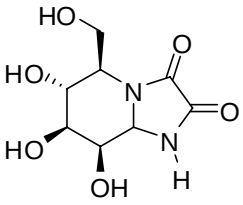 Kifunensine (**15**)	120 μM	jack bean [76]
	20-50 nM	mannosidase I (mung bean seedlings) [77]
	n.i.	mannosidase II (mung bean seedlings) [77]
	100 nM	Golgi-mannosidase I (rat liver) [77]
	n.i.	ER-mannosidase (rat liver) [77]

n.i. = no inhibition

Scheme 19: Structures of Mannostatin A, B and Kifunensine. IC_{50} toward various enzymes.

Swainsonine (**16**, Scheme 20), a polyhydroxylated indolizidine alkaloid, discovered in 1978 by Dorling and al.,[78] displayed reversible inhibition of class II α-mannosidases (lysosomal and Golgi α-mannosidases). Swa was first isolated in Australia from the plant *Swainsona canescens*,[79] which was toxic to livestock. Swa has then been identified as the toxic principle of locoism, a syndrome developed by animals ingesting the locoweed infested species *Astragalus* and *Oxytropis* species,[80] and more recently in the poisonous plant *Ipomea carnea*,[81] and the fungus *Rhizoctonia leguminocola*.[82] The clinical signs of locoism include nervousness, aggression, hyperactivity, increasing miscoodination, head tremors, loss of weight, reproductive alterations, weakness and death. These symptoms are attributed to lysosomal storage disease which is characterized by cytoplasmic vacuolation of cells of the central nervous system. However, purified Swa alone is now known not to be neurotoxic, but loco syndrome may be caused by ingestion of a combination of alkaloids found in *Swainsona canescens* or *Astragalus*.[83]

Dorling and al. recognized that the lysosomal storage disorder induced in animals grazing *Swainsona* species was biochemically and morphologically similar to the rare genetic mannosidosis that occurs in humans. This affection is characterized by accumulation in cells and excretion in urine of mannose-rich oligosaccharides, resulting from a deficiency of lysosomal α-mannosidase.[84] It has been found that Swa concentrates and accumulates in lysosomes of normal human fibroblasts and human lymphoblasts in culture, since it is almost fully ionized within the acidic environment of this organelle.[85] Such accumulation produces the inhibition of the intracellular lysosomal α-mannosidase which induces incomplete catabolism of the carbohydrate moiety of glycoproteins and storage of the remaining proteins which finally leads to disease as a consequence. It is assumed that this mode of action also occurs *in vivo*. Actually, Swa provides a valuable tool for the study of human mannosidosis despite the fact it also inhibits Golgi α-mannosidase II. [86]

---

[78] Dorling, P. R.; Huxtable, C. R.; Vogel, P. *Neuropathol. Appl. Neurobiol.* **1978**, *4*, 285-295.
[79] Colegate, S. M.; Dorling, P. R.; Huxtable, C. R.; *Aust. J. Chem.* **1979**, *32*, 2257-2264.
[80] Molyneux, R. J.; James, L. F.; Science **1982**, *216*, 190-191.
[81] Haraguchi, M.; Gorniak, S. L.; Ikeda, K.; Minami, Y.; Kato, A.; Watson, A. A.; Nash, R. J.; Molyneux, R. J.; Asano, N. *J. Agric. Food Chem.* **2003**, *51*, 4995-5000.
[82] Schneider, M. J.; Ungemach, F. S.; Broquist, H. P.; Haris, T. M. *Tetraheddron* **1983**, *39*, 29-32.
[83] Bowlin, T. L.; Sunkara, P. S. *Biochem. Biophys. Res. Commun.* **1988**, *151*, 859-864.
[84] Jolly, R. D.; Winchester, B. G.; Gehler, J.; Dorling, P. R.; Dawson, G. *J. Appl. Biochem.* **1981**, *3*, 273-291.
[85] a) Chotai, K.; Jennings, C.; Winchester, B.; Dorling, P.R. *J. Cell. Biochem.* **1983**, *21*, 107-117. b) Ikeda, K.; Kato, A.; Adachi, I.; Haraguchi, M.; Asano, N. *J. Agric. Food Chem.* **2003**, *51*, 7642-7646.
[86] a) Watson, A. A.; Fleet, G. W. J.; Asano, N.; Molyneux, R.; Nash, R. J. *Phytochemistry* **2001**, *56*, 265-295. b) Cenci di Bello, I.; Dorling, P.R.; Winchester, B.; *Biochem. J.* **1983**, *215*, 693-696.

Swa was the first compound able to alter glycoprotein processing. It displayed inhibitory ability toward jack bean α-mannosidase, rat liver Golgi α-mannosidase II but was without effect on Golgi α-mannosidase I.[87] In addition, Swa did not inhibit ER α-mannosidase or the soluble α-mannosidases of rat liver.[88] The selectivity of Swa toward α-mannosidases was established against other glycosidases such as α-glucosidase, β-galactosidase and β-glucoronidase and lysosomal β-mannosidases.[85a] The pKa of Swa was determined to be 7.4 which mean that Swa would be fully ionized at pH 4.0.[89] Molecular modelling has shown that the relative positions of the cationic ammonium center and the three hydroxyl groups mimic an intermediate cationic structure of the hydrolysis mediated by α-mannosidases II and thus accounts for the apparent specificity of Swa for α-mannosidases II.[85b]

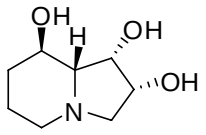

Swainsonine (**16**, Swa)

IC_{50}	Enzyme [Ref]
0.4-0.1 μM	jack bean [89, 104a]
70 nM	α-mannosidase (human liver lysosomal) [87c]
20 nM	α-mannosidase (rat lysosomal) [85b]
40 nM	α-mannosidase (human lysosomal) [85b]
n.i.	Golgi mannosidase I (rat liver) [87a]
200 nM	Golgi mannosidase II (rat liver) [87a]
160 nM	α-mannosidase (rat liver lysosomal) [75a]

n.i. = no inhibition

Scheme 20: Structure of Swainsonine. IC_{50} toward various enzymes.

Several research groups have developed synthetic pathways to more complex sugar mimetics[90] hoping to achieve more potent inhibition against selected glycosidases. Nevertheless, the inhibition values were generally lower than the activities provided by natural azasugars.

[87] a) Tulsiani, D. P. R.; Harris, T. M.; Touster, O. *J. Biol. Chem.* **1982**, *257*, 7936-7939. b) Tulsiani, D. P. R.; Broquist, H. P.; James, L. F.; Touster, O. *Arch. Biochem. Biophys.* **1988**, *264*, 607-617. c) Cenci di Bello, I.; Fleet, G.; Namgoong, S. K.; Tadano, K.-I..; Winchester, B.; *Biochem. J.* **1989**, *259*, 855-861.
[88] Bischoff, J.; Kornfeld, R. *J. Biol. Chem.* **1986**, *261*, 4758-4765.
[89] Dorling, P. R.; Huxtable, C. R.; Colegate, S. M. *Biochem. J.* **1980**, *191*, 649-651.
[90] Robina, I.; Vogel, P. *Synthesis* **2005**, *5*, 675-702 and refs cited therein.

The development of inhibitors of the recently disclosed endomannosidase,[19, 91] has also raised interest, as these enzymes are not inhibited by Swa. Spiro and al have shown that Glcα1,3(1-deoxy)mannonojirimycin (**17**, Scheme 21) in the presence of castanospermine, inhibited *in vivo* the endomannosidase mediated pathway thus preventing the synthesis of complex *N*-linked oligosaccharides.[92]

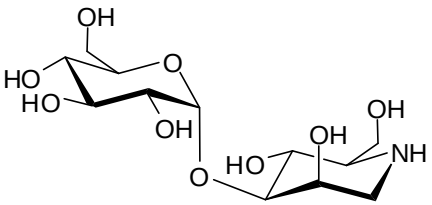

(**17**)

Scheme 21: Glcα1,3(1-deoxy)mannonojirimycin.

[91] Hamilton, S. R.; Li, H.; Wischnewski, H.; Prasad, A.; Kerley-Hamilton, J. S.; Mitchell, T.; Walling, A. J.; Davidson, R. C.; Wildt, S.; Gerngross, T. U. *Glycobiology* **2005**, *15*, 615-624.

[92] a) Hiraizumi, S.; Spohr, U.; Spiro, R. G. *J. Biol.Chem.* **1993**, *268*, 9927-9935. b) Rothblatt, J.; Novick, P.; Stevens, T. *Guidebook to the Secretory Pathway*, Oxford University Press, **1994**, 188-189.

1.6. Therapeutic applications of glycosidase inhibitors

1.6.1. Therapeutic applications not related to cancer

Because enzyme-catalyzed carbohydrate hydrolysis is a biologically widespread process, glycosidase inhibitors have many potential applications as agrochemicals and as therapeutic agents. Inhibition of glycosidases in living material can have profound effects on the quality control, maturation, transport, and secretion of glycoproteins, and can alter cell-cell or cell-pathogens recognition processes suggesting potential use of glycosidase inhibitors against viral and bacterial infections and cancer.[93]

1.6.1.1. Diabetes treatment

Since the late 1960s, the Bayer group has searched for inhibitors of intestinal sucrase for clinical development in the treatment of type II diabetes (non-insulinodependent). In our diet, carbohydrates consist mainly of starch and saccharose. Starch is hydrolyzed into maltose by α-amylase released by the pancreas in the small intestine. Saccharose is hydrolyzed into glucose and fructose by α-glucosidases by intestinal saccharase. These monosaccharides are then directly absorbed by intestinal cells and enter the blood stream. Diabetic patients are affected by hyperglycemia. Inhibition of α-glucosidases in the small intestine can slow down carbohydrate hydrolysis and thus prevent peaks in the blood sugar levels. The Bayer group discovered that the pseudotetrasaccharide acarbose (**18**, Scheme 22), from the fermentation broth of the *Actinoplanes* strain SE 50,[94] competes with saccharose for the binding to the active site of the saccharase. The inhibitory ability (IC_{50}) of acarbose toward the porcine intestinal saccharase has been measured as 0.5 μg/ml.[95] Actually, acarbose is commercialized as Glucobay® for the therapy of type II diabetes.[96]

[93] Asano, N. *Glycobiology* **2003**, *13*, 93R-104R.
[94] Schmidt, D. D.; Frommer, W.; Junge, B.; Müller, L.; Wingender, W.; Truscheit, E. *Naturwissenschaften* **1977**, *64*, 535-536.
[95] Kwon, Y.-I.; Son, H.-J.; Moon, K. S.; Kim, J. K.; Kim, J.-G.; Chun, H.-S.; Ahn, S. K.; Hong, C. I. *J. Antibiot.* **2002**, *55*, 462-466.
[96] Balfour, J.A.; McTavish, D. *Drugs* **1993**, *46*, 1025-1054.

A structure similar to acarbose is found in valienamine (**19**, Scheme 22) and its analogue valiolamine (**20**, Scheme 22) which were isolated from the culture broth of validamycin-producing organism, *Streptomyces hygroscopicus* var. *limoneus*. These compounds exhibit strong α-glucosidase inhibitory ability *in vivo* and *in vitro* but valiolamine presents a more potent α-glucosidase inhibitory activity toward porcine intestinal sucrase, maltase and isomaltase than valienamine.[97] Horii and co-workers synthesized numerous *N*-substituted valiolamine derivatives in order to enhance the α-glucosidase inhibitory efficacy *in vitro*. The derivative voglibose (**21**, Scheme 22), obtained by reductive amination of valiolamine with dihydroxyacetone, presents IC_{50} values of 15 nM and 46 nM toward maltase and sucrase, respectively.[98] Voglibose is now on the market for the therapy of type II diabetes in Japan under the name Basen®.

In 1976, DNJ was found to be even more active than acarbose for the inhibition of α-glucosidase. However, despite its excellent α-glucosidase inhibitory potential *in vitro*, its efficacy *in vivo* was only moderate.[99] Alternative DNJ analogues were then developed and hundreds of *N*-substituted and C-branched derivatives were synthesized and screened for their biological activity. The best derivatives were nearly two orders of magnitude more effective than acarbose but the *N*-hydroxyethyl derivative of DNJ (**22**, Scheme 22) was finally chosen for further development and clinical trials. It has been approved for the treatment of type II diabetes under the name of Miglitol®.[100]

Recently, the piperidine alkaloid isofagomine (**23**, Scheme 22), a strong inhibitor of β-glucosidase,[101] has been reported to inhibit hepatic glycogen phosphorylase with an IC_{50} value of 0.7 μM, and to prevent basal and glucagon-stimulated glycogen hydrolysis in cultured hepatocytes with IC_{50} values of 2-3 μM.[102] Inhibitors of glycogen phosphorylase have not yet been evaluated for the treatment of type II diabetes but are promising target.

---

[97] Kameda, Y.; Asano, N.; Yoshikawa, M.; Takeuchi, M.; Yamaguchi, T.; Matsui, K.; Horii, S.; Fukase, H. *J. Antibiot.* **1984**, *37*, 1301-1307.

[98] Horii, S.; Fukase, H.; Matsu, T.; Kameda, Y.; Asano, N.; Matsui, K. *J. Med. Chem.* **1986**, *29*, 1038-1046.

[99] Junge, B.; Matzke, M,; Stoltefuss, J. *Handbook of Experimental Pharmacology*; Kuhlmann, J.; Puls, W. Eds.; Springer: Berlin Heiderberg New York, **1996**, *119*, 411-482.

[100] a) Paulsen, H.; Stütz, A.E *Iminosugars as Glycosidase Inhibitors: Nojirimycin and Beyons*,Ed. Wiley-VCH, Weinheim, **1999**, Chapter 1. b) Jacob, G. S. *Curr. Opin. Struct. Biol.* **1995**, *5*, 605-611.

[101] Jespersen, T. M.; Dong, W.; Sierks, M. R.; Skrydstrup, T.; Lundt, I.; Bols, M. *Angew. Chem. Int. Ed. Engl.* **1994**, *33*, 1778-1779.

[102] Jakobsen, P.; Lundbeck, J. M.; Kristiansen, M.; Breinholt, J.; Demuth, H.; Pawlas, J.; Torres Candela, M. P.; Andersen, B.; Westergaard, N.; Lundgren, K.; Asano, N. *Bioorg. Med. Chem.* **2001**, *9*, 733-744.

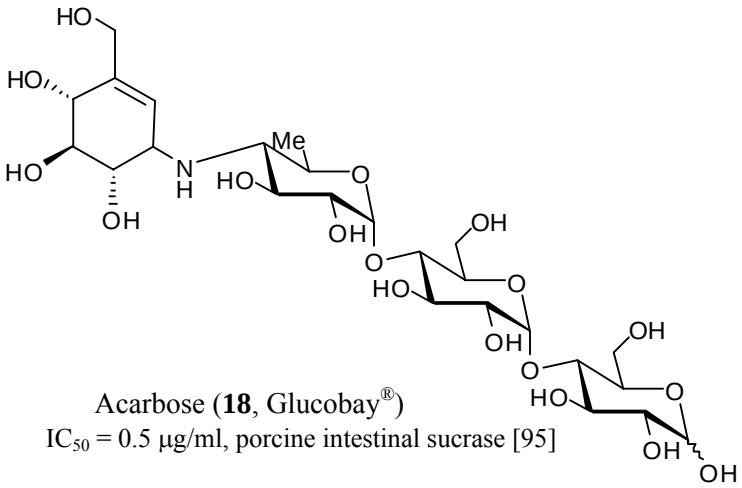

Acarbose (**18**, Glucobay®)
IC_{50} = 0.5 μg/ml, porcine intestinal sucrase [95]

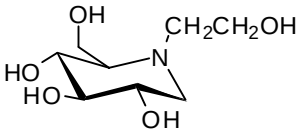

N-Hydroxyethyl deoxynojirimycin
(**22**, Miglitol®)

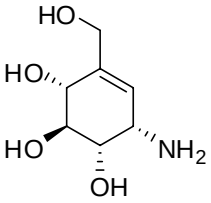

IC_{50}	Enzyme [Ref]
18 μM	α-glucosidase (yeast) [97]
53 μM	sucrase (porcine intestinal) [97]
340 μM	maltase (porcine intestinal) [97]
1 mM	isomaltase (porcine intestinal) [97]

Valienamine (**19**)

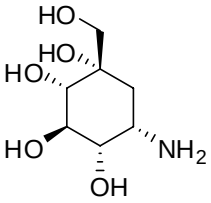

190 μM	α-glucosidase (yeast) [97]
49 nM	sucrase (porcine intestinal) [97]
2.2 μM	maltase (porcine intestinal) [97]
2.7 μM	isomaltase (porcine intestinal) [97]

Valiolamine (**20**)

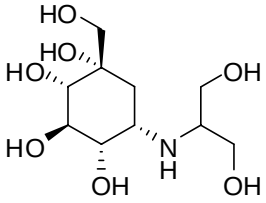

4.6 nM	sucrase (porcine intestinal) [98]
15 nM	maltase (porcine intestinal) [98]

Voglibose (**21**, Basen®)

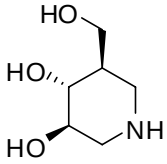

0.7 μM	hepatic glycogen phosphorylase [102]
0.11 μM	β-glucosidase (almonds) [101]

Isofagomine (**23**)

Scheme 22: Glycosidase inhibitors as anti-diabetic agents. IC_{50} toward various enzymes.

1.6.1.2. Antiviral treatment

Glycosidase inhibitors may also provide useful antiviral drugs as viruses carried coat glycoproteins which play an important role in their adhesion and their infectivity to cells. Thus, compounds that interfere with the glycosylation processes of viral glycoproteins can be expected to act as antiviral agents. An example of this strategy is illustrated by TM (**1**) which has been found to reduce transport of influenza viral glycoproteins to the cell surface.[103] Moreover, it has been shown that the absence of the carbohydrate side-chain from the viral glycopeptides of Herpes simplex type 1 virus particles grown in the presence of tunicamycin, does not affect the overall integrity of the virions but significantly decreases infectivity.[104]

α-Glucosidase inhibitors, such as DNJ[105] (**4**), *N*-butyl-deoxynojirimycin[106] (**24**, Bu-DNJ, Scheme 24) and CST[107] (**8**) are potent inhibitors of human immunodeficiency virus (HIV) replication.[108] All sugars mimetics showing anti-HIV activity have the common property to be potent inhibitors of processing α-glucosidase I. It is presumed that the anti-HIV activity results from the inhibition of processing ER α-glucosidase I, since there is a good correlation between the potency of inhibition toward this enzyme and viral control. Treatment of HIV-1-infected cells with an inhibitor such as Bu-DNJ causes a reduction of the release of infectious viruses.[109] This reduction is not induced by a decrease in the numbers of viral particles but of the modification of the structures of these particles rendering them unable to infect cells. Indeed, the process of fusion between the virus and the membrane of CD4 lymphocytes is prevented since gp120, the protein which is essential for the binding to CD4 lymphocyte is misfolded.[110]

---

[103] Saito, T.; Yamaguchi, I. *J. Vet. Med. Sci.* **2000**, *62*, 575-581.
[104] a) Katz, E.; Margalith, E.; Duksin, D. *Antimicrobial Agents Chemotherapy* **1980**, 17, 1014-1022. b) Elbein, A. D. *Ann. Rev. Biochem.* **1987**, *56*, 497-534. c) Schwarz, R. T.; Datema, R. *Adv. Carbohydrate Chem. Biochem.* **1982**, *40*, 287-379.
[105] Sunkara, P. S.; Bowlin, T. L.; Liu, P. S.; Sjoerdsma, A. *Biochem. Biophys. Res. Comm.* **1987**, *148*, 206-210.
[106] a) Karlsson, G. B.; Butters, T. D; Dwek, R. A.; Platt, F. M. *J. Biol. Chem.* **1993**, *268*, 570-576. b) Dedera, D.; Vander Heyen, N.; Ratner, L. *AIDS Res. Hum. Retrovirus* **1990**, *6*, 785-794. c) Karpas, A.; Fleet, G. W.; Dwek, R. A.; Tetursson, S.; Namgoong, S. K. and al. *Proc. Natl. Acad. Sci. USA* **1988**, *85*, 9229-9233.
[107] Walker, B. D.; Kowalski, M.; Goh, W. C.; Kozarsky, K.; Krieger, M.; Rosen, C.; Rohrschneider, L.; Haseltine, W. A.; Sodroski, J. *Proc. Natl. Acad. Sci.* **1987**, *84*, 8120-8124.
[108] Robina, I.; Moreno-Vargas, A. J.; Carmona, A. T.; Vogel, P. *Curr. Drug Metabolism* **2004**, *5*, 329-361.
[109] a) Taylor, D. L.; Nash, R.; Fellows, L. E.; Kang, M. S.; Tyms, A. S. *Antiviral Chem. Chemother.* **1992**, *3*, 273-277. b) Fischer, P. B.; Collin, M.; Karlsson, G. B.; James, W.; Butters, T. D.; Davis, S. J.; Gordon, S.; Dwek, R. A.; Platt, F. M. *J. Virol.* **1995**, *69*, 5791-5797.
[110] Dwek, R. A.; Butters, T. D.; Platt, F. M.; Zitzmann, N. *Nat. Rev. Drug Discov.* **2002**, *1*, 65-75.

Side effects such as diarrhea and problems in achieving therapeutic serum concentrations of Bu-DNJ needed to inhibit α-glucosidase I in humans may limit the practical use of this drug as an anti-HIV agent.[111]

Clinical trials combining Bu-DNJ (**24**) and zidovudine a nucleotide analogue (**25**, AZT, Scheme 23)[112] in a double-blind, randomized, multi-site Phase II study of 118 patients suggested that Bu-DNJ presents an anti-HIV activity. Nevertheless, diarrhea limited the maximum dose tolerated and precluded its use as an anti-HIV agent. To avoid this problem, the Bu-DNJ tetrabutanoate commercialized under the name glycovir (**27**, Scheme 24) was developed as a candidate for the treatment of AIDS (acquired immune deficiency syndrome). This prodrug is thought to be converted into the active Bu-DNJ after its passage through the intestine, thus avoiding diarrhea.[113] Other prodrug forms of Bu-DNJ, such as perbutyrylated ester, have been prepared to reduce gastrointestinal toxicity.[114]

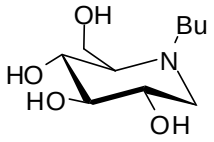

N-Butyl-deoxynojirimycin (**24**, Bu-DNJ)
IC_{50} = 56 μM, anti HIV activity [112]

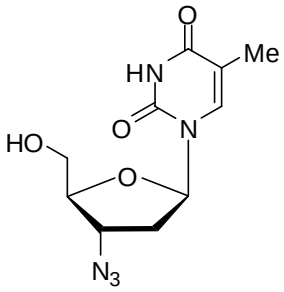

Zidovudine (**25**, AZT®)
IC_{50} = 0.1 μM, anti HIV activity [112]

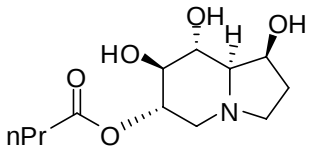

6-O-Butanoylcastanospermine (**26**, Bu-Cast)
IC_{50} = 1.1 μM, anti HIV activity [112]

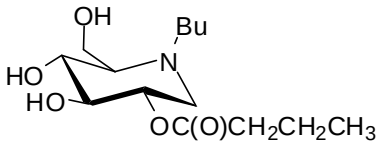

(**27**, Glycovir®)

Scheme 23: Structures of anti-HIV agents.

Another α-glucosidase inhibitor, currently undergoing Phase I clinical trials against HIV is 6-*O*-butanoylcastanospermine (**26**, Bu-Cast, Scheme 23). Its activity was compared with other inhibitors of glycoprotein-processing enzyme such as DNJ (**4**), Bu-DNJ (**24**) and CST (**9**), and

[111] Mehta, A.; Zitzmann, N.; Rudd, P. M.; Block, T. M.; Dwek, R. A. *FESB Lett.* **1998**, *430*, 17-22.
[112] Taylor, D. L.; Sunkara, P. S.; Liu, P. S.; Kang, M. S.; Bowlin, T. L.; Tyms, A. S. *AIDS* **1991**, *5*, 693-698.
[113] Cook, C. S.; Karabatsos, P. J.; Schoenhard, G. L.; Karim, A. *Pharm. Res.* **1995**, *12*, 1158-1164.
[114] Fischl, M. A.; Resnick, L.; Coombs, R.; Kremer, A. B.; Pottage, J. C.; Fass, R. J.; Fife, K. H.; Powderly, W. G.; Collier, A. C.; Aspinall, R. L. *J. Acquir. Immun. Defic. Syndr.* **1994**, *7*, 139-147.

compound **26** was the most potent against HIV.[112] An additional study reported that Bu-Cast was about 30 fold more potent than the parent CST for the inhibition of HIV replication in CD4+ T lymphocytes and for the inhibition of glycoprotein processing. This improved activity *in vitro* is probably the result of enhanced cellular uptake, suggesting that Bu-Cast may be hydrolyzed intracellularly to castanospermine through the action of cellular esterases.[115]

The treatment of the influenza virus can be achieved by zanamivir (**28**, Relenza®, Scheme 24) and oseltamivir (**29**, Tamiflu®, Scheme 24) which are neuraminidase inhibitors. After replication of the virus in the host cell, the virus binds to an inside cell-membrane glycoprotein containing a sialic acid (SA). The viral neuraminidase, found on the surface of the virus, cleaves this SA residue and enables the progeny virion to leave the infected cells. Thus, by blocking the release of the newly formed viral particles, neuraminidase inhibitors prevent further spread of the virus.[116] Both compounds **28** and **29** have been found to be highly potent inhibitors of the influenza neuraminidase and to inhibit influenza A and B virus infection in humans for both prophylactic and therapeutic treatments.[117] Zanamivir has low bioavailability and is administrated by inhalation, which can cause problems in patients with underlying respiratory disease. In contrast, the more lipophilic prodrug oseltamivir has a very high oral bioavailability and is readily absorbed from the gastrointestinal tract, converted by hepatic esterase to the active form of the compound and is finally distributed in the body. [118] Presently, the only potential drug for the pandemic threat of H5N1 influenza is oseltamivir, administrated in capsule.[119]

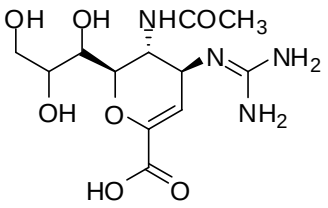

(**28**, Zanamivir, Relenza®)
< 1ng/ml, Influenza A, B, neuraminidase [117]

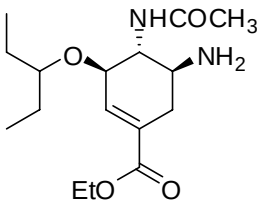

(**29**, Oseltamivir, Tamiflu®)
< 1ng/ml, Influenza A,B, neuraminidase [117]

Scheme 24: Neuraminidase inhibitors as antiviral agents.

[115] Taylor, D. L.; Kang, M. S.; Brennan, T. M.; Bridges, C. G.; Sunkara, P. S.; Tyms, A. S. *Antimicrob. Agents Chemotherapy* **1994**, *38*, 1780-1787.
[116] Moscona, A. *N. Engl. J. Med.* **2005**, *353*, 1363-1373.
[117] de Clercq, E. *Nature Rev. Drug Discovery* **2006**, *5*, 1015-1025.
[118] Farina, V.; Brown, J. D. *Ange. Chem. Int.* **2006**, *45*, 7330-7334.
[119] Wei, D.-Q.; Du, Q.-S.; Sun, H.; Chou, K.-C. *Bio. Biophys. Res. Comm.* **2006**, *344*, 1048-1055.

1.6.2. Therapeutic applications related to cancer treatment

1.6.2.1. Glycosylation and cancer

Glycosylation has been documented for human cancer, and it has been found that both catabolic and glycoprotein-processing glycosidases are involved in the transformation of normal cells to cancer cells. Glycans expressed by diseased cells are displayed at different levels or with different structures than by normal cells.[120] Many tumor cells display aberrant glycosylation due to an altered expression of glycosyltransferases.[121] It has also been known for a long time that the levels of glycosidases are elevated in the serum of many patients with various tumors,[122] and some secreted glycosidases are involved in the degradation of the extracellular matrix in tumor cell invasion.[123] Consequently, these enzymes constitute valuable targets for cancer treatment. In addition, alteration in the protein folding in tumor cells results in the destabilization of the tertiary structure, defects in glycoprotein recognition and thus elimination by the cell quality control.[124] This mechanism can be detrimental for the tumor cell and induce its elimination by the organism or beneficial and promote tumor progression.

Glycans are involved in many steps of the metastasis which is the primary cause of morbidity and mortality in cancer patients. For metastasis to occur, a number of highly specialized events must happen, including detachment from the original tumor, invasion through the extracellular matrix (ECM) and into the vascular or lymphatic system, extravasation from the vessel into the host tissue, and proliferation to a secondary site (Scheme 25).[125] Several critical steps in this metastatic cascade depend on cell-to-cell or cell-to-matrix interactions that involve cell surface molecules. Consequently, changes in oligosaccharides structures on the cell surface may have a strong influence on the behaviour of malignant cells.[126]

---

[120] Dube, D. H.; Bertozzi, C. R. *Nat. Rev. Drug Discov.* **2005**, *4*, 477-488.
[121] Hakomori, S.-I. *Cancer Res.* **1985**, *45*, 2405-2414.
[122] Woollen, J. W.; Turner, P.; *Clin. Chim. Acta* **1965**, *12*, 671-683.
[123] Bernacki, R. J.; Niedbala, M. J.; Korytnyk, W.; *Cancer Metastasis Rev.* **1985**, *4*, 81-101.
[124] Dennis, J. W.; Granovski, M.; Warren, C. E. *BioEssays* **1999**, *21*, 412-421.
[125] Fuster, M. M.; Esko, J. D.; *Nat. Rev. Drug Discov.* **2005**, *5*, 526-542.
[126] a) Hakomori, S.-I. *Cancer Res.* **1996**, *56*, 5309-5318. b) Roberts, J. D.; Klein, J.-L. D.; Palmantier, R.; Dhume, S. T.; George, M. D.; Olden, K. *Canc. Detect. Prev.* **1998**, *22*, 455-462.

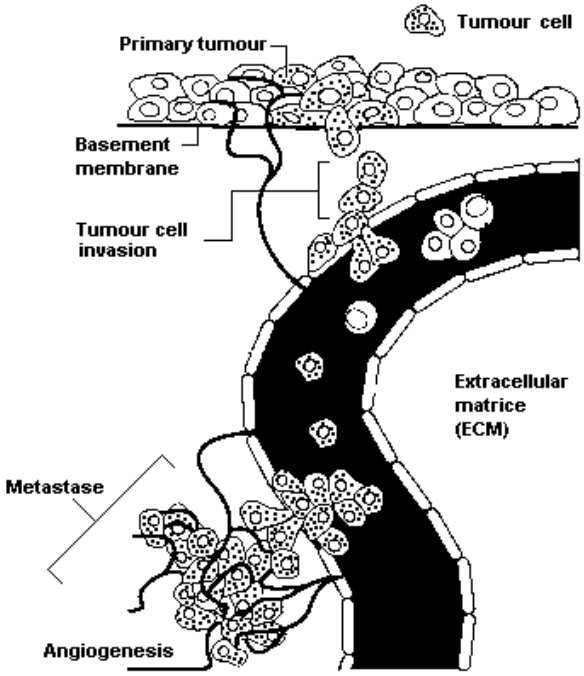

Scheme 25: Metastasis cascade.

Most classes of glycans exist as membrane-bound glycoconjugates or as secreted molecules, which can become integral parts of the ECM. These locations place glycans in a position to mediate cell adhesion and motility, as well as intracellular signalling events.[127]

In the tumor environment, changes in glycosylation allow neoplastic cells to mimic many of the events that occur during the development which allows tumor cells to invade and spread throughout the organism.[128] Examples of the importance of glycans are described below according to the main stages of tumor progression.

During tumor invasion, tumor cells detach one from another and from the ECM and migrate through neighbouring tissue.[129] Tumors also generate glycoconjugates that appear to serve a repulsive role, physically facilitating the detachment of invasive cells from the primary tumor. Indeed, tumor cells tend to produce increased levels of glycoconjugates containing sialic acid, an acidic sugar that imparts a negative charge to the glycans chains. The formation and the

[127] Varki, A.; Cummings, R.; Esko, J.; Freeze, H.; Hart, G.; Marth, J. *Essentials of Glycobiology*, Published by Cold Spring Harbor Laboratory Press, **1999**, 515-536.
[128] Varki, A.; Cummings, R.; Esko, J.; Freeze, H.; Hart, G.; Marth, J. *Essentials of Glycobiology*, Published by Cold Spring Harbor Laboratory Press, **1999**, 537-549.
[129] Nicolson, G. *Cancer Metastasis Rev.* **1988**, *7*, 143-188.

overexpression of polysialic acid occur in some tumor cells.[130] Enhanced sialic acid expression might promote cell detachment from the tumor mass through charge repulsion, which physically inhibits cell-cell apposition. Polysialylation is often associated with the increased invasive potential of tumor cells and its expression correlates with poor prognosis. Inhibitors of specific enzymes of the tumor cell glycosylation pathways could avoid this polysialylation and thus prevent detachment of tumor cells.

Invasion by tumor cells also involves the alteration of cell-matrix interactions, which are mediated by adhesion molecules present on the tumor cells that bind to ECM components. Malignant cells commonly exhibit increased expression of complex β1,6-branched *N*-linked glycans on their surface, caused by an increase in the expression of the enzyme *N*-acetylglucosamine transferase V (GlcNAcTV).[131] In the Golgi, this enzyme transfers a GlcNAc residue onto growing *N*-linked glycans so that subsequent glycosylation results in "multi-antennary" chains.[132] In tumor cells, the presence of such complex β1,6-glycans on E-cadherin, an adhesion molecule that mediates cell aggregation, reduces tumor cell-cell adhesion.[133] Therefore, increased expression of this enzyme by tumor cells promotes detachment and invasion. The same strategy occurs with integrins. The biological role of these adhesion molecules is modified by tumor cells through an altered glycosylation. Integrins represent a crucial class of cell-surface adhesion receptors that mediate attachment to important ECM protein ligands such as fibronectin and laminin. Increased GlNAcTV expression results in increased β1,6-glycans on integrins which disrupts the ability of integrins to bind ECM proteins. This alteration also increases tumor motility through the ECM as well as invasion across basement membranes.[134] Alteration of this abnormal glycosylation process with inhibitors of glycosidases that may act before the GlNAcTV would prevent the invasion of tumor cells and thus control cancer progression.

[130] a) Seidenfaden, R.; Krauter, A.; Schertzinger, F.; Gerardy-Schahn, R.; Hildebrandt, H. *Mol. Cell. Biol.* **2003**, *23*, 5908-5918. b) Dennis, J. W.; Pawling, J.; Cheung, P.; Partridge, E.; Demetriou, M. *Biochim. Biophys. Acta* **2002**, *1573*, 414-422.
[131] Dennis, J. W.; Granovsky, M.; Warren, C. E. *Biochim. Biophys. Acta* **1999**, *1473*, 21-34.
[132] a) Goss, P. E.; Baker, M. A.; Carver, J. P.; Dennis, J. W. *Clin. Cancer Res.* **1995**, *1*, 935-944. b) Varki, A.; Cummings, R.; Esko, J.; Freeze, H.; Hart, G.; Marth, J. *Essentials of Glycobiology*, Published by Cold Spring Harbor Laboratory Press, **1999**, 85-100.
[133] Yoshimura, M.; Ihara,Y.; Matsuzawa, Y.; Taniguchi, N. *J. Biol. Chem.* **1996**, *271*, 13811-13815.
[134] Guo, H. B.; Lee, I.; Kamar, M.; Aklyama, S. K.; Pierce, M. *Cancer Res.* **2002**, *62*, 6837-6845.

1.6.2.2. Glycosidase inhibitors as potent anti-cancer agents

Therapeutic targeting of the altered glycosylation pathways of tumor cells should be considered as anti-proliferative approaches. For example, the blockage of tumor *N*-glycosylation through the inhibition of GlcNAcTV and the blockage of sialylation pathways might offer promising strategies.[135] Nevertheless, there have been no specific inhibitors of GlcNATV reported so far. On the other hand, isoenzymes ST8SiaII and ST8SiaIV that catalyses the synthesis of polysialic acid in mammalian cells can be inhibited using synthetic sialic acid precursors.[136] But the use of these agents *in vivo* has not been reported yet. These two strategies still need further investigation to be validated.

However, the use of glycosidase inhibitors has recently appeared as a promising approach to treat cancers.[137] Transferases, α-glucosidases and α-mannosidases are the most relevant targets in the field of cancer for the development of cellular glycosidases inhibitors.

Tunicamycin (**1**), which inhibits the first step of *N*-oligosaccharides biosynthesis, has been shown to exhibit antimetastatic activity by reducing the adhesion of tumor cells to the vascular endothelium.[138] Moreover, TM significantly enhanced *in vitro* the sensitivity of head and neck carcinoma cells to cisplatin (cis-diaminedichloroplatinum(II)) a drug widely used to treat different cancers including testicular, head and neck, bladder and lung cancer. Furthermore, *in vivo* administration of TM in combination with cisplatin significantly inhibited local tumor growth and increased apoptosis of cisplatin-resistant tumor cells as compared to cisplatin alone.[139]

[135] Granovsky, M.; Fata, J.; Pawling, J.; Muller, W. J.; Khokha, R.; Dennis, J. W. *Nature Med.* **2000**, *6*, 306-312.
[136] Horstkorte, R.; Mühlenhoff, M.; Reutter, W.; Nöhring, S.; Zimmermann-Kordmann, M.; Gerardy-Schahn, R. *Exp. Cell. Res.* **2004**, *298*, 268-274.
[137] Humphries, M. J.; Olden, K. *Pharmac. Ther.* **1989**, *44*, 85-105.
[138] Humphries, M. J.; Matsumoto, K.; White, S. L.; Olden, K. *Cancer Res.* **1986**, *46*, 5215-5222.
[139] Noda, I.; Fujieda, S.; Seki, M.; Tanaka, N.; Sunaga, H.; Ohtsubo, T.; Tsuzuki, H.; Fan, G.-K.; Saito, H. *Int. J. Cancer* **1999**, *80*, 279-284.

Castanospermine (**8**), which is a potent inhibitor of α-glucosidase I, was tested for its potency to inhibit the ability of metastatic cells to cause platelet aggregation. Spearman and al. developed a series of T24-H-ras-transformed 10T1/2 fibroblasts, which display varying metastatic potential to form lung tumors when injected into the tail vein of syngeneic mice. When grown in the presence of CST (50 μM) and injected in mice, a significant reduction in their ability to aggregate platelets was observed and correlated with the ability of CST to inhibit tumor lung colonization by the treated cells.[140]

Other *in vivo* experiments with CST resulted in significant inhibition of tumor growth in nude mice. Indeed, tumor growth inhibition in animals treated with CST was about 50% less than in control animals when measured 13 days after treatment. However, little or no regression was observed when animals, treated with CST, were bearing large tumors (> 1cm). Since angiogenesis is an important contributor to tumor growth, the effect of CST on neovascularisation *in vivo* was assessed. Control animals exhibited a strong angiogenic response with abundant vessels while CST-treated animals showed significantly less vascularisation when injected with 50 mg CST/mouse/day. Moreover, in endothelial cells grown *in vitro*, CST or Me-DNJ (**5**) prevented capillary-like structure formation. Indeed, the ability of endothelial cells to adhere to extracellular matrix proteins was retained but CST- or Me-DNJ-treated cells exhibited increased cell aggregation and reduced cell migration, thus preventing their alignment and organization to form tubular structures. These results suggest that CST and Me-DNJ increased cell-cell adhesion by glycoside-dependent interactions resulting in the blockage of the reorganization of cells into capillary-like networks.[141]

Analogues of the natural ester Sintenin (**30**, Scheme 26), displaying moderate inhibitory activity toward α-glucosidase, exhibited significant cytoxicity toward human tumor cell lines from hepatocellular, nasopharyngeal, lung, prostate and cervical (adeno)carcinoma.[142]

[140] Spearman, M. A.; Ballon, J. M.; Gerrard, J. M.; Greenberg, A. H. Wright, J. A. *Cancer Lett.* **1991**, *60*, 185-191.
[141] Pili, R.; Chang, J.; Partis, R. A.; Mueller, R. A.; Chrest, F. J.; Passaniti, A. *Cancer Res.* **1995**, *55*, 2920-2926.
[142] Hu, L. H.; Zou, H. B.; Gong, J. X.; Li, H. B.; Yang, L. X.; Cheng, W.; Zhou, C. X.; Bai, H.; Guéritte, F.; Zhao, Y. *J. Nat. Prod.* **2005**, *68*, 342-348.

Streptozotocin (**31**, STZ, Scheme 26), a β-glycosidase inhibitor increased median survival of patients with metastatic pancreatic carcinoma of 64 weeks in combination with 5-fluorouracil. In combination with 5-fluorouracil and mitomycin, **31** increased median survival for 10 months.[143] STZ has been approved by the FDA (U.S. Food and Drug Administration) for treating metastatic cancer of pancreatic islet cells. Since the drug caries a substantial risk of side effects, due its toxicity against the insulin-producing beta cells of the pancreas, its use is generally limited to patients that can not be treated by other drugs.[144]

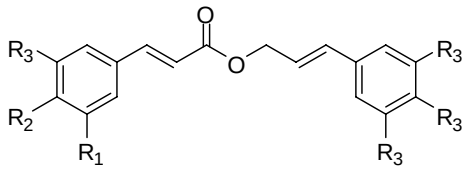

R_1	R_2	R_3	IC_{50}	Enzyme [Ref]
OMe	OMe	OMe	110 μM	α-glucosidase [142]
H	OH	H	65 μM	α-glucosidase [142]
OH	OH	H	97 μM	α-glucosidase [142]

Analogues of Sintenin (**30**)

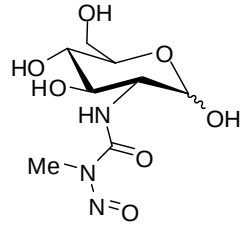

Streptozotocin (**31**)

Scheme 26: Anti-cancer agents based on glycosidase inhibition.

Although a number of polyhydroxylated alkaloids have been reported to show anti cancer activity, research has concentrated on the development of Swa (**16**, Scheme 20) as a drug candidate for the management of human malignancies. Experiments have shown that Swa has a complex mode of action such as inhibiting the growth of tumor cells, preventing the dissemination of malignant cells from the primary tumor to secondary sites and stimulating effect of the immune system.[145] Theses point will be discussed more in details below.

[143] Bukowski, R. M.; Schacter, L. P.; Groppe, C. W.; Hewlett, J. S.; Weick, J. K.; Livingston, R. B. *Cancer* **1982**, *50*, 197-200.
[144] Schnedl, W. J.; Ferber, S.; Johnson, J. H.; Newgard, C. B. *Diabetes* **1994**, *43*, 1326-1333.
[145] Olden, K.; Breton, P.; Grzegorzewski, K,; Yasuda, Y.; Gause, B. L.; Oredipe, O. A.; Newton, S. A.; White, S. L. *Pharmacol. Ther.* **1991**, *50*, 285-290.

The effect of Swa on different human cancer cell lines was evaluated. Treatment of human hepatoma cells with Swa resulted in an accelerated secretion of hybrid forms of the glycoproteins transferin, ceruloplasmin, α2-macroglobulin and α1-antitrypsin, whereas the secretion of non-glycoproteins was not affect. Moreover, the transport of these hybrid glycoproteins through the Golgi apparatus was faster than the transport of normal glycoproteins.[146] These results highlight the capacity of Swa to modify the metabolism of glycoproteins and thus their biological activity.

The decrease of tumor cell proliferation by Swa seems to be related to its activity on the inhibition of the processing of asparagine-linked oligosaccharides. Indeed, neoplastic transformation in both human and rodent tumor cells is often accompanied by increasing expression of β-1,6-branched oligosaccharides.[147] Swa is known to block the expression of complex-type oligosaccharides in malignant cells by its ability to inhibit Golgi α-mannosidase II.[15b] It seems that loss or truncation of β-1,6-branched oligosaccharides in metastatic tumor cells reduces cell motility by increasing cell adhesion.[148] *In vitro*, Swa increased the adhesion of bladder cancer cells to laminin, collagen IV and fibronectin.[149] Consequently, Swa reduced their capacity to invade other tissues and also reduced solid tumor growth.

Using Swa, Humphries and al. tested the hypothesis that specific glycans structures are required for pulmonary colonization by tumor cells. B16-F10 murine melanoma cells were treated with Swa in growth medium and then injected intravenously into syngeneic C57BL/6 mice. This treatment resulted in dramatic inhibition of colonization, but it had no effect on B16-F10 viability or tumorigenicity after subcutaneous implantation. Swa-treated radiolabeled B16-F10 cells were cleared from the lungs at a greater rate than control cells, suggesting that one effect of the treatment is to alter tumor cell retention in the target organ. These results implicate specific glycans structures in pulmonary colonization involved in tumor cell-organ recognition during metastasis.[150] Similarly, both the lymphoid tumor cell line MDAY-D2 and B16-F10 melanoma cells were less metastatic when grown in Swa (0.3 μg/ml) for 48 hours prior to injection of the cells into the lateral tail veins of mice.

---

[146] Yeo, T.-K.; Yeo, K.-T.; Parent, J. B.; Olden, K. *J. Biol. Chem.* **1985**, *260*, 2565-2569.
[147] Pierce, M.; Arango, J. *J. Biol. Chem.* **1986**, *261*, 10772-10777.
[148] Dennis, J. W.; Koch, K.; Yousefi, S.; VanderElst, I. *Cancer Res.* **1990**, *50*, 1867-1872.
[149] Przybylo, M.; Litynska, A.; Pochec, E. *Biochimie* **2005**, *87*, 133-142.
[150] Humphries, M. J.; Matsumoto, K.; White, S. L.; Olden, K. *Proc. Natl. Acad. Sci. USA* **1986**, *83*, 1752-1756.

Furthermore, the addition of Swa (2.5 μg/ml) to the drinking water of the mice further reduced the incidence of lung colonization by B16-F10 melanoma cells.[151] In experimental murine cancer models, administration of Swa in drinking water, before or after surgical excision of the primary tumor, inhibited by 95 and 88% the formation of spontaneous metastases to the liver and lungs of the highly invasive M5076 murine reticulosarcoma or B16-F10 murine melanoma cells.[145]

There is also considerable evidence that Swa enhances the natural antitumor defences of the body.[152] This information comes from the ability of Swa to activate immune effector cells such as natural killer cells,[153] T-lymphocytes and macrophages.[154] It seems that the anti-tumor properties of these cells are apparent only after they have been activated. Swa can also induce tumouricidal activity in resident tissue macrophages of both the lung and spleen, their activation being both time- and dose-dependent.[154b] This is relevant to the clinical management of metastatic diseases since visceral organs are common sites of metastasis.

Since all cellular glycoproteins which normally express complex-type oligosaccharides are affected by Swa treatment, investigations were carried out to determine whether the effects of Swa on cellular proliferation could be widespread amongst non-transformed tissues in the body. These studies showed that the effects of this compound would appear to be cell-specific, since it does not equally affect the processing of all glycoproteins.[155] Moreover, the systemic administration of high doses of Swa to sheep induces mannosidosis.[156] However, no evidence of an overt toxic reaction was observed when Swa was administrated orally to rodents[157] so it was considered that the mannosidosis induced by Swa could be species- or tissue specific phenomena.[158]

[151] Dennis, J. W. *Cancer Resarch* **1986**, *46*, 5131-5136.
[152] Kino, T.; Inamura, N.; Nakahara, K.; Kiyoto, S.; Goto, T.; Terano, H.; Kohsaka, M.; Aoki, H.; Imanaka, H. *J. Antibiot.* **1985**, *38*, 936-940.
[153] Humphries, M. J.; Matsumoto, K.; White, S. L.; Molyneux, R. J.; Olden, K. *Cancer Res.* **1988**, *48*, 1410-1415.
[154] a) White, S. L.; Nagai, T.; Akiyama, S. K.; Reeves, E. J.; Grzegorzewski, K.; Olden, K. *Cancer commun.* **1991**, *3*, 83-91. b) Das, P. C.; Roberts, J. D.; White, S.; Olden, K. *Oncology research* **1995**, *7*, 425-433.
[155] Spearman, M. A.; Damen, J. E.; Kolodka, T.; Greenberg, A. H.; Jamieson, J. C.; Wright, J. A.; *Cancer Lett.* **1991**, *57*, 7-13.
[156] Huxtable, C. R.; Dorling, P. R. *Am. Assoc. Pathol.* **1982**, *107*, 124-126.
[157] Huxtable, C. R.; Dorling, P. R. *Acta Neuropathol.* **1985**, *68*, 65-73.
[158] Tulsiani, D. R. P.; Touster, O. *J. Biol. Chem.* **1987**, *262*, 6506-6514.

These results were so encouraging that the efficacy of Swa was examined in phase I clinical trials in humans with advanced malignancies. In the first study, Swa was administrated to nineteen terminally-ill cancer patients with leukemia, breast, colon, lung, pancreatic, or head and neck cancers by continuous intravenous infusion over 5 days in the dose range from 50 to 550 μg/kg/day, repeated at once 28 days intervals. The serum concentrations of this drug reached 3 to 11.8 mg/l which is 100 to 400 times greater than the 50% inhibitory concentration for Golgi α-mannosidase II and lysosomal α-mannosidase.[159] Nevertheless, the patients had elevated levels of the liver enzyme aspartate aminotransferase in the serum that was indicative of hepatic toxicity and they also suffered from pulmonary and peripheral oedema. However, the patients with head and neck cancer presented a decrease of the tumor progression and two others showed symptomatic improvement.[160] A second clinical trial was undertaken to evaluate Swa by oral administration twice a week (dose range 50 to 600 μg/kg) to sixteen patients with advanced malignancies. Serum drug levels peaked 3 to 4 hours following a single oral dose. The maximum dose tolerated was found to be 300 μg/kg/day due to an increased level of aspartate aminotransferase in the serum and dyspnea similar to that observed in the previous trial.[161] Other side effects were observed included fatigue, anorexia, abdominal pain and neurological symptoms.

Seventeen patients with locally advanced or metastatic kidney carcinoma were enrolled in a phase II trial to assess the efficacy of oral chronic administration of GD0039 (Hydrochloride salt of Swa). Unfortunately, no evidence of anti-tumor activity of GD0039 was seen in this study and the seventeen patients discontinued the treatment due to toxicity.[162] Adverse events such as fatigue, anorexia, nausea and diarrhea were also observed.

In order to avoid these side effects, analogues of Swa with substituents at C(3) position have been synthesized in order to improve the selectivity for Golgi α-mannosidase II over lysosomal α-mannosidase (**32-35**, Scheme 27) which are class II retaining enzymes with high sequence homology.[163] These new derivatives, with α-oriented substituents (**32, 34**), were more potent inhibitors than the corresponding β-analogues (**33, 35**), which is consistent with

[159] Baptista, J. A.; Goss, P.; Nghiem, M.; Krepinsky, J. J.; Baker, M.; Dennis, J. W. *Clin. Chem.* **1994**, *40*, 426-430.
[160] Goss, P. E.; Baptiste J.; Fernandes, B.; Baker, M.; Dennis, J. W. *Cancer Res.* **1994**, *54*, 1450-1457.
[161] Goss, P. E.; Reid, C. L.; Bailey, D.; Dennis, J. W. *Clin. Cancer. Res.* **1997**, *3*, 1077-1986.
[162] Shaheen, P. E.; Stadler, W.; Elson, P.; Knox, J.; Winquist, E.; Bukowski, R. M. *Invest. New Drugs* **2005**, *23*, 577-581.
[163] Liao, Y.-F.; Lal, A.; Moremen, K. W. *J. Biol.Chem.* **1996**, *271*, 28348-28358.

the hypothesis that the C(3) substituent mimics the α-oriented carbohydrate that should be hydrolyzed by the α-mannosidase.[164]

Inhibitors with small substituents at C(3) position were not as potent as Swa, however derivatives **32** presented interesting biological properties toward jack bean α-mannosidase as they were more potent inhibitors of this enzyme than Swa. On the other hand, ring-expanded analogues[165] of Swa or derivatives of Swa[166] with substituents at C(6) and C(7) were not active toward the α-mannosidase from jack bean (structures not shown).

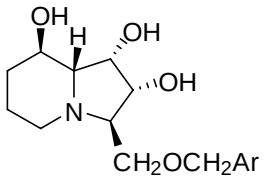

(**32**)

Ar	IC_{50} (jack bean) [164b]
Ph	0.39 μM
2-naphtyl	0.11 μM
4-Ph-Ph	0.08 μM
4-^{t}Bu-Ph	0.05 μM

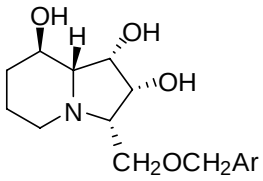

(**33**)

IC_{50} (jack bean) [164b]

100 μM

17 μM

200 μM

> 200 μM

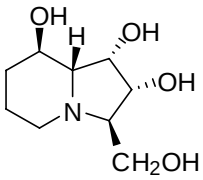

(**34**)

IC_{50} (jack bean) = 1.2 μM [164a]

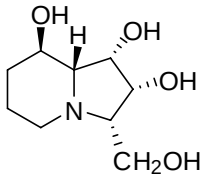

(**35**)

IC_{50} (jack bean) = 45 μM [164a]

Scheme 27: Analogues of Swa with substituents at the C(3) position. IC_{50} toward jack bean α-mannosidase *vs* Swa IC_{50} = 0.4-0.1 μM.

[164] a) Hembre, E. J.; Pearson, W. H. *Tetrahedron* **1997**, *53*, 11021-11032. b) Pearson, W. H.; Guo, L. *Tetrahedron Lett.* **2001**, *42*, 8267-8271.
[165] Pearson, W. H.; Hembre, E. J. *J. Org. Chem.* **1996**, *61*, 5537-5545.
[166] Pearson, W. H.; Hembre, E. J. *Tetrahedron Lett.* **2001**, *42*, 8273-8276.

Esters analogues of Swa have been synthesized to improve the specificity for Golgi α-mannosidase II and/or improve pharmacokinetics in order to enhance anti-tumoral effects and immune stimulatory activity. The results revealed that carbonoyloxy esters of Swa with substitutions at the alcohols on position C(2) and C(8) were 2-3 orders of magnitude less active than Swa as α-mannosidase inhibitors toward jack bean α-mannosidase. *In vivo*, among the various carbonoyloxy analogues of Swa, the 2-octanoyloxy-derivative **39** induced the highest increased rate of survival of mice 28 days after injection, which is similar to the rate obtained with Swa, suggesting that cellular esterases may convert this analogue into Swa inside the cells.[167]

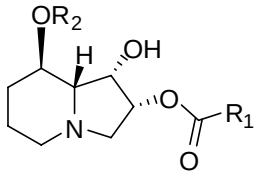

	R_1	R_2	IC_{50} (jack bean) [167]
Swa (**16**)	H	H	0.1 – 0.4 μM
2-benzoyloxy-Swa (**36**)	Bn	H	350 μM
2-toluoyloxy-Swa (**47**)	Bn-CH_3	H	350 μM
2-*p*-nitrobenzoyloxy-Swa (**38**)	Bn-NO_2	H	123 μM
2-octanoyloxy-Swa (**39**)	$(CH_2)_6CH_3$	H	123 μM
2-butanoyloxy-Swa (**40**)	$(CH_2)_2CH_3$	H	123 μM
8-palmitoyloxy-Swa (**41**)	H	$(CH_2)_{14}CH_3$	240 μM
8-myristinoyloxy-Swa (**42**)	H	$(CH_2)_{12}CH_3$	> 500 μM

Scheme 28: Analogues of Swa. IC_{50} toward jack bean α-mannosidase.

[167] Dennis, J. W.; White, S. L.; Freer, A. M.; Dime, D. *Biochem. Pharmacol.* **1993**, *46*, 1459-1466.

The following table (Table 1) summarizes the different inhibitors of glycosidases which have been studied and have shown interesting properties for the treatment of cancer.[168]

Compound (n°) [Ref]	**Targeted glycosidase**	**Type of cancer**	***In vitro*/ *In vivo***	**Results**
TM (**1**) [139]	Inhibition of the biosynthesis of "14 core unit"	Squamous cell carcinoma of head and neck	*In vitro*	Increased sensitivity of carcinoma cells to cis-platin
		Cis-platin resistant mouse model	*In vivo*	Inhibition of local tumor growth by administration of TM and cis-platin
Me-DNJ (**5**) [141]	α-glucosidase I α-glucosidase II	Endothelial cells	*In vitro*	Increased cell aggregation and reduced cell migration
Sintenin analogues (**30**) [142]	α-glucosidase I α-glucosidase II	Hepatocellular, Nasopharyngeal, Lung, Prostate, Cervical carcinoma cells	*In vitro*	Inhibition of growth
CST (**8**) [140,141]	α-glucosidase I	Lung	*In vivo*	Inhibition of platelets aggregation and tumor lung colonization
		Prostate	*In vivo*	Reduction of tumor growth, decrease of blood vessel infiltration
Swa (**16**) [53, 161] [145, 146] [149]	Golgi α-mannosidase II	Melanoma, Reticulocarcinoma,	*In vivo*	Inhibition of lung colonization, inhibition of metastases formation after excision of the primary tumor
		Bladder cells	*In vitro*	Increased adhesion of tumor cells to laminin, collagen IV and fibronectin. Decreased migratory ability
		Advanced tumors	*Phase I*	Reduction of tumor mass
2-carbonoyl-Swa (**38**-**40**) [167]	Poor inhibition of α-mannosidases	Melanoma	*In vivo*	Increased rate of survival 28 days after injection of treated cancer cells
STZ (**31**) [143]	Reduction of β-glycosidase activities in kidney	Carcinoid tumors	*Clinical use*	In combination with 5-florouracil: increased median survival of 64 weeks.
		Pancreatic tumors	*Clinical use*	In combination with 5-florouracil and mitomycin: increased median survival of 10 months.

Table 1: Glycosidase Inhibitors as Potential Anti-cancer agents.

[168] Gerber-Lemaire, S.; Juillerat-Jeanneret, L. *Mini-Rev. Medicinal Chem.* **2006**, *6*, 1043-1052.

Recently the Vogel's group has initiated a search for new potent inhibitors of α-mannosidase II with the hope to uncover a new anti-cancer lead. A combinatorial method was developed for the rapid discovery of inhibitors of α-mannosidase from jack bean (Scheme 29).[169]

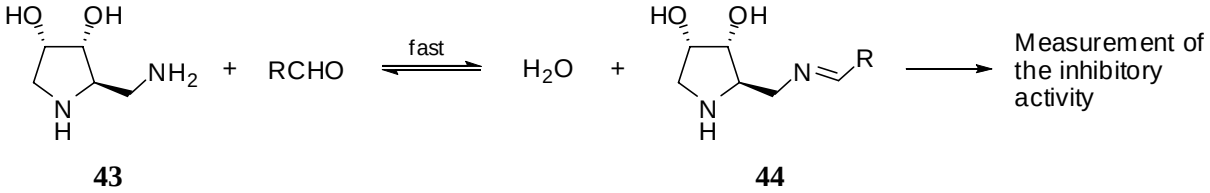

43 **44**

Scheme 29: Combinatorial methodology.

In this approach, amine **43** was mixed with a panel of commercially available aldehydes, in water and at low concentration, then the jack bean α-mannosidase was added to the corresponding imines (**44**) allowing direct measurement of the inhibitory ability of these imines. The equilibrium constant for imine formation from these partners was particularly high, due to an intramolecular promoting effect of the secondary β-amino moiety. It was also established that the imines were valid models of the corresponding diamines for the inhibitory ability.

Thus, this study allowed the determination of the more appropriate side chains to be introduced on the (2*R*,3*R*,4*S*)-2-aminomethylpyrrolidine 3,4-diol core to produce potent inhibitors of α-mannosidase from jack bean. Based on this approach, a new family of selective and competitive inhibitors of α-mannosidases was disclosed with K_i values ranging from 3 μM to 135 nM for the best congeners (**45-47**, Scheme 30).[170]

[169] Gerber-Lemaire, S.; Popowycz, F.; Rodriguez-Garcia, E.; Carmona Asenjo, A.T.; Robina, I.; Vogel, P. *ChemBioChem*. **2002**, 3, 466-470.

[170] a) Popowycz, F.; Gerber-Lemaire, S.; Rodríguez-García, E.; Schütz, C.; Vogel, P. *Helv. Chim. Acta* **2003**, *86*, 1914-1948. b) Popowycz, F.; Gerber-Lemaire, S.; Schütz, C.; Vogel, P. *Helv. Chim. Acta* **2004**, *87*, 800-810.

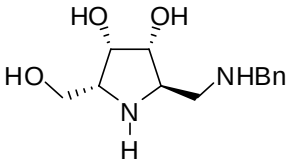

45

IC_{50} = 6.2 μM
K_i = 1.2 μM

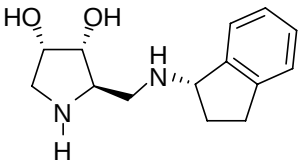

46

IC_{50} = 17 μM
K_i = 2.3 μM

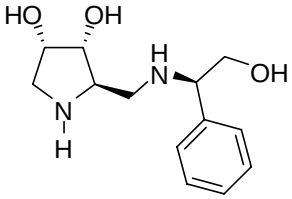

47

IC_{50} = 700 nM
K_i = 135 nM

Scheme 30: Dihydroxypyrrolidine derivatives as potent α-mannosidase inhibitors. IC_{50} toward α-mannosidase from jack bean.

Five membered iminocyclitols bearing hydroxyl groups have been shown to be potent inhibitors of α-mannosidases. The dihydroxypyrrolidine moiety is thought to mimic the shape and charge of the transition state of the reacting sugar moiety (**49**, Scheme 31). This pyrrolidine ring is similar to the oxocarbenium ion-like intermediate (**48**, Scheme 31) but is not hydrolysable due to the stability conferred by the nitrogen atom and thus knocks down the enzyme activity.[171] Furthermore, the five-membered ring confers an additional similitude with the oxocarbenium ion-like intermediate where the region around the cation is planar in contrast with the chair conformation of the sugar. The (3R,4S) configuration of the hydroxyl groups ensures selectivity towards mannosidases because of their similar orientation in space with mannose. On the other hand, a (3S,4R) configuration for example would lead to a selective inhibition of glucosidases.

[171] Popowycz, F.; Gerber-Lemaire, S.; Demange, R.; Rodríguez-García, E.; Carmona Asenjo, A. T.; Robina, I.; Vogel, P. *Bioorg. Med. Chem. Lett.* **2001**, *11*, 2489-2493.

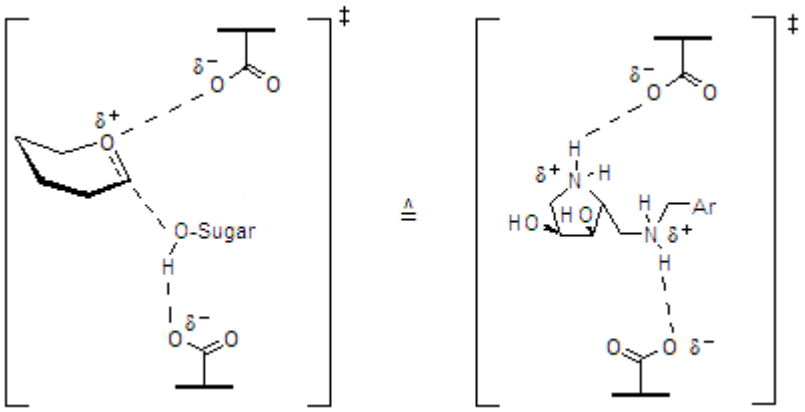

48 **49**

Scheme 31: Supposed interaction of the natural substrate and the inhibitor in the active site of a glycosidase.

Moreover, it has been suggested that the binding of a polyhydroxylated alkaloid to the active site of a glycosidase, protonation of the compound leads to the formation of an ion pair between the inhibitor and a carboxylate anion in the active site of the enzyme. The protonated inhibitor closely resembles the transition state of the natural substrate and hence the enzyme has a high affinity for the molecule. However, the strength of the binding and consequently the effectiveness of the inhibition depend on the ionization state of the inhibitor, dictated by its pKa, and the optimal pH of the enzyme.[172]

[172] Lalegerie, P.; Legler, G.; Yon, J. M. *Biochimie* **1982**, *64*, 977-1000.

2. Aim of the project

In view of the promising inhibitory activities obtained with compound **47** and analogues on α-mannosidase from jack bean and the anticancer properties of Swa, our project aimed at the development of a new family of anticancer agents based on the inhibition of α-mannosidases II.

We were first interested in performing structural analyses with *Drosophila melanogaster* Golgi α-mannosidase II, a reliable model of the human Golgi α-mannosidase II. These data will allow us to understand the binding mode of the first lead inhibitor **47** into the active site of the enzyme and open the door to a docking study to determine adequate computer tools for the prediction of the binding of inhibitors to α-mannosidases II. These analyses will focus our attention on various modifications that can be performed in order to improve the inhibitory activity of pyrrolidine derivatives previously disclosed in Vogel's group. Several chemical transformations such as the introduction of additional substituents on the pyrrolidine ring and derivatization of the primary alcohol will be envisaged (Scheme 32).

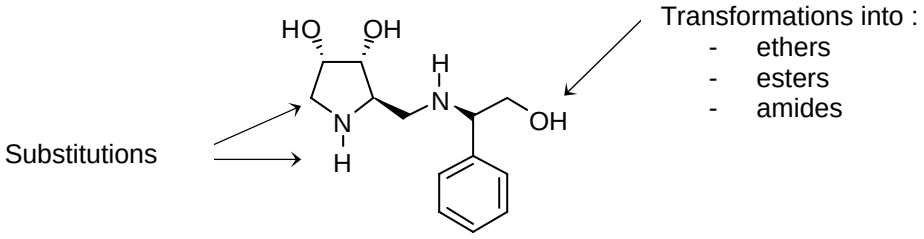

Scheme 32: Functionalization of pyrrolidine **47**.

After these structural modifications, the newly designed derivatives will be evaluated as inhibitors of model and human α-mannosidases II. The most active congeners will be further assessed for their potential anti cancer properties. Various tumoral cells lines will be tested such as glioblastoma (LNZ308 and LN18) and melanoma cells (Me237, Me275). Glioblastomas are associated with a high proliferative and invasive potential, multiple resistance toward conventional chemotherapeutic agents, and poor prognosis. It is thus of high interest to find new molecules that could inhibit the proliferation of these tumours.

The effect of the pyrrolidine derivatives on the growth of cancer cells will be first measured with the MTT ((3,4,5-dimethylthiazol-yl)-2,5-diphenyl tetrazolium) assay, which determines the number of metabolically active cells. For the best inhibitors, we will also determine DNA synthesis inhibition and protein synthesis inhibition by [^{3}H]-thymidine and [^{3}H]-leucine incorporation measurements, respectively. Comparative measurements on healthy cell lines from primary fibroblasts (PO05, PG95) will allow us to determine the selectivity of our derivatives.

3. Results and Discussion

3.1. Binding mode of dGMII:47 complex

In order to determine the different chemical modifications that could enhance the inhibitory ability of pyrrolidine derivative **47**, elucidation of the binding mode of this compound to α-mannosidase II represented the first aim of this study. As previously described, dGMII is a valid model of the structural and functional features of mammalian Golgi α-mannosidase II. In collaboration with the group of Prof. D. Rose (University of Toronto, Canada), we investigated the x-ray structure of the dGMII: **47** complex.[173]

Resolution of the synchrotron collected data at 1.30 Å allowed accurate analysis of the binding mode of **47** to the active site of dGMII as depicted in Scheme 33.

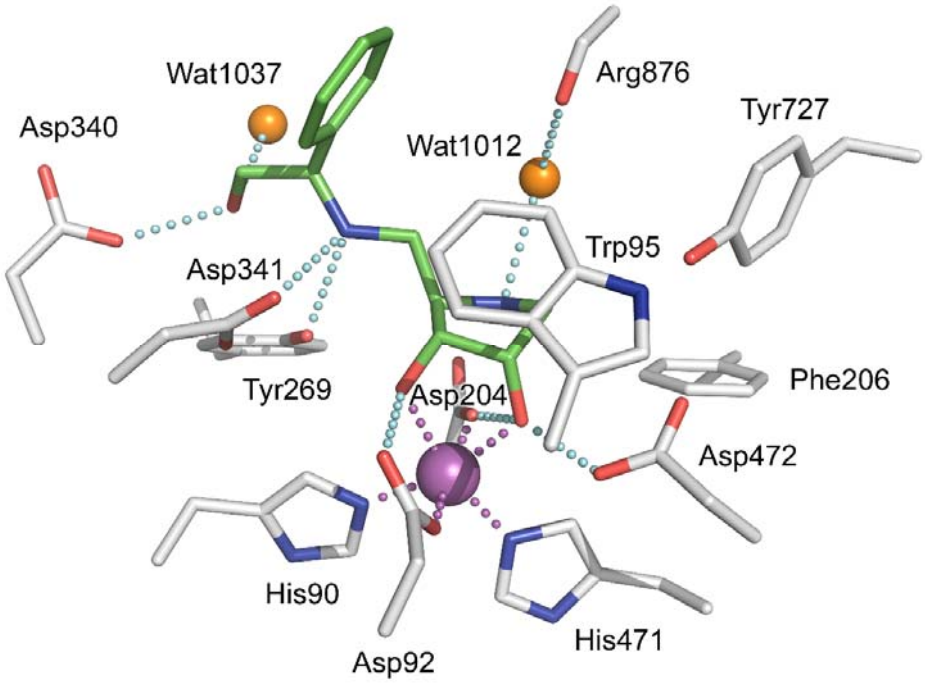

Scheme 33: Crystal structure of compound **47** complexed to dGMII. Interactions closer than 3.2 Å are indicated. The interactions with the zinc atom are drawn in magenta, water molecules appear as orange balls. Distances are presented in Table 3, page 63. The figure was generated with PyMOL.

[173] Measurements performed by Dr. D. Kuntz, University of Toronto, Canada.

The binding of inhibitor **47** in the active site of dGMII is illustrated in Scheme 33 and a list of interactions distance less than 3.2 Å is given in Table 3, page 63. These data revealed tight interactions between the hydroxyl groups at C(3) and C(4) positions of the pyrrolidine ring and the active site zinc which made additional interactions with His90, Asp92, Asp204 and His471. Furthermore, interactions were also revealed between the exocyclic N7 atom in the "tail" region of **47** and Asp341 and Tyr269. Trp95 made two important interactions with the inhibitors: (i) a T-shaped interaction between the aromatic ring of the inhibitor and the indole moiety of Trp95, the two planes being at near right angles of each other and (ii) Trp95 also made π-stacking hydrophobic interactions with the pyrrolidine ring, a common feature of dGMII complexes.

Comparison of dGMII: **47** structure with dGMII:Swa (dGMII:**16**) complex revealed that major changes of the binding modes of these two inhibitors occurred in the interactions of the terminal hydroxyl group (OH-9) of **47** with the active site of dGMII. Furthermore, in the case of Swa, an hydroxyl moiety was engaged in tight interactions with Asp472 and Tyr727. In the case of **47**, the absence of an alcohol group in this region of the active site resulted in a shift of 0.6 Å of the hydroxyl moiety of Tyr727 (Tyr727 OH) toward the hydroxyl moiety of Asp472 OD1 (Table 3, page 63).

This analysis revealed that the inhibitor **47** made numerous interactions with dGMII active site. Nevertheless, the region between Asp472 and Tyr727 should be able to accommodate additional substituents on the C(5) position of the pyrrolidine ring. We thus envisaged the introduction of a methyl group at this position.

3.2. Synthesis and Enzymatic test of 5-methylpyrrolidine-3,4-diol derivatives

The synthetic pathway started from L-5-trityloxymethyl-2-pyrroldinone (**50**) which was converted into the protected diol **51** in five steps following Ikota's methodology[174] with 20% overall yield (Scheme 34). Lactam **51** was treated through a sequence of Grignard addition followed by reduction of the resulting methyl ketone moiety and cyclization in basic medium to afford pyrrolidines **52** and **53**, as a 1:1 mixture of diastereoisomers separable by flash chromatography. On both isomers, the trityl protecting group was removed through Birch reduction,[175] allowing subsequent oxidation of the primary alcohol under Swern[176] or Ley's[177] conditions. The resulting carbaldehydes **54** and **56** were then engaged in a reductive amination procedure in the presence of D-(α)-phenylglycinol and $NaBH(OAc)_3$ for *in situ* reduction of the intermediate imines. Acidic removal of acetonide and carbamate protecting groups afforded **55** and **57** in 73% and 39% yield, respectively (2 steps).

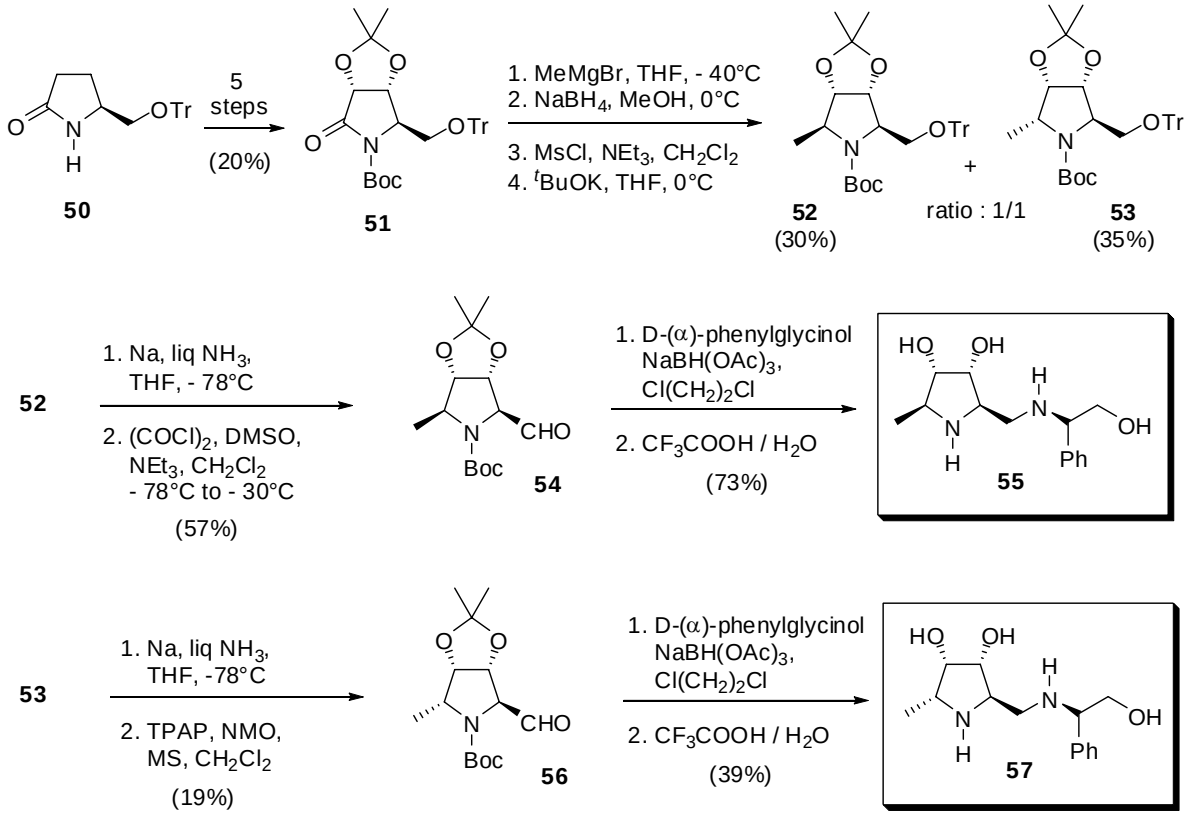

50 **51** **52** (30%) **53** (35%) **54** **55** **56** **57**

Scheme 34: Synthesis of 5-methylpyrrolidine-3,4diol derivatives.

[174] Ikota, N.; Hanaki, A. *Chem. Pharm. Bull.* **1989**, *4*, 1087-1089.
[175] Birch, A. J.; Nasipuri, D. *Tetrahedron* **1959**, *6*, 148-153.
[176] Mancuso, A. J.; Swern, D. *Synthesis* **1981**, *3*, 165-185.
[177] Ley, S. V.; Norman, J.; Griffith, W. P.; Marsden, S.P. *Synthesis* **1994**, *7*, 639-666.

The inhibitory ability of **55** and **57** was evaluated on dGMII[178] and on 16 commercially available glycosidases:[179] α-L-fucosidase (bovine kidney), two α-galactosidases (coffee beans and *Escherichia coli*), three β-galactosidases (*Escherichia coli*, bovine liver and *Aspergillus orizae*), two α-glucosidases (yeast and rice), two amyloglucosidases (*Aspergillus niger* and *Rhizopus mold*), β-glucosidase (almonds), α-mannosidase (jack beans), β-mannosidase (*Helix promatia*), β-xylosidase (*Aspergillus niger*) and two β-N-acetylglucosaminidases (jack beans and bovine kidney) at the optimal pH value of each enzyme. The collected data were compared to the inhibitory ability of compound **47** (Table 2).

		47[180]	**55**	**57**
β-glucosidase (almonds)	Inhibition (%) at 1mM	93%	n.i.	94%
	IC_{50}	46 μM	n.d.	40 μM
	K_i	9.5 μM	n.d.	n.d.
α-mannosidase (jack bean)	Inhibition (%) at 1mM	100%	n.i.	80%
	IC_{50}	700 nM	n.d.	134 μM
	K_i	135 nM	n.d.	53 μM
α-mannosidase (dGMII)	IC_{50}	80 μM	2-3 mM	1mM

n.i. = no inhibition n.d. = not determined

Table 2: Inhibitory ability of derivatives **47**, **56** and **57**.

Pyrrolidine derivative **55** did not display any inhibitory ability toward all the tested glycosidases. The other isomer **57** displayed about 200 times less inhibitory ability against α-mannosidase from jack bean than compound **47** (IC_{50} = 134 μM for **57** *vs* 0.7 μM for **47**) and was also less efficient toward dGMII (IC_{50} = 1 mM for **57** *vs* 0.08 mM for **47**). The introduction of a methyl group at C(5) position of the pyrrolidine ring was thus highly detrimental for the inhibition of α-mannosidases. As for compound **47**, the other enzymes were not affected by **57** except β-glucosidase from almonds (IC_{50} = 40 μM).

[178] Enzymatic assays performed according to the procedure described in Kuntz, D. A.; Ghavami, A.; Johnston, B. D.; Pinto, B. M.; Rose, D. R. *Tetrahedron: Assymetry* **2005**, *16*, 25-32.
[179] Enzymatic assays performed by Catherine Schütz, EPFL.
[180] Popowycz, F. These de doctorat n° 2866, EPFL, **2003**.

3.3. X-ray analysis of substituted pyrrolidine derivatives

This new substituted pyrrolidine derivative was also complexed to dGMII and the resulting crystal structure was analyzed by x-ray. A similar study was carried out on compound **58**, a stereoisomer of compound **47**.

A)

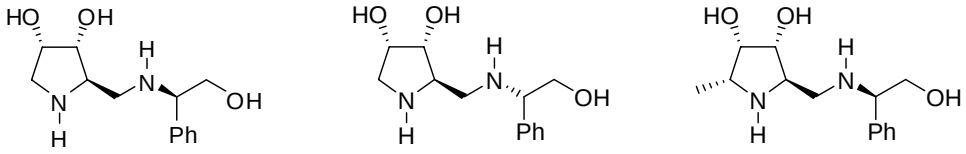

	47	**58**	**57**
IC_{50} dGMII (μM):	80	720	1000

B)

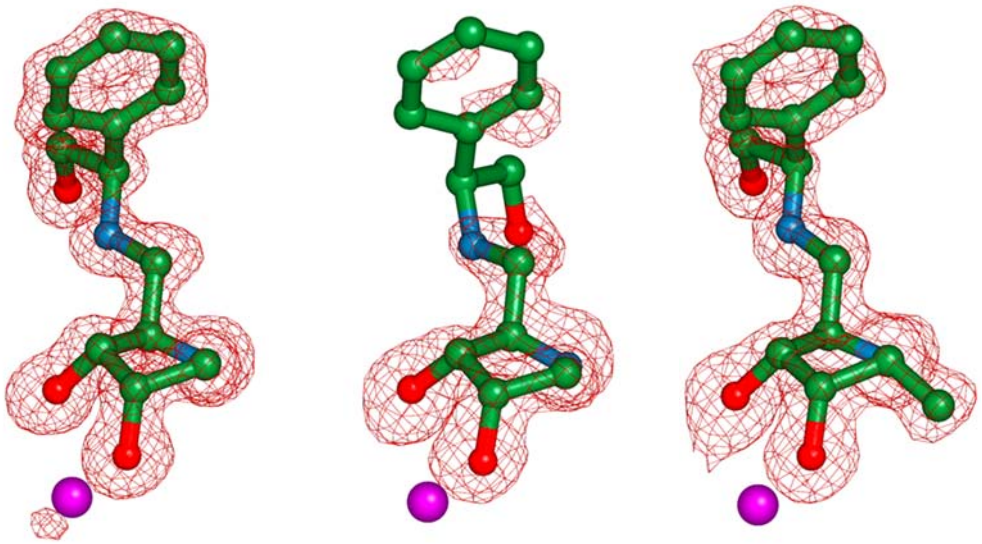

PDB code:	2F18	2F1A	2F1B
Resolution (Å):	1.30	1.45	1.45

Scheme 35: **A**) Structures of the three hydroxypyrrolidines crystallized in the active site of dGMII and their inhibitory ability (IC_{50}) toward dGMII. **B**) Electron density representation of the inhibitors, PDB code and Resolution. The active site zinc ion is represented by the magenta ball.

Scheme 35 shows the accuracy of the electron density around the bound pyrrolidine inhibitors. The density of **47** and **57** was much cleaner in the "tail" region of the aromatic ring than the similar region for inhibitor **58**. Indeed, the tail region of **58** was not clearly defined in the electron density which means that this region is an unfavourable location, and may be oscillating between several positions. Furthermore, this lack of good density correlated well with the lowest inhibitory ability of **58** (IC_{50} = 720 μM *vs* 80 μM for **47**).

Inhibitors **47** and **57** exhibited virtually identical binding modes in the active site of dGMII with the exception of the methyl group on C(5) of the pyrrolidine ring. An overlay of the binding mode of compounds **47** and **57**, Scheme 36, revealed that the active site region was opened up in the structure of **57** compared to structure of **47** whereas the Phe206 and Tyr727 were pushed away from the inhibitor. The distance between C2 in the inhibitors and CZ of Phe206 was 4.8 Å in the dGMII:**57** complex, while it was 4.3 Å in the dGMII:**47** adduct. The Tyr727 OH was shifted 0.4 Å away from C2. The additional methyl group in **57** was in a position normally occupied by a polar hydroxyl in other inhibitors; the conformational stress put on the enzyme to accommodate its binding might be a reason for the low affinity of **57** relative to **47** (IC_{50} = 1000 μM for **57** *vs* 80 μM for **47**).

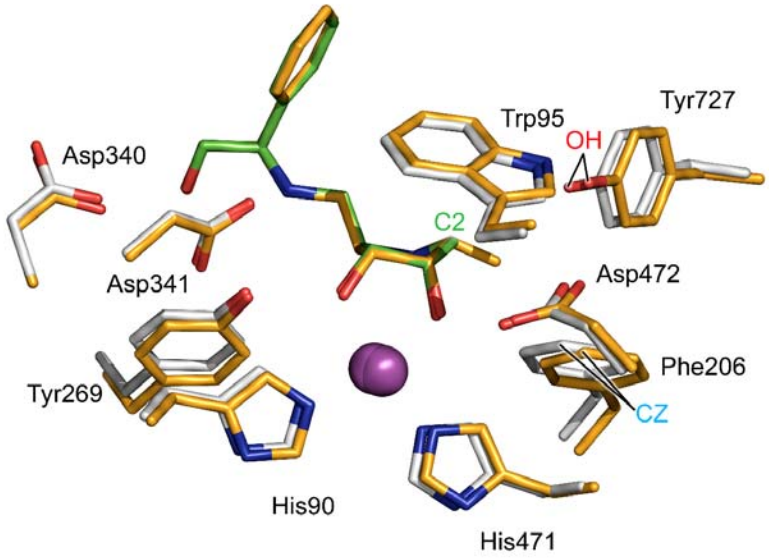

Scheme 36: Overlay of the conformations of the active site residues in the complexes of **47** (ligand green, protein grey) and **57** (ligand and protein orange) with dGMII. The zinc atoms appear as magenta balls. Distances are presented in Table 3, page 63. The figure was generated with PyMOL.

In the dGMII:**47** complex, the terminal oxygen of the inhibitor **47** (OH-9) made numerous hydrogen bonds. It was 2.7 Å from Asp340 OD1, 2.8 Å from a water molecule, 3.3 Å from Tyr269 OH and 3.5 Å from Asp341 OD1. An almost identical bonding pattern was seen for inhibitor **57**, although the interaction distances were slightly longer. The oxygen of compound **57** (OH-9) was 2.7 Å from Asp340 OD1, 2.8 Å from a water molecule, 3.5 Å from Tyr269 OH and 3.7 Å from Asp341 OD1 (Table 3).

Because of the different stereochemistry of the inhibitor **58**, the primary oxygen of compound **58** (OH-9) was placed in a different location and was now 4.8 Å from Asp340 OD1 and 4.5 Å from Asp341 OD1. Nevertheless, there were still interactions with Tyr269 and two water molecules (Table 3).

Zinc Interactions

Compound	Swa (**16**)	**47**	**58**	**57**
PDB	1HWW	2F18	2F1A	2F1B
Protein or Inhibitor Atom	**Distance (Å)**	**Distance (Å)**	**Distance (Å)**	**Distance (Å)**
His90 NE2	2.10	2.12	2.11	2.14
Asp92 OD1	2.24	2.13	2.16	2.17
Asp204 OD1	2.17	2.09	2.08	2.11
His471 NE2	2.09	2.11	2.09	2.13
OH-1 (**16**) or OH-3 (**47**, **58**, **57**)	2.20	2.18	2.20	2.20
OH-2 or OH-4	2.13	2.26	2.35	2.31

Protein/ligand Interactions

Compound	Swa (**16**)		**47**		**58**		**57**	
PDB	1HWW		2F18		2F1A		2F1B	
Protein Atom	**Atom**	**Distance (Å)**	**Atom**	**Distance (Å)**	**Atom**	**Distance (Å)**	**Atom**	**Distance (Å)**
Asp92 OD1	OH-1	3.03	OH-3	2.99	OH-3	2.98	OH-3	3.03
	OH-2	2.92	OH-4	3.11	OH-4	3.18	OH-2	3.12
Asp92 OD2	OH-2	2.54	OH-4	2.69	OH-4	2.61	OH-2	2.59
Asp204 OD1	OH-1	2.83	OH-3	2.76	OH-3	2.81	OH-3	2.77
	OH-2	2.97	OH-4	2.93	OH-4	2.96	OH-4	2.98
	N-4	2.75	N-1	2.81	N-1	2.88	N-1	2.81
Asp204 OD2	N-4	3.45	N-1	3.34	N-1	3.36	N-1	3.38
Tyr269 OH			N-7	3.00	N-7	2.88	N-7	3.14
			OH-9	3.30	OH-9	2.97	OH-9	3.52
Asp340 OD1			OH -9	2.67	OH -9	4.82	OH -9	2.66
Asp341 OD1			OH-9	3.49	OH-9	4.48	OH-9	3.70
Asp341 OD2			N-7	2.78	N-7	2.85	N-7	2.80
			OH-4	3.42	OH-4	3.49	OH-4	3.45
Asp472 OD1	OH-8	2.56	-	-	-	-	-	-
Asp472 OD2	OH-1	2.60	OH-3	2.49	OH-3	2.46	OH-3	2.59
Tyr727 OH	OH-8	2.64	-	-	-	-	-	-
WATERS			OH-9	2.78	OH-9	2.63	OH-9	2.78
			N-1	2.91	N-1	2.94	N	2.96

Table 3: Summary of interatomic distances (Å) between the inhibitors and dGMII.

3.4. Docking studies

Our goal, in collaboration with the group of Prof. N. Moitessier (McGill University, Montreal, Canada), was to determine, through a comparative evaluation of several docking programs, the most accurate computational tool for the design of α-mannosidase inhibitors.

3.4.1. Selection of the model enzyme and associated structures

Since we have obtained three x-ray structures of our inhibitors in the dGMII, we used these dGMII:inhibitor complexes as the starting point for computer-assisted design of new potent and selective inhibitors of α-mannosidases. No other models nearer the human enzyme, was available to perform this study. Indeed, mammalian mannosidases are difficult to purify in suitable quantities to be used for crystallization and thus x-ray assays. And only a single structure of bovine lysosomal mannosidase is available from the Protein Data Bank (PDB 107D) with a suboptimal resolution of 2.70 Å which hinders the possibility of performing accurate docking experiments on it.

To the three structures of dGMII:inhibitors described in paragraph 3.3 was added seven supplementary complexes selected from available crystal structures in the Protein Data Bank (Scheme 37). The ligands were selected to represent a large range of inhibitory activity against dGMII ranging from 20 nM to 7.5 mM . The PDB codes retained were: 1HWW (Swa), 1HXK (DMJ), 1PS3 (Kifunensine), 1R33, 1R34, 1TQS (Salacinol) and 1TQT.[40b,178,181,182] The structures with ligands that were not competitive inhibitors or structures with resolution worse than 2 Å were discarded.

[181] Shah, N.; Kuntz, D. A.; Rose, D. R. *Biochemistry* **2003**, *42*, 13812-13816.
[182] Kavlekar, L. M.; Kuntz, D. A.; Wen, X.; Johnston, B. D.; Svensson, B.; Rose, D. R.; Pinto, B. M. *Tetrahedron: Assymetry* **2005**, *16*, 1035-1046.

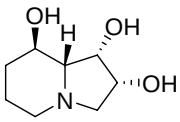

Swa, **16**

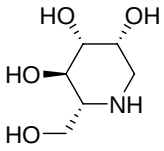

DMJ, **12**

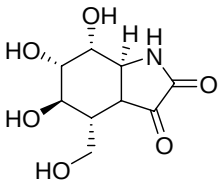

Kifunensine, **15**

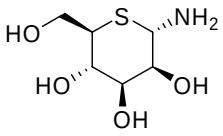

59

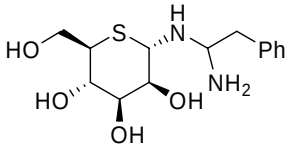

60

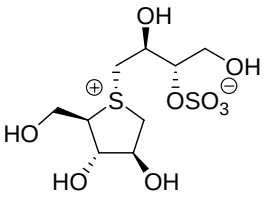

Salacinol, **61**

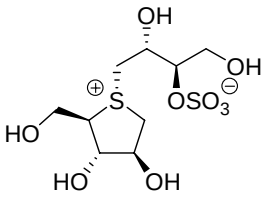

62

	Name	PDB code	Resolution (Å)	IC_{50} dGMII (μM)
16	Swainsonine (Swa)	1HWW	1.87	0.02
12	Deoxymannojirimycine (DMJ)	1HXK	1.50	400
15	Kifunensine	1PS3	1.80	1000
59		1R33	1.80	70
60		1R34	1.95	900
61	Salacinol	1TQS	1.30	7500
62		1TQT	1.90	7500

Scheme 37: Structures of seven dGMII:inhibitor complexes.

3.4.2. General considerations

For the last two decades, computational methods for structure-based drug design have evolved significantly. Their increasing accuracy has been followed with growing interest by the pharmaceutical industry. Among these methods, docking techniques have been extensively investigated and exploited in medicinal chemistry projects.

Computational molecular docking is a research technique for predicting whether one ligand will bind a target protein. Protein-ligand docking is done by modelling the interactions between the protein and the ligand. The success of a docking study depends on two mathematic tools: the search algorithm and the scoring function.

The search algorithm is the first mathematic tool used by the docking program to search all possible conformations of the ligand paired to the protein, which are called “poses”. The scoring function is the second mathematic tool of the program and is used to predict the affinity of the ligand for the protein in order to rank various inhibitors in function of their inhibitory ability.

3.4.3. Docking of dGMII inhibitors

3.4.3.1. Challenges for the docking on dGMII

A close look at the selected crystal structures revealed challenges for the accurate docking of GMII inhibitors. First, a zinc atom was involved in the catalytic activity of the enzyme and was strongly bound to the inhibitors. Second, some solvent-exposed moieties of the largest and more hydrophilic inhibitors were not completely inserted into the active site. Third, bound water molecules made important interactions with some inhibitors. Nevertheless, as none of the water molecules were conserved throughout the set of the 10 dGMII:inhibitor complexes, they were not considered for the docking study. Indeed, it would have been impossible to keep water molecules without biasing the self-docking of an inhibitor to its natural solvated receptor.

3.4.3.2. Selection of the docking program

Despite the extensive investigations that have been pursued during the last decade on docking techniques, no universal method applicable to any protein target has been discovered. Thus, the choice of the software has to be done wisely. A set of docking programs (Glide, GOLD, FlexX, AutoDock, eHiTs and FITTED) was used in order to identify the optimal software for the design of Golgi mannosidase II (GMII) inhibitors.[183] This study performed with Pablo Englebienne at McGill University was not intended to fully evaluate these docking programs but only to find the best one in the context of the α-mannosidase II inhibition.

The assessed programs covered a variety of conformational search methods in order to predict the binding mode of the inhibitor into the active site of the enzyme. GOLD, AutoDock and FITTED used a genetic algorithms, FlexX an incremental construction, eHiTs a rigid fragment docking and linking and finally Glide a multi-level search. Moreover, a large panel of scoring functions (e.g. ChemScore, GlideScore, GoldScore, AutoDock scoring function) were tested to evaluate their accuracy to predict the inhibitory ability of the inhibitors for the enzyme.

[183] Englebienne, P.; Fiaux, H.; Kuntz, D. A.; Corbeil, C. R.; Gerber-Lemaire, S.; Rose, D. R.; Moitessier, N. Proteins, **2007**, paper in press.

Some of the evaluated programs came with an interface that was used to prepare the protein structures, the ligands and some of the initial keyword files. However, in order to obtain the best performance from each docking program, the standalone versions with optimized parameters were used.

Glide, which I have personally tested in this comparative study, will be discussed in details.

3.4.3.3. Evaluation of Glide

Specificities of Glide:

Glide uses a funnel-type approach to search the conformational space. The best poses are then scored using the scoring function GlideScore.[184] Among the many terms of this scoring function is a term accounting for metal-ligand interactions that might have been well suited for the Zn-inhibitor interactions. However, this term is restricted to anionic ligands and single atom ligation. It thus does not account for the geometry of metal-ligands complexes. The selected ligands were neutral and the metal ligation would therefore be modelled as purely electrostatic.

Moreover, Glide proposes the use of constraints to force specific interactions. The user-defined constraints add an additional filter to the hierarchical filtering of the funnel. In order to evaluate the impact of constraints on accuracy, two studies (with and without constraints) were carried out. Unexpectedly, the addition of a constraint did not significantly increase the accuracy of the binding mode prediction.

The catalytic site, including two histidines (His90, His471), two aspartates (Asp92, Asp204) and a zinc ion, was studied in details. The formal charge of the zinc atom is +2, although it is clear that this charge was delocalized onto the chelating residues. Thus, the charges for the catalytic site residues and for the zinc atom were derived from density functional theory (DFT) calculations of a truncated binding site.

[184] Friesner, R. A.; Banks, J. L.; Murphy, R. B.; Halgren, T. A.; Klicic, J. J.; Mainz, D. T.; Repasky, M. P.; Knoll, E. H.; Shelley, M.; Perry, J. K.; Shaw, D. E.; Francis, P.; Shenkin, P. S. *J. Med. Chem.* **2004**, *47*, 1739-1749.

Principle of Glide:

Prior to the docking experiments, several operations are required by Glide to prepare the proteins and the ligands. Indeed, after addition of the hydrogen atoms, the ligands were separated from the protein to work in an independent way. The proteins were charged and prepared through minimization calculation and the ligands were prepared separately and optimized since, in a real drug design scenario, the final structure is not known (Scheme 38A). Then, the prepared proteins were used for computing grids, with and without constraints. Finally, the docking study was performed with the ten selected ligands which were docked to the ten protein structures for a total of 100 docking runs (10 self-docking runs where the ligands were docked-back to their own protein and 90 cross-docking runs, where the ligands were docked in the nine other x-ray structures of dGMII, Scheme 38B).

A) **B)**

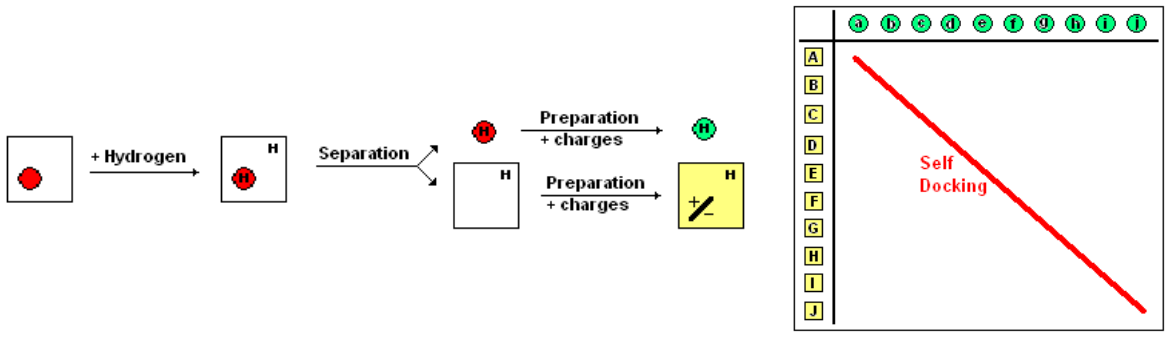

Scheme 38: **A**) Steps for the preparation of the proteins and ligands for docking studies. **B**) Representation of the 10 self-docking runs and 90 cross-docking runs.

Once the program has docked the ligand into the protein, the “poses” which are the simulated conformations of the ligand in the protein were examined and compared to the x-ray structure through a RMSD (Root mean square deviation) calculation. This value is thus an evaluation of the accuracy of the program to dock an inhibitor into the protein.

Results obtained with Glide on dGMII:

With Glide, the ligands were docked with RMSD's below 1.0 Å in 40% of the cases (Scheme 39A, dashed arrow) and below 2.0 Å in 48% (Scheme 39A, bold arrow). The other programs assessed were less accurate.

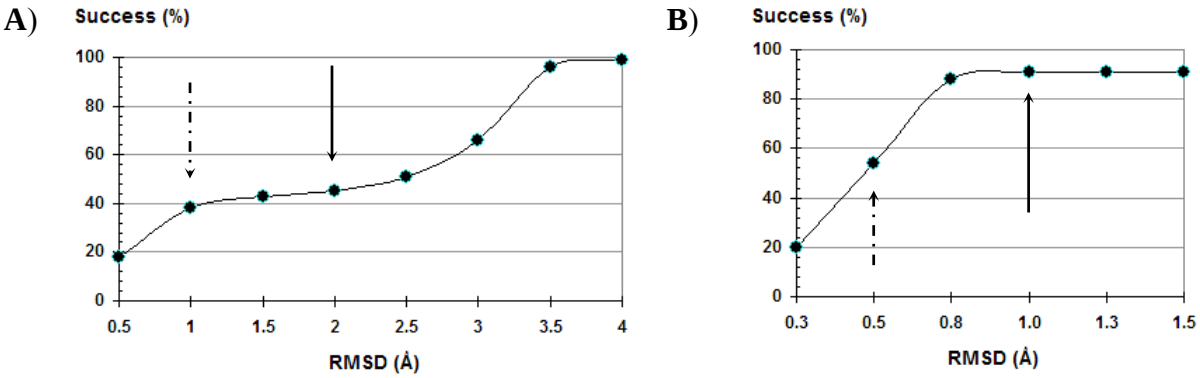

Scheme 39: Accuracy for Glide to dock the 10 ligands to the 10 protein structures. **A**) Deviation of the docked poses relatively to the crystal structure binding mode. **B**) Metal binding atoms.

The computed RMSD's indicated better accuracy for the self-docking of the smaller ligands which were docked back to their protein structure with RMSD's below 1.1 Å (data not shown). This observation was consistent with the results reported in the original Glide publication by Friesner and co-workers.[184] They observed that about 50% of the compounds were docked back with RMSD's below 1.0 Å. In the same study, about a third of the compounds were docked with RMSD between 1.0 Å and 2.0 Å. Nevertheless, in our study, ligands **47**, **57** and **58** were self-docked with RMSD values higher than 2.5 Å. To further evaluate the apparent poor docking accuracy observed for ligands **47**, **57** and **58** a closer inspection of the poses around the zinc atom was carried out and the docked conformations were inspected and compared to the experimental x-ray structures.

First, it was noticed that the experimentally observed zinc chelation by the diol or alcohol moieties was correctly predicted in most of the one hundred complexes. Indeed, in 54% of the cases the chelating alcohols or diols are predicted at 0.5 Å to the observed x-ray structure (Scheme 39B, dashed arrow) and 91% of the cases are located at 1.0 Å (Scheme 39B, bold arrow).

Second, a close look at the docked structures indicated that the docked pose was for the most part correct in many cases. The main deviation came from the solvent-exposed moieties and the orientation of the aromatic groups.

For instance, compound **47**'s phenyl group was predicted to interact with Arg228 through π interactions, while in the crystal structure it was interacting with Trp95 through a T-shaped π interaction (Scheme 40). In fact, Glide and the other programs were not able to predict this T-shaped interaction which is probably due to the poor description of this type of interaction by the commonly used scoring functions. Nevertheless, the pyrrolidine ring was perfectly orientated in all poses.

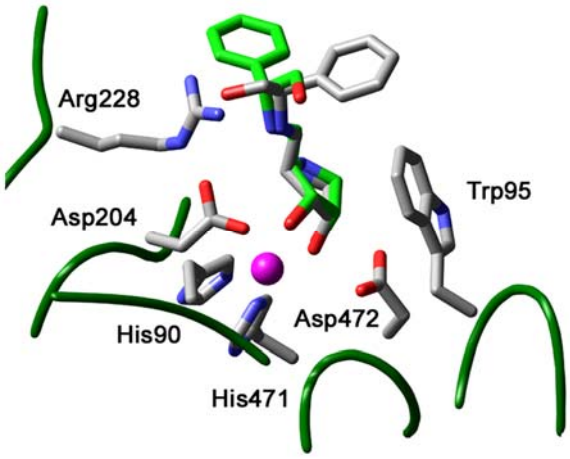

Scheme 40: Glide docked *vs* observed binding mode of compound **47**. The crystal structure appears in grey and the docked structure in green.

It is worth noting that the geometry of the ligands was optimized prior to docking. As a consequence, the ring conformation in the input file was already different from the crystal structure and thus contributed to a small part of the RMSD (< 0.3 Å).

So, the apparent poor accuracy of 48% should be considered with circumspection as most of the compounds were docked properly. The main deviation could be attributed to the solvent exposed moieties. When these moieties were not considered accuracies higher than 91% were calculated (Scheme 39). The other programs of the comparative study poorly predicted both the metal ligation and the location of the solvent exposed groups.

Despite the good docking accuracy of Glide, the scores obtained with the scoring function GlideScore (GScore) did not correlate well with the experimental biological activities (Scheme 41). The scores are negative and predict the inhibiting ability of the inhibitor for dGMII. More the score is negative, more efficient should be the inhibitor. But, Swa the most active compound (**16**, 1HWW, IC_{50} = 20 nM toward dGMII) was predicted to be one of the poorest active inhibitors of the set with a GScore of -10.78. Whereas **57** (2F1B, IC_{50} = 1mM toward dGMII) was predicted to be one of the most active compounds with a GScore evaluated at -12.83.

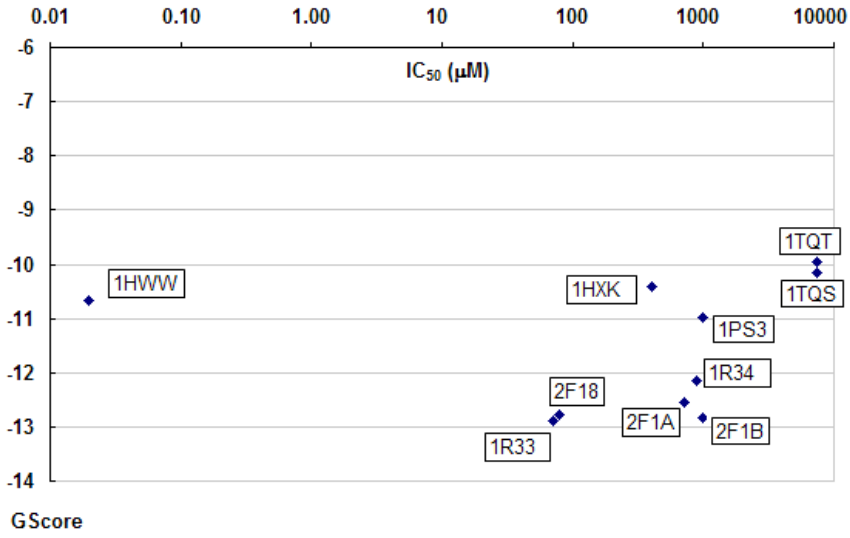

Scheme 41: Accuracy for Glide to predict the inhibitory activities. Correlation between the scores calculated with the scoring function GlideScore (GScore) and the inhibitory activities (IC_{50}) toward dGMII.

This study revealed that Glide could accurately discriminate the different poses and thus predict reasonable binding modes but the scoring function of the program was not able to predict the inhibitory activities of compounds with different affinities.

3.5. Functionalization of inhibitor 47 with polar substituents

As it was not possible to design relevant chemical modifications of our lead inhibitor **47** through computational methods, the x-ray structures of dGMII:**47**, dGMII:**57** and dGMII:**58** served as the basis for further functionalizations. In particular, comparison of the binding of **47** with Swa suggested that the introduction of polar groups at C(5) position of the pyrrolidine could enhance the affinity of the inhibitor for the enzyme. Additional interactions with the Asp472 and Tyr727 should thus provide more potent inhibition toward dGMII (Scheme 42).

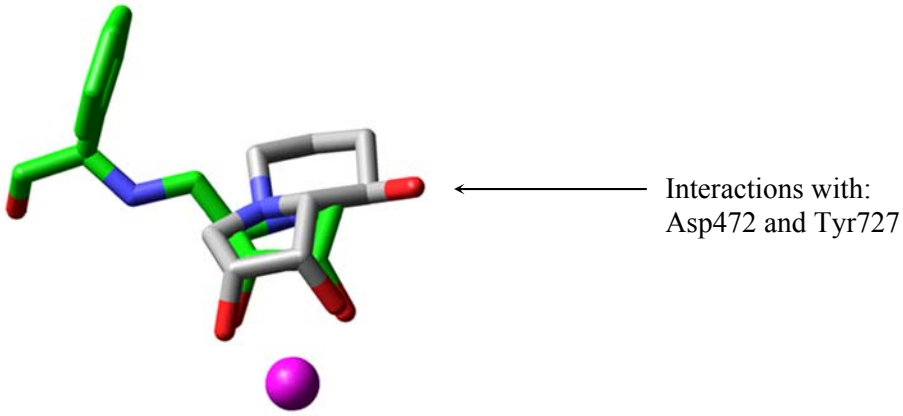

Scheme 42: Overlays of the binding of compound **47** with Swa (**16**). Molecule **47** is drawn in green, Swa in grey and the atom of zinc in purple.

3.5.1. Synthesis of 3,4,5-trihydroxypyrrolidine derivatives

Introduction of an hydroxyl group at the C(5) position of the pyrrolidine ring was first envisaged.[185] Starting from the intermediate **51**, reduction of the carbamate moiety in presence of sodium borohydride followed by subsequent protection of the resulting alcohol as methyloxymethyl ether afforded **63** as a mixture of two diastereoisomers, with 80% overall yield (2 steps). Birch reduction of the trityl moiety and oxidation of the resulting alcohol under Swern conditions provided aldehyde **64** (1:1 mixture of diastereoisomers, 75% yield). Reductive amination with D-(α)-phenylglycinol afforded diamine **65** with 46% yield.

[185] Steiner, C. Diploma work, EPFL, **2005**.

Several assays to remove the protecting groups in acidic medium (CF_3COOH/H_2O 4/1, 1M HCl) failed to afford the expected hemiaminal **66**, due mainly to decomposition. Indeed, the acidic conditions required for deprotection may lead to mixture of compounds including imines and dimmer. Defoin and al. have shown that simple 2-hydroxypyrrolidines could be obtained as equilibrium mixtures of the corresponding imine, 2-aminoalcohol and dimmer. The composition of these mixtures depended on the pH value of the medium and on the nature of ionic species in the buffers.

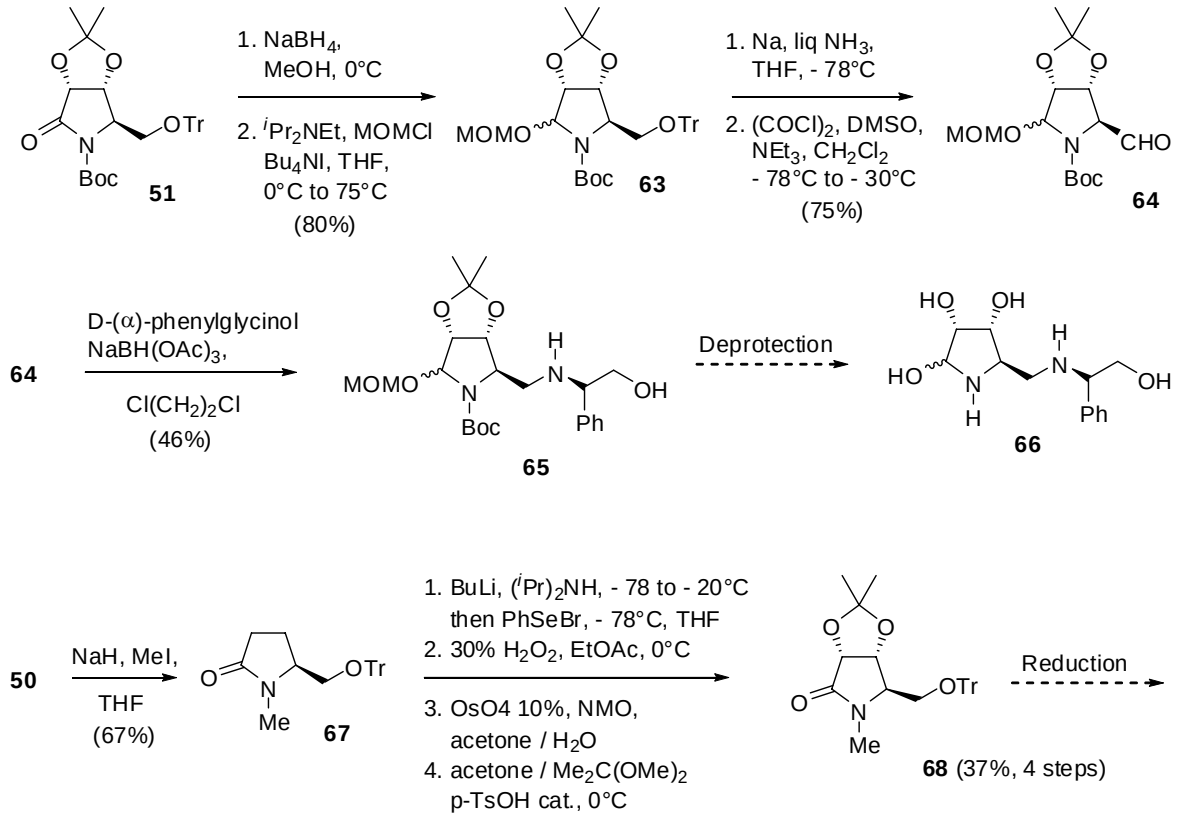

Scheme 43: Synthesis of 3,4,5-trihydroxypyrrolidine derivatives.

In order to prevent water elimination from the hemiaminal to form the corresponding imine, introduction of a methyl group on the amine of the pyrrolidine ring was envisaged. Methylation of L-5-trityloxymethyl-2-pyrroldinone **50** followed by introduction of the C(3), C(4) diol moiety according to the procedure of Ikota provided *N*-methyllactam **68** (Scheme 43). Reduction of the carbonyl moiety of **68** was then attempted under several conditions (Table 4). In the presence of $NaBH_4$, $LiBH_4$ or $LiBH(Et)_3$, only starting material was recovered. The use of stronger reducing agents (entries 5-7) afforded a compound which was not further analyzed, but may be the corresponding *N*-methylpyrrolidine.

	Hydride	Eq.	Solvent	Temp (°C)	Result
1	$NaBH_4$	1.5	MeOH	0°C to 25°C	Starting Material
2	$NaBH_4$	5.0	MeOH	25°C to reflux	Starting Material
3	$LiBH_4$	1.0	THF	-78°C to 25°C	Starting Material
4	$LiBH(Et)_3$	1.0	THF	-78°C to 25°C	Starting Material
5	$LiAlH_4$	1.0	THF	-20°C to 25°C	*N*-Methylpyrrolidine
6	DIBAL-H	1.0 + 1.2	CH_2Cl_2	-78°C to 25°C	*N*-Methylpyrrolidine
7	K-Selectride	1.0 + 2.0	THF	-78°C to 25°C	*N*-Methylpyrrolidine

Table 4: Conditions for the reduction of lactam **68**.

As a carbamate protecting group was necessary to achieve reduction of the lactam, introduction of a benzylcarbamate was chosen (Scheme 44) as this group can be removed under non-acidic conditions after reduction of the carbonyl moiety. Further methylation of the pyrrolidine nitrogen will prevent imine formation during final deprotection. L-5-trityloxymethyl-2-pyrroldinone **50** was converted into carbamate **69** in 91% yield.[186] Ikota's procedure then provided the protected lactam **70** in poor yield. Reduction of the carbonyl group was achieved with lithium borohydride in almost quantitative yield. But protection of the alcohol as a methyloxymethyl ether followed by the cleavage of the carbamate released a complex mixture of non-separable compounds that could not be identified by NMR (nuclear magnetic reasonance).

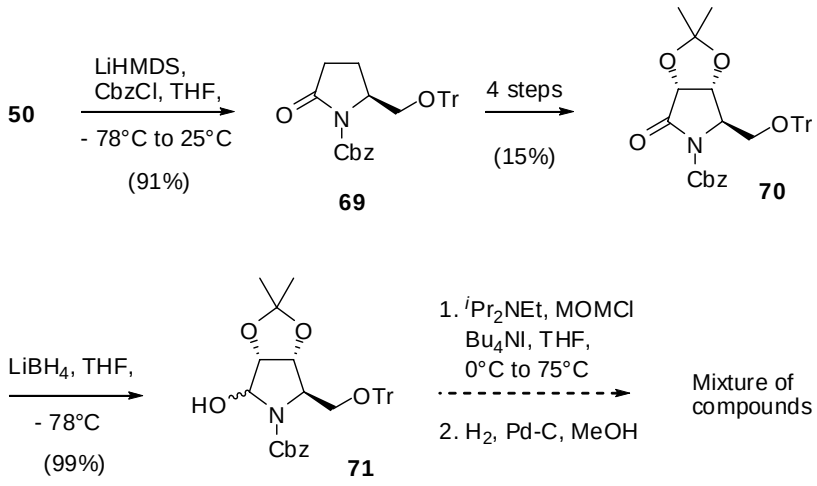

Scheme 44: Synthesis with a benzylcarbamate protecting group.

[186] Hannessian, S.; Kornienko, A.; Swayze, E. E. *Tetrahedron* **2003**, *59*, 995-1007.

As introduction of an hydroxyl group at C(5) position of the pyrrolidine ring was unsuccessful, fluorination of this position was also attempted (Scheme 45). However, neither treatment of hydroxycarbamate **72** with DAST, nor transformation into the corresponding triflate or mesylate for further displacement with fluoride anion afforded the targeted derivative.

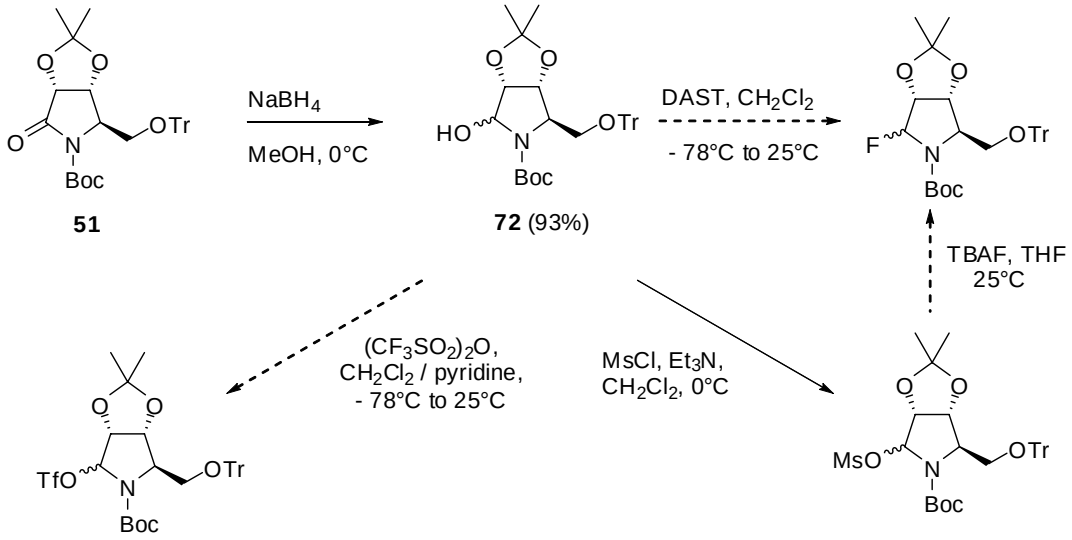

Scheme 45: Attempt of fluorination at C(5) position of the pyrrolidine ring.

Consequently, we wondered whether a pyrrolidinone instead of a pyrrolidine scaffold could provide additional interactions with Asp472 and Tyr727 residues of the active site of dGMII and if modifications on the phenylglycinol moiety could improve the biological activities toward α-mannosidases.

3.5.2. Synthesis of dihydroxypyrrolidinone derivatives

As removal of trityl moiety required strong basic conditions, we decided to replace it with a silyl ether. 5-oxo-L-proline **73** was converted into the primary alcohol **74** with 84% yield. Protection as a *tert*-butyldimethylsilyl ether followed by introduction of a *tert*-butyl carbamate (**75**) or a methyl group (**81**) on the nitrogen atom afforded lactams in good yields. Ikota's procedure provided diols **76** and **82** in 43% and 41% yield, respectively. Protection of the diol moieties as acetonides (**77** and **83**) followed by cleavage of the silyl ether in presence of tetrabutylammonium fluoride allowed oxidation of the resulting primary alcohol with Dess-Martin periodinane.[187] Other oxidative reagents (Swern, PCC) failed to afford reasonable yield of the expected aldehydes **79** and **85**. Reductive amination with D-(α)-phenylglycinol provided protected lactam intermediates that were treated under acidic conditions to afford 3,4-dihydroxypyrrolidinone derivatives **80** and **86** in 12% and 28% yield, respectively (Scheme 46).

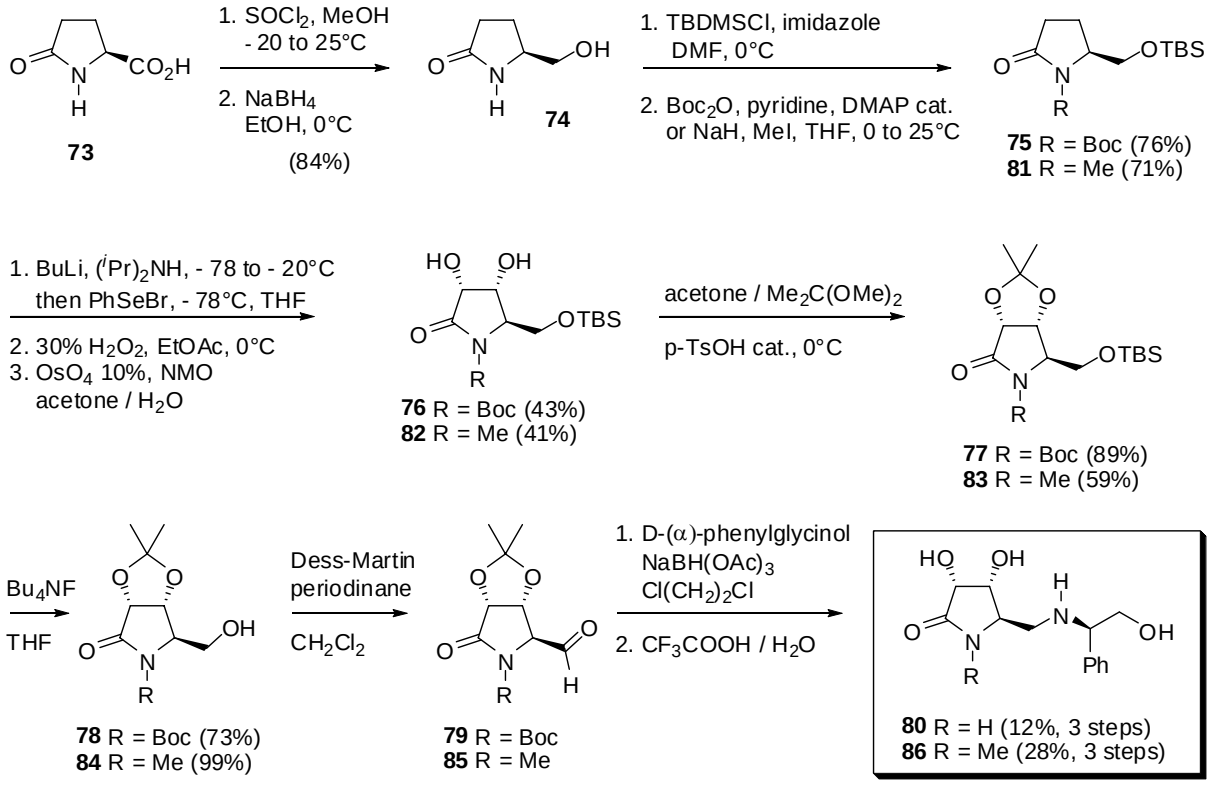

Scheme 46: Synthesis of 3,4-dihydroxypyrrolidinone derivatives.

[187] Dess, D. B.; Martin, J. C. *J. Org. Chem.* **1983**, *48*, 4155-4156.

3.5.3. Modification of the phenylglycinol moiety

In the frame of our study, modification of the phenylglycinol moiety was also envisaged to modulate the inhibitory ability of our pyrrolidine-based inhibitors. Elongation of the aromatic chain to produce compound **89** was achieved by coupling carbaldehyde **87**,[188] with D-(α)-phenylalaninol **88** followed by acidic removal of the protecting groups (Scheme 47).

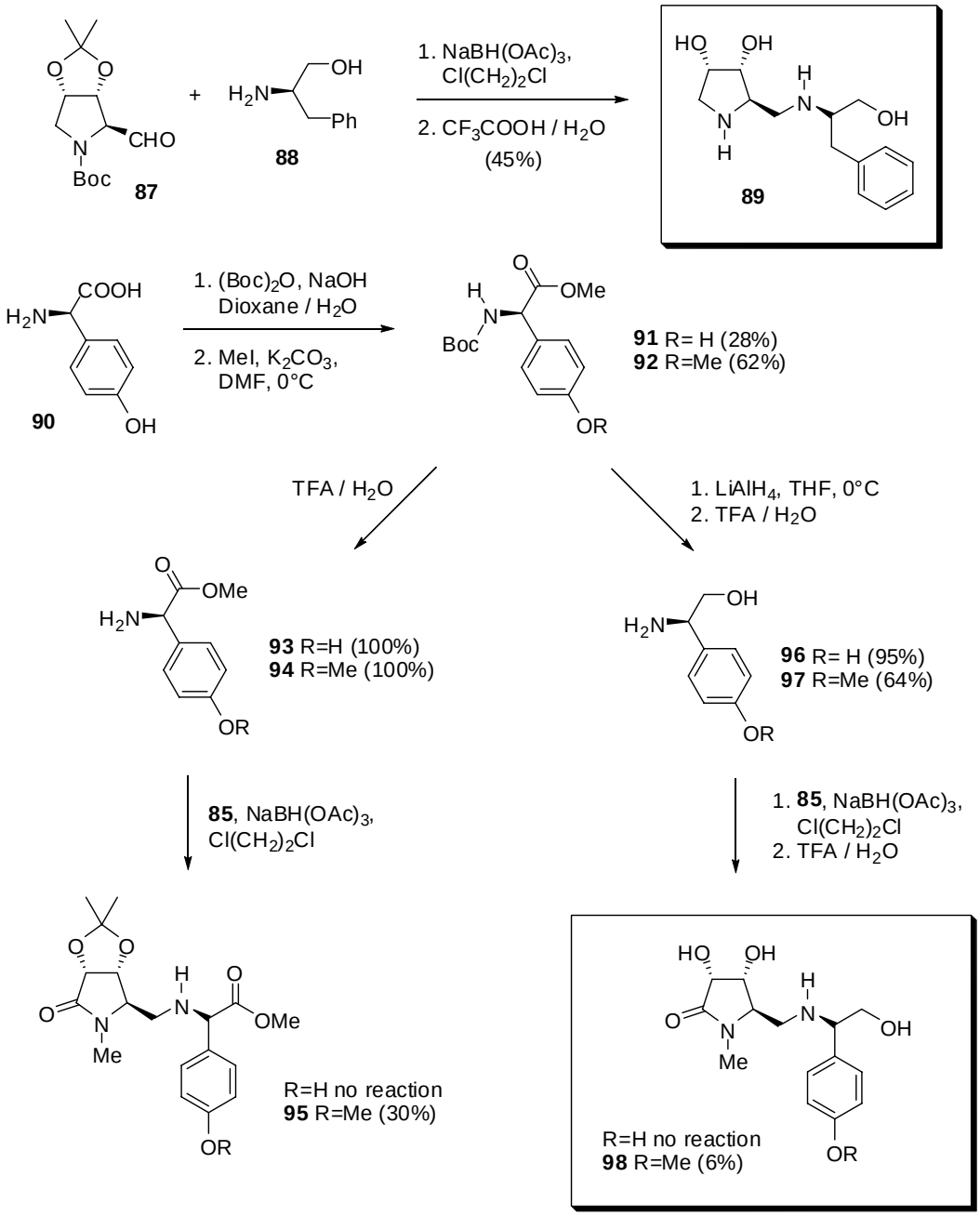

Scheme 47: Functionalization of the phenyl group.

[188] Fleet, G. W. J.; Son, J. C. *Tetrahedron* **1988**, *44*, 2637-2647.

Functionalization of the aromatic moiety of phenylglycinol with polar groups that may influence the solubility of the corresponding inhibitors in physiologic medium was initiated. For that purpose, 4-hydroxyphenylglycine **90** was protected as tert-butylcarbamate and treated with methyliodide in basic medium to afford **91** and **92** in 28% and 62% yield, respectively (Scheme 46).[189] Deprotection of the amine under acidic conditions followed by reductive amination with aldehyde **85** provided the methyloxyphenyl derivative **95** in moderate yield. Phenol **93** did not react under these conditions. Our attempt to reduce the methyl ester moiety failed to give the expected primary alcohol. Thus, reduction of the methyl ester was performed on compounds **91** and **92** with lithium aluminium hydride. Deprotection of the amine allowed reductive amination with aldehyde **85**. The phenol derivative **96** was not reactive toward the reductive amination whereas the methyloxyphenyl intermediate **97** led to a very low yield of the corresponding pyrrolidinone. Further acidic cleavage of acetonide protecting group afforded **98** with good yield and purity. Until now, optimization of this synthetic route was not assessed.

3.5.4. Inhibition of jack bean α-mannosidase and dGMII

The inhibitory potential of compounds **58**, **80**, **86, 89** and **98** toward α-mannosidase from jack bean and dGMII was determined and compared to the activity of our lead inhibitor **47** and of Swa (**16**) as a reference inhibitor of α-mannosidase II.

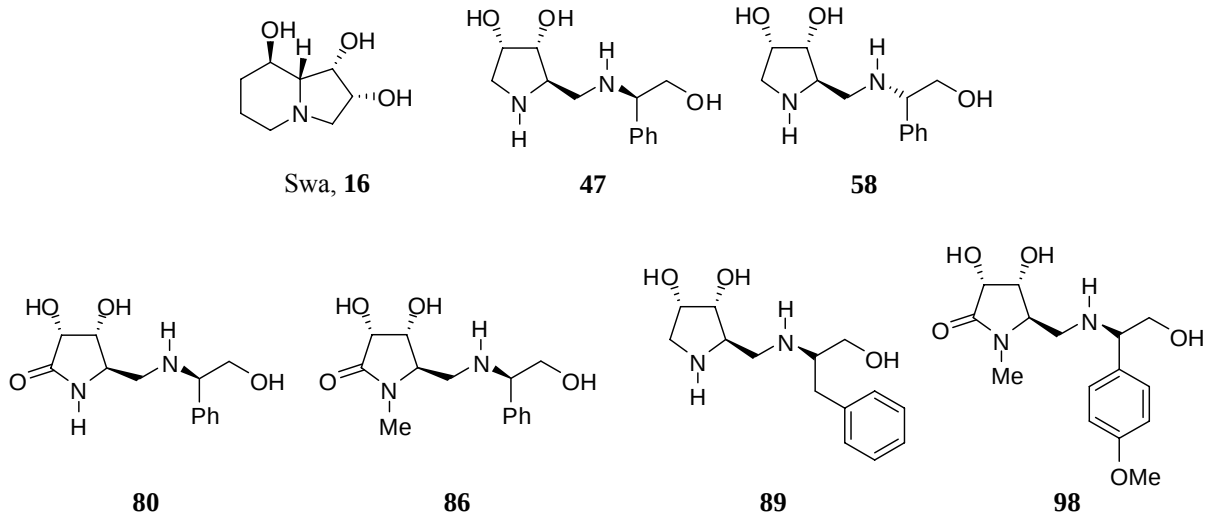

Scheme 48: Overview of pyrrolidine and pyrrolidinone compounds for enzymatic tests.

[189] Chen, Y. T.; Seto, C. T. *J. Med. Chem.* **2002**, *45*, 3946-3952.

		α-mannosidase from jack bean	dGMII
Swa (**16**)	IC_{50}	398 nM	30 nM
	K_i	155 nM (C)	n.d.
47	IC_{50}	705 nM	80 µM
	K_i	135 nM (C)	n.d.
58	IC_{50}	90 µM	720 µM
	K_i	173 µM (C)	n.d.
80	IC_{50}	4.5 µM	7 µM
	K_i	4.0 µM (C)	n.d.
86	IC_{50}	150 nM	500 nM
	K_i	206 nM (C)	n.d.
89	IC_{50}	1 mM	n.d.
98	IC_{50}	30 nM	n.d.

(C) = competitive inhibition n.d. = not determined

Table 5: Inhibitory activities toward α-mannosidase from jack bean and dGMII.

The configuration of the phenylglycinol moiety was clearly determinant in the inhibition of both enzymes as **58** was a poor inhibitor (IC_{50} = 720 µM for **58** *vs* 80 µM for **47** toward dGMII). Homologation of the aromatic chain by one methylene group also resulted in a dramatic loss of inhibitory potency against α-mannosidase from jack bean (IC_{50} = 1mM for **89** *vs* 705 nM for **47**). Replacement of the pyrrolidine moiety by a pyrrolidinone system also resulted in a significant decrease of the inhibitory potency toward α-mannosidase from jack bean (**80**). On the other hand substitution of the lactam moiety by a methyl group induced an improvement of the IC_{50} toward this enzyme (IC_{50} = 150 nM for **86** *vs* 750 nM for **47**) and compound **86** appeared to be as potent as Swa (K_i = 206 nM for **86** *vs* 155 nM for **16**). The anisole analogue **98** was even more potent with an IC_{50} of 30 nM against α-mannosidase from jack bean. However, the very little quantities obtained thus far did not allow further investigations on this derivative.

The inhibition of dGMII by pyrrolidine **47** was very modest while transformation into a pyrrolidinone system led to a net improvement of the inhibitory ability. In particular, derivative **86** presented an IC_{50} of 500 nM toward dGMII which make it one of the best inhibitor of this enzyme. Nevertheless, it remained 15 times less active than Swa on dGMII.

*3.5.5. X-ray structure of dGMII:**86** complex*

Compound **86** was co-crystallized in the active site of dGMII in order to evaluate its binding mode (Scheme 49). In comparison with our lead **47**, the carbonyl group of the *N*-methyl-pyrrolidinone inhibitor made additional interactions with Tyr727 and Asp472 which may account for the increased inhibition of **86** toward dGMII (IC_{50} = 500 nM for **86** *vs* 80 μM for **47**). The stacking interactions with Trp95 (Scheme 50) and the polar interactions with the zinc atom and Asp340, Asp341 and Tyr269 are similar for the both inhibitors **47** and **86**.

A 3.23 Å long hydrogen bond between the O-2 of compound **86** and the NE1 of Trp95 assumingly stabilizes the observed stacking between this residue and the inhibitor. A further new interaction of **86** that has neither been observed with Swa nor with **47** is a hydrogen bond between NE2 of His471 and the 3-hydroxyl group of **86** which apparently causes additional improvement in binding affinity and stabilization of the compound in the active site (Table 6). Introduction of a methyl substituent on the nitrogen center of the pyrrolidinone ring was fundamental to allow a global shift of the inhibitor into the active site. Indeed, the inhibitory ability of the free lactam **80** was significantly lower than the activity of the *N*-methyl substituted analogue **86** (IC_{50} = 7 μM for **80** *vs* 500 nM for **86**).

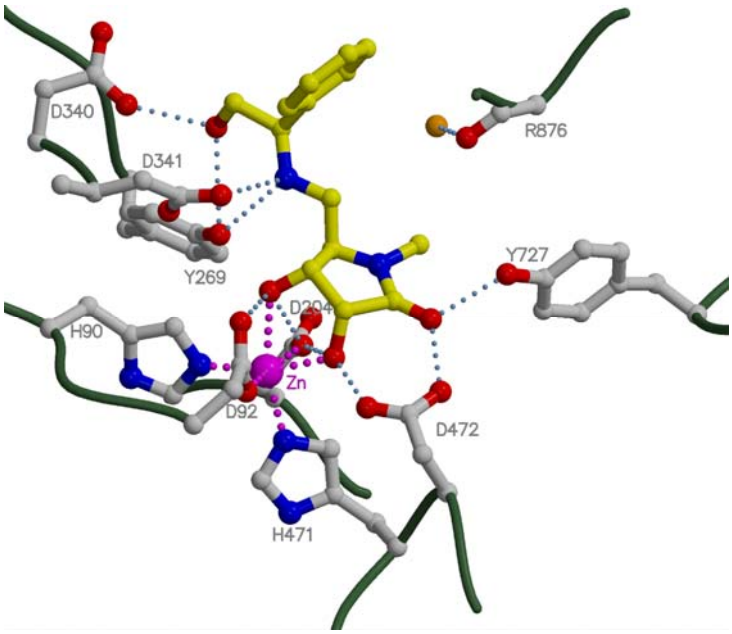

Scheme 49: Crystal structure of dGMII:**86** complex. Interactions closer than 3.5 Å are indicated and the interactions with the zinc atom are drawn in magenta. Distances are presented in Table 6. The figure was generated with Molscript.

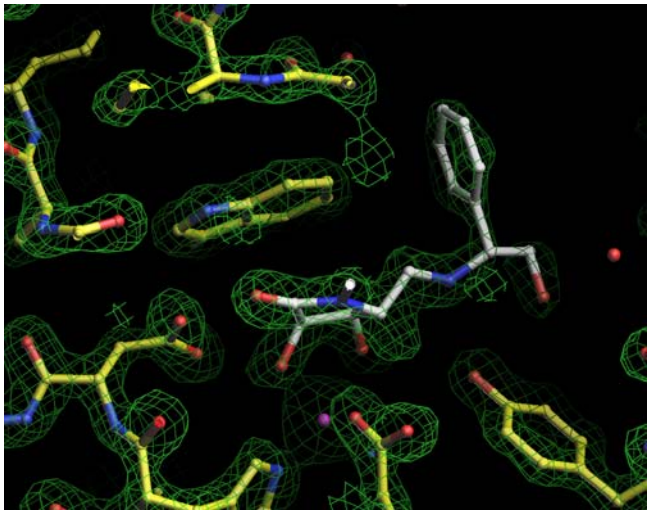

Scheme 50: Electron density map of dGMII:**86** complex. The active site zinc ion is presented by a magenta ball and the inhibitor in white.

Superimposition of the binding modes of compounds **86** and of Swa, Scheme 51, revealed that the hydroxyl moiety (OH-8) of Swa pointed out in the same direction than the carbonyl moiety of inhibitor **86**. It is noteworthy that the distance between the carbonyl oxygen O-2 of **86** and the hydroxyl group of Tyr727 is almost equal to the distance between the hydroxyl group (OH-8) of Swa and the same residue (2.65 Å for **86** *vs* 2.64 Å for Swa). For the interactions with Asp472, the same observation was made (d(O-2, Asp472 OD1) = 2.47 Å for **86** *vs* d(OH-8, Asp472 OD1) = 2.56 Å for Swa). Table 6 summarized the distances of interaction between these two inhibitors with the amino acids groups of dGMII.

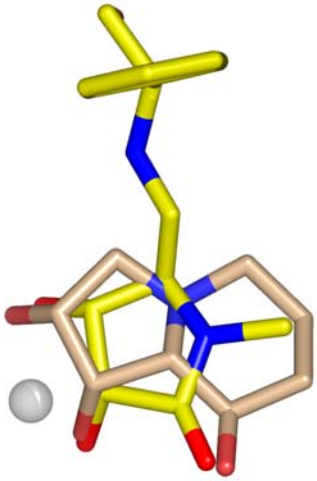

Scheme 51: Superimposition of the structures dGMII:**86** and dGMII:Swa complexes. The zinc atom is presented in grey, Swa in pink and compound **86** in yellow.

Zinc Interactions		
Compound	Swa (**16**)	**86**
Protein or Inhibitor Atom	**Distance (Å)**	**Distance (Å)**
His90 NE2	2.10	2.05
Asp92 OD1	2.24	2.20
Asp204 OD1	2.17	2.09
His471 NE2	2.09	2.14
OH-1 (**16**) / OH-3 (**86**)	2.20	2.24
OH-2 or OH-4	2.13	2.42

Protein/ligand Interactions				
Compound		Swa (**16**)	**86**	
Protein Atom	**Atom**	**Distance (Å)**	**Atom**	**Distance (Å)**
Asp92 OD1	OH-1	3.03	OH-3	2.92
	OH-2	2.92	OH-4	3.29
Asp92 OD2	OH-2	2.54	OH-4	2.55
Trp95 NE1	-	-	**O-2**	**3.23**
Asp204 OD1	OH-1	2.83	OH-3	2.86
	OH-2	2.97	OH-4	2.97
	N-4	2.75	N-1	4.37
Asp204 OD2	N-4	3.45	N-1	3.61
Tyr269 OH	-	-	N-7	3.01
			OH-9	3.13
Asp340 OD1	-	-	OH -9	2.75
Asp341 OD1			OH-9	3.34
Asp341 OD2	-	-	N-7	2.81
			OH-4	3.27
His471 NE2	-	-	OH-3	3.16
Asp472 OD1	OH-8	2.56	**O-2**	**2.47**
Asp472 OD2	OH-1	2.60	OH-3	2.59
Tyr727 OH	OH-8	2.64	**O-2**	**2.65**

Table 6: Comparison of interatomic distances (Å) between inhibitors Swa or **86** and dGMII.

3.6. Biological Assays

We next evaluated, *in vitro*, the activity of pyrrolidine and pyrrolidinone derivatives that displayed potent inhibitory properties against α-mannosidases, on tumor cells in collaboration with the group of Dr. L. Juillerat (CHUV, Lausanne).

Biological assays were performed on different human cancer cell lines derived from melanoma,[190] and glioblastoma,[191] which are tumors associated with a high proliferative and invasive potential, multiple resistance toward conventional chemotherapeutics agents and poor prognosis. Human cerebral endothelial cells (HCEC),[192] were also included in the study and human fibroblasts were used as models for non tumoral cells.

3.6.1. MTT assay

To study cell viability, the MTT assay was selected.

3.6.1.1. Principle of MTT assay

Metabolically active cells reduce the tetrazolium salt MTT ((3,4,5-dimethylthiazol-yl)-2,5-diphenyl tetrazolium) to afford a formazan dye which can be quantified in a multiwell plate reader at 540 nm (Scheme 52).

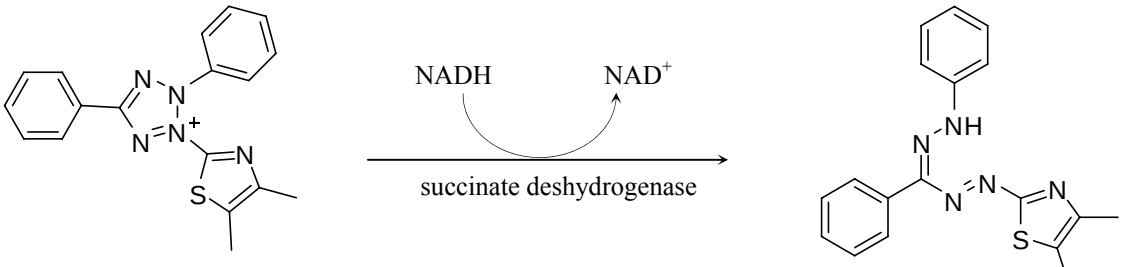

MTT **Formazan**

Scheme 52: Metabolization of MTT to a formazan salt by viable cells.

[190] Bullani, R. R.; Wehrli, P.; Viard-Leveugle, I.; Rimoldi, D.; Cerottini, J.-C.; Saurat, J.-H.; Tschopp, J.; French, L. E. *Melanoma Res.* **2002**, *12*, 263-270.
[191] Dieserens, A. C.; de Tribolet, N.; Martin-Achard, A.; Gaide, A. C.; Schnegg, J. F.; Carrel, S. *Acta Neuropathol.* **1981**, *53*, 21-28.
[192] Muruganandam, A.; Herx, L. M.; Monette, R.; Durkin, J. P.; Stanimirovic, D. B. *FASEB J.* **1997**, *11*, 1187-1197.

3.6.1.2. Preliminary results of the MTT assay

First, the effects of compound **47**, **86** and Swa, as a reference, were determined in human LN18 and LNZ308 glioblastoma cells using the MTT assay (Scheme 53). None of these potent inhibitors of α-mannosidase from jack bean and dGMII displayed significant inhibition of glioblastoma cells growth.

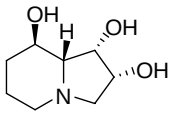

Swa (**16**)

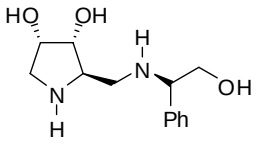

47

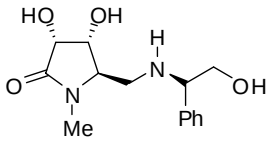

86

Scheme 53: First compounds tested on glioblastoma cells.

As the hydrophilic character of these molecules may hinder their transport across cell membranes, a series of more lipophilic derivatives of our lead **47** was synthesized. Indeed, derivative **47** was transformed into more lipophilic compounds such as ethers, esters and amides in order to allow internalization by human cancer cells.

3.6.1.3. Introduction of lipophilic groups

D-(α)-phenylglycinol **99** was transformed into diallylamine **100** (79%) allowing protection of the primary alcohol as simple ethers (benzyl and methyl ethers) with good to quantitative yields.[180] Substituted benzyl ethers were also introduced. Palladium promoted cleavage of the allyl moieties in the presence of 2-mercaptobenzoic acid as an allyl scavenger,[193] followed by a reductive amination with carbaldehyde **87** led to diamines **103** and **106**, after deprotection in acidic medium. Deallylation of the 3-fluorobenzyl ether **107** resulted in a poor yield of the corresponding amine **108** while the 4-fluorobenzyl ether **110** decomposed during the reaction. Amine **108** was then submitted to reductive amination and acidic deprotection to provide the functionalized pyrrolidine **109** (Scheme 54).

[193] Lemaire-Audoire, S.; Savignac, M.; Genet, J.-P. *Tetrahedron Lett.* **1995**, *36*, 1267-1270.

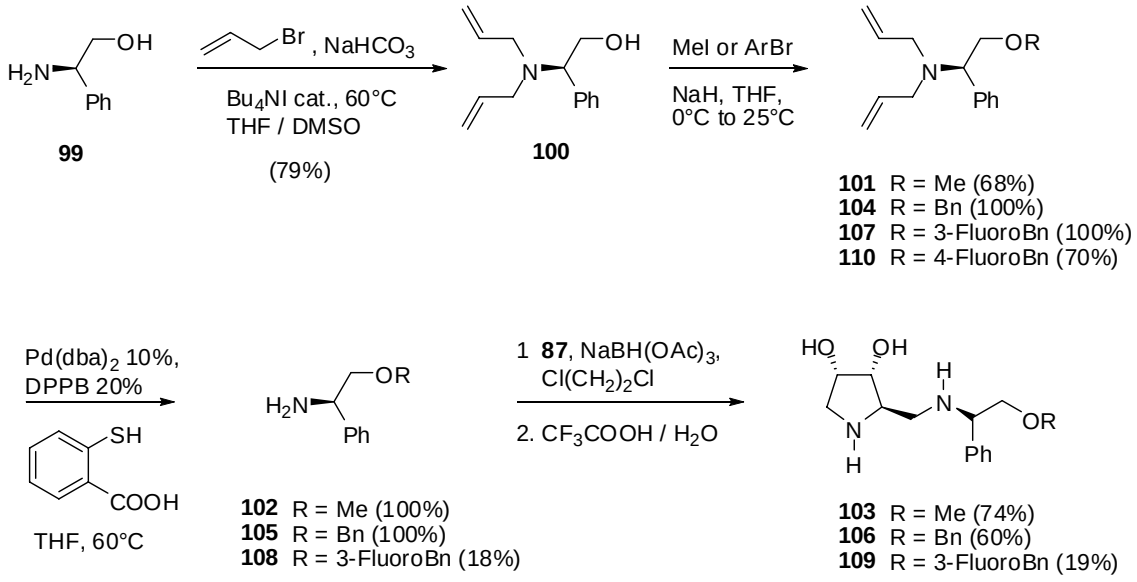

Scheme 54: Derivatization into ethers.

Introduction of ester moieties on the primary hydroxyl group of derivative **47** was also carried out (Scheme 55). D-(α)-phenylglycinol (**99**) was protected as a *tert*-butyl carbamate **111**, allowing acylation of the primary alcohol with aliphatic and substituted aromatic acyl chlorides. After acidic treatment, the resulting amines **112-122** were engaged in a reductive amination procedure with pyrrolidine carbaldehyde **87** to provide compounds **123-133** after quantitative cleavage of the Boc and acetonide protecting groups.[194]

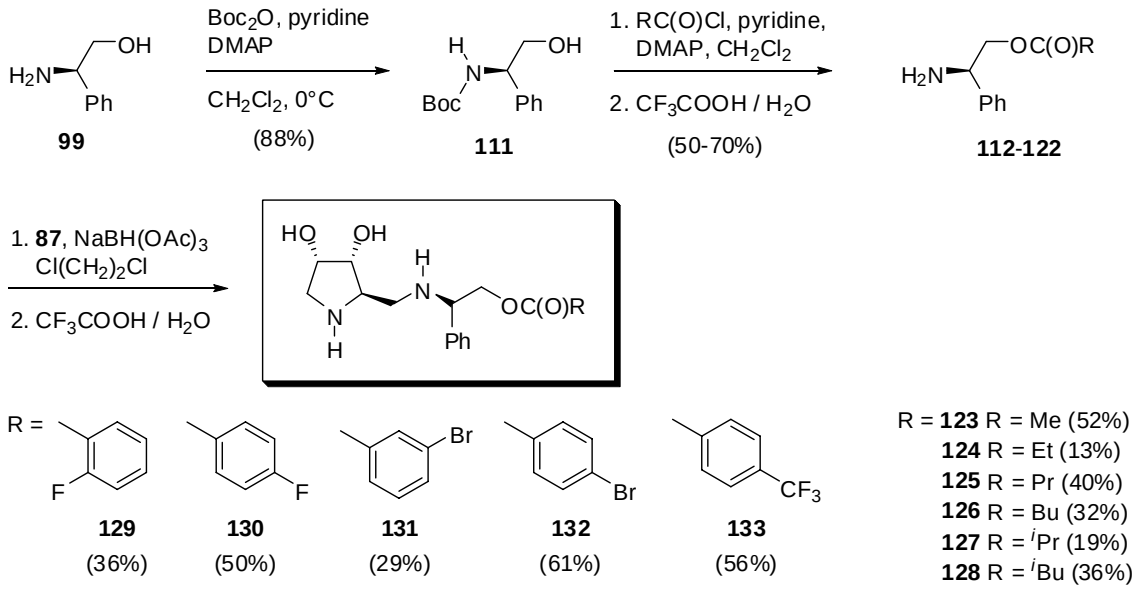

Scheme 55: Derivatization into aliphatic and aromatic esters.

[194] Fiaux, H.; Schütz, C.; Vogel, P.; Juillerat-Jeanneret, L.; Gerber-Lemaire *Chimia* **2006**, *60*, 185-189.

In order to evaluate the influence of the configuration of the phenylglycinol moiety, compound **134** (Scheme 57) was synthesized according to the same procedure starting from L-(α)-phenylglycinol.

Intermediate **111** was also converted into the corresponding primary amine **135** and used to introduce amide groups on the lateral side chain of the pyrrolidine (Scheme 56).[195] Reaction with 3-bromobenzoyl chloride followed by acidic treatment afforded the corresponding aminoamide **136**. Subsequent reductive amination with carbaldehyde **87** and sodium triacetoxyborohydride, followed by acid-catalyzed removal of acetonide and Boc moieties provided the targeted pyrrolidine **137** in 74% yield (2 steps).

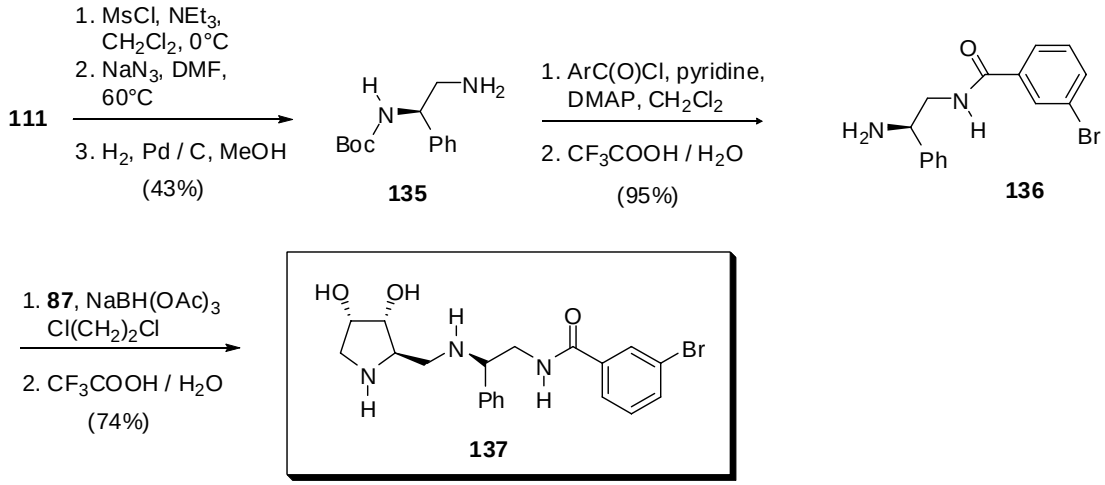

Scheme 56: Derivatization into aromatic amide.[196]

The effects of these derivatives on human glioblastoma cells were determined using the MTT assay after 24 hours of exposure. The data are summarized in Table 7.

[195] Favre, S.; Fiaux, H.; Schütz, C.; Vogel, P.; Juillerat-Jeanneret, L.; Gerber-Lemaire, S. *Heterocycles* **2006**, *69*, 179-192.
[196] Favre, S. Diploma work, EPFL, **2005**

3.6.1.4. Results of the MTT assay

Scheme 57 summarized all the products tested on tumoral cells lines:

Reference and Primary Alcohols:

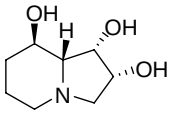

Swa (**16**)

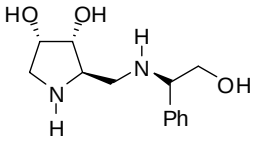

47

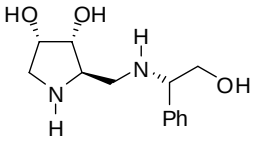

58

Esters:

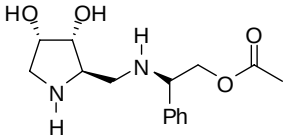

123

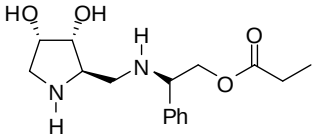

124

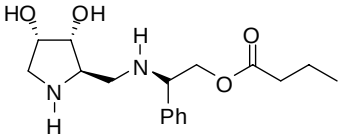

125

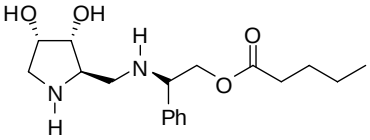

126

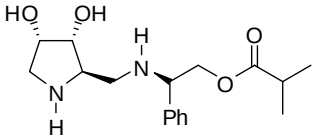

127

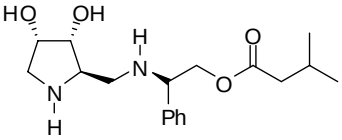

128

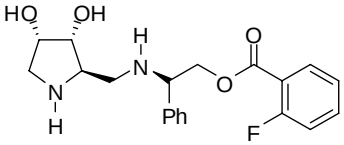

129

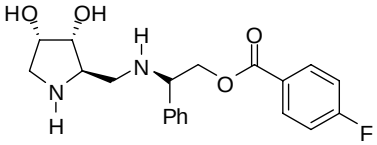

130

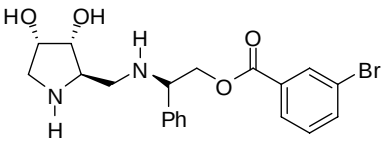

131

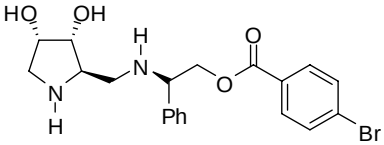

132

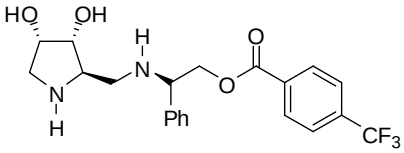

133

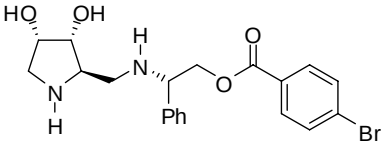

134

Ether and Amide:

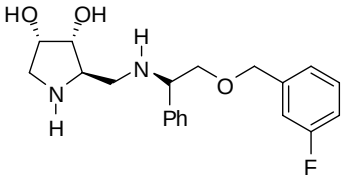

109

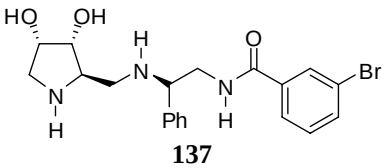

137

Scheme 57: Overview of the products tested on tumoral cells lines.

		100 μM	200 μM	300 μM
Swa (**16**)	LN18	7	18	13
	LNZ308	25	24	16
47	LN18	13	19	22
	LNZ308	0	8	26
58	LN18	0	17	7
	LNZ308	0	4	28
80	LN18	0	0	0
	LNZ308	0	0	1
86	LN18	1	0	0
	LNZ308	3	5	10
Ether	LN18	2	19	27
109	LNZ308	2	14	34
Ester aliphatic	LN18	5	0	11
123	LNZ308	3	9	17
124	LN18	21	7	22
	LNZ308	17	11	20
125	LN18	6	38	38
	LNZ308	16	17	25
126	LN18	6	9	16
	LNZ308	11	15	7
127	LN18	6	7	14
	LNZ308	12	6	20
128	LN18	4	0	20
	LNZ308	3	0	22
Ester aromatic	LN18	0	17	26
129	LNZ308	0	18	23
130	LN18	9	22	20
	LNZ308	4	16	21
131	LN18	8	10	16
	LNZ308	5	5	17
132	LN18	**5**	**67**	**92**
	LNZ308	**11**	**60**	**87**
133	LN18	0	12	11
	LNZ308	4	15	27
134	LN18	0	25	32
	LNZ308	0	6	26
Amide	LN18	15	30	52
137	LNZ308	2	20	50

Table 7: Growth inhibition of glioblastoma cells by functionalized pyrrolidines. Cells were exposed for 24 hours to 0, 100, 200 or 300 μM of the various synthetic derivatives then the MTT assay was performed for the last 2 hours of incubation. The % of residual mitochondrial activity was calculated as the ratio of absorbance of treated to control cells.

Introduction of an ether moiety slightly decreased the growth of glioblastoma cells. The aliphatic ester groups did not significantly increased the anti-proliferative activity. Among the aromatic ester derivatives, the 4-bromobenzoate (**132**) demonstrated a concentration-dependant inhibition of growth with almost complete inhibition at 300 µM. Replacement of the bromo substituent by a fluoro group or placing the halide substituent in meta position of the aromatic ring resulted in the loss of antiproliferative properties. The use of an amide bond rather than an ester linkage (**137**) also decreased the efficacy. As for the inhibition of α-mannosidase from jack bean and dGMII, inversion of the configuration of the phenylglycinol moiety (**134**) decreased the anti-proliferative properties toward glioblastoma cells.

Neither 4-bromobenzoïc acid, nor ethyl 4-bromobenzoate, which may result from the hydrolysis of **132** by cell esterases, affected glioblastoma cell growth (data not shown), which excludes an effect of the aromatic substituent.

Since derivatization into 4-bromobenzoate promoted the antiproliferative properties of α-mannosidase inhibitor **47**, the same transformation was carried out on the second generation inhibitors **80** and **86** to afford **138** and **139** (Scheme 58).

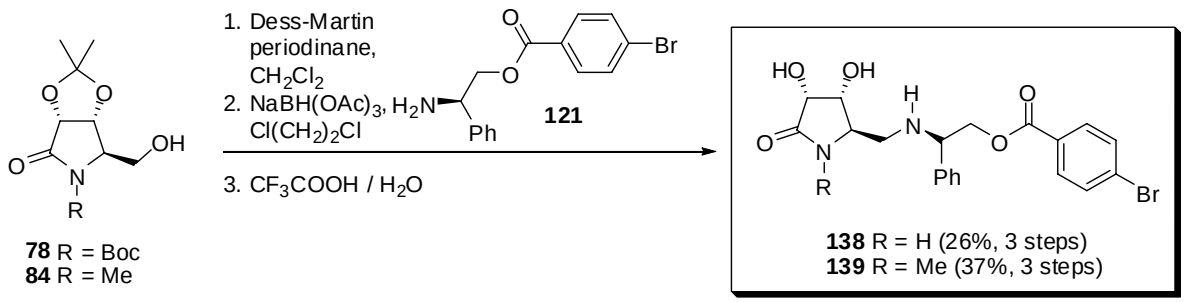

Scheme 58: Pyrrolidinone derivative from aromatic phenylglycinol esters.

These ester derivatives **138** and **139** were evaluated on the growth of glioblastoma LN18 and LNZ308 cells after exposition for 24, 48 or 72 hours, and were compared to **132** (Table 8).

	Conc	LN18 24h	LN18 48h	LN18 72h	LNZ308 24h	LNZ308 48h	LNZ308 72h
132	**100 μM**	5	17	31	11	15	24
	200 μM	67	48	68	60	33	56
	300 μM	92	95	97	87	78	96
138	**100 μM**	24	-	-	0	-	-
	200 μM	52	-	-	16	-	-
	300 μM	59	-	-	51	-	-
139	**100 μM**	4	52	-	6	15	-
	200 μM	49	89	-	50	61	-
	300 μM	92	95	-	98	99	-

Table 8: Time-course of growth inhibition of glioblastoma cells. Cells were exposed for 24, 48 or 72 hours to 0, 100, 200 or 300 μM of the various synthetic derivatives, then the MTT assay was performed for the last 2 hours of incubation. The % of residual mitochondrial activity was calculated as the ratio of absorbance of treated to control cells.

Increasing the time of exposure led to a significant improvement of growth inhibition, especially at low concentration of compounds. The *N*-methylpyrrolidinone derivative **139** displayed comparable anti-proliferative activity as its pyrrolidine analogue **132** whereas its inhibitory potency against α-mannosidase from jack bean and dGMII was higher. The non-substituted pyrrolidinone **138** was ineffective on inhibiting glioblastoma cell growth.

A dose-response evaluation (300 μM to 100 μM, 24 hours of exposure to the inhibitors) of the antiproliferative effects of the best derivatives **132** and **139** was carried out on both glioblastoma cell lines and on HCEC cells to compare the profile of inhibition (Scheme 59).

A)

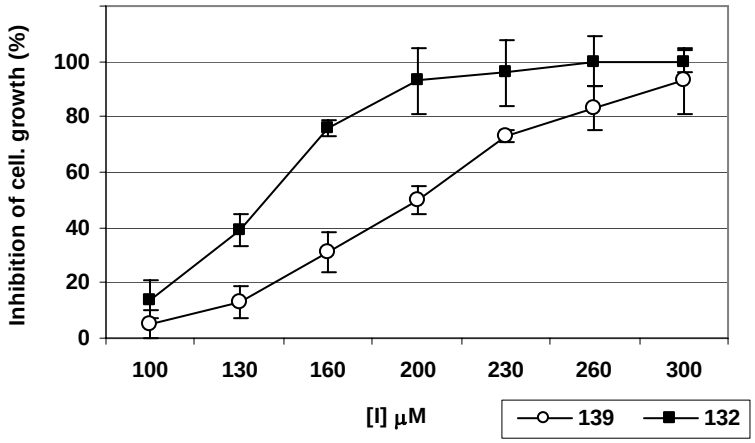

B)

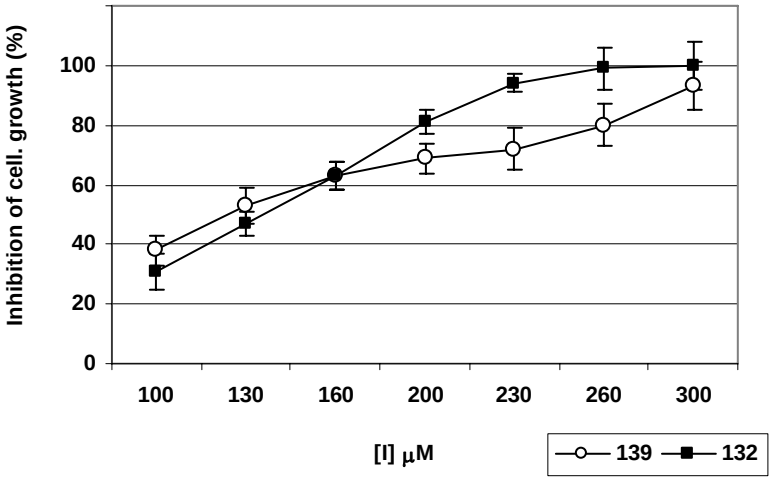

Scheme 59: Growth inhibition of human glioblastoma and HCEC cells by **132** and **139** after 24 hours of incubation. **A**) LN18 glioblastoma cells **B**) HCEC cells. Results are shown as means ± SD of triplicate wells of one representative experiment out of three.

Comparison of the inhibition profile on LN18 and LNZ308 cells revealed a slightly improved efficiency for the pyrrolidine derivative **132** (IC_{50} = 130 µM and 120 µM for **132** *vs* 200 µM and 200 µM for **139** toward LN18 and LNZ308 cells, respectively). Growth inhibition of LN18 is presented in Scheme 59A. The same experiment on HCEC cells showed similar growth inhibition for both derivative **132** and **139** (IC_{50} = 130 µM for **132** *vs* 120 µM for **139** toward HCEC cells) (Scheme 59B).

These data demonstrated that 4-bromobenzoate derivatives of α-mannosidases inhibitors **132** and **139** have the ability to inhibit glioblastoma cell growth, whereas Swa was ineffective under the same conditions. The aromatic ester promoted likely, the transport of the inhibitors across cells membrane and was probably cleaved by cellular esterases to release the more hydrophilic derivative **47** and **86**, respectively.

In view of these promising results, the mode of action of derivative **132** was studied in more detail.

3.6.2. Inhibition of DNA and proteins synthesis

3.6.2.1. Principle of incorporation of [^{3}H]-thymidine and [^{3}H]-leucine

Metabolic incorporation of tritiated thymidine ([^{3}H]-thymidine) into cellular DNA and tritiated leucine ([^{3}H]-leucine) into protein are widely used protocols to monitor rates of DNA synthesis and protein synthesis, respectively.

The cells are incubated in the presence of the inhibitor and then [^{3}H]-thymidine is added. During each cell division, the cells incorporate [^{3}H]-thymidine into its DNA. The incorporation of the labelled thymidine is thus proportional to the multiplication of the cells. Then, the amount of radioactivity is counted in a scintillation counter.

The same strategy is used with tritiated leucine. Indeed, during each cell division, the cells incorporate the labelled leucine into their proteins, which allow a quantification of the proteins newly synthesized.

3.6.2.2. Results of the inhibition of DNA and Protein synthesis

We evaluated whether **132** had the potential to diminish cell growth by inhibiting the synthesis of DNA and of proteins by glioblastoma cells. The evaluation of the incorporation of [^{3}H]-thymidine and [^{3}H]-leucine, after 6 hours of exposure of the cells to compound **132**, demonstrated that **132** inhibited thymidine incorporation (DNA synthesis) (Scheme 60A) at slightly lower concentration and to a higher extent than leucine incorporation (protein synthesis) (Scheme 60B). These results suggested that this derivative acted initially by

inhibiting DNA synthesis (93% inhibition at 300 μM in LN18) which then led to a decrease of protein synthesis (82% at 300 μM in LN18) and ultimately resulted in diminished cell survival.

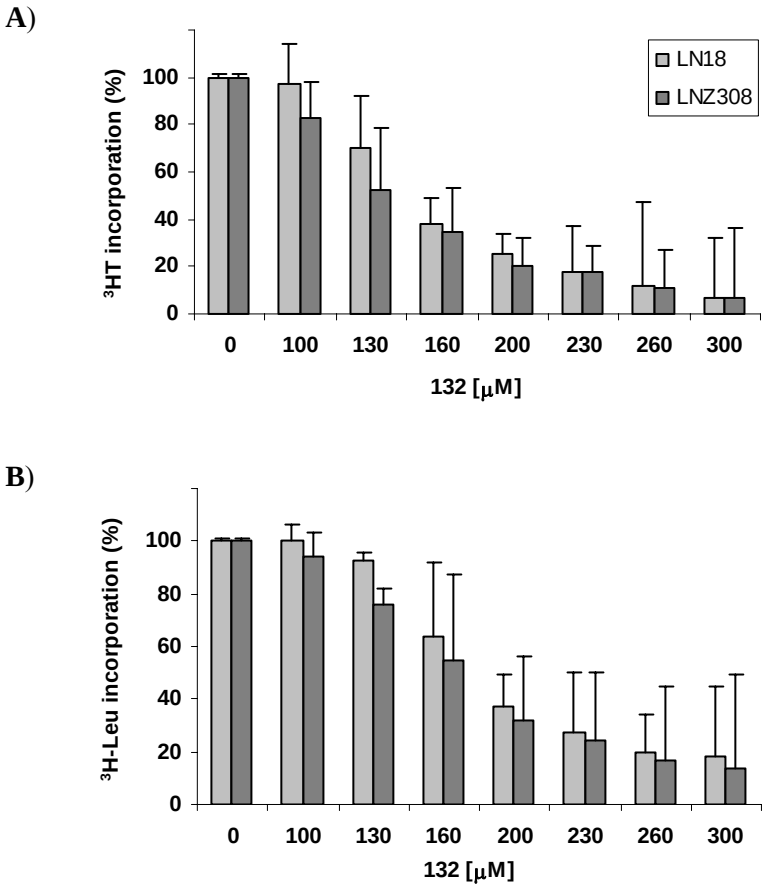

Scheme 60: Inhibition of DNA and protein synthesis by **132** in human glioblastoma cells: LN18 are represented with light gray bars and LNZ308 with dark gray bars. Cells were exposed for 6 hours to increasing concentrations of **132**. The incorporation of either **A**) radioactive thymidine (^{3}HT) or **B**) radioactive leucine (^{3}H-Leu) was performed for the last 2 hours. Results are shown as means ± SD of triplicate wells of one representative experiment out of three.

*3.6.3. Evaluation of **132** toward melanoma and fibroblasts cells*

We further evaluated whether compound **132** was able to inhibit DNA and protein syntheses and survival in human cancer cells originating from a tumor different from glioblastoma, the melanoma cells (Me237 and Me275).

A)

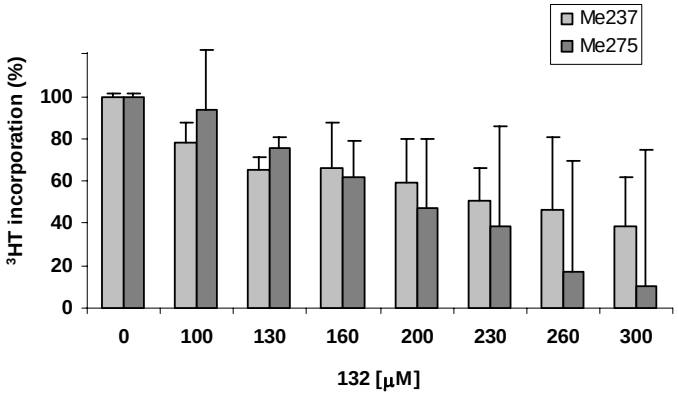

B)

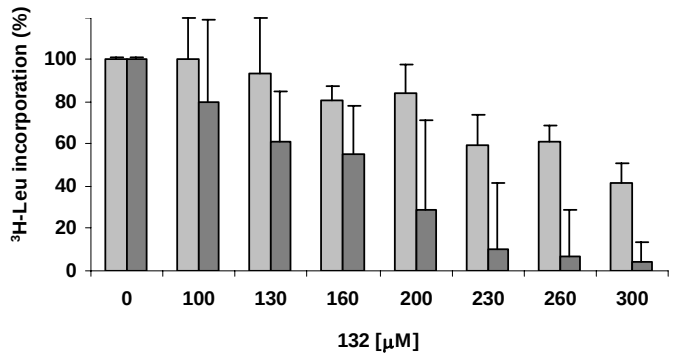

C)

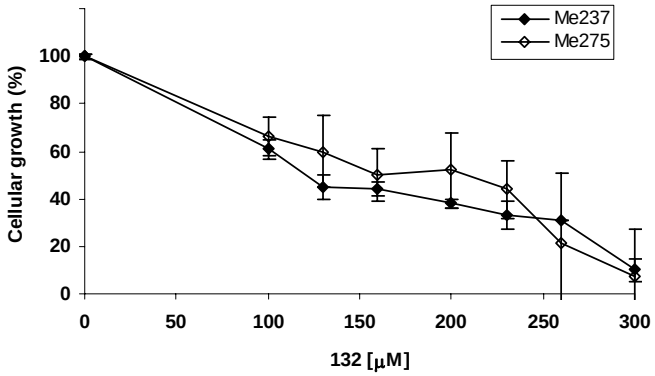

Scheme 61: Inhibition by **132** of DNA synthesis (**A**), protein synthesis (**B**) and growth (**C**) in human melanoma cells: Me237 are represented with light gray bars and Me275 with dark gray bars. Cells were exposed to increasing concentrations of **132**. The incorporation of radioactive thymidine (^{3}HT) or radioactive leucine (^{3}H-Leu) were performed for the last 2 hours after 6 hours of incubation of **132**. MTT assay was performed after 24 hours of incubation of **132**. Results are shown as means ± SD of triplicate wells of one representative experiment out of three.

Exposure of human Me237 and Me275 melanoma cells for 6 hours to **132** resulted in a blockage of DNA (Scheme 61A) and protein syntheses (Scheme 61B). After 24 hours, the number of metabolically active melanoma cells decreased as determined by the MTT assay (Scheme 61C).

Finally, the sensitivity of human fibroblasts, a model of non-tumoral cells, was evaluated with increased concentration of **132** (Scheme 62).

A)

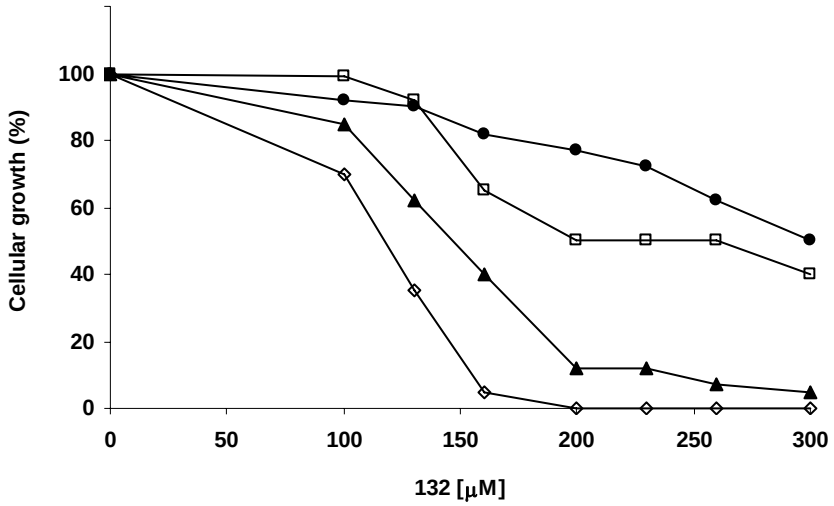

B)

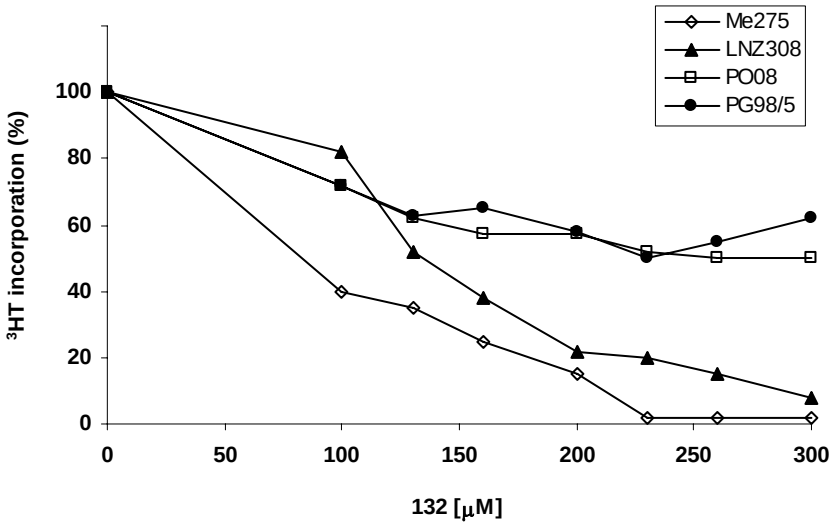

Scheme 62: Comparison of the growth inhibition induced by **132** in human primary fibroblasts (PG98/5 and PO08) and human tumor cells (LNZ308 glioblastoma and Me237 melanoma cells). Cells were exposed to increasing concentrations of **132**. **A**) Incorporation of radioactive thymidine (^{3}HT) was performed for the last 2 hours after 6 hours of incubation of **132** and **B**) the MTT assay was performed after 24 hours of incubation of **132**. Results are shown as means ± SD of triplicate wells of one representative experiment out of three.

Fibroblasts were less sensitive to **132** than glioblastoma and melanoma cells for the inhibition of DNA synthesis after 6 hours of exposure (Scheme 62A) or survival after 24 hours of incubation (Scheme 62B) suggesting some cell selectivity of **132** between tumoral and nontumoral cells.

*3.6.4. Physicochemical parameters of compounds **47**, **86**, **132** and **139***

In view of the different activities of the esters **132** and **139** compared to their parent alcohols **47** and **86**, evaluation of their physicochemical parameters was performed in collaboration with Dr. B. Faller at NOVARTIS, Basel. Data were collected for: solubility, pKa, permeability,[197] and LogPo/w,[198] the octanol-water partition coefficient which measures the hydrophobicity and/or hydrophilicity of the substance. Table 9 summarizes the collected data.

pKa[c)]
Experimental (calculated)[d)] values

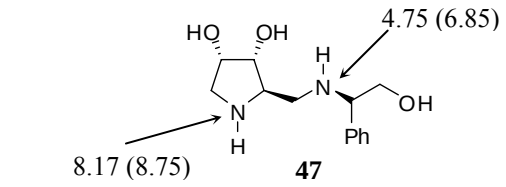

47

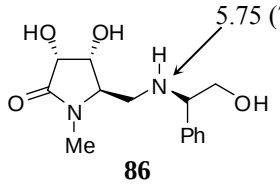

86

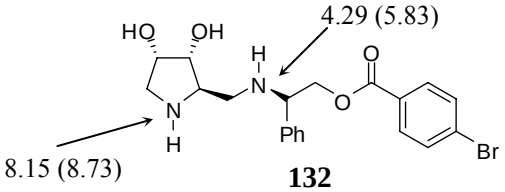

132

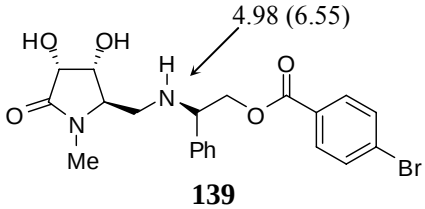

139

LopPo/w, Permeability and Solubility

		47	**86**	**132**	**139**
LogPo/w[a)]		2.4	n.d.	3.3	3.5
Permeability[b)]		n.d.	n.d.	H	H
Solubility (μg/ml)	pH 1.0	n.d.	n.d.	449	450
	pH 6.8	n.d.	n.d.	289	299

n.d. = not determined
a) Range of LogPo/w is measured between [-2;7]
LogPo/w > 5 = product toxic, due to a high lipophilicity
b) L=low; M=Medium; H=High
c) pKa values of the conjugate acids
d) calculation program : ACD/pKa DB release version 9.04

Table 9: LogPo/w, pKa, solubility and permeability across artificial membrane of compounds **47**, **86**, **132** and **139**.[199]

[197] Wohnsland, F.; Faller, B. *J. Med. Chem.* **2001**, *44*, 923-930.
[198] Faller, B.; Grimm, H. P.; Loeuillet-Ritzler, F.; Arnold, S.; Briand, X. *J. Med. Chem.* **2005**, *48*, 2571-2576.
[199] Measurement performed by Xavier Briand, Novartis, Basel.

In accordance with the previous data on growth inhibition of tumor cells, ester derivatives **132** and **139** are more lipophilic than the parent alcohols (LogPo/w = 3.3 for **132** *vs* 2.4 for **47**). LogPo/w of **86** was not obtained because of low absorbance intensity. The high permeability of compounds **132** and **139** place them as potential candidates for drug development.

Discrepancies were noticed between the calculated and the experimental pKa values for the amino group on the lateral chain (two pKa units for all compounds). The stronger acidity of this ammonium group compared with the expected value may result from a poor solvatation due to the presence of the aromatic ring. These experimental data for pKa values could account for the difference of solubility observed between derivatives **132** and **139** in pH 7 buffer, which corresponds to the conditions used in the MTT assay. Indeed, **132** in its ammonium form seemed to be more soluble than its neutral pyrrolidinone analogue **139**.

In summary, a series of functionalized pyrrolidine and pyrrolidinone inhibitors of α-mannosidases have been prepared and evaluated. Derivatives **47** and **86** are potent, selective and competitive inhibitors of α-mannosidase from jack bean and dGMII. However, they did not inhibit the growth of human cancer cells. It was postulated that their hydrophilic character prevented their internalization by cells. In support of this hypothesis, the more lipophilic esters **132** and **139** inhibited the growth of human glioblastoma and HCEC cells more efficiently than Swa, a potential antitumoral agent (Scheme 59). Moreover, compound **132** inhibited the growth of glioblastoma and melanoma cells more than the growth of fibroblasts, as models of non-tumoral cells (Scheme 62). Measurements of the lipophilicity supported these observations as the LogPo/w values were higher for the ester derivatives than for the parent alcohols (Table 9).

In order to get more insights into the mode of action of our lead compounds **47** and **86**, evaluation of their inhibitory activities on cellular α-mannosidases was envisaged.

3.6.5. Human α-mannosidases

3.6.5.1. Various human α-mannosidases

As already presented in the introduction, there are several cellular α-mannosidases II that display similar molecular weight and sequences at their active sites.

These α-mannosidases II can be separated into three groups:
(i) The acidic/lysosomal (MAN2B1, EC 3.2.1.24) α-mannosidases with the human lysosomal α-mannosidase II widely distributed and active at pH 4-4.5. The single chain precursor has a molecular weight of 110kD, which is processed to 3 fragments of 70, 42 and 15 kD.[200] Increased expression of this enzyme has been previously demonstrated in extracts of glioblastoma and correlated with malignancy.[201]

(ii) The intermediate/Golgi (MAN2A1, EC 3.2.1.114) α-mannosidases with the human Golgi α-mannosidase II, active at pH 5.5-6, with a molecular weight of 130 kD and with its gene located to chromosome 5.[202]

(iii) Neutral/cytosolic (MAN2C1/6A8) α-mannosidases with the human cytosol α-mannosidase II recently cloned as the 6A8-mab-reactive protein, active at neutral pH. Its molecular weight has been evaluated at 120 kD.[203] This enzyme is inhibited by Swa with less efficiency than Golgi α-mannosidase with IC_{50} of 20 μM *vs* 20 nM for Golgi α-mannosidase II.

[200] Beccari, T.; Stinchi, S.; Orlacchio, A. *Bioscience Reports* **1999**, *19*, 157-162.
[201] Wielgat, P.; Walczut, U.; Szajda, S.; Bien, M.; Zimnoch, L.; Mariak, Z.; Zwierz, K. *J. Neurooncol.* **2006**, *80*, 243-249.
[202] Moremen, K. W.; Robbins, P. W.; *J. Cell. Biol.* **1991**, *115*, 1521-1534.
[203] Li, B.; Wang, Z. Z.; Ma, F. R.; Shi, G. X.; Zhang, L. X.; Zeng, X.; Liu, Y.; Zhao, F. T.; Zhu, L. P. *Eur. J. Biochem.* **2000**, *267*, 7176-7183.

3.6.5.2. Inhibitory activities toward human α-mannosidases

The inhibitory potency of compounds **47** and **86** on α-mannosidases extracts from human glioblastoma and HCEC was determined and compared to the inhibitory ability of Swa.[204]

A first set of measurements was performed for derivatives **47**, **86** and Swa on glioblastoma cell lines LNZ308, LN18 and HCEC cells at three different pH values, with a pre-incubation time of 10 minutes of inhibitor in cell extracts at 25°C (Table 10).

IC_{50} (μM)

	LNZ308			**LN18**			**HCEC**		
	pH 5.0	**pH 6.5**	**pH 7.3**	**pH 5.0**	**pH 6.5**	**pH 7.3**	**pH 5.0**	**pH 6.5**	**pH 7.3**
Swa(**16**)	0.03	4	4	25	4	4	0.05	4	4
47	30	1000	500	1000	> 1000	750	75	500	350
86	< 2.5	500	>1000	500	750	> 1000	2.5	750	> 1000

Table 10: Inhibitory ability of Swa (**16**), compounds **47** and **86** on human α-mannosidases from glioblastoma and HCEC extracts at three different pH values. Pre-incubation of inhibitor in cell extracts: 10 minutes at 25°C.

For all cell lines, a decrease of the pH resulted in a higher inhibition. The pH for further experiments was thus fixed at 5.0 and it was also anticipated that increasing the pre-incubation time to 30 minutes and the temperature to 37°C could result in improved inhibition (Table 11).

The first generation inhibitor **47** presented a moderate inhibitory potency on α-mannosidases from both glioblastoma cell lines (IC_{50} = 50 μM) and HCEC (IC_{50} = 25 μM, Table 11). As observed for the inhibition of the model enzymes (jack bean α-mannosidase and dGMII), the homologated analog **89** was much less active on enzymes of all extracts. Introduction of an oxo moiety at the C(5) position of the five membered ring did not afford significant improvement of the inhibition (**80**). However, the *N*-methyl pyrrolidinone **86** displayed potent inhibitory ability on α-mannosidases from LNZ308 and LN18 (IC_{50} = 500 nM and 2.0 μM, respectively) and from HCEC (IC_{50} = 500 nM).

[204] Fiaux, H.; Kuntz, D. A.; Hoffman, D.; Janzer, R. C.; Gerber-Lemaire, S.; Rose, D. R.; Juillerat-Jeanneret, L. ; Functionalized pyrrolidine inhibitors of human α-mannosidase II in cancer: optimizing the fit to the active site, paper in preparation.

	IC_{50}		
Compounds	**LNZ308**	**LN18**	**HCEC**
Swa (**16**)	20 nM	50 nM	10 nM
47	50 μM	50 μM	25 μM
89	500 μM	750 μM	200 μM
80	50 μM	350 μM	75 μM
86	**500 nM**	**2.0 μM**	**500 nM**
Ethyl 4-bromobenzoate	n.i.	n.i.	n.i.
Acid 4-bromobenzoate	n.i.	n.i.	n.i.
128	300 μM	n.d.	n.d.
130	250 μM	n.d.	n.d.
131	350 μM	n.d.	n.d.
132	75 μM	200 μM	75 μM
133	> 1 mM	> 1 mM	> 1 mM
134	150 μM	750 μM	75 μM
137	300 μM	n.d.	n.d.
139	**7.5 μM**	**75 μM**	**750 nM**

n.i. = no inhibition n.d. = not determined

Table 11: Inhibitory ability (IC_{50}) on human α-mannosidases from glioblastoma and HCEC extracts at pH 5.0. Pre-incubation of inhibitors in cell extracts: 30 minutes at 37°C.

Amide **137** or ester derivatives **128**, **130**, **131** and **133** as well as the corresponding 4-bromobenzoate ester **132**, **134** and **139** presented a decreased inhibitory ability on glioblastoma cell extracts. These data were expected as the loss of interactions between the primary alcohol and residues of the active site of the enzyme decreased the affinity of the inhibitors for the enzyme. Nevertheless, a moderate inhibition was maintained for compound **139** (IC_{50} = 7.5 μM and 75 μM on LNZ308 and LN18 extracts, respectively) strengthening the hypothesis that the ester linkage is cleaved by cellular esterases to release the free primary alcohol. Within the incubation time, this process may only be partial, resulting in a higher IC_{50} values than for the parent inhibitors **47**, **80** and **86**. Interestingly, in HCEC cells this hydrolytic process seemed to be more rapid as the activity of the 4-bromobenzoate derivatives was similar to the inhibition induced by the parent alcohols (IC_{50} = 75, 75 and 0.75 μM for **132**, **138** and **139** *vs* 25, 75 and 0.50 μM for **47**, **80** and **86**).

These data correlated with the inhibitory abilities measured on dGMII, a reliable model of human α-mannosidases II. The additional interactions with the active site of dGMII observed for derivative **86** may account for the improved inhibitory potency on dGMII and human α-mannosidase in comparison with the lead inhibitor **47**. However, Swa presented higher potency than our derivatives.

Nevertheless the pyrrolidinone derivatives **86** revealed an improved efficacy in comparison with our first generation inhibitor **47** and thus constitute new promising scaffolds for the inhibition of human cellular α-mannosidases. Furthermore and for the first time in our group, it was shown to be active toward human enzymes.

3.6.5.3. Property of human α-mannosidases

In order to get additional information on the nature of the cellular targets of our derivatives, gel-filtration chromatography was performed on cellular extracts from glioblastoma and HCEC cells.

Principle of gel-filtration:

The principle of this experiment was to separate proteins inversely to their apparent molecular weight. As sepharose 4B allows fractioning in the range of 60 to 20'000 kD, this gel was selected as stationary phase (Scheme 63).

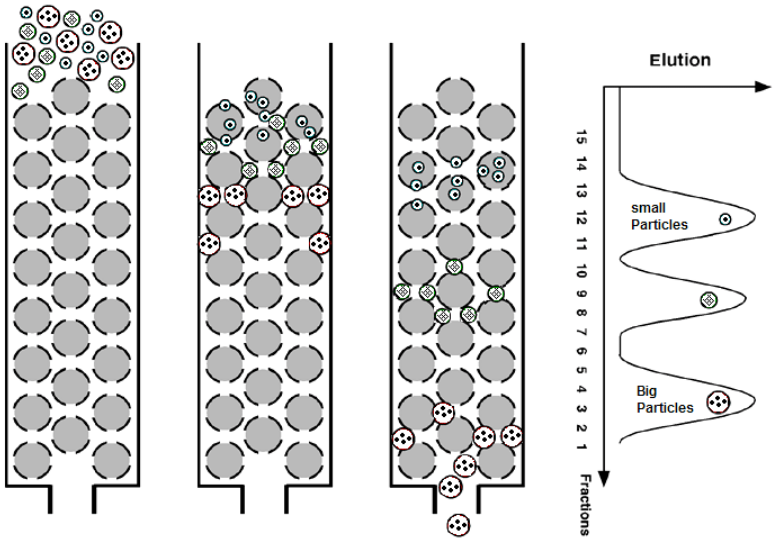

Scheme 63: Principle of gel-filtration.

Results for gel-filtration:

Scheme 64 represents the results obtained for LNZ308 cells line extracted with a detergent. The other cells displayed the same elution profile. For all tested cell lines (LN18, LNZ308 and HCEC) the main enzymatic activity was easily extracted in the presence as well as in the absence of detergent and migrated as a protein of apparent molecular weight of about 120 kD.

The molecular weight value obtained from this experiment is in accordance with the molecular weights reported in the literature for α-mannosidases II (3.6.5.1). Nevertheless, it was not possible to distinguish between lysosomal, cytosolic or Golgi α-mannosidases II.

The main peak displayed an optimum activity at neutral pH and was inhibited by our lead molecule **86** (IC_{50} = 500 µM, pH 6.5) in agreement with the values obtained in cellular extracts (Table 10, page 99).

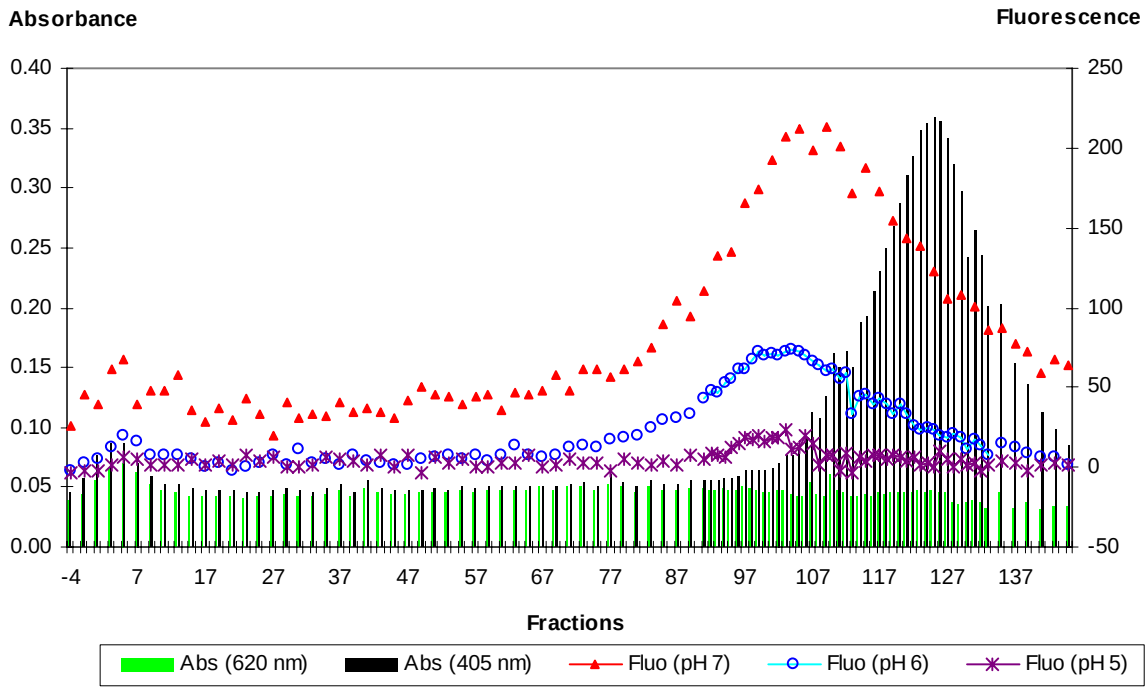

Scheme 64: Gel-filtration on Sepharose 4B of LNZ308 glioblastoma cells extracts in presence of detergent. Absorbance of blue dextran (2'000 kD) and Haemoglobin (60 kD) was measured at 620 and 405 nm, respectively. Kinetic measurement was performed during 30 min, at 3 different pH values (5.0; 6.5 and 7.3), with α-mannoside-4-methyl-umbelliferyl as substrate.

4. Conclusions and Perspectives

The first lead compound **47** was co-crystallized in the active site of Golgi α-mannosidase II from *Drosophila melanogaster* which presents a high sequence homology with the human enzyme. The x-ray structure revealed a zinc-binding site and the interactions between the inhibitor and specific amino acids of the active site.

This study combined with docking experiments allowed us to design new inhibitors by introducing polar substituents on the C(5) position of the pyrrolidine ring to form the pyrrolidinone derivative **86** with an additional methyl group on the amine of the ring. The x-ray structure of dGMII:**86** complex revealed two additional interactions between the carbonyl group of the pyrrolidinone ring and Asp472 and Tyr267 residues of the protein which can account for the higher affinity of this new lead (IC_{50} = 80 μM for **47** *vs* 500 nm for **86**).

The two leads have been evaluated as anti cancer agents and their effects were determined on human glioblastoma cells using the MTT assay, which determines the number of metabolically active cells. Unfortunately, these compounds were not able to inhibit cellular growth. As the hydrophilic character of these molecules may hinder their transport across cell membranes, we prepared analogues that could improve cell penetration. Different lipophilic groups have been introduced and we have discovered that introduction of a 4-bromobenzoyl moiety resulted in an improvement of cellular uptake, leading to growth inhibition of cancer cells. A dose-response evaluation (100 μM to 300 μM) of the anti-proliferative effects on glioblastoma cells demonstrated that (2*R*)-2-({[(2*R*,3*R*,4*S*)-3,4-dihydroxypyrrolidin-2-yl]methyl}amino)-2-phenylethyl 4-bromobenzoate **132** and (2*R*)-2-({[(2*R*,3*R*,4*R*)-3,4-dihydroxy-1-methyl-5-oxopyrrolidin-2-yl]methyl}amino)-2-phenylethyl 4-bromobenzoate **139** induced complete cellular death at 300 μM concentration. The physicochemical profile of these derivatives revealed that the ionization state, at the pH used for the biological assay, may not be the same which can account for the slight difference of inhibition profile. Furthermore, melanoma cells, another tumoral cells, HCEC cells, an immortal non-tumoral cells line and fibroblasts, a model for non tumoral cells were also exposed to these derivatized inhibitors. Evaluation of the inhibition of incorporation of [^{3}H]-leucine and [^{3}H]-thymidine revealed that the synthesis of DNA was stopped before the synthesis of new proteins.

The exposure of tumor cells to ester derivatives results in two advantages: first, the hydrolysis of the ester could release molecules more active toward mannosidases (**47** and **86**) than the corresponding prodrugs (**132** and **139**) and secondly, the hydrophilic character of the active molecules following their intracellular hydrolysis by esterases can prevent their passive diffusion out of the cells. Therefore, functionalized pyrrolidine represent promising lead agents able to control the progression of human glioblastoma and melanoma, to inhibit DNA and protein synthesis and to display some selectivity toward tumoral cells compared to non-tumoral cells.

The inhibitory potency of our new derivatives on α-mannosidases from human glioblastoma and HCEC extracts was determined and compared to the activity of Swa. For all cell lines, a decrease of the pH of the medium resulted in a higher inhibitory activity. The first generation inhibitor **47** presented a moderate inhibitory potency on α-mannosidases from both tumoral cells whereas introduction of an oxo moiety at C(5) position and a methyl group on the pyrrolidinone system (**86**) resulting in potent inhibitory activity on human α-mannosidases (IC_{50} = 50 μM toward LNZ308 glioblastoma or HCEC cells for **47** *vs* 500 nM for **86**).

Migration of the α-mannosidases extracted from human glioblastoma cells (LNZ308 and LN18) and HCEC cells demonstrated an apparent molecular weight of about 120 kD by gel filtration. Nevertheless, further experiments will be required to determine the precise cellular target of our derivatives (Golgi α-mannosidase II, cytosolic α-mannosidase or lysosomal α-mannosidase).

Additional investigations will be performed to determine the localisation (i.e. lysosome, Golgi, or cytosol) of the α-mannosidases II inhibited by our derivatives and other cancer cell lines will be tested. Furthermore, lectin arrays recently became commercially available (Qproteome, Quiagen) to determine glycosylation state of eukaryotic proteins, based on lectin spotting on array slides. Preliminary results[205] using micro-arrays donated by Quiagen, in the context of a field test, have given promising information but this study is still under investigation. The modifications of the glycosylation pattern of cellular target proteins may be estimated using commercially available carbohydrate-selective biotin-labelled lectins after

[205] Measurements performed in collaboration with C. Chapuis, CHUV, **2006**.

separation of the cellular proteins in polyacrylamide gels and transfer onto a nylon membrane that will be the object of future studies.

Improving the cell selectivity of these derivatives by conjugation to targeting moieties may also be of high interest in the context of this study.

5. Experimental Part

5.1. General Methods

5.1.1. Crystallography

Crystallization, data collection and structural refinement were carried out essentially as outlined by Kuntz *et al*.[41a] with the exceptions noted below.

Crystals of dGMII were grown overnight, washed with phosphate buffered solution,[181] and soaked with 10 mM of inhibitors for at least 3 hours. In case of **57**, crystals were soaked in Tris-buffered reservoir solution without phosphate washing. Data were collected on Beamline 191D at the Advanced Photon Source for crystals of **47** and **62** and at Beamline A1 at the Cornell High Energy Synchrotron Source for **57** and **86**. 400 Frames with 0.5 degree oscillation/frame were collected. To obtain a data set with good completeness, data on 2 crystals of **47** were collected and the data merged with Scalepack.

5.1.2. Preparation of structures and parametrization of Glide

The 10 structures were retrieved from the PDB (PDB codes: 1HWW, 1HXK, 1PS3, 1R33, 1R34, 1TQS, 1TQT, as well as the newly determined 2F18, 2F1A, 2F1B) and prepared using Maestro 7.0[206] from Schrödinger.

Water molecules were removed from the x-ray structures and the resulting proteins were aligned based on the α-carbon trace. Hydrogen atoms were added to both protein and ligands and bonds between amino acids and the zinc atom were broken. Charges and atom types were assigned automatically with Macromodel/OPLS2003 to the protein and the ligands. Neutral zones (as defined in Glide) of 10-20 Å around the ligands were defined and the inhibitor/proteins were refined using the local optimization procedure proposed in Glide. Then, charges of the catalytic site residues were corrected following a DFT[207] calculation at the B3LYP/6-31G** level of theory (using Jaguar 6.0[208]) carried out on a truncated site consisting of His90, His471, Asp92, Asp204 and Zn. The zinc parameters, obtained from the

[206] Maestro 70, Schrödinger LLC: Portland OR 2004 http://www.schrodinger.com.
[207] DFT calculation = Density Functional Theory calculation.
[208] Jaguar 60, Schrödinger LLC: Portland OR 2004 http://www.schrodinger.com.

literature,[209] were added to the OPLS2003 force field definition and the specific charge, obtained with the DFT calculation, was assigned to the zinc atom. Finally, the structures of the ligands were all optimized through energy minimization (Tripos force field) prior to the docking.

At this stage, the proteins and ligands were ready for docking. Grids were prepared for each protein with the exact same center and size of 40 Å around the zinc atom. Moreover, a constraint that forced the interaction with the metal ion was included. During the grid preparation, a specific keyword (CMAE) has to be employed to maintain the partial charges computed from DFT. Four hours per protein were needed to do the preparation, refinement and grid calculation on an SGI R16K. The ligands were minimized using the OPS2003 forcefield and submitted to Glide for docking. 25 runs were performed for each inhibitors in one protein. In order to ensure convergence, the following parameters were used and fixed to their mamimum values: ligvdwscale factor 1.0; maxkeep 50,000; maxconf 10,000; nreport 5,000; maxref 4,000; scorecut 100. Using these parameters, the docking of the ten inhibitors on a single receptor was performed in an average time of 44 minutes on an SGI R16K. During the docking, a specific keyword (reference) was needed to report the RMSD values.

5.1.3. Biological Evaluation

5.1.3.1. Inhibition of purified plant glycosidases

The experiments were performed essentially as previously described by Brandi et al.[210] Briefly, 0.01 to 0.5 units/ml of enzyme (Aldrich, 1 unit = 1 enzyme unit liberates 1 μmol of glycoside per minute from *p*-nitrophenyl glycoside) and various concentrations of inhibitor were pre-incubated for 10 or 30 min at 37°C. The kinetic reaction, measured at 37°C, started by addition of the appropriate *p*-nitrophenyl glycoside substrate (Sigma) buffered to the optimum pH of the enzyme. The reaction was stopped by addition of 2.5 volumes of 0.2 M sodium borate buffer (pH 9.8). The *p*-nitrophenolate formed was quantified at 410 nm and IC_{50} were calc. or double-reciprocal plots (Lineweaver and Burk) were used to determine the inhibition kinetics values.

[209] Tiraboschi, G.; Gresh, N.; Giessner-Prettre, C.; Pedersen, L. G.; Deerfield, D. W. *J. Comp. Chem.* **2000**, *21*, 1011-1039.
[210] Brandi, A.; Cicchi, S,; Cordero, F. M.; Frignoli, B.; Goti, A.; Picasso, S.; Vogel, P. *J. Org. Chem.* **1995**, *60*, 6806-6812.

5.1.3.2. Cell culture and Treatments.

Human LN18 and LNZ308 glioblastoma cell lines (a kind gift of A. C. Diserens, Neurosurgery Department, CHUV, Lausanne, Switzerland) were routinely maintained in Dulbecco's Modified Eagle Medium (DMEM, Gibco, Invitrogen, Basel, Switzerland) containing 4.5 g/l glucose, 5% foetal calf serum (FCS, Gibco) and antibiotics. Human Me237 and Me275 melanoma cell lines (a kind gift of D. Rimoldi, Ludwig Institute, Lausanne, Switzerland) were grown in RPMI medium (Gibco) containing 10% FCS and antibiotics. Human primary fibroblasts were prepared from surgical skin (PG 98/5, a kind gift of M. Benattan, Dermatology Department, CHUV, Lausanne, Switzerland) or lung (PO 08, a kind gift of J.-D. Aubert, Pneumology Department, CHUV, Lausanne, Switzerland) biopsies derived in the CHUV using the explant technique, and were grown in DMEM medium containing 4.5 g/l glucose, 10% FCS and antibiotics. HCEC cells are immortalized human brain-derived endothelial cells (a kind gift of D. Stanimirovic, Ottawa, Canada) and were grown in DMEM medium containing 4.5 g/l glucose, 10% FCS and antibiotics.

For the experiments, cells were grown in 48-wells plates (Costar, Corning, NY) for 24 to 72 hours in presence of FCS until 60-75% confluence, then exposed for the indicated time to increasing concentrations of the synthetic derivatives (from 0 to 300 μM, stock solutions in methanol/PBS 1/20) in fresh complete medium. Then either metabolically active cells were quantified using the MTT assay, or DNA synthesis or protein synthesis as evaluated using [^{3}H]-Thymidine or [^{3}H]-leucine incorporation. Experiments were performed in triplicate wells and were repeated at least three times. Means $\pm$ sd have been calculated.

5.1.3.3. Evaluation of Cell Proliferation by the MTT Assay

MTT ((3,4,5-dimethylthiazol-yl)-2,5-diphenyl tetrazolium, Sigma, Buchs, Switzerland) was used to quantify the number of metabolically active cells. Following treatment with pyrrolidine derivatives, the cells were exposed to 0.2 mg/ml MTT in DMEM medium for 2 hours. The supernatant was aspirated and the precipitated formazan was dissolved in HCl 0.1 N in 2-propanol and quantified at 540 nm in a multiwell plate reader (iEMS Reader MF, Labsystems, Bioconcepts, Switzerland).

5.1.3.4. Evaluation of DNA and Protein Synthesis

Thymidine and leucine incorporation were used to assess DNA and protein syntheses, respectively. [^{3}H]-Thymidine (Amersham-Pharmacia, Dübendorf, Switzerland, 400 nCi/puit/ml) or [^{3}H]-Leucine (American Radiolabeled Chemicals, St-Louis MO, USA, 400 nCi/puit/ml) were added to treated or control cells for the last 2 hours of incubation with the pyrrolidine derivatives. The cell layer was washed, precipitated with 10% trichloracetic acid and the precipitate was dissolved in 1% SDS in NaOH 0.1 N. Then 5 ml of scintillation cocktail (Optiphase, Wallac, Regensdorf, Switzerland) was added, and the radioactivity was measured in a β-counter (WinSpectral, Wallac).

5.1.3.5. Evaluation of molecular weight of α-mannosidases

Confluent layers of cells grown on a plate of Petri (9 cm, FalconL) were washed with PBS (Phosphate buffer saline, pH 7.3) and extracted in 0.55 ml of PBS-0.1% Triton X-100 (Fluka, Switzerland). After centrifugation at 800 g for 5 min, 2.5 mg Blue Dextran (2000 kD, Pharmacia, gel filtration kit, Switzerland) and 2.1 mg bovine haemoglobin (67 kD, Fluka, Switzerland) were added to 0.5 ml of the cell extract supernatant. The solution was applied to a 0.9 cm x 115 cm Sepharose 4B column (Pharmacia, Amersham, Genf, Switzerland) in PBS-0.1% Triton at 4°C. Collected fractions (350 µl) were measured at 620 nm (Blue Dextran) and 405 nm (Haemoglobin) and assayed for enzymatic activities at three different pH values (5.0, 6.5 and 7.3) using the fluororogenic substrate 4-Methyl-Umbelliferyl-α-D-mannopyranoside (Fluka) by measuring the fluorescence increase in a multiwell plate reader (Cytofluor, PerSeptive BioSystems) thermostated at 37 °C, λ_{ex} = 360 nm; λ_{em} = 460 nm, for 30 min.

5.2. Synthesis

5.2.1. Reagents and Solvents

All commercially available reagents (Fluka, Aldrich, Acros) were used without further purification.

Technical solvents were used for extraction without any purification. For reactions requiring anhydrous conditions, dry solvents were bought (Fluka) or filtered prior to use (Innovative Technology).

In absence of any particular notification, experiments were carried out under argon atmosphere.

5.2.2. Chromatography techniques

Reactions were monitored by thin layer chromatography (Merck silica gel $60F_{254}$ plates). Revelation was carried out by UV light (254nm) and $KMnO_4$ [3g of $KMnO_4$, 20g of K_2CO_3, 0.25 ml of AcOH and 300 ml of H_2O] or Pancaldi [21g of $(NH_4)_6Mo_4$, 1g of $Ce(SO_4)_2$, 31 ml of H_2SO_4 and 470 ml of H_2O] reagents. Purifications were performed by flash chromatography (Fluka silica gel 60, 230-400 mesh, 0.04-0.063mm).

Analytical high-performance liquid chromatography (HPLC) was performed on a Waters 600 apparatus, equipped with a Waters absorbance detector set at 214 nm and C_4, C_8 and C_{18} Grace Vydac columns. Elution was performed using the following gradient over 30 min, 100% (0.9% CF_3COOH in H_2O) to 100% (0.9% CF_3COOH in MeCN).

5.2.3. Analysis

^{1}H-NMR spectra were recorded on Bruker ARX-400 and DPX-400 spectrometers at 400 MHz. Chemical shifts δ(H) were assigned relatively to the reference solvent peak in ppm (MeOD: δ(H) = 3.34; $CDCl_3$: δ(H) = 7.27). Coupling constants *J* are given in Hz.
Multiplicity: s = singlet, d = doublet, t = triplet, b = broad.

^{13}C-NMR spectra were recorded on Bruker ARX-400 and DPX-400 spectrometers at 101 MHz. References for solvent used in ppm (MeOD: δ(C) = 49.0; $CDCl_3$: δ(C) = 77.0).

IR spectra were recorded on a Perkin Elmer Paragon 1000 FT-IR spectrometer.

UV spectra were recorded on a Kontron Uvikon 810 CW spectrophotometer.

Optical rotations were recorded at 25°C on a *J*asco P-1020 polarimeter. [α] values are given in units of 10^{-1}deg cm^2g^{-1}.

Mass spectra were recorded on a GC-MS spectrometer (Nermag R-10-10C in chemical ionisation mode with NH_3), on a MALDI-TOF spectrometer (Axima-CFR^{+}, Kratos, Manchester), on a ESI-Q spectrometer (Finnigan SSQ 710C, Thermoquest, UK) and on a ESI-QT of Ultima spectrometer (Micromass, Manchester).

Microanalyses were performed by Ilse Beetz Laboratory (Kronach, Germany).

5.2.4. Synthesis Procedures

Procedure 1: General method for the reductive amination

To a solution of aldehyde RCHO (1.0 eq) in anhydrous 1,2-dichloroethane were added a primary amine R'NH_2 (1.0 - 1.5 eq) and sodium triacetoxyborohydride (1.4 eq) portionwise. The mixture was stirred at 25°C for 12 hours. After complete consumption of starting aldehyde (tlc monitoring), the solution was poured into a saturated aqueous solution of $NaHCO_3$. The aqueous layer was extracted 3 times with EtOAc and the combined organic extracts were dried over $MgSO_4$. Solvent evaporation *in vacuo* and flash chromatography on silica gel afforded pure diamines.

Procedure 2: General method for deprotection of Boc and acetonide groups

Procedure 2a: A 5-10 % solution of protected diamine in CF_3COOH/H_2O (4/1) was stirred at 25°C for 1-12 hours. After evaporation *in vacuo*, the residue was purified by flash chromatography on silica gel (CH_2Cl_2/MeOH or MeCN/NH_4OH).

Procedure 2b: A 5-10 % solution of diamine in 4M HCl_{aq} was stirred at 25°C for 1-12 hours. After evaporation in *vacuo*, the residue was purified by flash chromatography on silica gel (CH_2Cl_2/MeOH or MeCN/NH_4OH).

Procedure 3: General method for preparation of phenyl glycinol esters

To a solution of primary alcohol (1.0 eq) in anhydrous CH_2Cl_2, at 0°C, were added NEt_3 (4.0 eq), R''C(O)Cl (1.4 - 2.0 eq) and DMAP (0.2 eq). The mixture was allowed to warm up to 25°C and was stirred until consumption of starting alcohol. The resulting mixture was poured into a saturated aqueous solution of $NaHCO_3$ and the aqueous layer was extracted with CH_2Cl_2 (10 ml, 3 times). The combined organic extracts were washed with a saturated aqueous solution of NH_4Cl (10 ml) and brine (10 ml), dried over $MgSO_4$, filtered and concentrated *in vacuo*. Purification by flash chromatography on silica gel afforded pure ester derivatives.

Tert-butyl (3a*S*,4*R*,6*R*,6a*R*)-2,2,4-trimethyl-6-{[(triphenylmethyl)oxy]methyl}tetrahydro-5*H*-[1,3]dioxolo[4,5-c]pyrrole-5-carboxylate ((-)-53)

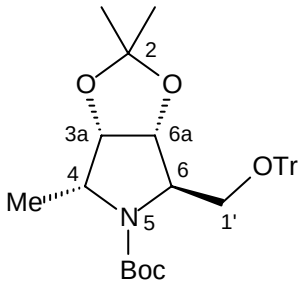

To a solution of **51**[174] (3.7 g, 6.9 mmol, 1.0 eq) in anhydrous THF (35 ml), cooled to -50°C, was added MeMgBr (3.5 ml of a 3M solution in Et_2O, 10.4 mmol, 1.5 eq) dropwise. The reaction mixture was stirred at -40°C for 30 minutes. The mixture was poured into a saturated aqueous solution of NH_4Cl (50 ml), water was added (30 ml) and the aqueous layer was extracted with EtOAc (25 ml, 3 times). The combined organic extracts were dried over $MgSO_4$, filtered and concentrated *in vacuo*. Flash chromatography on silica gel (pentane/EtOAc 3/1) afforded an intermediate amide (3.4 g, 87 %) as a yellow oil.

To a solution of this amide (1.3 g, 2.4 mmol, 1.0 eq) in anhydrous MeOH (24 ml), cooled to 0°C, was added $NaBH_4$ (371 mg, 9.8 mmol, 4.0 eq) portionwise. The mixture was warmed up to 25°C and stirred for 45 minutes. The resulting mixture was poured into brine (30 ml) and the aqueous layer was extracted with EtOAc (20 ml, 3 times). The combined organic extracts were dried over $MgSO_4$, filtered and concentrated *in vacuo* to afford a mixture of two diastereoisomeric alcohols (1.2 g) as a white foam.

To a solution of this crude mixture (1.2 g, 2.5 mmol, 1.0 eq) in anhydrous CH_2Cl_2 (24 ml), cooled to 0°C, were added NEt_3 (512 µl, 3.7 mmol, 1.5 eq) and MsCl (285 µl, 3.7 mmol, 1.5 eq) dropwise. The mixture was stirred at 0°C for 30 minutes. The resulting solution was poured into a saturated aqueous solution of $NaHCO_3$ (20 ml) and the aqueous layer was extracted with EtOAc (15 ml, 3 times). The combined organic extracts were dried over $MgSO_4$, filtered and concentrated *in vacuo* to afford a crude mesylate (1.5 g) as a white foam.

To a solution of this mesylate (1.5g, 2.5 mmol, 1.0 eq), in anhydrous THF (25 ml), cooled to 0°C, was added ^{t}BuOK (688 mg, 6.1 mmol, 2.5 eq) and the mixture was stirred at 0°C for 30 minutes. The resulting mixture was poured into brine (20 ml) and the aqueous layer was extracted with EtOAc (15 ml, 3 times). The combined organic extracts were dried over $MgSO_4$, filtered and concentrated *in vacuo.* Flash chromatography on silica gel (pentane/EtOAc 17/1) afforded **52** (455 mg, 35 %, 3steps) and **53** (517 mg, 40 %, 3steps) as pale yellow oils.

Data for 53, mixture of rotamers (α/β 1/1.6):

$[\alpha]_{589}^{25}$ = -59, $[\alpha]_{577}^{25}$ = -62, $[\alpha]_{435}^{25}$ = -117, $[\alpha]_{405}^{25}$ = -136 (c = 0.41, $CHCl_3$).

IR (film): 3455, 2980, 2935, 1695, 1375, 1170, 1080, 1030, 755, 700 cm^{-1}.

^{1}H-NMR (400 MHz, MeOD):
7.39-7.11 (m, $15H_{arom}$); **4.84** (m, 1H, H-C($3a_\alpha$)); **4.76** (m, 1H, H-C($3a_\beta$)); **4.46** (m, 1H, H-C($6a_\beta$)); **4.41** (m, 1H, H-C($6a_\alpha$)); **4.18-4.11** (m, 3H, H-C(4_α), H-C(4_β), H-C(6_α)); **4.05** (m, 1H, H-C(6_β)); **3.85** (bd, 1H, $^2J_{gem}$ = 8.9, H-C(1'$_\alpha$)); **3.45** (dd, 1H, ^3J(H-C(1'$_\beta$), H-C(6_β)) = 2.5, $^2J_{gem}$ = 8.9, H-C(1'$_\beta$)); **3.07** (bd, 1H, $^2J_{gem}$ = 8.9, H-C(1'$_\beta$)); **2.95** (bd, 1H, $^2J_{gem}$ = 8.9, H-C(1'$_\alpha$)); **1.54** (s, 9H, Me_3C_α); **1.51** (s, 3H, Me); **1.44** (d, 3H, ^3J(Me, H-C(4)) = 6.5, Me_β-C(4)); **1.38** (d, 3H, ^3J(Me, H-C(4)) = 5.6, Me_α-C(4)); **1.34** (s, 9H, Me_3C_β); **1.32** (s, 3H, Me).

^{13}C-NMR (101 MHz, MeOD):
154.2 (s, N*C*(O)O); **143.6** (s, $3C_{arom}$); **128.6** (d, ^1J(C,H) = 159, $6C_{arom}$); **127.9** (d, ^1J(C,H) = 160, $6C_{arom}$); **127.1** (d, ^1J(C,H) = 161, $3C_{arom}$); **110.9** (s, O*C*Me_2); **87.1** (s, O*C*Ph_3); **81.8** (d, ^1J(C,H) = 158, C($6a_\beta$)); **81.4** (d, ^1J(C,H) = 159, C($6a_\alpha$)); **81.3** (d, ^1J(C,H) = 159, C($3a_\alpha$)); **80.6** (d, ^1J(C,H) = 158, C($3a_\beta$)); **79.8** (s, O*C*$Me_{3\alpha}$); **79.4** (s, O*C*$Me_{3\beta}$); **63.5** (t, ^1J(C,H) = 143, C(1'$_\alpha$)); **62.7** (C(1'$_\beta$), C(6_α), C(6_β)); **58.0** (d, ^1J(C,H) = 140, C(4_α)); **57.7** (d, ^1J(C,H) = 140, C(4_β)); **28.6** (q, ^1J(C,H) = 130, Me_3C); **28.4** (q, ^1J(C,H) = 130, Me_3C); **25.8** (q, ^1J(C,H) = 128, Me-C(2)); **25.0** (q, ^1J(C,H) = 128, Me-C(2)); **16.9** (q, ^1J(C,H) = 128, Me_α-C(4)); **15.5** (q, ^1J(C,H) = 128, Me_β-C(4)).

ESI-MS: 552.30 $(M+Na)^+$.
HRMS ($C_{33}H_{39}NO_5$ + Na): calc. 552.2726; found 552.2781.

The other isomer **52** was not fully characterized but directly engaged in the next step.

(2*R*,3*R*,4*S*,5*R*)-2-({[1*R*]-2-Hydroxy-1-phenylethyl]amino}methyl) -5-methylpyrrolidine -3,4-diol ((-)-57)

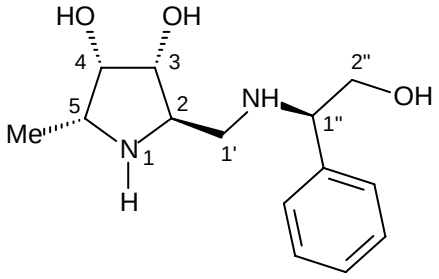

Metallic sodium chips (387 mg, 16.9 mmol, 15.0 eq) were added to liquid NH_3 (55 ml, condensed at -78°C) and a solution of **53** (596 mg, 1.1 mmol, 1.0 eq) in anhydrous THF (10 ml) was added dropwise. After stirring at –78°C for 50 minutes, solid NH_4Cl was added until complete decoloration of the blue mixture. The solution was allowed to warm up to 25°C and stirred to the end of gas evolution. The residue was diluted with EtOAc and water, filtered on a pad of Celite and concentrated *in vacuo*. Purification by flash chromatography on silica gel (pentane/EtOAc 1/1) afforded an intermediate primary alcohol (295 mg, 91 %) as a colourless oil.

To a solution of this primary alcohol (219 mg, 0.76 mmol, 1.0 eq) in anhydrous CH_2Cl_2 (8 ml), were added 4Å molecular sieves (380 mg), NMO (124 mg, 0.92 mmol, 1.2 eq) and Pr_4NRuO_4 (27 mg, 0.08 mmol, 0.1 eq). The mixture was stirred at 25°C for 1 hour, filtered on a pad of Celite and concentrated *in vacuo*. Purification by flash chromatography on silica gel (pentane/EtOAc 3/1) afforded the aldehyde **56** (46 mg, 21 %) as a colourless oil.

Procedure 1. **D-(-)-α-phenylglycinol** (**99**) (26 mg, 0.19 mmol, 1.2 eq), aldehyde **56** (46 mg, 0.16 mmol, 1.0 eq), $NaBH(OAc)_3$ (46 mg, 0.22 mmol, 1.4 eq), $Cl(CH_2)_2Cl$ (2 ml). Flash chromatography (CH_2Cl_2/MeOH 9/1) afforded 59 mg (0.15 mmol, 92 %, colourless oil) of the fully protected compound which was directly engaged in **procedure 2b**. Purification by flash chromatography (MeCN/NH_4OH 8/1) afforded **57** (16 mg, 42 %) as a brown oil.

$[\alpha]_{589}^{25}$ = -5, $[\alpha]_{435}^{25}$ = -7, $[\alpha]_{405}^{25}$ = -8 (c = 0.20, $CHCl_3$).

IR (film): 3415, 3020, 2930, 1645, 1455, 1215, 1140, 755 cm^{-1}.

^{1}H-NMR (400 MHz, MeOD):
7.41-7.21 (m, $5H_{arom}$); **4.03-4.01** (m, 2H, H-C(3), H-C(1’’)); **3.84** (m, 1H, H-C(4)); **3.72-3.64** (m, 3H, H-C(5), 2H-C(2’’)); **3.45** (m, 1H, H-C(2)); **2.95** (dd, 1H, ^3J(H-C(1’), H-C(2)) = 3.8, $^2J_{gem}$ = 13.2, H-C(1’)); **2.80** (dd, 1H, ^3J(H-C(1’), H-C(2)) = 9.4, $^2J_{gem}$ = 13.2, H-C(1’)); **1.42** (d, 3H, ^3J(Me, H-C(5)) = 6.6, Me-C(5)).

^{13}C-NMR (101 MHz, MeOD):
141.5 (s, $1C_{arom}$); **129.7** (d, ^1J(C,H) = 160, $2C_{arom}$); **128.8** (d, ^1J(C,H) = 160, $1C_{arom}$); **128.6** (d, ^1J(C,H) = 158, $2C_{arom}$); **75.6** (d, ^1J(C,H) = 144, C(3)); **73.3** (d, ^1J(C,H) = 153, C(1’’)); **67.3** (t, ^1J(C,H) = 144, C(2’’)); **66.6** (d, ^1J(C,H) = 143, C(4)); **63.0** (d, ^1J(C,H) = 146, C(2)); **58.2** (d, ^1J(C,H) = 141 , C(5)); **48.0** (t, ^1J(C,H) = 136, C(1’)); 1**2.1** (q, ^1J(C,H) = 129, Me-C(5)).

MALDI-TOF: 267.12 $(M+H)^+$.
HRMS ($C_{14}H_{22}N_2O_3$ + H): calc. 267.1709; found 267.1748.

^{1}H-NMR spectrum of **53**

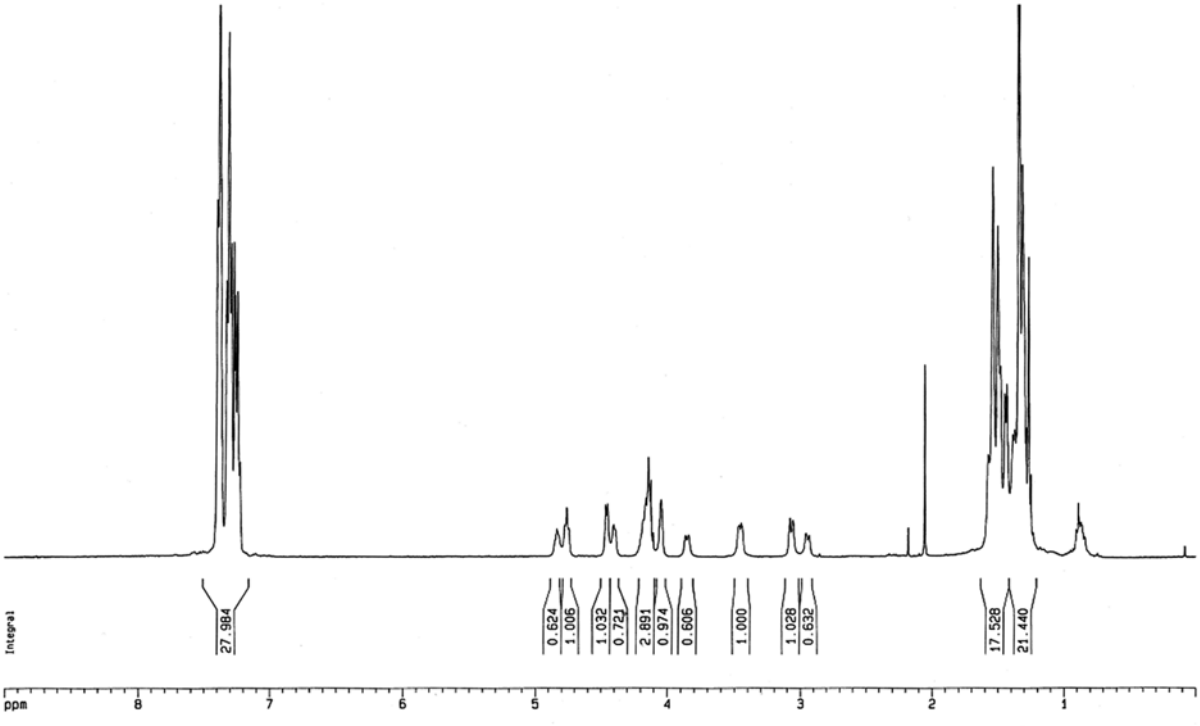

^{1}H-NMR spectrum of **57**

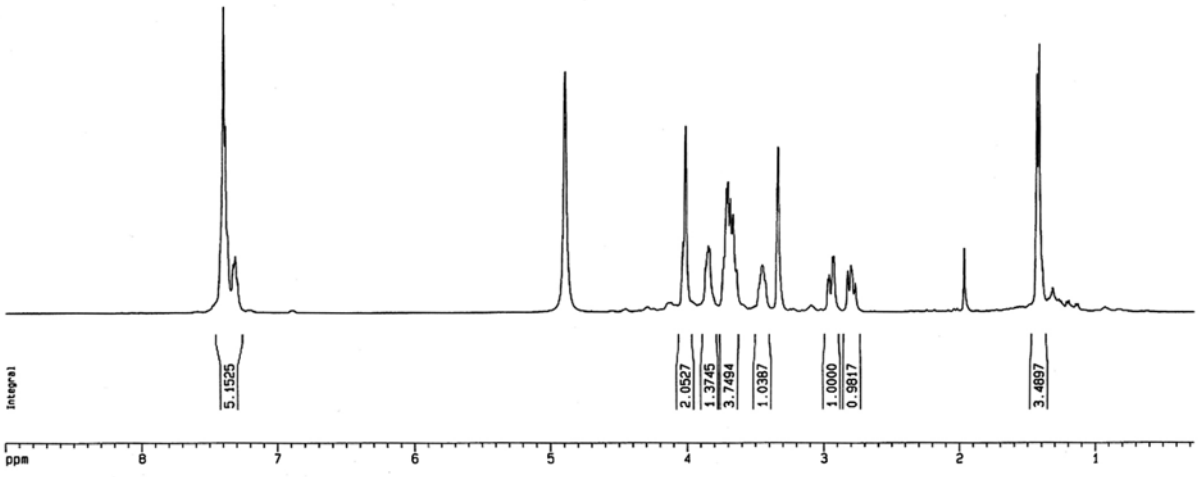

(2*R*,3*R*,4*S*,5*S*)-2-({[1*R*]-2-Hydroxy-1-phenylethyl]amino}methyl) -5-methylpyrrolidine-3,4-diol ((-)-55)

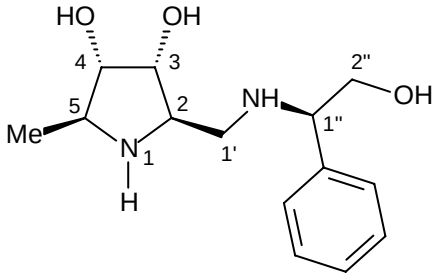

Metallic sodium chips (296 mg, 12.9 mmol, 15.0 eq) were added to liquid NH_3 (42 ml, condensed at –78°C) and a solution of **52** (455 mg, 0.86 mmol, 1.0 eq) in anhydrous THF (8 ml) was added dropwise. After stirring at –78°C for 50 minutes, solid NH_4Cl was added until complete decoloration of the blue mixture. The solution was allowed to warm up to 25°C and stirred to the end of gas evolution. The residue was diluted with EtOAc and water, filtered on a pad of Celite and concentrated *in vacuo*. Purification by flash chromatography on silica gel (pentane/EtOAc 1/1) afforded an intermediate primary alcohol (222 mg, 90 %) as a colourless oil.

To a solution of oxalyl chloride (79 µl, 0.93 mmol, 1.2 eq) in anhydrous CH_2Cl_2 (6 ml), cooled to -78°C, was added DMSO (132 µl, 1.9 mmol, 2.4 eq). After 20 minutes, the intermediate primary alcohol (222 mg, 0.77 mmol, 1.0 eq), in solution in anhydrous CH_2Cl_2 (2 ml), was added dropwise. After 20 minutes, NEt_3 (539 µl, 3.87 mmol, 5.0 eq) was added and the mixture was warmed to -30°C for 20 minutes. The mixture was poured into water (30 ml) and extracted with EtOAc (15 ml, 3 times). The combined organic layers were washed with brine (20 ml), dried over $MgSO_4$, filtered and concentrated *in vacuo* to afford aldehyde **54** (140 mg, 63 %).

Procedure 1. **D-(-)-α-phenylglycinol** (**99**) (40 mg, 0.29 mmol, 1.2 eq), aldehyde **54** (70 mg, 0.24 mmol, 1.0 eq), $NaBH(OAc)_3$ (72 mg, 0.34 mmol, 1.4 eq), $Cl(CH_2)_2Cl$ (2.5 ml). Flash chromatography (CH_2Cl_2/MeOH 11/1) afforded 73 mg (0.18 mmol, 74 %) of the fully protected compound which was directly engaged in **procedure 2b**. Purification by flash chromatography (MeCN/NH_4OH 8/1) afforded **55** (48 mg, 98 %) as a brown oil.

$[\alpha]_{589}^{25}$ = -4, $[\alpha]_{577}^{25}$ = -7, $[\alpha]_{435}^{25}$ = -9 (c = 0.17, $CHCl_3$).

IR (film): 3055, 1670, 1445, 1200, 1140, 840, 800, 725 cm^{-1}.

^{1}H-NMR (400 MHz, MeOD):
7.53 (m, $2H_{arom}$); **7.46** (m, $3H_{arom}$); **4.34** (t, 1H, ^3J(H-C(1''), H-C(2'')) = 5.9, H-C(1'')); **4.10** (dd, 1H, ^3J(H-C(3), H-C(4)) = 5.2, ^3J(H-C(3), H-C(2)) = 7.0, H-C(3)); **3.95** (d, 2H, ^3J(H-C(2''), H-C(1'')) = 5.9, H-C(2'')); **3.90** (dd, 1H, ^3J(H-C(4), H-C(5)) = 4.9, ^3J(H-C(4), H-C(3)) = 5.2, H-C(4)); **3.77** (ddd, 1H, ^3J(H-C(2), H-C(1')) = 4.8, ^3J(H-C(2), H-C(3)) = 7.0, ^3J(H-C(2), H-C(1')) = 8.9, H-C(2)); **3.65** (qd, 1H, ^3J(H-C(5), H-C(4)) = 4.9, ^3J(H-C(5)), Me = 7.0, H-C(5)); **3.42** (dd, 1H, ^3J(H-C(1'), H-C(2)) = 8.9, $^2J_{gem}$ = 13.6, H-C(1')); **3.26** (dd, 1H, ^3J(H-C(1'), H-C(2)) = 4.8, $^2J_{gem}$ = 13.6, H-C(1')); **1.45** (d, 3H, ^3J(Me, H-C(5)) = 7.0, Me-C(5)).

^{13}C-NMR (101 MHz, MeOD):
135.7 (s, $1C_{arom}$); **130.5** (d, ^1J(C,H) = 161, $1C_{arom}$); **130.3** (d, ^1J(C,H) = 161, $2C_{arom}$); **129.4** (d, ^1J(C,H) = 159, $2C_{arom}$); **75.4** (d, ^1J(C,H) = 149, C(4)); **73.5** (d, ^1J(C,H) = 146, C(3)); **66.3** (d, ^1J(C,H) = 142, C(1'')); **64.3** (t, ^1J(C,H) = 145, C(2'')); **61.7** (d, ^1J(C,H) = 147, C(5)); **61.4** (d, ^1J(C,H) = 147, C(2)); **47.0** (t, ^1J(C,H) = 143, C(1')); 1**6.0** (q, ^1J(C,H) = 128, Me-C(5)).

MALDI-TOF: 267.04 $(M+H)^+$.
HRMS ($C_{14}H_{22}N_2O_3$): calc. 266.1630; found 266.1629.

^{1}H-NMR spectrum of **55**

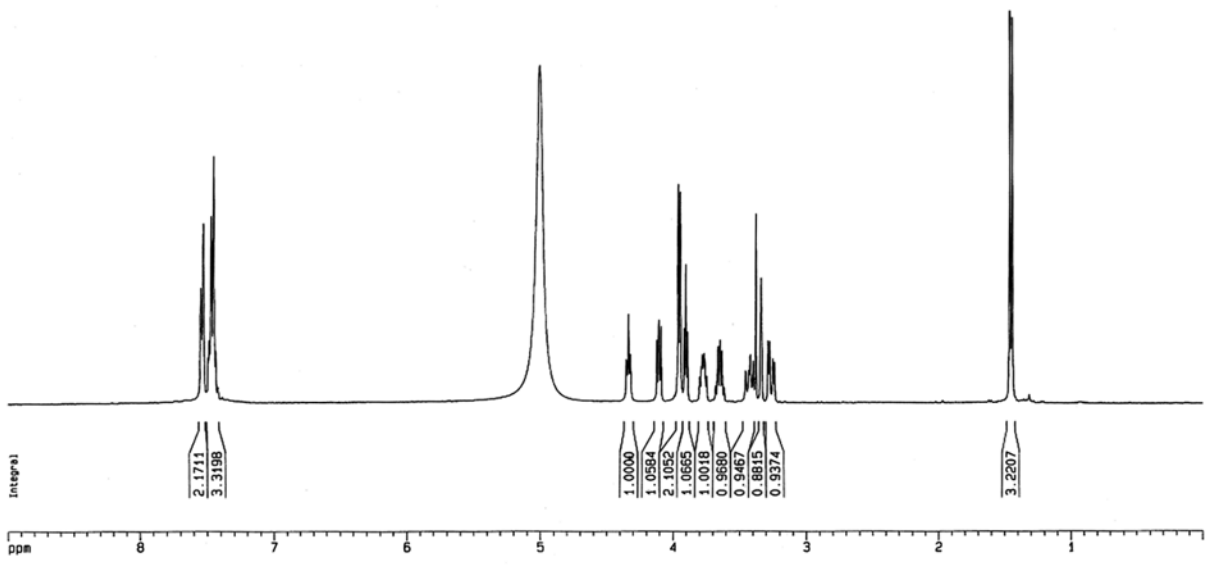

Tert-butyl (3a*R*,6*R*,6a*R*)-4-hydroxy-2,2-dimethyl-6-[(trityloxy)methyl]tetrahydro-5*H*-[1,3]dioxolo[4,5-c]pyrrole-5-carboxylate ((-)-72)

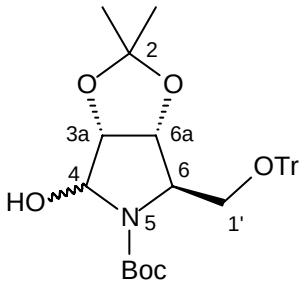

To a solution of **51**[174] (1.54 g, 2.91 mmol, 1.0 eq) in anhydrous MeOH (30 ml) at 0°C was added sodium borohydride (0.17 g, 4.37 mmol, 1.5 eq) and the solution was stirred at 0°C for 15 min. The resulting mixture was diluted with EtOAc (30 ml), poured into a saturated aqueous solution of $NaHCO_3$ (30 ml). The aqueous layer was extracted with EtOAc (10 ml, 3 times). The combined organic extracts were dried over $MgSO_4$, filtered and concentrated *in vacuo*. Flash chromatography on silica gel (EtOAc/pentane 1/6) afforded alcohol **72** (1.44 g, 93%) as a white foam.

$[\alpha]_{589}^{25}$ = -57, $[\alpha]_{577}^{25}$ = -57, $[\alpha]_{435}^{25}$ = -108, $[\alpha]_{405}^{25}$ = -128 (c = 0.32, CH_2Cl_2).

UV (MeCN) : 260 (1500), 217 (11500), 196 (5500).

IR (film) : 3470, 2985, 2940, 2880, 1690, 1430, 1365, 1260, 1215, 1170, 1130, 1080, 780, 765, 755, 705 cm^{-1}.

^{1}H-NMR (400MHz, $CDCl_3$):
7.38-7.25 (m, $15H_{arom}$) ; **5.64** (bs, 1H, H-C(4_{maj})) ; **5.52** (bs, 1H, H-C(4_{min})) ; **4.84** (dd, 1H, ^3J = 5.8, ^3J = 5.8, H-C(3a)) ; **4.32** (d, 1H, ^3J(H-C(6a), H-C(3a)) = 5.1, H-C(6a)) ; **4.13** (d, 1H, ^3J (H-C(6), H-C(1')) = 3.8, H-C(6_{min})) ; **4.04** (s, 1H, H-C(6_{maj})) ; **3.90** (d, 1H, $^2J_{gem}$ = 8.3, H-C($1'_{min}$)) ; **3.59** (d, 1H, $^2J_{gem}$ = 9.3, H-C($1'_{maj}$)) ; **2.98** (d, 1H, $^2J_{gem}$ = 9.2, H-C($1'_{maj}$)) ; **2.90** (d, 1H, $^2J_{gem}$ = 8.6, H-C($1'_{min}$)) ; **1.58** (s, 6H, $2CH_3$-C($2)_{maj}$) ; **1.40** (s, 9H, Me_3C) ; **1.34** (s, 6H, $2CH_3$-C($2)_{min}$).

^{13}C-NMR (101MHz, $CDCl_3$):
154.8 (s, NC(O)O_α) ; **154.3** (s, NC(O)O_β) ; **143.4** (s, $1C_{arom}$) ; **128.5** (d, ^1J(C-H) = 159, $2C_{arom}$) ; **128.0** (d, ^1J(C-H) = 160, $2C_{arom}$) ; **127.2** (d, ^1J(C-H) = 161, $1C_{arom}$) ; **112.1** (s, O*C*Me_2) ; **87.3** (s, O*C*Ph_3) ; **81.6** (d, ^1J(C-H) = 171, C(6a)) ; **81.3** (s, O*C*Me_3) ; **80.9** (d, ^1J(C-H) = 167, C(4)) ; **77.8** (d, ^1J(C-H) = 161, C(3a)) ; **63.0** (t, ^1J(C-H) = 145, C(1')) ; **60.3** (d, ^1J(C-H) = 147, C(6)) ; **28.4** (q, ^1J(C-H) = 131, Me_3C) ; **25.7** (q, ^1J(C-H) = 124, $2CH_3$-C($2)_{maj}$) ; **25.2** (s, ^1J(C-H) = 125, $2CH_3$-C($2)_{min}$).

MALDI-TOF: 570.12 $(M+K)^{+\cdot}$, 554.17 $(M+Na)^+$.

Tert-butyl (3a*R*,6*R*,6a*R*)-4-(methoxymethoxy)-2,2-dimethyl-6-[(trityloxy)methyl]tetrahydro-5*H*-[1,3]dioxolo[4,5-c]pyrrole-5-carboxylate ((-)-63)

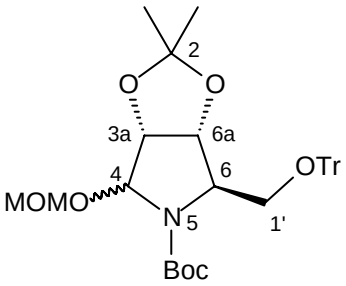

To a solution of alcohol **72** (2.13 g, 4.00 mmol, 1.0 eq) in anhydrous THF (50ml) at 0°C were added *N*-ethyl diisopropylamine (5.47 ml, 31.99 mmol, 8.0 eq), chloromethyl methyl ether (1.82 ml, 23.99 mmol, 6.0 eq) and a catalytic amount of tetrabutylammonium iodide. The mixture was stirred at reflux for 12 hours. The resulting mixture was diluted with EtOAc (70 ml), poured into a saturated aqueous solution of $NaHCO_3$ (50 ml) and the aqueous layer was extracted with EtOAc (20 ml, 3 times). The combined organic extracts were dried over $MgSO_4$, filtered and concentrated *in vacuo*. Flash chromatography on silica gel (EtOAc/pentane 1/8) afforded **63** (1.32 g, 58%), as a light yellow foam and the starting material (0.94 g, 44%).

$[\alpha]_{589}^{25}$ = -38, $[\alpha]_{577}^{25}$ = -39, $[\alpha]_{435}^{25}$ = -72, $[\alpha]_{405}^{25}$ = -85 (c = 0.91, MeOH).

UV (MeCN): 260 (1500), 233 (7500), 226 (1000).

IR (film): 2925, 1705, 1365, 1215, 1160, 1025, 865, 800, 750 cm-^{1}.

^{1}H-NMR (400MHz, $CDCl_3$):
7.37-7.25 (m, 15H_{arom}) ; **5.42** (d, 1H, ^{3}J(H-C(4), H-C(3a)) = 5.4, H-C(4_{maj})) ; **5.33** (d, 1H, ^{3}J(H-C(4), H-C(3a)) = 5.0, H-C(4_{min})) ; **5.10-5.01** (m, 1H, 1OCH_2O) ; **4.79** (bs, 1H, 1OCH_2O) ; **4.79** (bs, 1H, ^{3}J(H-C(3a), H-C(6a)) = 4.7, H-C(3a)) ; **4.29** (d, 1H, ^{3}J(H-C(6a), H-C(3a)) = 4.7, H-C($6a_{maj}$)) ; **4.20** (d, 1H, ^{3}J(H-C(6a), H-C(3a)) = 4.7, H-C($6a_{min}$)) ; **4.14** (s, 1H, H-C(6_{min})) ; **4.08** (s, 1H, H-C(6_{maj})) ; **4.00** (d, 1H, $^{2}J_{gem}$ = 9.1, H-C(1'$_{min}$)) ; **3.59** (d, 1H, $^{2}J_{gem}$ = 9.1, H-C(1'$_{maj}$)) ; **3.52** (s, 3H, OCH_3) ; **3.08** (d, 1H, $^{2}J_{gem}$ = 9.1, H-C(1'$_{maj}$)) ; **2.94** (d, 1H, $^{2}J_{gem}$ = 9.1, H-C(1'$_{min}$)) ; **1.60, 1.61** (2s, 6H, 2CH_3-C($2)_{maj}$) ; **1.56** (s, 9H, Me_3C_β) ; **1.35** (s, 9H, Me_3C_α) ; **1.31, 1.22** (2s, 6H, 2CH_3-C($2)_{min}$).

^{13}C-NMR (101MHz, $CDCl_3$):
153.8 (s, N*C*(O)O) ; **143.7** (s, 1$C_{arom\ min}$) ; **143.5** (s, 1$C_{arom\ maj}$) ; **128.6** (d, ^{1}J(C-H) = 159, 2C_{arom}) ; **128.0** (d, ^{1}J(C-H) = 160, 2C_{arom}) ; **127.2** (d, ^{1}J(C-H) = 161, 1C_{arom}) ; **112.4** (s, O*C*Me_2) ; **97.2** (t, ^{1}J(C-H) = 165, OCH_2O) ; **86.9** (s, O*C*Ph_3) ; **86.5** (d, ^{1}J(C-H) = 164, C(4_{min})) ; **85.8** (d, ^{1}J(C-H) = 162, C(4_{maj})) ; **81.9** (d, ^{1}J(C-H) = 160, C($6a_{maj}$)) ; **81.4** (d, ^{1}J(C-H) = 164, C($6a_{min}$)) ; **80.9** (s, O*C*Me_3) ; **79.2** (d, ^{1}J(C-H) = 155, C($3a_{min}$)) ; **78.2** (d, ^{1}J(C-H) = 155, C($3a_{maj}$)) ; **62.8** (t, ^{1}J(C-H) = 145, C(1'$_{maj}$)) ; **61.4** (t, ^{1}J(C-H) = 145, C(1'$_{min}$)) ; **59.7** (d, ^{1}J(C-H) = 141, C(6_{min})) ; **59.4** (d, ^{1}J(C-H) = 141, C(6_{maj})) ; **56.7** (q, ^{1}J(C-H) = 141, O$\underline{C}H_{3min}$) ; **56.3** (q, ^{1}J(C-H) = 141, O*C*H_{3maj}) ; **29.6** (q, ^{1}J(C-H) = 127, *Me*$_3C_\beta$) ; **29.3** (q, ^{1}J(C-H) = 127, *Me*$_3C_\alpha$) ; **25.7** (q, ^{1}J(C-H) = 128, 2*C*H_3-C($2)_{min}$) ; **25.3** (q, ^{1}J(C-H) = 126, 2*C*H_3-C($2)_{maj}$).

MALDI-TOF: 614.06 $(M+K)^+$, 598.10 $(M+Na)^+$; 574.79 (M^+).

^{1}H-NMR spectrum of **72**

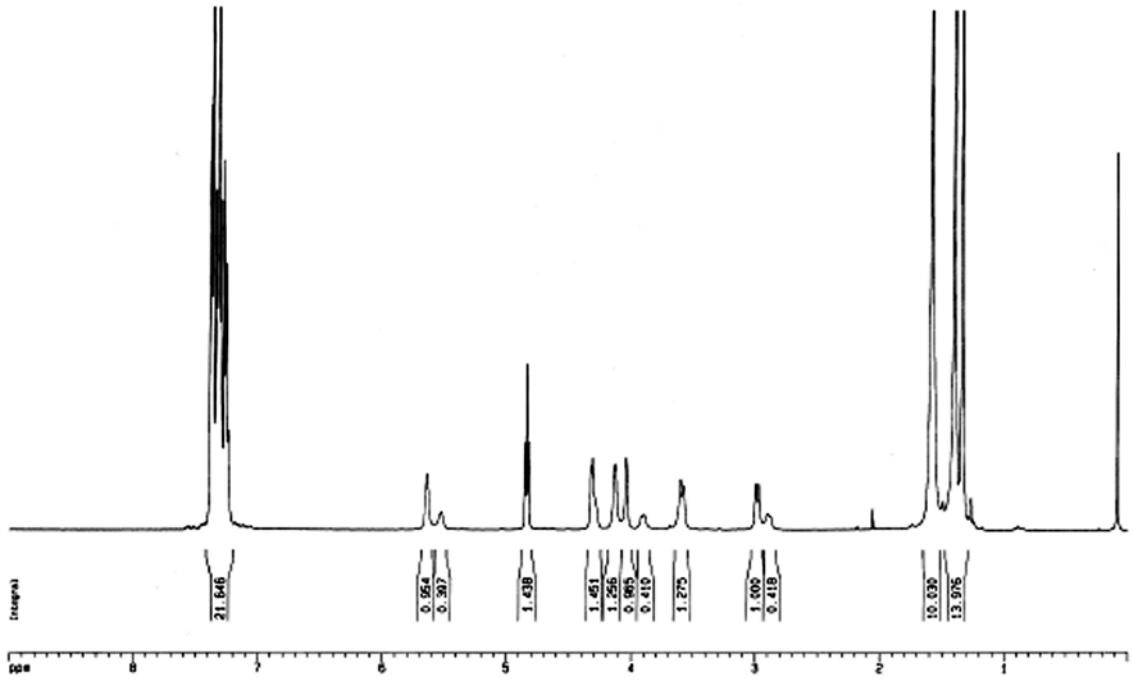

^{1}H-NMR spectrum of **63**

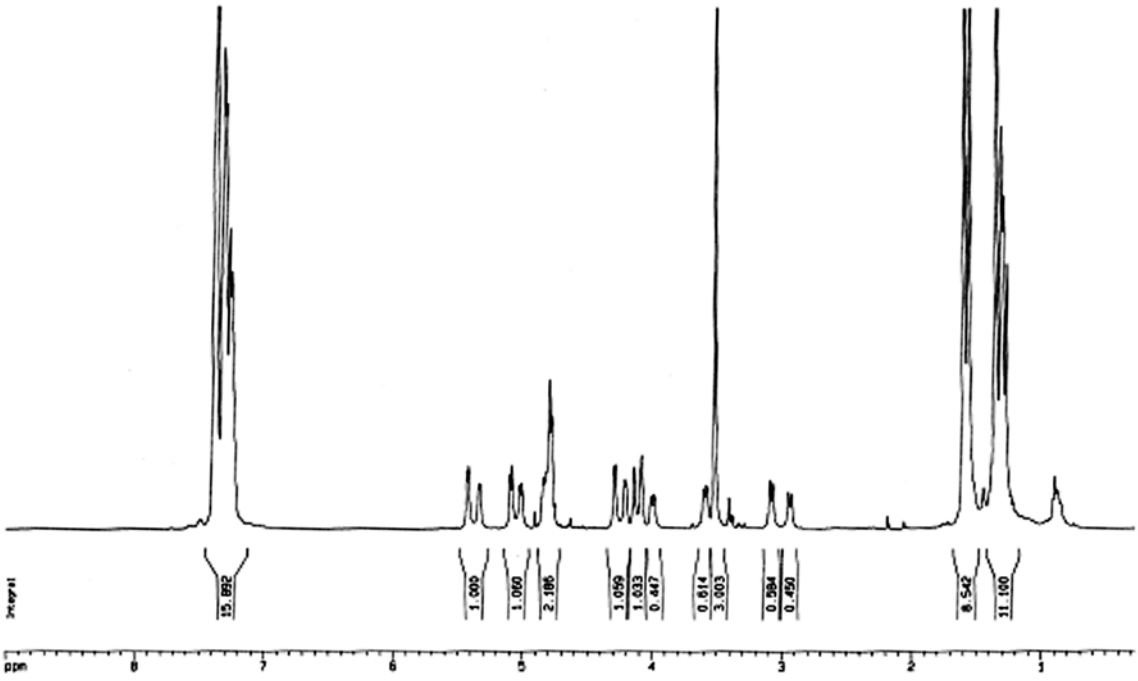

Tert-butyl (3a*R*,4*S*,6a*R*)-4-formyl-6-(methoxymethoxy)-2,2-dimethyltetrahydro-5*H*-[1,3] dioxolo[4,5-c]pyrrole-5-carboxylate ((-)-64)

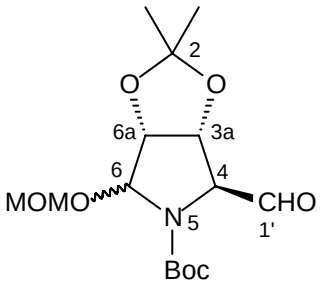

Metallic sodium chips (0.77 g, 33.59 mmol, 15.0 eq) were added to liquid NH_3 (130 ml, condensed at -78°C) and a solution of **63** (1.29 g, 2.24 mmol, 1.0 eq) in anhydrous THF (25 ml) was added dropwise. After stirring at –78°C for 50 minutes, solid NH_4Cl was added until complete decoloration of the blue mixture. The solution was allowed to warm up to 25°C and stirred to the end of gas evolution. The residue was diluted with EtOAc and water, filtered on a pad of Celite and concentrated *in vacuo*. Purification by flash chromatography on silica gel (pentane/EtOAc 1/1) afforded an intermediate primary alcohol (0.61 g, 82 %) as a pale yellow transparent solid.

To a solution of oxalyl chloride (0.28 g, 2.21 mmol, 1.2 eq) in anhydrous CH_2Cl_2 (6 ml), cooled to -78°C, was added DMSO (315 µl, 4.42 mmol, 2.4 eq). After 20 minutes, the intermediate primary alcohol (0.61 g, 1.84 mmol, 1.0 eq), in solution in anhydrous CH_2Cl_2 (6 ml), was added dropwise. After 20 minutes, NEt_3 (1.28 ml, 9.22 mmol, 5.0 eq) was added and the mixture was warmed to -30°C for 20 minutes. The mixture was poured into water (50 ml) and extracted with EtOAc (20 ml, 3 times). The combined organic layers were washed with brine (20 ml), dried over $MgSO_4$, filtered and concentrated *in vacuo*. Purification by flash chromatography on silica gel (pentane/EtOAc 2/1) afforded aldehyde **64** (0.56 g, 91%) as a white foam.

$[\alpha]_{589}^{25}$ = -71, $[\alpha]_{577}^{25}$ = -72, $[\alpha]_{435}^{25}$ = -148, $[\alpha]_{405}^{25}$ = -183 (c = 0.30, CH_2Cl_2).

UV (MeCN): 294 (10500), 282 (10000), 234 (9500).

IR (KBr): 2985, 2365, 2945, 1735, 1675, 1405, 1380, 1370, 1210, 1150, 1110, 1085, 1015, 970, 920, 855, 775 cm^{-1}.

^{1}H-NMR (400MHz, $CDCl_3$):
9.65 (s, 1H, H-C(1'$_{min}$)) ; **9.56** (s, 1H, H-C(1'$_{maj}$)) ; **5.46** (d, 1H, ^3J(H-C(6), H-C(6a)) = 5.4, H-C(6$_{maj}$)) ; **5.31** (d, 1H, ^3J(H-C(6), H-C(6a)) = 5.3, H-C(6$_{min}$)) ; **5.03-4.75** (m, 2H, OCH_2O) ; **4.68-4.56** (m, 2H, H-C(6a), H-C(3a)) ; **4.57** (s, 1H, H-C(4$_{maj}$)) ; **4.52** (s, 1H, H-C(4$_{min}$)) ; **3.47** (s, 3H, OCH_3) ; **1.68, 1.61** (2s, 6H, $2CH_3$-C(2)$_{min}$) ; **1.55, 1.46** (2s, 9H, *Me*$_3$C) ; **1.42, 1.31** (2s, 6H, $2CH_3$-C(2)$_{maj}$).

^{13}C-NMR (101MHz, $CDCl_3$):
197.4 (d, ^1J(C-H) = 191, C(1')) ; **154.0** (s, NC(O)O_β) ; **153.1** (s, NC(O)O_α) ; **114.0** (s, O$\underline{C}Me_2$) ; **96.6** (t, ^1J(C-H) = 166, COCH_2O) ; **84.7** (d, ^1J(C-H) = 165, C(6_{min})) ; **84.4** (d, ^1J(C-H) = 164, C(6_{maj})) ; **82.3** (s, OCMe$_{3min}$) ; **82.1** (s, OCMe$_{3maj}$) ; **79.1** (d, ^1J(C-H) = 156, C($6a_{maj}$)) ; **78.9** (d, ^1J(C-H) = 155, C($6a_{min}$)) ; **78.0** (d, ^1J(C-H) = 152, C(3a)) ; **67.6** (d, ^1J(C-H) = 176, C(4_{maj})) ; **67.1** (d, ^1J(C-H) = 176, C(4_{maj})) ; **56.5** (q, ^1J(C-H) = 141, OCH_{3min}) ; **56.2** (q, ^1J(C-H) = 142, OCH_{3maj}) ; **28.0** (q, ^1J(C-H) = 127, *Me*$_3$C) ; **25.7** (q, ^1J(C-H) = 126, 2CH$_3$-C($2)_{maj}$) ; **25.3** (q, ^1J(C-H) = 127, 2CH$_3$-C($2)_{min}$).

MALDI-TOF: 370.13 $(M+K)^+$, 354.17 $(M+Na)^+$.

^{1}H-NMR spectrum of **64**

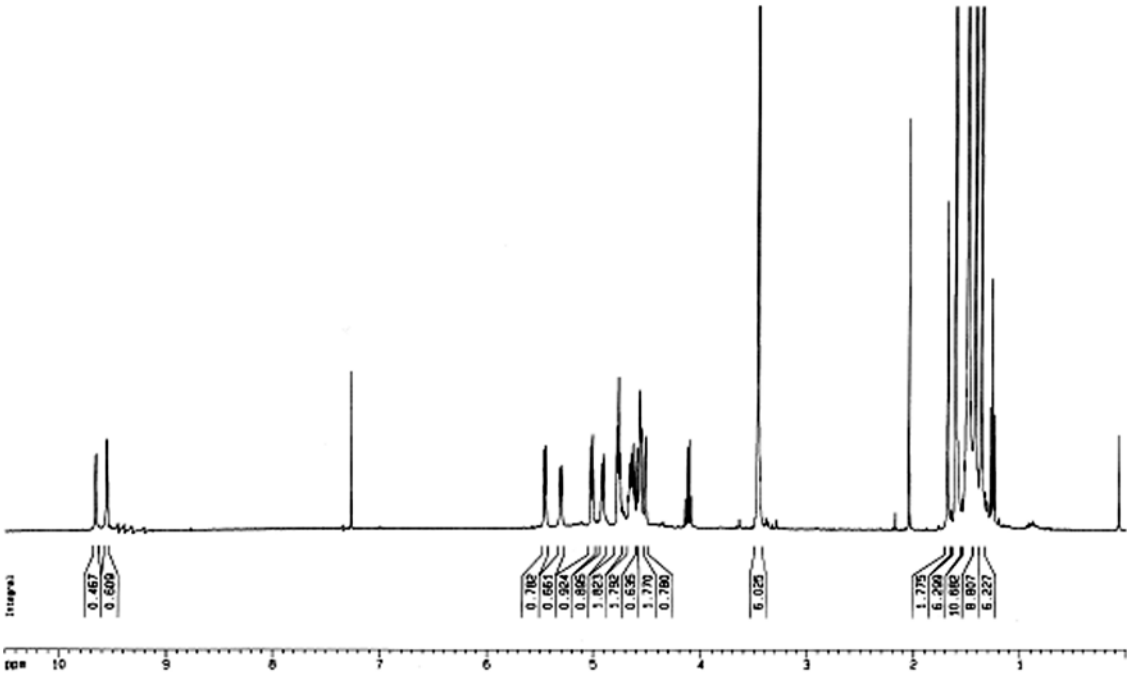

***Tert*-butyl (3a*R*,4*R*,6a*R*)-4-({[(1*R*)-2-hydroxy-1-phenylethyl]amino}methyl)-6-(methoxymethoxy)-2,2-dimethyltetrahydro-5*H*-[1,3]dioxolo[4,5-c]pyrrole-5-carboxylate ((-)-65)**

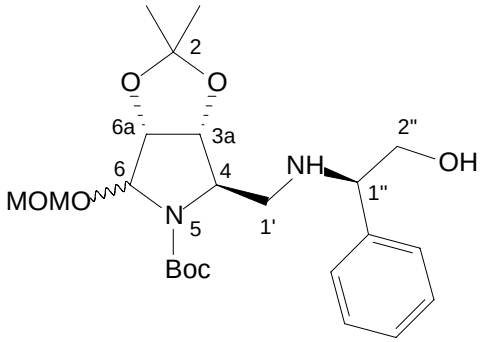

Procedure 1. **D-(-)-α-phenylglycinol** (**99**) (50 mg, 0.37 mmol, 1.2 eq), aldehyde **64** (100 mg, 0.31 mmol, 1.0 eq), $NaBH(OAc)_3$ (100 mg, 0.46 mmol, 1.5 eq), $Cl(CH_2)_2Cl$ (4 ml). Flash chromatography (CH_2Cl_2/MeOH 30/1) afforded **65** (60 mg, 46%) as a colourless oil.

$[\alpha]_{589}^{25}$ = -82, $[\alpha]_{577}^{25}$ = -83, $[\alpha]_{435}^{25}$ = -165, $[\alpha]_{405}^{25}$ = -198 (c = 0.20, CH_2Cl_2).

UV (MeCN): 295 (8500), 290 (8500), 235 (7500).

IR (film): 3455, 2930, 2360, 1700, 1455, 1370, 1245, 1215, 1160, 1110, 1025, 920, 755 cm^{-1}.

^{1}H-NMR (400MHz, MeOD):
7.37-7.25 (m, $5H_{arom}$) ; **5.19** (bs, 1H, H-C(6_{maj})) ; **5.06** (bs, 1H, H-C(6_{min})) ; **4.99** (bs, 1H, $1OCH_2O_{maj}$) ; **4.89** (bs, 1H, $1OCH_2O_{min}$) ; **4.77-4.63** (m, 3H, $1OCH_2O$, H-C(3a), H-C(6a)) ; **3.97** (bs, 1H, H-C(3')) ; **3.73-3.70** (m, 1H, H-C(4)) ; **3.63** (dd, 1H, $^2J_{gem}$ = 10.9, ^3J(H-C(1'), H-C(4)) = 4.5, H-C(1')) ; **3.54** (dd, 1H, $^2J_{gem}$ = 10.8, ^3J(H-C(1'), H-C(4)) = 8.4, H-C(1')) ; **3.47** (s, 3H, OCH_3) ; **2.75** (d, 1H, $^2J_{gem}$ = 10.9, H-C(4')) ; **2.60** (bs, 1H, H-C(4')) ; **1.58** (s, 6H, $2CH_3$-$C(2)_{min}$) ; **1.53** (s, 9H, Me_3C_α) ; **1.39** (s, 6H, $2CH_3$-$C(2)_{maj}$) ; **1.31** (s, 3H, Me_3C_β).

^{13}C-NMR (101MHz, MeOD):
155.5 (s, NC(O)O) ; **142.4** (s, $1C_{arom}$) ; **129.6** (d, ^1J(C-H) = 159, $2C_{arom}$) ; **128.6** (d, ^1J(C-H) = 156, $2C_{arom}$) ; **113.6** (s, O*C*Me_2) ; **98.4** (t, ^1J(C-H) = 165, OCH_2O_{min}) ; **98.0** (t, ^1J(C-H) = 165, OCH_2O_{maj}) ; **87.8** (d, ^1J(C-H) = 164, C(6_{min})) ; 87.2 (d, ^1J(C-H) = 168, C(6_{maj})) ; **83.3** (d, ^1J(C-H) = 160, C($3a_{maj}$)) ; **82.6** (d, ^1J(C-H) = 160, C($3a_{min}$)) ; **81.6** (s, O*C*Me_3) ; **80.0** (d, ^1J(C-H) = 155, C($6a_{min}$)) ; **79.3** (d, ^1J(C-H) = 156, C($6a_{maj}$)) ; **67.9** (t, ^1J(C-H) = 141, C(1')) ; **66.6** (d, ^1J(C-H) = 135, C(4)) ; **61.4** (d, ^1J(C-H) = 147, C(3')) ; **57.0** (q, ^1J(C-H) = 139, OCH_{3min}) ; **56.7** (q, ^1J(C-H) = 142, OCH_{3maj}) ; **28.6** (q, ^1J(C-H) = 127, *Me*$_3$C) ; **26.1** (q, ^1J(C-H) = 126, 2*C*H_3-$C(2)_{maj}$) ; **25.7** (q, ^1J(C-H) = 126, 2*C*H_3-$C(2)_{min}$).

MALDI-TOF: 454.03 $(M+H)^+$, 453.05 (M^+).

^{1}H-NMR spectrum of **65**

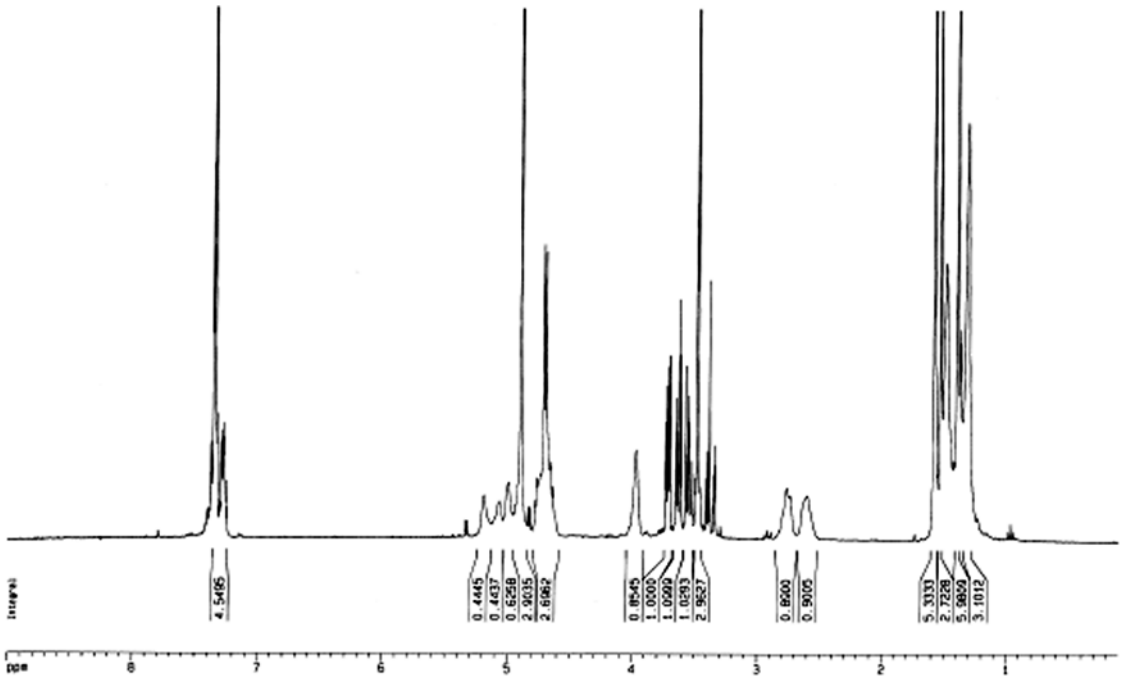

(5*S*)-1-methyl-5-[(trityloxy)methyl]pyrrolidin-2-one ((-)-67)

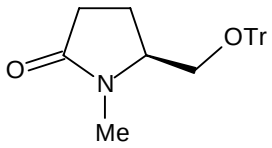

To a solution of **L-(5)-trityloxymethyl-2-pyrrolidinone** (**50**) (500 mg, 1.4 mmol, 1.0 eq) in anhydrous THF (3 ml), cooled to 0°C, was added sodium hydride (183 mg, 4.2 mmol, 3.0 eq 55 % in oil) and the mixture was stirred at 0°C for 5 minutes. Methyl iodide (611 µl, 9.8 mmol, 7.0 eq) was added and the mixture was allowed to warm up to 25°C. After 4 hours, water was added carefully. The resulting mixture was poured into a saturated aqueous solution of NH_4Cl (15 ml) and the aqueous layer was extracted with EtOAc (15 ml, 3 times). The combined organic extracts were dried over $MgSO_4$, filtered and concentrated *in vacuo*. Flash chromatography on silica gel (pentane/EtOAc 4/5) afforded **67** (347 mg, 67 %) as a pale yellow solid.

$[\alpha]_{589}^{25}$ = -3, $[\alpha]_{577}^{25}$ = -6 (c = 0.47, $CHCl_3$).

IR (film): 3450, 3060, 2920, 1685, 1485, 1445, 1400, 1295, 1250, 1220, 1155, 1075, 1035, 995, 755, 705 cm^{-1}.

^{1}H-NMR (400 MHz, $CDCl_3$):
7.64-7.07 (m, $15H_{arom}$); **3.62** (m, 1H, H-C(5)); **3.31** (dd, 1H, ^3J(H-C(1'), H-C(5)) = 3.7, $^2J_{gem}$ = 10.0, H-C(1')); **3.17** (dd, 1H, ^3J(H-C(1'), H-C(5)) = 4.5, $^2J_{gem}$ = 10.0, H-C(1')); **2.79** (s, 3H, Me-N); **2.55** (m, 1H, H-C(3)); **2.34** (ddd, 1H, ^3J(H-C(3), H-C(4)) = 4.7, ^3J(H-C(3), H-C(4)) = 4.8, $^2J_{gem}$ = 10.1, H-C(3)); **2.12** (m, 1H, H-C(4)); **1.87** (m, 1H, $^2J_{gem}$ = 9.4, H-C(4)).

^{13}C-NMR (101 MHz, $CDCl_3$):
175.4 (s, C(2)); **143.6** (s, $3C_{arom}$); **128.6** (d, ^1J(C,H) = 159, $6C_{arom}$); **127.9** (d, ^1J(C,H) = 160, $6C_{arom}$); **127.2** (d, ^1J(C,H) = 161, $3C_{arom}$); **86.9** (s, O*C*Ph_3); **64.2** (t, ^1J(C,H) = 142, C(1')); **60.0** (d, ^1J(C,H) = 144, C(5)); **30.2** (t, ^1J(C,H) = 133, C(3)); **28.4** (q, ^1J(C,H) = 138, Me); **21.6** (t, ^1J(C,H) = 133, C(4)).

MALDI-TOF: 372.15 $(M+H)^+$.
Anal. for $C_{25}H_{25}NO_2$ (371.48): calc. C 80.83, H 6.78, N 3.77; found C 80.75, H 6.82, N 3.83.
M.P: 115-117°C.

^{1}H-NMR spectrum of **67**

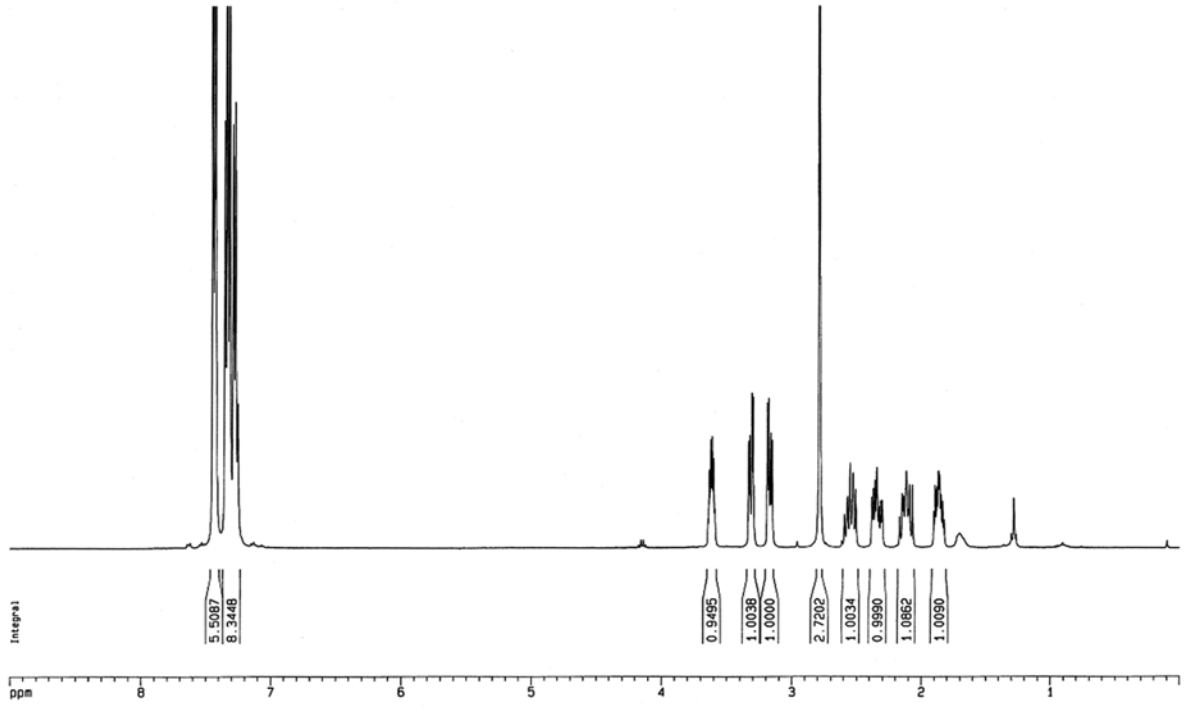

(3a*R*,6*R*,6a*R*)-2,2,5-trimethyl-6-[(trityloxy)methyl]tetrahydro-4*H*-[1,3]dioxolo[4,5-c] pyrrol-4-one ((-)-68)

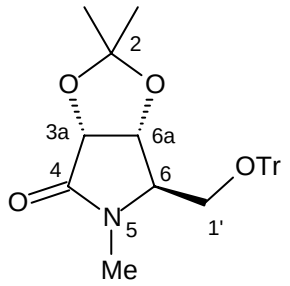

Butyllithium (2.2 eq, 1.6 M in hexane, 40.8 mmol, 25 ml) was added to a solution of diisopropylamine (5.7 ml, 40.8 mmol, 2.2 eq) in anhydrous THF (41 ml) at –78°C. The mixture was stirred at –78°C for 10 minutes, followed by addition of a solution of **67** (6.9 g, 18.5 mmol, 1.0 eq) in anhydrous THF (25 ml). The mixture was stirred at –78°C for 10 minutes, at –30°C for 10 minutes and then at –78°C for 15 minutes. After addition of a solution of PhSeBr (5.3 g, 22.3 mmol, 1.2 eq) in anhydrous THF (25 ml), the mixture was stirred at –78°C for 30 minutes. The solution was dissolved in EtOAc (35 ml) and washed with a saturated aqueous solution of NH_4Cl (50 ml). The organic layer was dried over $MgSO_4$, filtered and concentrated *in vacuo* at 20°C to give the corresponding 3-selenopyrroldinone which was directly engaged in the next step.

This 3-selenopyrrolidinone (18.5 mmol, 1.0 eq) was dissolved in a mixture of EtOAc/H_2O_2 (3/1, 160 ml) and cooled to 0°C. After stirring for 1 hour, water and EtOAc were added. The organic layer was washed with a saturated aqueous solution of $NaHCO_3$, NH_4Cl and brine to reach neutral pH. Drying over $MgSO_4$ and concentration *in vacuo* afforded a crude enone as a yellow foam.

This crude enone (18.5 mmol, 1.0 eq), OsO_4 (0.1 eq, 0.1 M in H_2O, 1.85 mmol, 18.5 ml) and NMO monohydrate (3.76 g, 27.8 mmol, 1.5 eq) in a mixture of acetone/H_2O (7/3, 160 ml) were stirred at 25°C for 12 hours. After addition of sodium pyrosulfite (2.5 g) at 0°C, the aqueous layer was extracted with EtOAc (30 ml, 3 times). The combined organic extracts were dried over $MgSO_4$ and concentrated *in vacuo*. Flash chromatography on silica gel (CH_2Cl_2/MeOH 97/3) afforded an intermediate diol (3.34 g, 45 %, 3 steps) as a yellow foam.

To a solution of this diol (140 mg, 0.35 mmol, 1.0 eq) in a mixture of acetone/2,2-dimethoxypropane (3/1, 3.5 ml), cooled to 0°C, was added a catalytic amount of *p*-TsOH. The solution was stirred at 0°C for 1 hour. After dilution with EtOAc (10 ml), the mixture was washed with a saturated aqueous solution of $NaHCO_3$ (15 ml) and H_2O (15 ml), dried over $MgSO_4$, filtered and concentrated *in vacuo*. Flash chromatography on silica gel (pentane/EtOAc 7/3) afforded **68** (130 mg, 83 %) as a pale yellow solid.

$[\alpha]_{589}^{25}$ = -32, $[\alpha]_{577}^{25}$ = -37, $[\alpha]_{435}^{25}$ = -63, $[\alpha]_{405}^{25}$ = -74 (c = 0.46, $CHCl_3$).

IR (film): 2990, 2930, 1705, 1490, 1450, 1380, 1220, 1075, 1000, 755, 705 cm^{-1}.

^{1}H-NMR (400 MHz, $CDCl_3$):
7.39-7.25 (m, $15H_{arom}$); **4.89** (d, 1H, ^3J(H-C(3a), H-C(6a)) = 5.7, H-C(3a)); **3.48** (d, 1H, ^3J(H-C(6a), H-C(3a)) = 5.7, H-C(6a)); **3.57** (bs, 1H, H-C(6)) **3.48** (dd, 1H, ^3J(H-C(1'), H-C(6)) = 2.5, $^2J_{gem}$ = 10.3, H-C(1')); **3.22** (dd, 1H, ^3J(H-C(1'), H-C(6)) = 2.4, $^2J_{gem}$ = 10.3, H-C(1')); **2.77** (s, 3H, Me-N); **1.44** (s, 3H, Me-C(2)); **1.39** (s, 3H, Me-C(2)).

^{13}C-NMR (101 MHz, $CDCl_3$):
171.7 (s, C(4)); **143.0** (s, $3C_{arom}$); **128.4** (d, ^1J(C,H) = 159, $6C_{arom}$); **128.0** (d, ^1J(C,H) = 160, $6C_{arom}$); **127.4** (d, ^1J(C,H) = 161, $3C_{arom}$); **111.9** (s, C(2)); **87.2** (s, O*C*Ph_3); **77.8** (d, ^1J(C,H) = 158, C(3a)); **76.3** (d, ^1J(C,H) = 160, C(6a)); **63.9** (d, ^1J(C,H) = 144, C(6)); **60.1** (t, ^1J(C,H) = 143, C(1')); **28.1** (q, ^1J(C,H) = 139, Me-N); **27.2** (q, ^1J(C,H) = 128, Me-C(2)); **25.8** (q, ^1J(C,H) = 128, Me-C(2)).

MALDI-TOF: 482.14 $(M+K)^+$, 466.16 $(M+Na)^+$, 444.19 $(M+H)^+$.
Anal. for $C_{28}H_{29}NO_4$ (443.54): calc. C 75.82, H 6.59, N 3.16; found C 75.79, H 6.64, N 3.05.
M.P: 150-155°C.

^{1}H-NMR spectrum of **68**

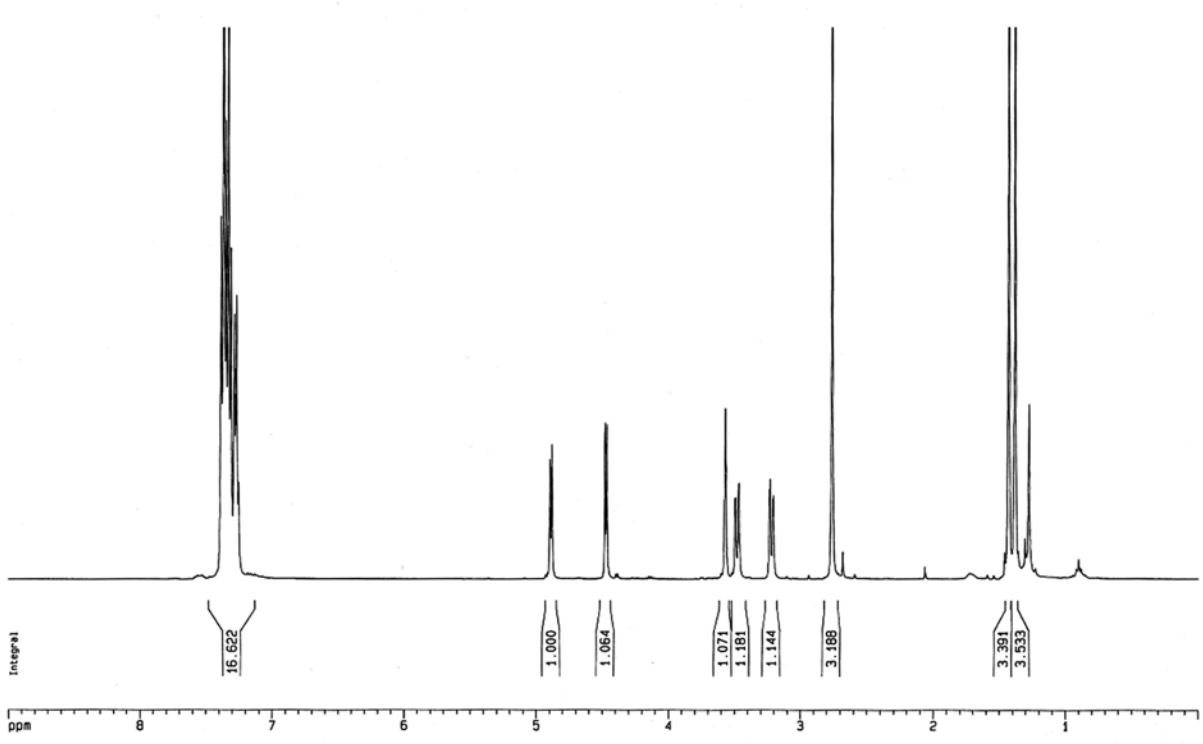

Phenylmethyl (5*S*)-2-oxo-5-{[(triphenylmethyl)oxy]methyl}pyrrolidine-1-carboxylate ((-)-69)

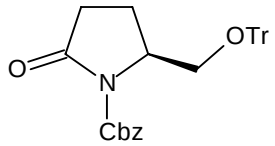

To a solution of **L-(5)-trityloxymethyl-2-pyrrolidinone** (**50**) (200 mg, 0.56 mmol, 1.0 eq) in anhydrous THF (5 ml), cooled to -78°C, was added a solution of LiHMDS (1.1 eq, 1M in THF, 500 µl). After 30 minutes, CbzCl (79 µl, 0.56 mmol, 1.0 eq) was added dropwise. The mixture was allowed to warm up to 25°C and was stirred for 2 hours. After dilution with EtOAc (3 ml), the mixture was washed with NH_4Cl (10 ml) and the aqueous layer was extracted with EtOAc (15 ml, 3 times). The combined organic extracts were dried over $MgSO_4$, filtered and concentrated *in vacuo*. Flash chromatography on silica gel (pentane/EtOAc 3/1) afforded **69** (250 mg, 91 %) as a pale yellow foam.

$[\alpha]_{589}^{25}$ = -48, $[\alpha]_{577}^{25}$ = -49, $[\alpha]_{435}^{25}$ = -96, $[\alpha]_{405}^{25}$ = -115 (c = 0.63, $CHCl_3$).

IR (film): 3025, 2955, 2880, 1785, 1750, 1720, 1490, 1450, 1380, 1290, 1220, 1080, 1035, 755, 705 cm^{-1}.

^{1}H-NMR (400 MHz, $CDCl_3$):
7.43-7.24 (m, 15H_{arom}); **5.22** (2H, AB, OC*H*$_2$Ph); **4.32** (m, 1H, H-C(5)); **3.54** (dd, 1H, ^3J(H-C(1'), H-C(5)) = 4.2, $^2J_{gem}$ = 9.6, H-C(1')); **3.22** (dd, 1H, ^3J(H-C(1'), H-C(5)) = 2.0, $^2J_{gem}$ = 9.6, H-C(1')); **2.88** (m, 1H, H-C(3)); **2.47** (m, 1H, H-C(3)); **2.13** (m, 1H, H-C(4)); **2.00** (m,1H, H-C(4)).

^{13}C-NMR (101 MHz, $CDCl_3$):
174.5 (s, C(2)); **150.9** (s, N*C*(O)O); **143.4** (s, 3C_{arom}); **135.1** (s, 1C_{arom}); **128.5** (d, ^1J(C,H) = 159, 2C_{arom}); **128.4** (d, ^1J(C,H) = 159, 6C_{arom}); **128.2** (d, ^1J(C,H) = 159, 1C_{arom}); **128.0** (d, ^1J(C,H) = 159, 2C_{arom}); **127.8** (d, ^1J(C,H) = 161, 6C_{arom}); **127.0** (d, ^1J(C,H) = 160, 3C_{arom}); **87.0** (s, O*C*Ph$_3$); **67.7** (t, ^1J(C,H) = 148, O*C*H$_2$Ph); **64.1** (t, ^1J(C,H) = 144, C(1')); **57.4** (d, ^1J(C,H) = 148, C(5)); **32.0** (t, ^1J(C,H) = 135, C(3)); **21.2** (t, ^1J(C,H) = 134, C(4)).

HRMS ($C_{32}H_{29}NO_4$ + Na): calc. 514.1994; found 514.1957.
Anal. for $C_{32}H_{29}NO_4$ (491.59): calc. C 78.19, H 5.95, N 2.85; found C 78.14, H 5.97, N 2.76.

^{1}H-NMR spectrum of **69**

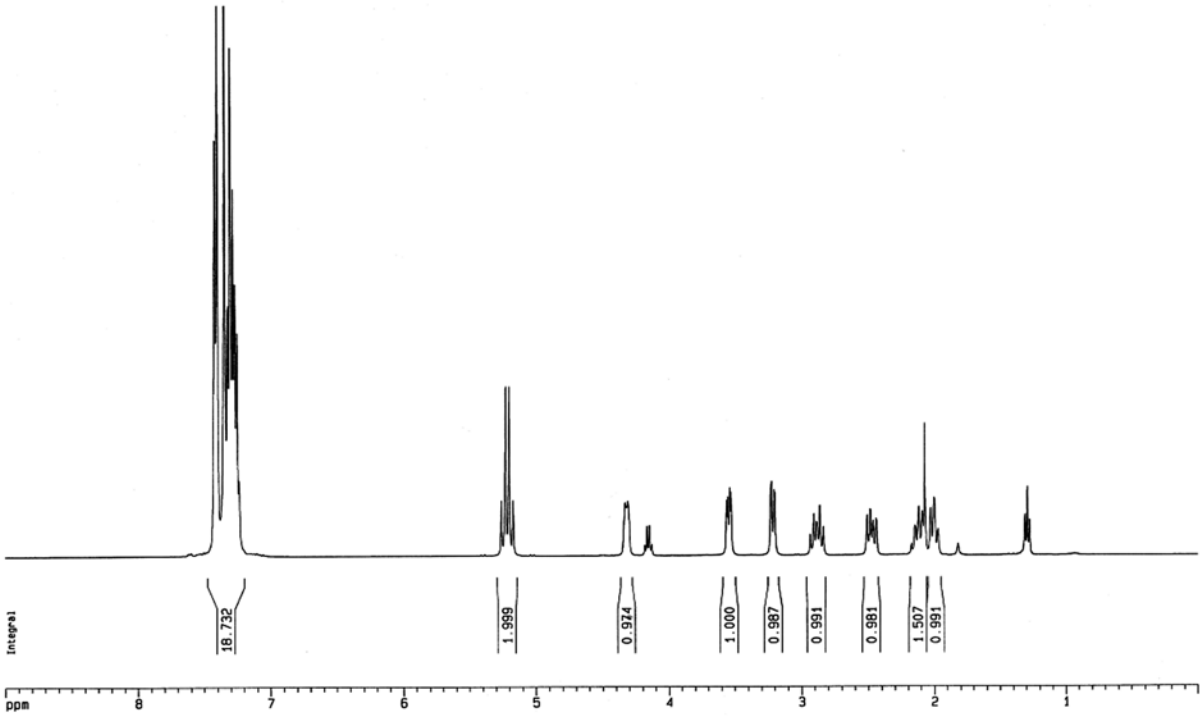

Phenylmethyl (3a*R*,6*R*,6a*R*)-2,2-dimethyl-4-oxo-6-{[(triphenylmethyl)oxy]methyl}tetrahydro-5*H*-[1,3]dioxolo[4,5-c]pyrrole-5-carboxylate ((-)-70)

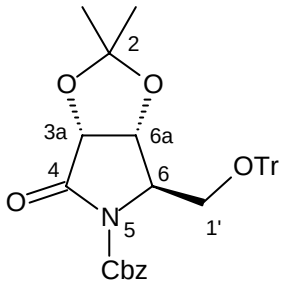

Butyllithium (2.2 eq, 1.6 M in hexane, 9.1 mmol, 5.7 ml) was added to a solution of diisopropylamine (1.3 ml, 9.1 mmol, 2.2 eq) in anhydrous THF (9 ml) at –78°C. The mixture was stirred at –78°C for 10 minutes, followed by addition of a solution of **69** (2.0 g, 4.1 mmol, 1.0 eq) in anhydrous THF (20 ml). The mixture was stirred at –78°C for 10 minutes, at –30°C for 10 minutes and then at –78°C for 15 minutes. After addition of a solution of PhSeBr (1.17 g, 4.95 mmol, 1.2 eq) in anhydrous THF (6 ml), the mixture was stirred at -78°C for 30 minutes. The solution was dissolved in EtOAc (15 ml) and washed with a saturated aqueous solution of NH_4Cl (20 ml). The organic layer was dried over $MgSO_4$, filtered and concentrated *in vacuo* at 20°C to give the corresponding 3-selenopyrroldinone which was directly engaged in the next step.

This 3-selenopyrrolidinone (4.1 mmol, 1.0 eq) was dissolved in a mixture of EtOAc/H_2O_2 (3/1, 32 ml), at 0°C. After stirring for 1 hour, water and EtOAc were added. The organic layer was successively washed with a saturated aqueous solution of $NaHCO_3$, NH_4Cl and brine to reach neutral pH, dried over $MgSO_4$ and concentrated *in vacuo* to afford a crude enone.

This crude enone (4.1 mmol, 1.0 eq), OsO_4 (0.1 eq, 0.1 M in H_2O, 0.41 mmol, 4.1 ml) and NMO monohydrate (836 mg, 6.2 mmol, 1.5 eq) in a mixture of acetone/H_2O (7/3, 40 ml) were stirred at 25°C for 12 hours. After addition of sodium pyrosulfite (250 mg) at 0°C, the aqueous layer was extracted with EtOAc (25 ml, 3 times). The combined organic extracts were dried over $MgSO_4$ and concentrated *in vacuo*. Flash chromatography on silica gel (CH_2Cl_2/MeOH 97/3) afforded an intermediate diol (609 mg, 28 %, 3 steps) as a white foam.

To a solution of this diol (609 mg, 1.16 mmol, 1.0 eq) in a mixture of acetone/2,2-dimethoxypropane (3/1, 10 ml), cooled to 0°C, was added a catalytic amount of *p*-TsOH. The solution was stirred at 0°C for 1 hour. After dilution with EtOAc (20 ml), the mixture was washed with a saturated aqueous solution of $NaHCO_3$ (20 ml) and water (20 ml), dried over $MgSO_4$, filtered and concentrated *in vacuo*. Flash chromatography on silica gel (pentane/EtOAc 7/3) afforded **70** (354 mg, 54 %) as a white solid.

$[\alpha]_{589}^{25}$ = -58, $[\alpha]_{577}^{25}$ = -60, $[\alpha]_{435}^{25}$ = -116, $[\alpha]_{405}^{25}$ = -158 (c = 0.56, $CHCl_3$).

IR (film): 3060, 3025, 2985, 2885, 1795, 1765, 1725, 1490, 1450, 1380, 1290, 1220, 1155, 1090, 1000, 750, 705 cm^{-1}.

^{1}H-NMR (400 MHz, $CDCl_3$):
7.51-7.08 (m, 20H_{arom}); **5.25** (2H, AB, OCH_2Ph); **4.97** (d, 1H, ^3J(H-C(3a), H-C(6a)) = 5.3, H-C(3a)); **4.38** (d, 1H, ^3J(H-C(6a), H-C(3a)) = 5.3, H-C(6a)); **4.29** (bs, 1H, H-C(6)); **3.74** (dd, 1H, ^3J(H-C(1'), H-C(6)) = 2.4, $^2J_{gem}$ = 10.2, H-C(1')); **3.22** (dd, 1H, ^3J(H-C(1'), H-C(6)) = 1.3, $^2J_{gem}$ = 10.2, H-C(1')); **1.45** (s, 3H, Me-C(2)); **1.37** (s, 3H, Me-C(2)).

^{13}C-NMR (101 MHz, $CDCl_3$):
171.1 (s, C(4)); **151.1** (s, N*C*(O)O); **143.0** (s, 3C_{arom}); **134.9** (s, 1C_{arom}); **128.6** (d, ^1J(C,H) = 160, 1C_{arom}); **128.4** (d, ^1J(C,H) = 158, 8C_{arom}); **128.1** (d, ^1J(C,H) = 160, 8C_{arom}); **127.3** (d, ^1J(C,H) = 161, 3C_{arom}); **112.2** (s, C(2)); **87.7** (s, O*C*Ph_3); **78.1** (d, ^1J(C,H) = 160, C(3a)); **75.7** (d, ^1J(C,H) = 161, C(6a)); **68.3** (t, ^1J(C,H) = 150, O*C*H_2Ph); **61.8** (t, ^1J(C,H) = 145, C(1')); **60.6** (d, ^1J(C,H) = 149, *C*(6)); **27.2** (q, ^1J(C,H) = 127, Me-C(2)); **25.7** (q, ^1J(C,H) = 127, Me-C(2)).

HRMS ($C_{35}H_{33}NO_6$ + Na): calc. 586.2206; found 586.2238.
Anal. for $C_{35}H_{33}NO_6$ (563.65): calc. C 74.58, H 5.90, N 2.48; found C 74.59, H 5.96, N 2.55.
M.P: 191-196°C.

^{1}H-NMR spectrum of **70**

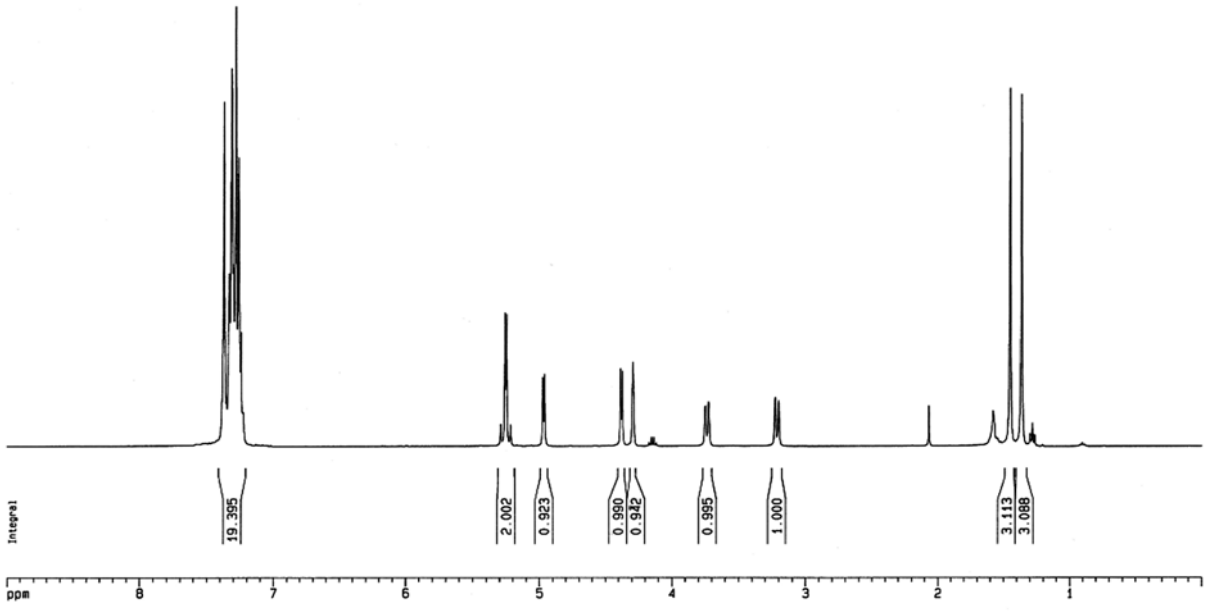

***Tert*-butyl (2*S*)-2-({[(1,1-dimethylethyl)(dimethyl)silyl]oxy}methyl)-5-oxopyrrolidine-1-carboxylate ((-)-75)**

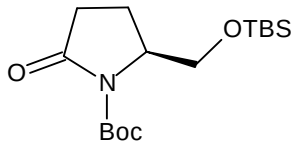

To a solution of **(S)-5-(hydroxymethyl)-2-pyrrolidinone** (**74**) (200 mg, 1.74 mmol, 1.0 eq) in DMF (15 ml), cooled to 0°C, were added imidazole (296 mg, 4.35 mmol, 2.5 eq) and TBDMSCl (393 mg, 2.61 mmol, 1.5 eq). The solution was stirred at 0°C for 1 hour. After concentration *in vacuo*, the residue was diluted with EtOAc (5 ml) and washed with a saturated aqueous solution of $NaHCO_3$ (10 ml, 3 times). The organic layer was dried over $MgSO_4$, filtered and concentrated *in vacuo*. Flash chromatography on silica gel (CH_2Cl_2/MeOH 97/3) afforded the protected alcohol (339 mg, 85 %) as a yellow oil.

To a solution of this protected alcohol (2.8 g, 12.5 mmol, 1.0 eq) in pyridine (50 ml) were added Boc_2O (3.0 g, 13.8 mmol, 1.1 eq) and a catalytic amount of DMAP. The reaction mixture was stirred at 25°C for 12 hours and then concentrated *in vacuo*. The residue was dissolved in EtOAc (35 ml) and washed with a saturated aqueous solution of NH_4Cl (20 ml) and a saturated aqueous solution of $NaHCO_3$ (20 ml). The organic layer was dried over $MgSO_4$, filtered and concentrated *in vacuo*. Flash chromatography on silica gel (CH_2Cl_2/MeOH 97/3) afforded **75** (3.7 g, 89 %) as a brown oil.

$[\alpha]_{589}^{25}$ = -57, $[\alpha]_{577}^{25}$ = -60, $[\alpha]_{435}^{25}$ = -120, (c = 0.41, $CHCl_3$).

IR (film): 3415, 2955, 2935, 2890, 2860, 1785, 1750, 1710, 1465, 1365, 1310, 1255, 1160, 1110, 1030, 840, 780 cm^{-1}.

^{1}H-NMR (400 MHz, $CDCl_3$):
4.17 (m, 1H, H-C(2)); **3.92** (dd, 1H, ^3J(H-C(1'), H-C(2)) = 3.8, $^2J_{gem}$ = 10.6, H-C(1')); **3.69** (dd, 1H, ^3J(H-C(1'), H-C(2)) = 2.2, $^2J_{gem}$ = 10.6, H-C(1')); **2.70** (ddd, 1H, ^3J(H-C(4), H-C(3)) = 10.2, ^3J(H-C(4), H-C(3)) = 10.7, $^2J_{gem}$ = 17.7, H-C(4)); **2.40** (ddd, 1H, ^3J(H-C(4), H-C(3)) = 2.2, ^3J(H-C(4), H-C(3)) = 9.7, $^2J_{gem}$ = 17.7, H-C(4)); **2.10-2.03** (m, 2H, H-C(3)); **1.54** (s, 9H, Me_3C); **0.88** (s, 9H, Me_3CSi); **0.05, 0.04** (2s, 6H, Me_2Si).

^{13}C-NMR (101 MHz, $CDCl_3$):
174.9 (s, C(5)); **150.1** (s, N*C*(O)O); **82.7** (s, O*C*Me_3); **64.3** (t, ^1J(C,H) = 142, C(1')); **58.9** (d, ^1J(C,H) = 145, C(2)); **32.3** (t, ^1J(C,H) = 132, C(4)); **28.1** (q, ^1J(C,H) = 127, *Me*$_3$C); **25.8** (q, ^1J(C,H) = 125, *Me*$_3$CSi); **21.1** (t, ^1J(C,H) = 134, C(3)); **18.2** (s, Me_3*C*Si); **-5.55, -5.60** (2q, ^1J(C,H) = 118, *Me*$_2$Si).

ESI-MS: 330.38 $(M+H)^+$.
Anal. for $C_{16}H_{31}NO_4Si$ (329.51): calc. C 58.32, H 9.48, N 4.25, Si 8.52; found C 58.43, H 9.43, N 4.30 Si 8.44.

^{1}H-NMR spectrum of **75**

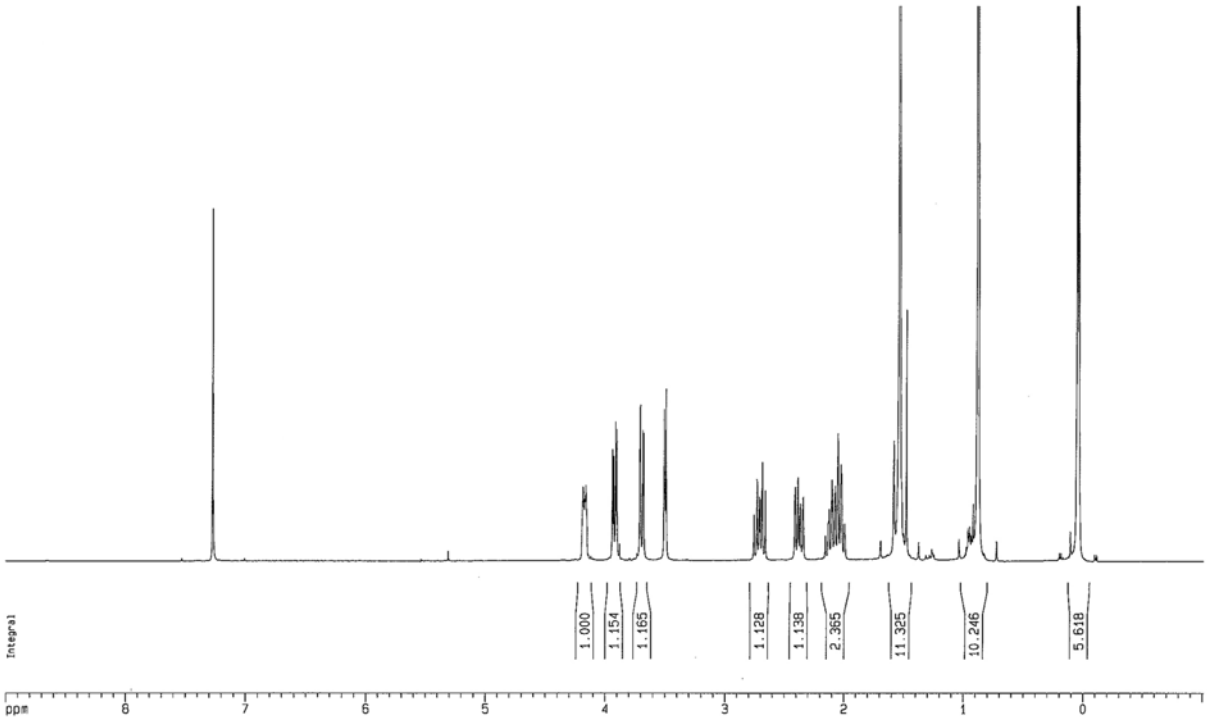

Tert-butyl (2_R_,3_R_,4_R_)-2-({[(1,1-dimethylethyl)(dimethyl)silyl]oxy}methyl)-3,4-dihydroxy-5-oxopyrrolidine-1-carboxylate ((-)-76)

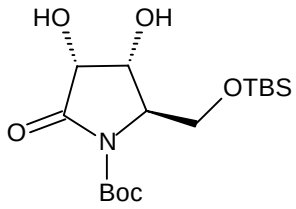

Butyllithium (2.4 eq, 1.6 M in hexane, 25.5 mmol, 16 ml) was added to a solution of diisopropylamine (3.6 ml, 25.5 mmol, 2.4 eq) in anhydrous THF (25 ml) at –78°C. The mixture was stirred at –78°C for 10 minutes, followed by addition of a solution of **75** (3.5 g, 10.6 mmol, 1.0 eq) in anhydrous THF (35 ml). The mixture was stirred at –78°C for 10 minutes, at –30°C for 10 minutes and then at –78°C for 15 minutes. After addition of a solution of PhSeBr (3.0 g, 12.7 mmol, 1.2 eq) in anhydrous THF (20 ml), the mixture was stirred at –78°C for 30 minutes. The solution was dissolved in EtOAc (35 ml) and washed with a saturated aqueous solution of NH_4Cl (20 ml). The organic layer was dried over $MgSO_4$, filtered and concentrated *in vacuo* at 20°C to give the corresponding 3-selenopyrroldinone which was directly engaged in the next step.

This 3-selenopyrrolidinone (10.6 mmol, 1.0 eq) was dissolved in a mixture of EtOAc/H_2O_2 (3/1 80 ml), at 0°C. After stirring for 1 hour, water and EtOAc were added. The organic layer was washed with a saturated aqueous solution of $NaHCO_3$, NH_4Cl and brine to reach neutral pH, dried over $MgSO_4$ and concentrated *in vacuo* to afford a crude enone.

This crude enone (10.6 mmol, 1.0 eq), OsO_4 (0.1 eq, 0.1 M in H_2O, 1.06 mmol, 10.6 ml) and NMO monohydrate (2.15 g, 15.9 mmol, 1.5 eq) in a mixture of acetone/H_2O (7/3 80 ml) were stirred at 25°C for 12 hours. After addition of sodium pyrosulfite at 0°C, the aqueous layer was extracted with EtOAc (30 ml, 3 times). The combined organic extracts were dried over $MgSO_4$ and concentrated *in vacuo*. Purification by flash chromatography on silica gel (CH_2Cl_2/MeOH 95/5) afforded **76** as a white foam (1.18 g, 43 %, 3 steps).

$[\alpha]_{589}^{25}$ = -12, $[\alpha]_{577}^{25}$ = -12, $[\alpha]_{435}^{25}$ = -24, $[\alpha]_{405}^{25}$ = -30 (c = 0.36, $CHCl_3$).

IR (film): 3440, 2955, 2885, 2860, 1780, 1465, 1370, 1300, 1255, 1155, 995, 945, 835, 755 cm^{-1}.

^{1}H-NMR (400 MHz, $CDCl_3$):
4.57 (d, 1H, ^3J(H-C(4), H-C(3)) = 4.8, H-C(4)); **4.36** (d, 1H, ^3J(H-C(3), H-C(4)) = 4.8, H-C(3)); **4.12** (m, 1H, H-C(2)); **3.99** (dd, 1H, ^3J(H-C(1'), H-C(2)) = 2.9, $^2J_{gem}$ = 10.9, H-C(1')); **3.83** (dd, 1H, ^3J(H-C(1'), H-C(2)) = 1.6, $^2J_{gem}$ = 10.9, H-C(1')); **1.55** (s, 9H, Me_3C); **0.87** (s, 9H, Me_3CSi); **0.04, 0.03** (2s, 6H, Me_2Si).

^{13}C-NMR (101 MHz, $CDCl_3$):
173.6 (s, C(5)); **149.6** (s, N*C*(O)O); **83.8** (s, O*C*Me_3); **71.5** (d, ^1J(C,H) = 154, C(4)); **69.2** (d, ^1J(C,H) = 167, C(3)); **64.7** (d, ^1J(C,H) = 150, C(2)); **61.7** (t, ^1J(C,H) = 145, C(1')); **28.0** (q, ^1J(C,H) = 127, *Me*$_3$C); **25.8** (q, ^1J(C,H) = 125, *Me*$_3$CSi); **18.2** (s, Me_3*C*Si); **-5.64, -5.65** (2q, ^1J(C,H) = 118, Me_2Si).

HRMS ($C_{16}H_{31}NO_6Si$ + Na): calc. 384.1818; found 384.1822.
Anal. for $C_{16}H_{31}NO_6Si$ (361.51): calc. C 53.16, H 8.64, N 3.87, Si 7.77; found C 53.20, H 8.64.

^{1}H-NMR spectrum of **76**

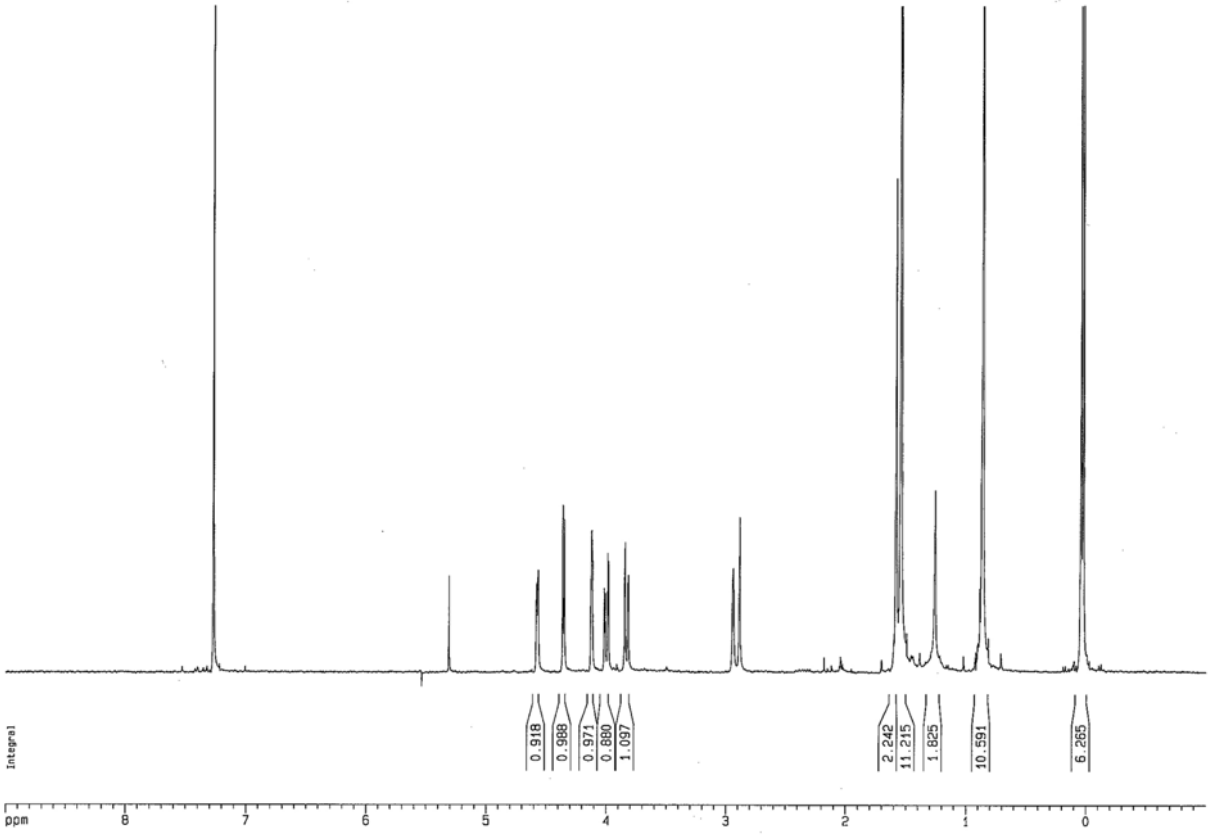

***Tert*-butyl (3a*R*,4*R*,6a*R*)-4-({[(1,1-dimethylethyl)(dimethyl)silyl]oxy}methyl)2,2-dimethyl -6-oxotetrahydro-5*H*-[1,3]dioxolo[4,5-c]pyrrole-5-carboxylate ((-)-77)**

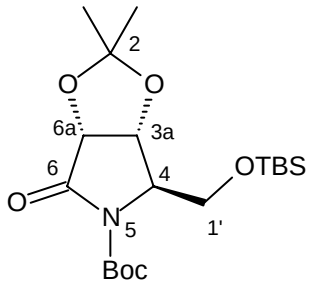

To a solution of diol **76** (1.18g, 3.28 mmol, 1.0 eq) in a mixture of acetone/2,2-dimethoxypropane (3/1 35 ml), cooled to 0°C, was added a catalytic amount of *p*-TsOH. The solution was stirred at 0°C for 3 hours. After dilution with EtOAc (15 ml), the mixture was washed with a saturated aqueous solution of $NaHCO_3$ (15 ml) and water (15 ml), dried over $MgSO_4$, filtered and concentrated *in vacuo*. Flash chromatography on silica gel (pentane/EtOAc 9/1) afforded **77** (1.1 g, 89 %) as a brown oil.

$[\alpha]_{589}^{25}$ = -78, $[\alpha]_{577}^{25}$ = -81, $[\alpha]_{435}^{25}$ = -159, $[\alpha]_{405}^{25}$ = -192 (c = 0.56, $CHCl_3$).

IR (film): 3425, 3020, 1640, 1520, 1475, 1425, 1375, 1305, 1215, 1155, 1045, 925, 760 cm^{-1}.

^{1}H-NMR (400 MHz, $CDCl_3$):
4.65 (d, 1H, ^3J(H-C(6a), H-C(3a)) = 5.4, H-C(6a)); **4.52** (d, 1H, ^3J(H-C(3a), H-C(6a)) = 5.4, H-C(3a)); **4.23** (m, 1H, H-C(4)); **4.00** (dd, 1H, ^3J(H-C(1'), H-C(4)) = 2.2, $^2J_{gem}$ = 10.9, H-C(1')); **3.78** (dd, 1H, ^3J(H-C(1'), H-C(4)) = 1.3, $^2J_{gem}$ = 10.9, H-C(1')); **1.54** (s, 9H, Me_3C); **1.46** (s, 3H, Me-C(2)); **1.38** (s, 3H, Me-C(2)); **0.86** (s, 9H, Me_3CSi); **0.03, 0.02** (2s, 6H, Me_2Si).

^{13}C-NMR (101 MHz, $CDCl_3$):
170.9 (s, C(6)); **150.0** (s, N*C*(O)O); **111.8** (s, C(2)); **83.5** (s, O*C*Me_3); **78.2** (d, ^1J(C,H) = 160, C(6a)); **75.7** (d, ^1J(C,H) = 161, C(3a)); **62.0** (t, ^1J(C,H) = 144, C(1')); **61.8** (d, ^1J(C,H) = 148, C(4)); **28.0** (q, ^1J(C,H) = 127, *Me*$_3$C); **27.1** (q, ^1J(C,H) = 125, Me-C(2)); **25.8** (q, ^1J(C,H) = 125, *Me*$_3$CSi); **25.6** (q, ^1J(C,H) = 126, Me-C(2)); **18.2** (s, Me_3*C*Si); **-5.64, -5.75** (2q, ^1J(C,H) = 118, Me_2Si).

MALDI-TOF: 424.16 $(M+Na)^+$.
Anal. for $C_{19}H_{35}NO_6Si$ (401.58): calc. C 56.83, H 8.78, N 3.49, Si 6.99; found C 56.81, H 8.72.

^{1}H-NMR spectrum of **77**

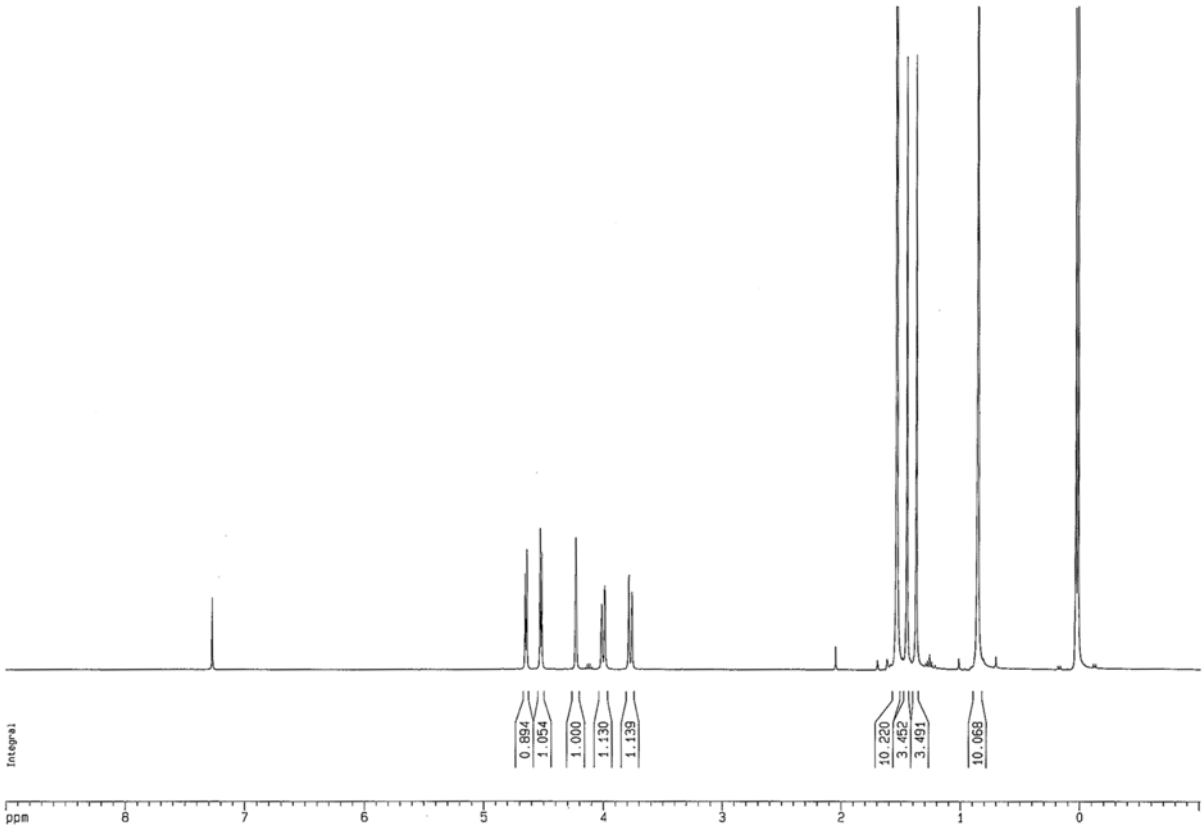

***Tert*-butyl (3a*R*,6a*R*)-4-(hydroxymethyl)-2,2-dimethyl-6-oxotetrahydro-5*H*-[1,3]dioxolo [4,5-c]pyrrole-5-carboxylate ((-)-78)**

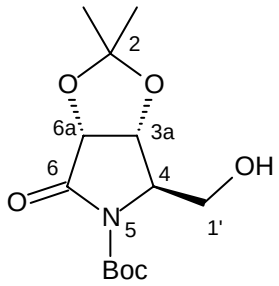

TBAF (2.0 eq, 1 M in THF, 1.0 mmol, 1.0 ml) was added to a solution of **77** (200 mg, 0.5 mmol, 1.0 eq) in anhydrous THF (5 ml) at 0°C. The mixture was stirred at 0°C for 1 hour and then concentrated *in vacuo*. The residue was purified by flash chromatography on silica gel (CH_2Cl_2/MeOH 96/4) to afford **78** (105 mg, 73 %) as a white foam.

$[\alpha]_{589}^{25}$ = -56 (c = 0.43, $CHCl_3$).

IR (film): 3495, 2985, 2360, 1780, 1720, 1460, 1370, 1305, 1240, 1155, 1095, 985, 845, 755 cm^{-1}.

^{1}H-NMR (400 MHz, $CDCl_3$):
4.77 (d, 1H, ^3J(H-C(6a), H-C(3a)) = 5.4, H-C(6a)); **4.60** (d, 1H, ^3J(H-C(3a), H-C(6a)) = 5.4, H-C(3a)); **4.23** (m, 1H, H-C(4)); **3.97** (ddd, 1H, ^3J(H-C(1'), H-C(4)) = 2.2, ^3J(H-C(1'), OH) = 4.8, $^2J_{gem}$ = 11.5, H-C(1')); **3.80** (ddd, 1H, ^3J(H-C(1'), H-C(4)) = 1.9, ^3J(H-C(1'), OH) = 6.1, $^2J_{gem}$ = 11.5, H-C(1')); **2.98** (dd, 1H, ^3J(OH, H-C(1')) = 4.8, ^3J(OH, H-C(1')) = 6.1, OH-C(1')); **1.53** (s, 9H, Me_3C); **1.45**(s, 3H, Me-C(2)); **1.37** (s, 3H, Me-C(2)).

^{13}C-NMR (101 MHz, $CDCl_3$):
172.2 (s, C(6)); **149.8** (s, N*C*(O)O); **111.8** (s, C(2)); **83.9** (s, O*C*Me_3); **78.0** (d, ^1J(C,H) = 160, C(6a)); **75.4** (d, ^1J(C,H) = 162, C(3a)); **62.1** (d, ^1J(C,H) = 149, C(4)); **61.3** (t, ^1J(C,H) = 144, C(1')); **28.0** (q, ^1J(C,H) = 127, Me_3C); **27.0** (q, ^1J(C,H) = 127, Me-C(2)); **25.5** (q, ^1J(C,H) = 127, Me-C(2)).

ESI-MS: 288.32 $(M+H)^+$.
HRMS ($C_{13}H_{21}NO_6$ + Na): calc. 310.1267; found 310.1273.

^{1}H-NMR spectrum of **78**

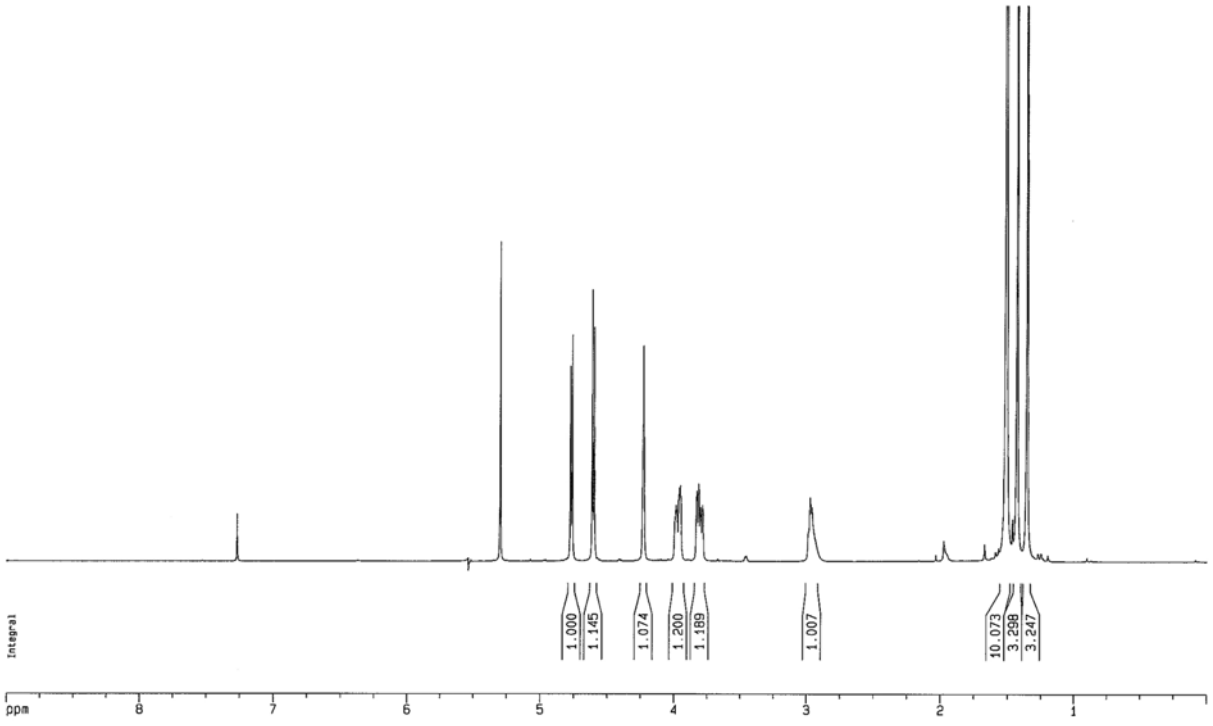

(3*R*,4*R*,5*R*)-3,4-Dihydroxy-5-({[(1*R*)-2-hydroxy-1-phenylethyl]amino}methyl)pyrrolidin-2-one ((-)-80)

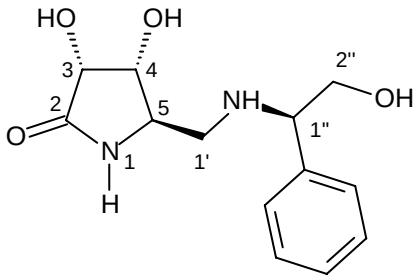

To a solution of oxalyl chloride (70 µl, 0.83 mmol, 1.2 eq) in anhydrous CH_2Cl_2 (6 ml), cooled to -78°C, was added DMSO (118 µl, 1.66 mmol, 2.4 eq). After 15 minutes, alcohol **78** (199 mg, 0.69 mmol, 1.0 eq) in solution in anhydrous CH_2Cl_2 (1 ml) was added dropwise. After 30 minutes, NEt_3 (483 µl, 3.47 mmol, 5.0 eq) was added and the mixture was warmed to –30°C for 20 minutes. The mixture was poured into water (10 ml) and extracted with EtOAc (10 ml, 3 times). The combined organic extracts were washed with brine (20 ml), dried over $MgSO_4$, filtered and concentrated *in vacuo* to afford the corresponding aldehyde **79** as a white foam.

Procedure 1. **D-(-)-α-phenylglycinol** (**99**) (49 mg, 0.36 mmol, 1.0 eq), aldehyde **79** (103 mg, 0.36 mmol, 1.0 eq), $NaBH(OAc)_3$ (107 mg, 0.5 mmol, 1.4 eq), $Cl(CH_2)_2Cl$ (4 ml). Flash chromatography (CH_2Cl_2/MeOH 96/4) afforded 29 mg (0.07 mmol, 19 %, 2 steps, colourless oil) of the fully protected compound which was directly engaged in **procedure 2b**. Purification by flash chromatography (MeCN/NH_4OH 6/1) afforded **80** (12 mg, 63 %) as a brown oil.

$[\alpha]_{589}^{25}$ = -8 (c = 0.56, MeOH).

IR (film): 3320, 3020, 2925, 1695, 1450, 1215, 1125, 1050, 760 cm^{-1}.

^{1}H-NMR (400 MHz, MeOD):
7.39-7.34 (m, $4H_{arom}$); **7.31-7.26** (m, $1H_{arom}$); **4.22** (d, 1H, ^3J(H-C(3), H-C(4)) = 5.4, H-C(3)); **4.10** (dd, 1H, ^3J(H-C(4), H-C(5)) = 1.4, ^3J(H-C(4), H-C(3)) = 5.4, H-C(4)); **3.78** (dd, 1H, ^3J(H-C(1''), H-C(2'')) = 4.4, ^3J(H-C(1''), H-C(2'')) = 8.1, H-C(1'')); **3.66** (dd, 1H, ^3J(H-C(2''), H-C(1'')) = 4.4, $^2J_{gem}$ = 10.9, H-C(2'')); **3.58** (dd, 1H, ^3J(H-C(2''), H-C(1'')) = 8.1, $^2J_{gem}$ = 10.9, H-C(2'')); **3.50** (ddd, 1H, ^3J(H-C(5), H-C(4)) = 1.4, ^3J(H-C(5), H-C(1')) = 6.1, ^3J(H-C(5), H-C(1')) = 6.1, H-C(5)); **2.59** (d, 2H, ^3J(H-C(1'), H-C(5)) = 6.1, 2H-C(1')).

^{13}C-NMR (101 MHz, MeOD):
177.8 (s, C(2)); **141.9** (s, C_{arom}); **129.6** (d, ^1J(C,H) = 160, $2C_{arom}$); **128.7** (d, ^1J(C,H) = 158, $2C_{arom}$); **128.6** (d, ^1J(C,H) = 161, C_{arom}); **72.2** (d, ^1J(C,H) = 153, C(4)); **71.2** (d, ^1J(C,H) = 144, C(3)); **67.7** (t, ^1J(C,H) = 143, C(2'')); **66.6** (d, ^1J(C,H) = 134, C(1'')); **61.6** (d, ^1J(C,H) = 145, C(5)); **50.8** (t, ^1J(C,H) = 136, C(1')).

MALDI-TOF: 267.13 $(M+H)^+$.
HRMS ($C_{13}H_{18}N_2O_4$ + H): calc. 267.1345; found 267.1347.

(5*S*)-5-({[(1,1-Dimethylethyl)(dimethyl)silyl]oxy}methyl)-1-methylpyrrolidin-2-one ((+)-81)

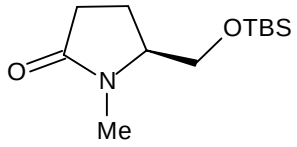

To a solution of **(S)-5-(hydroxymethyl)-2-pyrrolidinone** (**74**) (200 mg, 1.74 mmol, 1.0 eq) in DMF (15 ml), cooled to 0°C, were added imidazole (296 mg, 4.35 mmol, 2.5 eq) and TBDMSCl (393 mg, 2.61 mmol, 1.5 eq). The solution was stirred at 0°C for 1 hour. After concentration *in vacuo*, the residue was diluted with EtOAc (5 ml) and washed with a saturated aqueous solution of $NaHCO_3$ (10 ml, 3 times). The organic layer was dried over $MgSO_4$, filtered and concentrated *in vacuo*. Flash chromatography on silica gel (CH_2Cl_2/MeOH 97/3) afforded the protected alcohol (339 mg, 85 %) as a yellow oil.

To a solution of this protected alcohol (100 mg, 0.44 mmol, 1.0 eq) in anhydrous THF (4 ml), cooled to 0°C, was added sodium hydride (26 mg, 1.1 mmol, 2.5 eq, 55 % in oil). After stirring for 5 minutes, methyl iodide (190 µl, 3.1 mmol, 7.0 eq) was added and the mixture was allowed to warm up to 25°C. After 1.5 hours, water was added carefully, the resulting mixture was poured into a saturated aqueous solution of NH_4Cl (15 ml) and the aqueous layer was extracted with EtOAc (15 ml, 3 times). The combined organic extracts were dried over $MgSO_4$, filtered and concentrated *in vacuo*. Flash chromatography on silica gel (pentane/EtOAc 1/1) afforded **81** (177 mg, 83 %) as a yellow oil.

$[\alpha]_{589}^{25} = 2$, $[\alpha]_{577}^{25} = 2$, $[\alpha]_{435}^{25} = 10$, $[\alpha]_{405}^{25} = 13$ (c = 0.40, $CHCl_3$).

IR (film): 3445, 1650, 1465, 1400, 1255, 1110, 1030, 940, 775 cm^{-1}.

^{1}H-NMR (400 MHz, $CDCl_3$):
3.74 (dd, 1H, ^3J(H-C(1'), H-C(5)) = 3.5, $^2J_{gem}$ = 10.2, H-C(1')); **3.64-3.53** (dd and m, 2H, ^3J(H-C(1'), H-C(5)) = 4.2, $^2J_{gem}$ = 10.2, H-C(1') and H-C(5)); **2.86** (s, 3H, Me-N); **2.45** (m, 1H, H-C(3)); **2.31** (ddd, 1H, ^3J(H-C(3), H-C(4)) = 5.1, ^3J(H-C(3), H-C(4)) = 10.2, $^2J_{gem}$ = 16.6, H-C(3)); **2.09** (m, 1H, H-C(4)); **1.85** (ddd, 1H, ^3J(H-C(4), H-C(3)) = 5.1, ^3J(H-C(4), H-C(3)) = 10.2, $^2J_{gem}$ = 17.6, H-C(4)); **0.89** (s, 9H, Me_3CSi); **0.07, 0.06** (2s, 6H, Me_2Si).

^{13}C-NMR (101 MHz, $CDCl_3$):
175.4 (s, C(2)); **63.8** (t, ^1J(C,H) = 141, C(1')); **61.3** (d, ^1J(C,H) = 141, C(5)); **30.2** (t, ^1J(C,H) = 135, C(3)); **28.2** (q, ^1J(C,H) = 137, Me-N); **25.7** (q, ^1J(C,H) = 125, Me_3CSi); **21.1** (t, ^1J(C,H) = 131, C(4)); **18.1** (s, Me_3CSi); **-5.52** (q, ^1J(C,H) = 118, Me_2Si).

HRMS ($C_{12}H_{25}NO_2Si$ + Na): calc. 266.1552; found 266.1554.
Anal. for $C_{12}H_{25}NO_2Si$ (243.42): calc. C 59.21, H 10.35, N 5.75, Si 11.54; found C 59.33, H 10.23, N 5.72 Si 11.40.

^{1}H-NMR spectrum of **80**

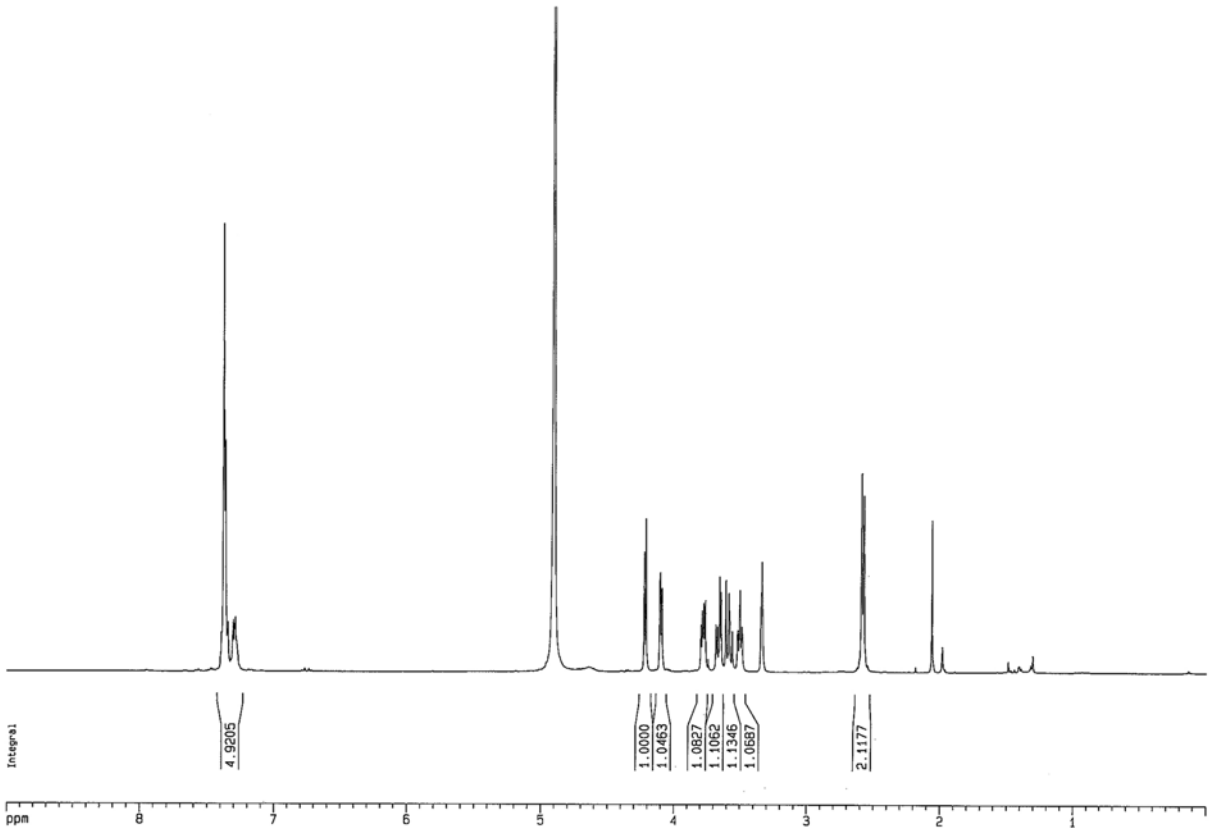

^{1}H-NMR spectrum of **81**

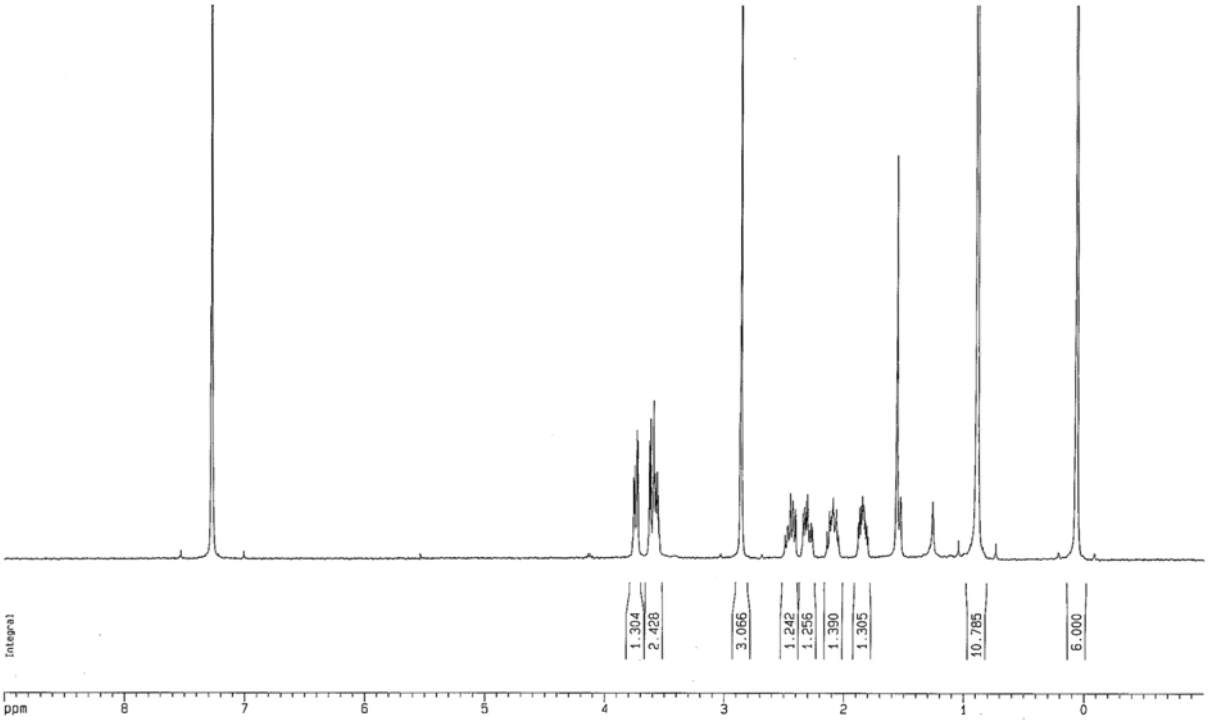

(3a*R*,6*R*,6a*R*)-6-({[(1,1-Dimethylethyl)(dimethyl)silyl]oxy}methyl)-2,2,5-trimethyltetrahydro-4*H*-[1,3]dioxolo[4,5-c]pyrrol-4-one ((-)-83)

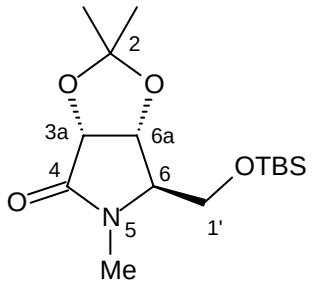

Butyllithium (2.4 eq, 2.5 M in hexane, 100.6 mmol, 40 ml) was added to a solution of diisopropylamine (14.1 ml, 100.6 mmol, 2.4 eq) in anhydrous THF (100 ml) at -78°C. The mixture was stirred at –78°C for 10 minutes, followed by addition of a solution of **81** (10.2 g, 41.9 mmol, 1.0 eq) in anhydrous THF (40 ml). The mixture was stirred at -78°C for 10 minutes, at –30°C for 10 minutes and then at –78°C for 15 minutes. After addition of a solution of PhSeBr (11.9 g, 50.3 mmol, 1.2 eq) in anhydrous THF (30 ml) at -78°C, the mixture was stirred for 30 minutes. The solution was dissolved in EtOAc (40 ml) and washed with a saturated aqueous solution of NH_4Cl (40 ml). The organic extract was dried over $MgSO_4$, filtered and concentrated *in vacuo* at 20°C to give the corresponding 3-selenopyrroldinone which was directly engaged in the next step.

This 3-selenopyrrolidinone (41.9 mmol, 1.0 eq) was dissolved in a mixture of EtOAc/H_2O_2 (3/1, 240 ml) and cooled at 0°C. After stirring for 1 hour, water and EtOAc were added. The organic layer was washed with a saturated aqueous solution of $NaHCO_3$, NH_4Cl and brine to reach neutral pH, dried over $MgSO_4$ and concentrated *in vacuo* to afford a crude enone.

This crude enone (41.9 mmol, 1.0 eq), OsO_4 (0.1 eq, 0.1 M in H_2O, 4.2 mmol, 42 ml) and NMO monohydrate (8.5 g, 62.9 mmol, 1.5 eq) in a mixture of acetone/H_2O (7/3 235 ml) was stirred at 25°C for 12 hours. After addition of sodium pyrosulfite (2.5 g) at 0°C, the aqueous layer was extracted with EtOAc (50 ml, 3 times). The combined organic extracts were dried over $MgSO_4$ and concentrated *in vacuo*. Purification by flash chromatography on silica gel (CH_2Cl_2/MeOH 97/3) afforded **82** (4.7 g, 41 %, 3 steps) as a white foam.

To a solution of diol **82** (4.7 g, 17.1 mmol, 1.0 eq) in a mixture of acetone/2,2-dimethoxypropane (3/1, 170 ml), cooled to 0°C, was added a catalytic amount of *p*-TsOH. The solution was stirred at 0°C for 3 hours. After dilution with EtOAc (40 ml), the mixture was washed with a saturated aqueous solution of $NaHCO_3$ (25 ml) and H_2O (25 ml), dried over $MgSO_4$, filtered and concentrated *in vacuo*. Flash chromatography on silica gel (pentane/EtOAc 7/3) afforded **83** (3.14 g, 59 %) as a white solid.

$[\alpha]_{589}^{25}$ = -33, $[\alpha]_{577}^{25}$ = -34, $[\alpha]_{435}^{25}$ = -60, $[\alpha]_{405}^{25}$ = -71 (c = 0.35, $CHCl_3$).

IR (film): 3450, 2935, 1645, 1465, 1380, 1255, 1220, 1125, 1075, 835, 775 cm^{-1}.

^{1}H-NMR (400 MHz, MeOD):
4.61 (d, 1H, ^3J(H-C(3a), H-C(6a)) = 5.9, H-C(3a)); **4.52** (d, 1H, ^3J(H-C(6a), H-C(3a)) = 5.9, H-C(6a)); **3.81** (dd, 1H, ^3J(H-C(1'), H-C(6)) = 1.9, $^2J_{gem}$ = 10.8, H-C(1')); **3.72** (dd, 1H, ^3J(H-C(1'), H-C(6)) = 1.5, $^2J_{gem}$ = 10.8, H-C(1')); **3.57** (m, 1H, H-C(6)); **2.86** (s, 3H, Me-N); **1.43** (s, 3H, Me-C(2)); **1.39** (s, 3H, Me-C(2)); **0.88** (s, 9H, Me_3CSi); **0.07, 0.05** (2s, 6H, Me_2Si).

^{13}C-NMR (101 MHz, $CDCl_3$):
171.7 (s, C(4)); **111.8** (s, C(2)); **77.8** (d, ^1J(C,H) = 158, C(3a)); **76.5** (d, ^1J(C,H) = 160, C(6a)); **65.3** (d, ^1J(C,H) = 142, C(6)); **60.4** (t, ^1J(C,H) = 142, C(1')); **27.9** (q, ^1J(C,H) = 139, Me-N); **27.2** (q, ^1J(C,H) = 128, Me); **25.8** (q, ^1J(C,H) = 127, Me); **25.8** (q, ^1J(C,H) = 126, Me_3CSi); **18.1** (s, Me_3CSi); **-5.58, -5.64** (2q, ^1J(C,H) = 118, Me_2Si).

HRMS ($C_{15}H_{29}NO_4Si$ + H): calc. 316.1944; found 316.1945.
Anal. for $C_{15}H_{29}NO_4Si$ (315.49): calc. C 57.11, H 9.27, N 4.44, Si 8.90; found C 57.15, H 9.24, N 4.46, Si 8.88.

M.P: 93-97°C.

^{1}H-NMR spectrum of **83**

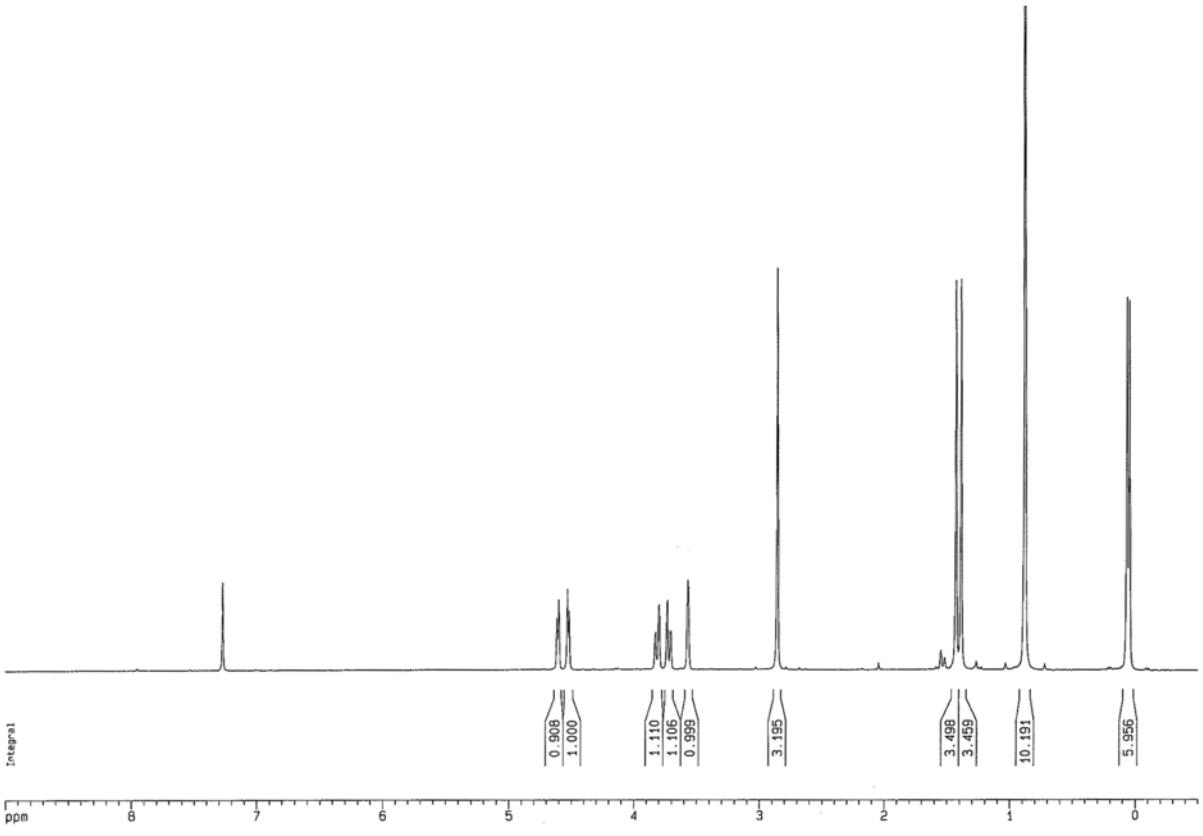

(3*R*,4*R*,5*R*)-3,4-Dihydroxy-5-({[(1*R*)-2-hydroxy-1-phenylethyl]amino}methyl)-1-methyl pyrrolidin-2-one ((-)-86)

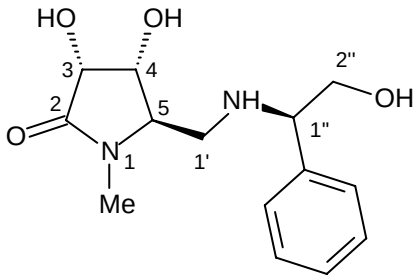

TBAF (1.7 eq, 1 M in THF, 9.0 mmol, 9.0 ml) was added to a solution of **83** (1.68 g, 5.3 mmol, 1.0 eq) in anhydrous THF (40 ml) at 0°C. The mixture was stirred at 0°C for 1 hour and then concentrated *in vacuo*. The crude product was directly purified by flash chromatography on silica gel (CH_2Cl_2/MeOH 94/6) to afford an intermediate primary alcohol **84** (1.06 g, 99 %).

To a solution of this primary alcohol **84** (60 mg, 0.29 mmol, 1.0 eq) in anhydrous CH_2Cl_2 (2.5 ml) was added Dess-Martin periodinane (189 mg, 0.45 mmol, 1.5 eq). The mixture was stirred at 25°C for 1 hour and was directly purified by flash chromatography on silica gel (CH_2Cl_2/MeOH 95/5) to afford aldehyde **85**.

Procedure 1. **D-(-)-α-phenylglycinol** (**99**) (45 mg, 0.33 mmol, 1.1 eq), aldehyde **85** (59 mg, 0.29 mmol, 1.0 eq), $NaBH(OAc)_3$ (88 mg, 0.42 mmol, 1.4 eq), $Cl(CH_2)_2Cl$ (3 ml). Flash chromatography (CH_2Cl_2/MeOH 95/5) afforded 33 mg (0.10 mmol, 36 %, 2 steps, colourless oil) of the fully protected compound which was directly engaged in **procedure 2b**. Purification by flash chromatography (MeCN/NH_4OH 10/1) afforded **86** (22 mg, 78 %) as a colourless oil.

$[\alpha]_{589}^{25}$ = -9, $[\alpha]_{577}^{25}$ = -25 (c = 0.25, MeOH).

IR (film): 3145, 3040, 1675, 1405, 1200, 1135, 1075, 755, 700 cm^{-1}.

^{1}H-NMR (400 MHz, MeOD):
7.38-7.26 (m, 5H_{arom}); **4.39** (d, 1H, ^3J(H-C(3), H-C(4)) = 5.4, H-C(3)); **4.26** (d, 1H, ^3J(H-C(4), H-C(3)) = 5.4, H-C(4)); **3.76** (dd, 1H, ^3J(H-C(1''), H-C(2'')) = 4.4, ^3J(H-C(1''), H-C(2'')) = 8.5, H-C(1'')); **3.63** (dd, 1H, ^3J(H-C(2''), H-C(1'')) = 4.4, $^2J_{gem}$ = 10.9, H-C(2'')); **3.55** (dd, 1H, ^3J(H-C(2''), H-C(1'')) = 8.5, $^2J_{gem}$ = 10.9, H-C(2'')); **3.38** (dd, 1H, ^3J(H-C(5), H-C(1')) = 3.4, ^3J(H-C(5), H-C(1')) = 6.1, H-C(5)); **2.84** (dd, 1H, ^3J(H-C(1'), H-C(5)) = 3.4, $^2J_{gem}$ = 13.0, H-C(1')); **2.66** (s, 3H, Me-N); **2.51** (dd, 1H, ^3J(H-C(1'), H-C(5)) = 6.1, $^2J_{gem}$ = 13.0, H-C(1')).

^{13}C-NMR (101 MHz, MeOD):
175.4 (s, C(2)); **142.0** (s, C_{arom}); **129.6** (d, ^1J(C,H) = 160, 2C_{arom}); **128.9** (d, ^1J(C,H) = 160, 2C_{arom}); **128.7** (d, ^1J(C,H) = 160, C_{arom}); **71.7** (d, ^1J(C,H) = 145, C(3)); **70.8** (d, ^1J(C,H) = 154, C(4)); **68.2** (d, ^1J(C,H) = 155, C(5)); **67.7** (t, ^1J(C,H) = 143, C(2'')); **66.6** (d, ^1J(C,H) = 135, C(1'')); **46.7** (t, ^1J(C,H) = 134, C(1')); **28.7** (q, ^1J(C,H) = 138, Me-N).

ESI-MS: 281.33 $(M+H)^+$.
HRMS ($C_{14}H_{20}N_2O_4$ + H): calc. 281.1501; found 281.1491.

^{1}H-NMR spectrum of **86**

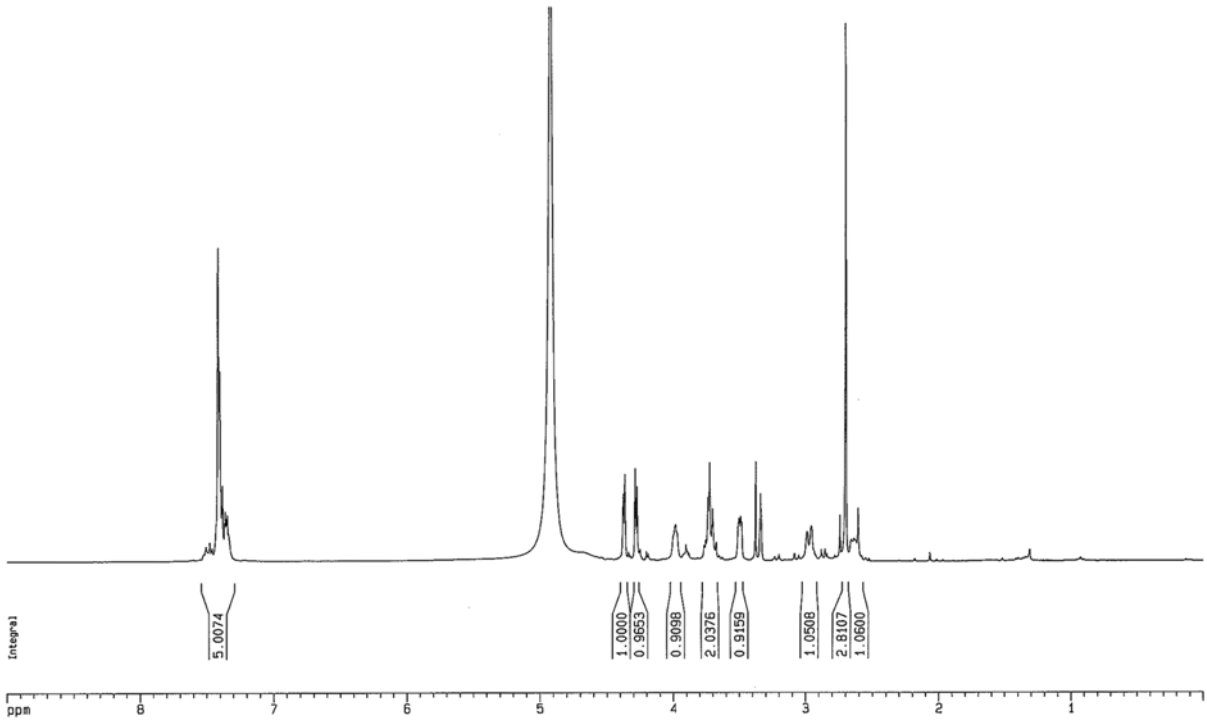

(2*R*,3*R*,4*S*)-2-[{(1*R*)-1-Hydroxymethyl-2-phenyl-ethylamino}-methyl]-pyrrolidine-3,4-diol ((+)-89)

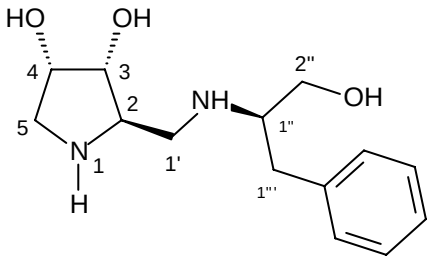

Procedure 1. **D-α-phenylalaninol** (**99**) (168 mg, 1.11 mmol, 1.0 eq), **87** (300 mg, 1.11 mmol, 1.0 eq), $NaBH(OAc)_3$ (328 mg, 1.55 mmol, 1.4 eq), $Cl(CH_2)_2Cl$ (11 ml). Flash chromatography (CH_2Cl_2/MeOH 12/1) afforded 239 mg (0.59 mmol, 53 %, brown oil) of the fully protected compound which was directly engaged in **procedure 2b**. Purification by flash chromatography (CH_2Cl_2/MeOH 12/1 to 10/4) afforded **89** (133 mg, 85 %) as a pale yellow solid after lyophilisation.

$[\alpha]_{589}^{25}$ = 2 (c = 0.17, $CHCl_3$).

UV (MeCN): 229 (500), 213 (200).

IR (film): 3020, 1680, 1215, 755, 670 cm^{-1}.

^{1}H-NMR (400 MHz, MeOD):
7.35-7.29 (m, $5H_{arom}$); **4.22** (ddd, 1H, ^3J(H-C(4), H-C(3)) = 7.6, ^3J(H-C(4), H-C(5)) = 4.2, ^3J(H-C(4), H-C(5)) = 2.3, H-C(4)); **3.90** (dd, 1H, ^3J(H-C(3), H-C(4)) = 7.6, ^3J(H-C(3), H-C(2)) = 4.3, H-C(3)); **3.62** (dd, 1H, ^3J(H-C(2''), H-C(1'')) = 4.0, $^2J_{gem}$ = 11.1, H-C(2'')); **3.44** (dd, 1H, ^3J(H-C(2''), H-C(1'')) = 6.0, $^2J_{gem}$ = 11.1, H-C(2'')); **3.38** (m, 1H, H-C(2)); **3.28** (dd, 1H, ^3J(H-C(5), H-C(4)) = 4.2, $^2J_{gem}$ = 12.4, H-C(5)); **3.12** (dd, 1H, ^3J(H-C(5), H-C(4)) = 2.3, $^2J_{gem}$ = 12.4, H-C(5)); **3.08** (dd, 1H, ^3J(H-C(1'), H-C(2)) = 4.4, $^2J_{gem}$ = 13.1, H-C(1')); **2.93** (m, 1H, H-C(1'')); **2.84** (dd, 1H, ^3J(H-C(1'), H-C(2)) = 8.2, $^2J_{gem}$ = 13.1, H-C(1')); **2.79** (m, 2H, H-C(1''')).

^{13}C-NMR (101 MHz, MeOD):
140.2 (s, $1C_{arom}$); **130.4** (d, ^1J(C,H) = 162, $2C_{arom}$); **129.6** (d, ^1J(C,H) = 160, $2C_{arom}$); **127.5** (d, ^1J(C,H) = 161, $1C_{arom}$); **75.2** (d, ^1J(C,H) = 144, C(3)); **71.7** (d, ^1J(C,H) = 152, C(4)); **63.6** (t, ^1J(C,H) = 153, C(2'')); **62.7** (d, ^1J(C,H) = 142, C(2)); **62.5** (d, ^1J(C,H) = 134, C(1'')); **51.1** (t, ^1J(C,H) = 143 , C(5)); **47.5** (t, ^1J(C,H) = 134, C(1')); **38.6** (t, ^1J(C,H) = 112, C(1''')).

MALDI-TOF: 267.46 $(M+H)^+$.
HRMS ($C_{14}H_{22}N_2O_3$): calc. 266.1630; found 266.1631.
M.P: 89-93°C.

^{1}H-NMR spectrum of **89**

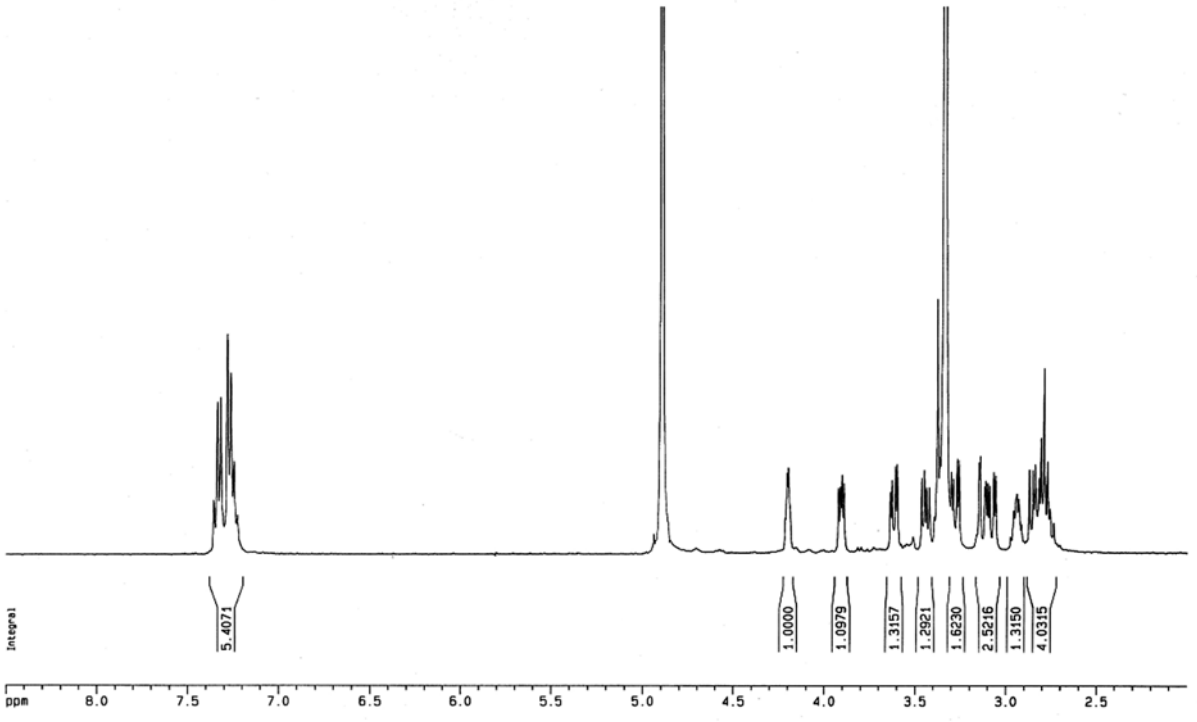

(2*R*)-2-Amino-2-[4-(methyloxy)phenyl]ethanol ((-)-97)

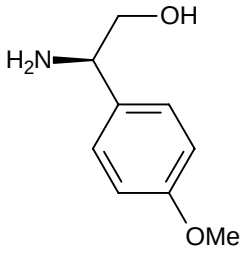

To a solution of **4-Hydroxy-D-phenylglycine**[211] (**90**) (3.0 g, 18.0 mmol, 1.0 eq) in a mixture of H_2O/Dioxane/1M NaOH (1/2/1 72 ml) was added $(Boc)_2O$ (4.3 g, 19.8 mmol, 1.1 eq). The mixture was stirred at 25°C for 4 hours and dioxane was evaporated *in vacuo*. The aqueous layer was washed with Et_2O (25 ml, 2 times), acidified with $KHSO_4$ and extracted with EtOAc (25 ml, 3 times). The combined organic extracts were dried over $MgSO_4$, evaporated *in vacuo* to afford the corresponding carbamate (4.9 g, 98 %) as a white foam.

To a solution of this carbamate (1.0 g, 3.74 mmol, 1.0 eq) in DMF (35 ml), cooled to 0°C, were added K_2CO_3 (2.6 g, 18.71 mmol, 5.0 eq) portionwise and, after 5 minutes, MeI (0.9 ml, 14.96 mmol, 4.0 eq) dropwise. The solution was stirred for 1 hour at 0°C and the resulting mixture, diluted with Et_2O (15 ml), was poured into a saturated aqueous solution of $NaHCO_3$ (15 ml). The aqueous layer was extracted with Et_2O (15 ml, 3 times). The combined organic extracts were dried over $MgSO_4$, filtered and concentrated *in vacuo*. Flash chromatography on silica gel (pentane/EtOAc 2/1) afforded an intermediate methyl ester **92** (680 mg, 62 %) as a colourless oil.

To a solution of this methyl ester **92** (200 mg, 0.68 mmol, 1.0 eq) in anhydrous THF (4 ml), cooled to 0°C, was added $LiAlH_4$ (39 mg, 1.02 mmol, 1.5 eq) portionwise. The mixture was stirred at 0°C for 1 hour. After addition of water (1 ml), the mixture was filtered through a pad of Celite and concentrated *in vacuo*. The resulting primary alcohol was directly engaged in **procedure 2b**. Purification by flash chromatography (MeCN/NH_4OH 10/1) afforded **97** (73 mg, 64 %, 2 steps) as a pale yellow solid.

[211] Salituro, G.M.; Townsend, C.A., *Jacs* **1990**, *112*, 760-770.

$[\alpha]_{589}^{25}$ = -17, $[\alpha]_{435}^{25}$ = -30, $[\alpha]_{405}^{25}$ = -34 (c = 0.27, MeOH).

IR (film): 3415, 1650, 1515, 1465, 1250, 1180, 1030, 830 cm^{-1}.

^{1}H-NMR (400 MHz, MeOD):
7.30 (d, ^3J=8.5, $2H_{arom}$); **6.93** (d, ^3J=8.5, $2H_{arom}$); **3.95** (dd, 1H, ^3J(H-C(1), H-C(2)) = 4.4, ^3J(H-C(1), H-C(2)) = 8.1, H-C(1)); **3.81** (s, 3H, OMe); **3.67** (dd, 1H, ^3J(H-C(2), H-C(1)) = 4.4, $^2J_{gem}$ = 10.9, H-C(2)); **3.56** (dd, 1H, ^3J(H-C(2), H-C(1)) = 8.1, $^2J_{gem}$ = 10.9, H-C(2)).

^{13}C-NMR (101 MHz, MeOD):
160.6 (s, C_{arom}); **134.7** (s, C_{arom}); **129.1** (d, ^1J(C,H) = 156, $2C_{arom}$); **114.9** (d, ^1J(C,H) = 159, $2C_{arom}$); **68.6** (t, ^1J(C,H) = 143, C(2)); **58.1** (d, ^1J(C,H) = 134, C(1)); **55.7** (q, ^1J(C,H) = 144, OMe).

ESI-MS: 168.36 $(M+H)^+$.
CI-MS (NH_3): 168 ($M+H^+$, 44), 151 (100), 136 (40).
HRMS ($C_9H_{13}NO_2$ + H): calc. 168.1024; found 168.1025.
M.P: 122-125°C.

^{1}H-NMR spectrum of **97**

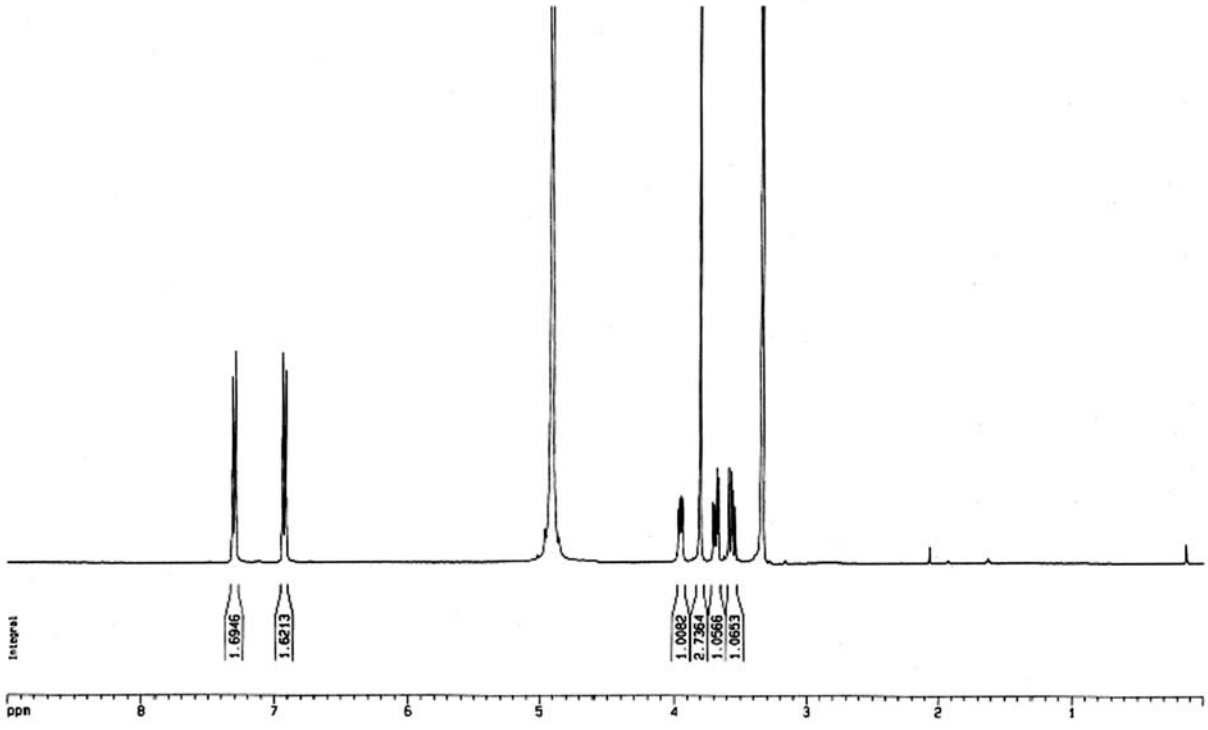

(3*R*,4*R*,5*S*)-3,4-Dihydroxy-5-[({(1*R*)-2-hydroxy-1-[4-(methyloxy)phenyl]ethyl}amino) methyl]-1-methylpyrrolidin-2-one ((-)-98)

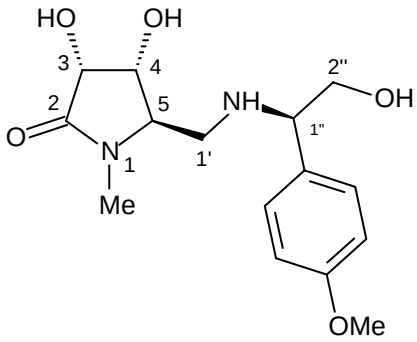

Procedure 1. Amine **97** (65 mg, 0.39 mmol, 1.0 eq), aldehyde **85** (78 mg, 0.39 mmol, 1.0 eq), $NaBH(OAc)_3$ (116 mg, 0.55 mmol, 1.4 eq), $Cl(CH_2)_2Cl$ (4.5 ml). Flash chromatography (CH_2Cl_2/MeOH 96/4) afforded 9.6 mg (0.03 mmol, 7 %, 2 steps) of the fully protected compound which was directly engaged in **procedure 2b**. Purification by flash chromatography (MeCN/NH_4OH 12/1) afforded **98** (6.8 mg, 80 %) as a pale yellow oil.

^{1}H-NMR (400 MHz, MeOD):
7.28 (d, ^3J=8.5, $2H_{arom}$); **6.94** (d, ^3J=8.5, $2H_{arom}$); **4.36** (d, 1H, ^3J(H-C(3), H-C(4)) = 5.4, H-C(3)); **4.23** (d, 1H, ^3J(H-C(4), H-C(3)) = 5.4, H-C(4)); **3.81** (m, 4H, OMe and H-C(1'')); **3.64** (dd, 1H, ^3J(H-C(2''), H-C(1'')) = 4.4, $^2J_{gem}$ = 10.9, H-C(2'')); **3.60** (dd, 1H, ^3J(H-C(2''), H-C(1'')) = 8.5, $^2J_{gem}$ = 10.9, H-C(2'')); **3.41** (dd, 1H, ^3J(H-C(5), H-C(1')) = 3.4, ^3J(H-C(5), H-C(1')) = 7.1, H-C(5)); **2.88** (dd, 1H, ^3J(H-C(1'), H-C(5)) = 3.4, $^2J_{gem}$ = 13.2, H-C(1')); **2.68** (s, 3H, Me-N); **2.56** (dd, 1H, ^3J(H-C(1'), H-C(5)) = 7.1, $^2J_{gem}$ = 13.2, H-C(1')).

^{13}C-NMR (101 MHz, MeOD):
175.2 (s, C(2)); **161.3** (s, C_{arom}); **130.2** (d, ^1J(C,H) = 156, $2C_{arom}$); **115.3** (d, ^1J(C,H) = 159, $2C_{arom}$); **115.2** (s, C_{arom}); **71.4** (d, ^1J(C,H) = 143, C(3)); **70.7** (d, ^1J(C,H) = 154, C(4)); **66.8** (d, ^1J(C,H) = 146, C(5)); **66.4** (t, ^1J(C,H) = 146, C(2'')); **65.8** (d, ^1J(C,H) = 135, C(1'')); **55.8** (q, ^1J(C,H) = 144, OMe); **46.0** (t, ^1J(C,H) = 137, C(1')); **28.8** (q, ^1J(C,H) = 140, Me-N).

ESI-MS: 311.35 $(M+H)^+$.
HRMS ($C_{15}H_{22}N_2O_5$ + H): calc. 311.1607; found 311.1610.

^{1}H-NMR spectrum of **98**

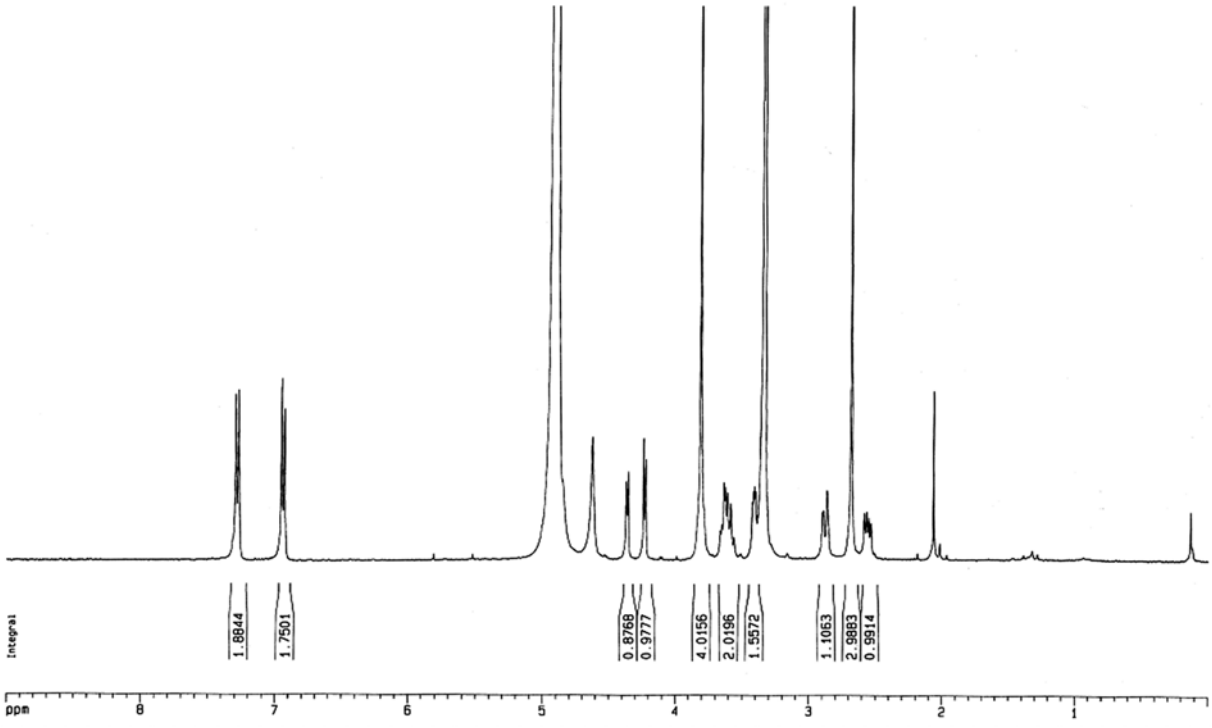

(2*R*)-2-(Diallylamino)-2-phenylethanol ((-)-100)

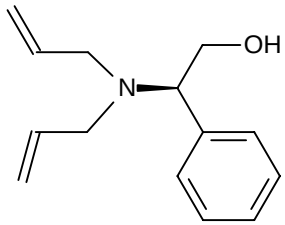

To a solution of **D-(-)-α-phenylglycinol** (**99**) (2.0 g, 14.6 mmol, 1.0 eq) in THF/DMSO (4/1 50 ml), were added $NaHCO_3$ (2.4 g, 29.2 mmol, 2.0 eq) and allyl bromide (5.1 ml, 58.3 mmol, 4.0 eq). A catalytic amount of Bu_4NI (1.62 g, 4.38 mmol, 0.3 eq) was added and the reaction mixture was stirred at 60°C for 3 hours. After cooling to 25°C, water (30 ml) was added. The reaction mixture was extracted with CH_2Cl_2 (30 ml, 3 times). The combined organic extracts were dried over $MgSO_4$, filtered and concentrated *in vacuo*. The residue was purified by flash chromatography (PE/EtOAc 5/1) to afford **100** (2.5 g, 79 %) as a light yellow oil.

$[\alpha]_{589}^{25}$ = -84, $[\alpha]_{577}^{25}$ = -92, $[\alpha]_{546}^{25}$ = -102, $[\alpha]_{435}^{25}$ = -186, $[\alpha]_{405}^{25}$ = -230 (*c* = 0.39, CH_2Cl_2).

UV (MeCN): 260 (1000), 211 (9500).

IR (film): 3440, 3080, 2930, 2885, 2820, 1640, 1495, 1455, 1420, 1350, 1265, 1220, 1030, 920, 760, 705 cm^{-1}.

^{1}H-NMR (400 MHz, MeOD):
7.39-7.30 (m, $3H_{arom}$); **7.22-7.20** (m, $2H_{arom}$); **5.82** (dddd, 2 H, ^3J(H-C(2'), H-C(1')) = 4.5, ^3J(H-C(2'), H-C(1')) = 8.2, ^3J(H-C(2'), H-C(3')) = 10.2, ^3J(H-C(2'), H-C(3')) = 14.2, H-C(2')); **5.19** (m, 4 H, H-C(3')); **4.01** (m, 2H, H-C(1), H-C(2)); **3.63** (dd, 1H, ^3J(H-C(1), H-C(2)) = 4.1, $^2J_{gem}$ = 9.6, H-C(1)); **3.40** (m, 2H, H-C(1')); **2.73** (dd, 2H, ^3J(H-C(1'), H-C(2')) = 8.2, $^2J_{gem}$ = 14.2, H-C(1')).

^{13}C-NMR (101 MHz, MeOD):
136.4 (d, ^1J(C,H) = 152, C(2')); **135.7** (s, C_{arom}); **129.0** (d, ^1J(C,H) = 158, $2C_{arom}$); **128.3** (d, ^1J(C,H) = 160, $2C_{arom}$); **127.8** (d, ^1J(C,H) = 160, C_{arom}); **117.7** (t, ^1J(C,H) = 153, C(3')); **63.4** (d, ^1J(C,H) = 137, C(2)); **60.4** (t, ^1J(C,H) = 145, C(1)); **52.4** (t, ^1J(C,H) = 133, C(1')).

CI-MS (NH_3): 218 ($M+H^+$, 100), 186 (32), 98 (4).

_N_,_N_-Diallyl-_N_-[(1_R_)-2-((3-fluorobenzyl)oxy)-1-phenylethyl]amine ((-)-107)

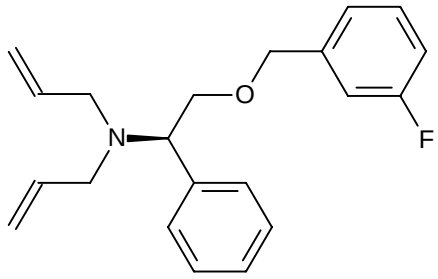

Diallylamine **100** (300 mg, 1.38 mmol, 1.0 eq) was dissolved in anhydrous THF (10 ml) and the temperature was cooled to 0°C. Sodium hydride (73 mg, 1.66 mmol, 1.2 eq, 55 % in oil) was added and the reaction mixture was stirred at 0°C for 10 minutes. 3-fluorobenzyl bromide (365 mg, 1.93 mmol, 1.4 eq) was added portionwise and the mixture was warmed to 60°C for 6 hours. The resulting mixture was poured into a saturated aqueous solution of $NaHCO_3$ (15 ml) and the aqueous layer was extracted with EtOAc (20 ml, 3 times). The combined organic extracts were dried over $MgSO_4$, filtered and concentrated *in vacuo*. Flash chromatography on silica gel (EtOAc/PE 1/10) afforded **107** (449 mg, 100 %) as a brown oil.

UV (MeCN): 218 (6000).

IR (film): 3585, 3070, 2925, 2855, 2360, 1590, 1490, 1450, 1360, 1260, 1140, 1105, 920, 785, 690 cm^{-1}.

^{1}H-NMR (400 MHz, $CDCl_3$):
7.39-7.25 (m, 5H_{arom}); **7.13** (m, 1H_{arom}); **7.03-6.93** (m, 3H_{arom}); **5.91-5.81** (m, 2H, H-C(2')); **5.19-5.12** (m, 4H, H-C(3')); **4.52** (s, 2H, OCH_2Ar); **4.08** (dd, 1H, ^3J(H-C(1), H-C(2)) = 6.1, ^3J(H-C(1), H-C(2)) = 6.4, H-C(1)); **3.89** (dd, 1H, ^3J(H-C(2), H-C(1)) = 6.1, $^2J_{gem}$ = 9.7, H-C(2)); **3.79** (dd, 1H, ^3J(H-C(2), H-C(1)) = 6.4, $^2J_{gem}$ = 9.7, H-C(2)); **3.27** (dd, 2H, ^3J(H-C(1'), H-C(2')) = 5.2, $^2J_{gem}$ = 14.4, H-C(1')); **3.01** (dd, 2H, ^3J(H-C(1'), H-C(2')) = 6.8, $^2J_{gem}$ = 14.4, H-C(1')).

^{13}C-NMR (101 MHz, $CDCl_3$):
164.1, **140.1**, **139.5** (3s, 3C_{arom}); **136.5** (d, ^1J(C,H) = 154, C(2')); **129.7** (d, ^1J(C,H) = 168, 1C_{arom}); **128.5** (d, ^1J(C,H) = 164, 2C_{arom}); **128.1** (d, ^1J(C,H) = 158, 2C_{arom}); **127.1** (d, ^1J(C,H) = 139, 1C_{arom}); **122.8** (d, ^1J(C,H) = 161, 1C_{arom}); **116.9** (t, ^1J(C,H) = 155, C(3')); **114.4** (d, ^1J(C,H) = 183, 1C_{arom}); **114.2** (d, ^1J(C,H) = 183, 1C_{arom}); **72.3** (t, ^1J(C,H) = 142, OCH_2Ar); **71.4** (t, ^1J(C,H) = 141, C(2)); **62.9** (d, ^1J(C,H) = 134, C(1)); **53.2** (t, ^1J(C,H) = 134, C(1')).

MALDI-TOF: 326.52 $(M+H)^+$.
HRMS ($C_{21}H_{24}FNO$ + H): calc. 326.1920; found 326.1920.

^{1}H-NMR spectrum of **100**

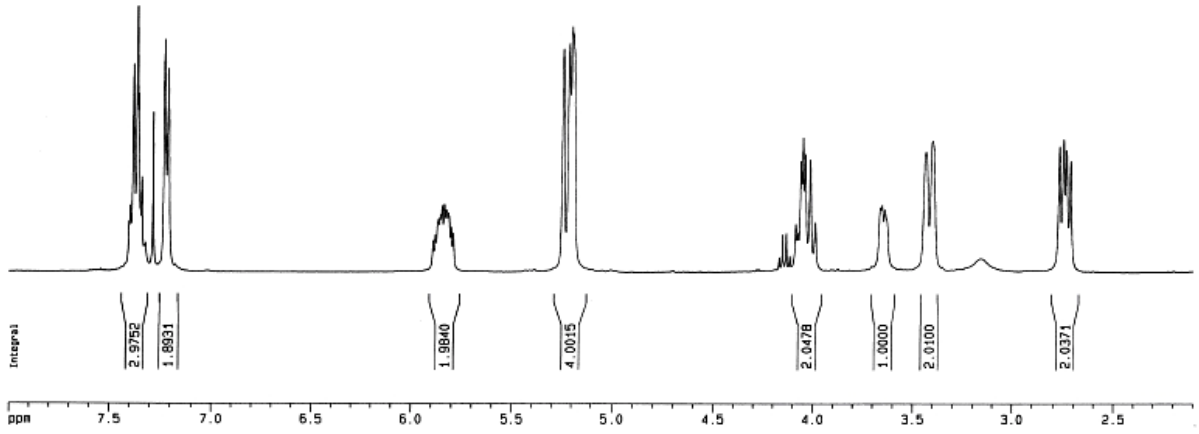

^{1}H-NMR spectrum of **107**

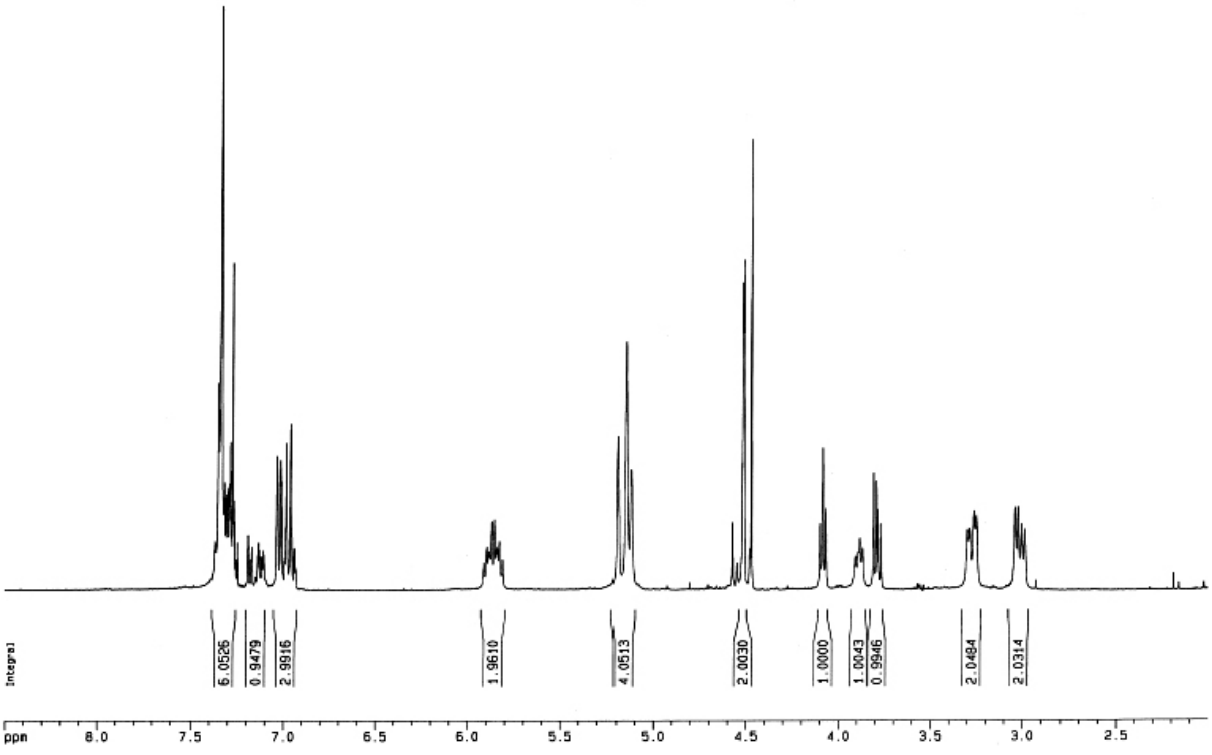

(1*R*)-2-((3-Methylbenzyl)oxy)-1-phenylethanamine ((-)-108)

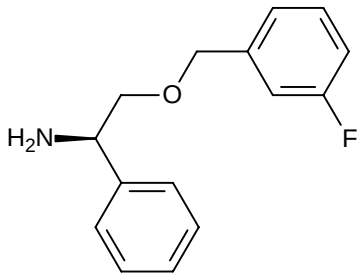

To a solution of ether **107** (225 mg, 0.69 mmol, 1.0 eq) and 2-mercaptobenzoic acid (234 mg, 1.52 mmol, 2.2 eq) in anhydrous THF were added $Pd(dba)_2$ (79 mg, 0.14 mmol, 0.2 eq) and DPPB (47 mg, 0.11 mmol, 0.16 eq). The mixture was warmed to 80°C and stirred for 6 hours. The solution was diluted with EtOAc (15 ml) and extracted with 1M HCl_{aq} (15 ml, 3 times). The combined aqueous layers were basified with 2.5M NaOH and extracted with EtOAc (15 ml, 3 times). The combined organic extracts were dried over $MgSO_4$, filtered and concentrated *in vacuo*. Flash chromatography on silica gel (CH_2Cl_2/MeOH 30/1) afforded **108** (30 mg, 18 %) as a brown oil.

^{1}H-NMR (400 MHz, MeOD):
7.40-7.26 (m, $6H_{arom}$); **7.13** (m, $1H_{arom}$); **7.07** (m, $1H_{arom}$); **7.01** (m, $1H_{arom}$); **4.57** (s, 2H, O*C*H_2Ar); **4.16** (m, 1H, H-C(1)); **3.66-3.55** (m, 2H, H-C(2)).

^{13}C-NMR (101 MHz, MeOD):
164.0, **144.0**, **143.6** (3s, $3C_{arom}$); **132.0** (d, ^1J(C,H) = 163, $1C_{arom}$); **130.4** (d, ^1J(C,H) = 160, $2C_{arom}$); **129.4** (d, ^1J(C,H) = 144, $1C_{arom}$); **128.9** (d, ^1J(C,H) = 160, $2C_{arom}$); **125.1** (d, ^1J(C,H) = 159, $1C_{arom}$); **116.2** (d, ^1J(C,H) = 158, $1C_{arom}$); **116.0** (d, ^1J(C,H) = 168, $1C_{arom}$); **78.0** (7, ^1J(C,H) = 143, C(2)); **74.2** (t, ^1J(C,H) = 143, O*C*H_2Ar); **57.4** (d, ^1J(C,H) = 138, C(1)).

CI-MS (NH_3): 246 ($M+H^+$, 5), 149 (10), 106 (100).
HRMS ($C_{15}H_{16}FNO$ + H): calc. 246.1294; found 246.1296.

(2*R*,3*S*,4*R*)-2-({[(1*R*)-2-(3-Fluorophenoxy)-1-phenylethyl]amino}methyl)pyrrolidin-3,4 diol ((-)-109)

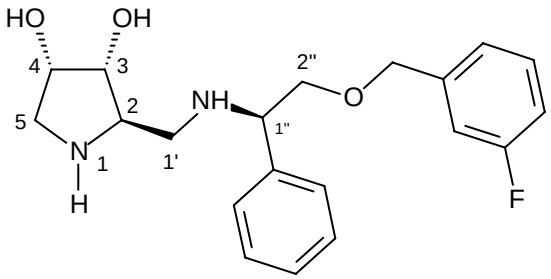

Procedure 1. Amine **108** (30 mg, 0.12 mmol, 1.0 eq), **87** (33.1 mg, 0.12 mmol, 1.0 eq), $NaBH(OAc)_3$ (36.2 mg, 0.17 mmol, 1.4 eq), $Cl(CH_2)_2Cl$ (4 ml). The crude product was directly engaged in **procedure 2b**. Purification by flash chromatography ($MeCN/NH_4OH$ 10/1) afforded **109** (9 mg, 19 %) as a brown foam after lyophilisation.

^{1}H-NMR (400 MHz, MeOD):
7.40 (m, $6H_{arom}$); **7.16** (m, $2H_{arom}$); **7.07** (m, $1H_{arom}$); **4.57** (s, 2H, OCH_2Ar); **3.98** (m, 2H, H-C(4), H-C(1'')); **3.98** (m, 3H, 2H-C(2''), H-C(3)); **3.11** (m, 2H, H-C(5), H-C(2)); **2.84** (m, 1H, H-C(5)); **2.66** (m, 1H, H-C(1')); **2.56** (m, 1H, H-C(1')).

^{13}C-NMR (101 MHz, MeOD):
142.6, **141.6**, **131.9** (3s, $3C_{arom}$); **129.6**, **129.4**, **128.9**, **128.8**, **124.3**, **115.4**, **115.1** (7d, $9C_{arom}$); **76.9** (d, ^1J(C,H) = 149, C(3)); **76.1** (t, ^1J(C,H) = 144, C(2'')); **73.3** (d, ^1J(C,H) = 144, C(4)) ; **72.5** (t, ^1J(C,H) = 149, OCH_2Ar); **64.4** (d, ^1J(C,H) = 137, C(1'')); **62.7** (d, ^1J(C,H) = 139, C(2)); **52.2** (t, ^1J(C,H) = 140, C(5)); **50.8** (t, C(1')).

HRMS ($C_{20}H_{25}FN_2O_3$ + H): calc. 361.1927; found 361.1929.
Purity measured by HPLC (C_{18}, C_8, C_4 columns): 92%, 100%, 100%.

^{1}H-NMR spectrum of **109**

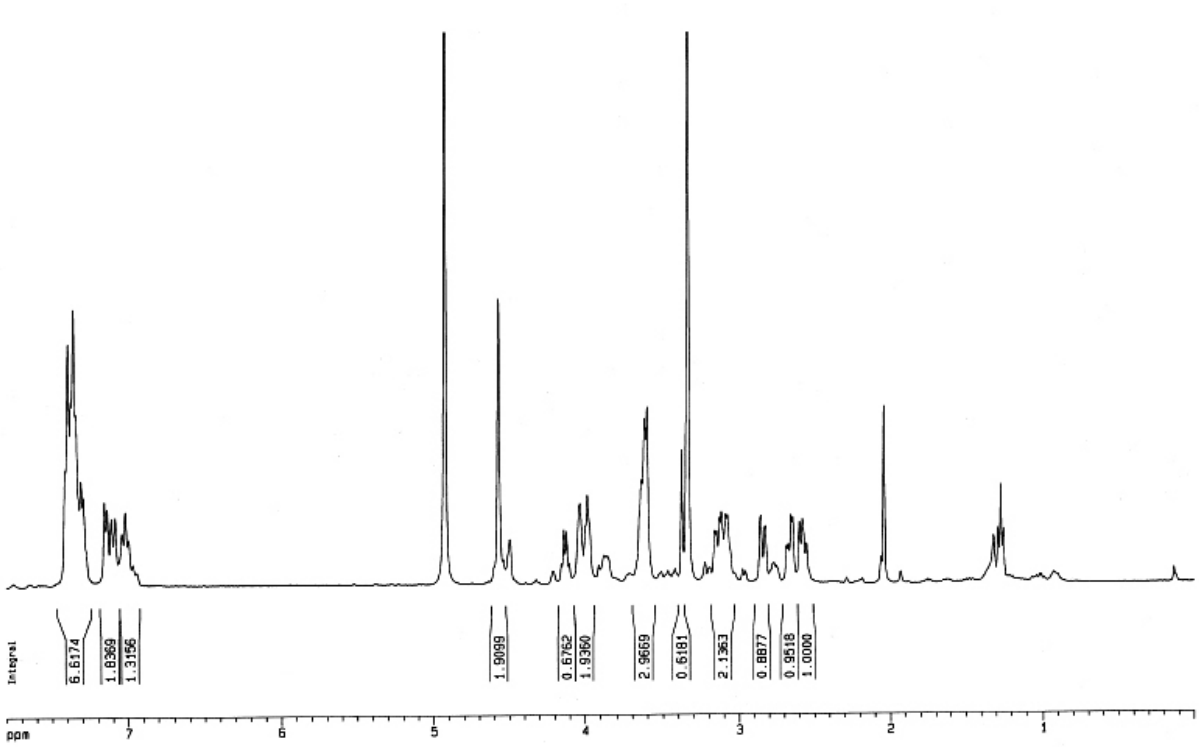

***Tert*-butyl ((1*R*)-2-hydroxy-1-phenylethyl) carbamate ((-)-111)**

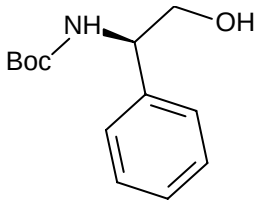

To a solution of **D-(-)-α-phenylglycinol** (**99**) (5.0 g, 36.5 mmol, 1.0 eq) in anhydrous CH_2Cl_2 (350 ml) were added pyridine (5.9 ml, 73 mmol, 2.0 eq), $(Boc)_2O$ (8.0 g, 36.5 mmol, 1.0 eq) and a catalytic amount of DMAP. The mixture was stirred at 0°C for 1 hour and poured into a saturated aqueous solution of $NaHCO_3$ (150 ml). The aqueous layer was extracted with CH_2Cl_2 (80 ml, 2 times). The combined organic extracts were dried over $MgSO_4$ and concentrated *in vacuo*. The residue was purified by flash chromatography (CH_2Cl_2/MeOH 20/1) to afford **111** (7.6 g, 88 %) as a pale yellow solid.

$[\alpha]_{589}^{25}$ = -49, $[\alpha]_{577}^{25}$ = -50, $[\alpha]_{435}^{25}$ = -107, $[\alpha]_{405}^{25}$ = -134 (*c* = 0.515, CH_2Cl_2).

UV (MeCN): 215 (4000).

IR (film): 3310, 3240, 3060, 2980, 2930, 2900, 2300, 1955, 1875, 1750, 1670, 1560, 1490, 1365, 1265, 1170, 1055, 840, 730, 700 cm^{-1}.

^{1}H-NMR (400 MHz, $CDCl_3$):
7.38-7.23 (m, $5H_{arom}$); **4.73** (m, 1H, H-C(2)); **3.80** (m, 2H, H-C(1)); **1.40** (s, 9H, Me_3C).

^{13}C-NMR (101 MHz, $CDCl_3$):
156.1 (s, N*C*(O)O); **139.4** (s, $1C_{arom}$); **128.7** (d, ^1J(C,H) = 161, $2C_{arom}$); **127.7** (d, ^1J(C,H) = 154, $1C_{arom}$); **126.5** (d, ^1J(C,H) = 158, $2C_{arom}$); **72.5** (s, O*C*Me$_3$); **66.9** (t, ^1J(C,H) = 148, C(1)); **56.3** (d, ^1J(C,H) = 143, C(2)); **28.3** (q, ^1J(C,H) = 127, Me_3C).

MALDI-TOF: 276.44 $(M+K)^+$, 260.47 $(M+Na)^+$.
HRMS ($C_{13}H_{19}NO_3$ + Na): calc. 260.1263; found 260.1266.

M.P: 120-126°C.

(2*R*)-2-Amino-2-phenylethyl acetate (112)

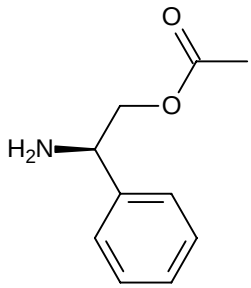

Procedure 3. Primary alcohol **111** (300 mg, 1.26 mmol, 1.0 eq), NEt_3 (705 µl, 5.06 mmol, 4.0 eq), acetyl chloride (180 µl, 2.53 mmol, 2.0 eq), DMAP (cat), CH_2Cl_2 (13 ml), 4.5 hours. Flash chromatography (pentane/EtOAc 4/1) afforded 230 mg (0.82 mmol, 65 %, white solid) of the *N*-protected intermediate which was directly engaged in **procedure 2b** to provide **112** (147 mg, quantitative) as a brown oil without any purification.

^{1}H-NMR (400 MHz, MeOD):
7.50 (m, 5H$_{arom}$); **4.66** (dd, 1H, ^3J(H-C(2'), H-C(1')) = 8.3, ^3J(H-C(2'), H-C(1')) = 4.4, H-C(2')); **4.44** (m, 2H, 2H-C(1')); **2.14** (s, 3H, C(O)*Me*).

^{13}C-NMR (101 MHz, MeOD):
171.9 (s, C=O); **134.9** (s, 1C$_{arom}$); **130.8** (d, ^1J(C,H) = 165, 1C$_{arom}$); **130.5** (d, ^1J(C,H) = 164, 2C$_{arom}$); **128.4** (d, ^1J(C,H) = 158, 2C$_{arom}$); **65.7** (7, ^1J(C,H) = 151, C(1')); **55.2** (d, ^1J(C,H) = 145, C(2')); **20.5** (q, ^1J(C,H) =130, C(O)*Me*).

MALDI-TOF: 180.31 $(M+H)^+$.
HRMS ($C_{10}H_{13}NO_2$ + H): calc. 180.1024; found 180.1022.

(2*R*)-2-Amino-2-phenylethyl propionate (113)

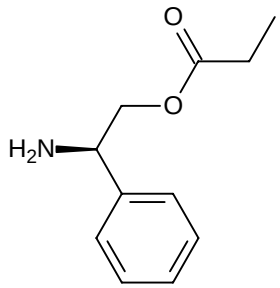

Procedure 3. Primary alcohol **111** (300 mg, 1.26 mmol, 1.0 eq), NEt_3 (705 µl, 5.06 mmol, 4.0 eq), propionyl chloride (221 µl, 2.53 mmol, 2.0 eq), DMAP (cat), CH_2Cl_2 (13 ml), 3 hours. Flash chromatography (pentane/EtOAc 9/1) afforded 297 mg (1.02 mmol, 80 %, white solid) of the *N*-protected derivative which was directly engaged in **procedure 2b** to provide **113** (196 mg, quantitative) as a brown oil without any purification.

^{1}H-NMR (400 MHz, MeOD):
7.51 (m, $5H_{arom}$); **4.67** (dd, 1H, ^3J(H-C(2'), H-C(1')) = 7.4, ^3J(H-C(2'), H-C(1')) = 4.5, H-C(2')); **4.47** (m, 2H, 2H-C(1')); **2.47** (q, 2H, ^3J(H-C(2), H-C(3)) = 7.5, H-C(2)); **1.16** (t, 3H, ^3J(H-C(3), H-C(2)) = 7.5, H-C(3)).

^{13}C-NMR (101 MHz, MeOD):
175.2 (s, C=O); **134.9** (s, $1C_{arom}$); **130.9** (d, ^1J(C,H) = 164, $1C_{arom}$); **130.5** (d, ^1J(C,H) = 162, $2C_{arom}$); **128.4** (d, ^1J(C,H) = 159, $2C_{arom}$); **65.6** (t, ^1J(C,H) = 148, C(1')); **55.3** (d, ^1J(C,H) = 144, C(2')); **27.9** (t, ^1J(C,H) =126, C(2)); **9.2** (q, ^1J(C,H) =128, C(3)).

MALDI-TOF: 194.26 $(M+H)^+$.
HRMS ($C_{11}H_{15}NO_2$ + H): calc. 194.1181; found 194.1183.

(2*R*)-2-Amino-2-phenylethyl butyrate (114)

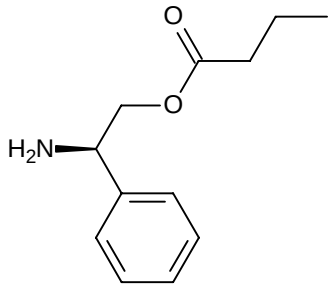

Procedure 3. Primary alcohol **111** (300 mg, 1.26 mmol, 1.0 eq), NEt_3 (705 µl, 5.06 mmol, 4.0 eq), butyryl chloride (265 µl, 2.53 mmol, 2.0 eq), DMAP (cat), CH_2Cl_2 (13 ml), 8 hours. Flash chromatography (pentane/EtOAc 9/1) afforded 296 mg (0.96 mmol, 76 %, white solid) of the *N*-protected intermediate which was directly engaged in **procedure 2b** to provide **114** (198 mg, quantitative) as a brown oil without any purification.

^{1}H-NMR (400 MHz, MeOD):
7.50 (m, 5H_{arom}); **4.67** (dd, 1H, ^3J(H-C(2'), H-C(1')) = 7.9, ^3J(H-C(2'), H-C(1')) = 4.7, H-C(2')); **3.50** (m, 2H, 2H-C(1')); **2.42** (t, 2H, ^3J(H-C(2), H-C(3)) = 7.4, H-C(2)); **1.66** (tq, 2H, ^3J(H-C(3), H-C(4)) = 7.4, ^3J(H-C(3), H-C(2)) = 7.4, H-C(3)); **0.96** (t, 3H, ^3J(H-C(4), H-C(3)) = 7.4, H-C(4)).

^{13}C-NMR (101 MHz, MeOD):
174.4 (s, C=O); **135.0** (s, 1C_{arom}); **130.7** (d, ^1J(C,H) = 162, 1C_{arom}); **130.4** (d, ^1J(C,H) = 160, 2C_{arom}); **128.4** (d, ^1J(C,H) = 165, 2C_{arom}); **65.5** (t, ^1J(C,H) = 148, C(1')); **55.2** (d, ^1J(C,H) = 143, C(2')); **36.4** (t, ^1J(C,H) =128, C(2)); **19.1** (t, ^1J(C,H) =128, C(3)); **13.9** (q, ^1J(C,H) =125, C(4)).

MALDI-TOF: 208.36 $(M+H)^+$.
HRMS ($C_{12}H_{17}NO_2$ + H): calc. 208.1337; found 208.1339.

(2*R*)-2-Amino-2-phenylethyl pentanoate (115)

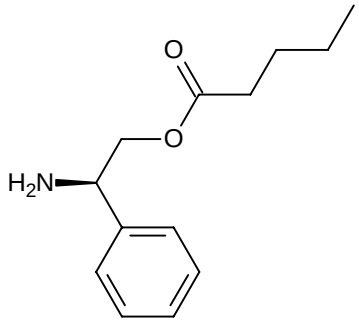

Procedure 3. Primary alcohol **111** (300 mg, 1.26 mmol, 1.0 eq), NEt_3 (705 µl, 5.06 mmol, 4.0 eq), valeroyl chloride (215 µl, 1.77 mmol, 1.4 eq), DMAP (cat), CH_2Cl_2 (10 ml), 4 hours. Flash chromatography (pentane/EtOAc 9/1) afforded 249 mg (0.77 mmol, 62 %, colourless oil) of the *N*-protected intermediate which was directly engaged in **procedure 2b** to provide **115** (170 mg, quantitative) as a pale yellow oil without any purification.

^{1}H-NMR (400 MHz, MeOD):
7.51 (m, 5H_{arom}); **4.67** (dd, 1H, ^3J(H-C(2'), H-C(1')) = 7.1, ^3J(H-C(2'), H-C(1')) = 4.7, H-C(2')); **4.45** (m, 2H, 2H-C(1')); **2.45** (t, 2H, ^3J(H-C(2), H-C(3)) = 7.4, H-C(2)); **1.63** (tt, 2H, ^3J(H-C(3), H-C(2)) = 7.4, ^3J(H-C(3), H-C(4)) = 7.6, H-C(3)); **1.37** (m, 2H, ^3J(H-C(4), H-C(3)) = 7.6, ^3J(H-C(4), H-C(5)) = 7.3, H-C(4)); **0.95** (t, 3H, ^3J(H-C(5), H-C(4)) = 7.3, H-C(5)).

^{13}C-NMR (101 MHz, MeOD):
174.5 (s, C=O); **135.0** (s, 1C_{arom}); **130.8** (d, ^1J(C,H) = 162, 1C_{arom}); **130.4** (d, ^1J(C,H) = 168, 2C_{arom}); **128.4** (d, ^1J(C,H) = 163, 2C_{arom}); **65.5** (t, ^1J(C,H) = 150, C(1')); **55.2** (d, ^1J(C,H) = 145, C(2')); **34.3** (t, ^1J(C,H) =128, C(2)); **27.9** (t, ^1J(C,H) =130, C(3)); **23.2** (t, ^1J(C,H) =122, C(4)); **14.0** (q, ^1J(C,H) =125, C(5)).

MALDI-TOF: 243.48 $(M+Na)^+$, 222.46 $(M+H)^+$.
HRMS ($C_{13}H_{19}NO_2$ + H): calc. 222.1494; found 222.1495.

(2*R*)-2-Amino-2-phenylethyl-2-methylpropionate (116)

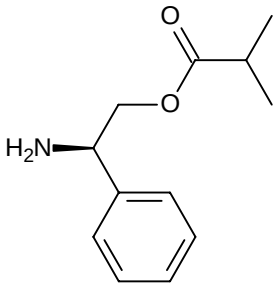

Procedure 3. Primary alcohol **111** (300 mg, 1.26 mmol, 1.0 eq), NEt_3 (705 µl, 5.06 mmol, 4.0 eq), isobutyryl chloride (186 µl, 1.77 mmol, 1.4 eq), DMAP (cat), CH_2Cl_2 (12 ml), 5 hours. Flash chromatography (pentane/EtOAc 9/1) afforded 285 mg (1.19 mmol, 94 %, white solid) of the *N*-protected intermediate which was directly engaged in **procedure 2b** to provide **116** (246 mg, quantitative) as a brown oil without any purification.

^{1}H-NMR (400 MHz, MeOD):
7.54-7.47 (m, $5H_{arom}$); **4.68** (dd, 1H, ^3J(H-C(2''), H-C(1'')) = 7.5, ^3J(H-C(2''), H-C(1'')) = 5.1, H-C(2'')); **4.45** (m, 2H, 2H-C(1'')); **2.68** (qq, 1H, ^3J(H-C(2), H-C(3)) = 7.0, ^3J(H-C(2), H-C(1')) = 7.0, H-C(2)); **1.19** (d, 3H, ^3J(H-C(3), H-C(2)) = 7.0, H-C(3)); **1.18** (d, 3H, ^3J(H-C(1'), H-C(2)) = 7.0, H-C(1')).

^{13}C-NMR (101 MHz, MeOD):
177.9 (s, C=O); **135.0** (s, $1C_{arom}$); **130.7** (d, ^1J(C,H) = 161, $1C_{arom}$); **130.4** (d, ^1J(C,H) = 163, $2C_{arom}$); **128.4** (d, ^1J(C,H) = 159, $2C_{arom}$); **65.6** (t, ^1J(C,H) = 148, C(1'')); **55.1** (d, ^1J(C,H) = 145, C(2'')); **34.8** (d, ^1J(C,H) =131, C(2)); **19.2** (q, ^1J(C,H) =128, C(3)); **19.1** (q, ^1J(C,H) =128, C(1')).

MALDI-TOF: 208.63 $(M+H)^+$.
HRMS ($C_{12}H_{17}NO_2$ + H): calc. 208.1337; found 208.1338.

(2*R*)-2-Amino-2-phenylethyl-3-methylbutanoate (117)

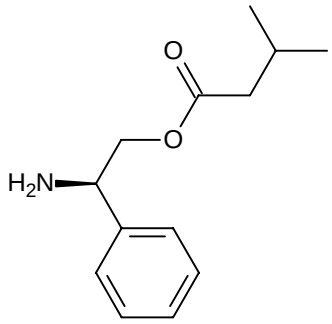

Procedure 3. Primary alcohol **111** (300 mg, 1.26 mmol, 1.0 eq), NEt_3 (705 µl, 5.06 mmol, 4.0 eq), isovaleroyl chloride (217 µl, 1.77 mmol, 1.4 eq), DMAP (cat), CH_2Cl_2 (10 ml), 6 hours. Flash chromatography (pentane/EtOAc 7/3) afforded 297 mg (0.92 mmol, 73 %, white solid) of the *N*-protected intermediate which was directly engaged in **procedure 2b** to provide **117** (203 mg, quantitative) as a brown oil without any purification.

^{1}H-NMR (400 MHz, MeOD):
7.51 (m, $5H_{arom}$); **4.67** (dd, 1H, ^3J(H-C(2''), H-C(1'')) = 6.1, ^3J(H-C(2''), H-C(1'')) = 4.8, H-C(2'')); **4.46** (m, 2H, 2H-C(1'')); **2.32** (d, 2H, ^3J(H-C(2), H-C(3)) = 7.1, H-C(2)); **2.10** (m, 1H, ^3J(H-C(3), H-C(2)) = 7.1, ^3J(H-C(3), Me) = 6.6, H-C(3)); **0.97** (d, 6H, ^3J(Me, H-C(3)) = 6.6, 2x*Me*(^{i}Pr)).

^{13}C-NMR (101 MHz, MeOD):
173.7 (s, C=O); **135.0** (s, $1C_{arom}$); **130.8** (d, ^1J(C,H) = 162, $1C_{arom}$); **130.6** (d, ^1J(C,H) = 161, $2C_{arom}$); **128.4** (d, ^1J(C,H) = 156, $2C_{arom}$); **65.4** (t, ^1J(C,H) = 149, C(1'')); **55.2** (d, ^1J(C,H) = 145, C(2'')); **43.6** (t, ^1J(C,H) =126, C(2)); **26.6** (d, ^1J(C,H) =129, C(3)); **22.6** (q, ^1J(C,H) =125, 2x*Me*(^{i}Pr)).

MALDI-TOF: 222.30 $(M+H)^+$.
HRMS ($C_{13}H_{19}NO_2$ + H): calc. 222.1494; found 222.1496.

Atom numbering according to the international union of pure and applied chemistry (IUPAC) names for compounds:

((-)-123); (124); ((-)-125); ((-)-126); ((-)-129); ((+)-130); ((-)-131); ((-)-132); ((+)-133); ((+)-134) and ((+)-137)

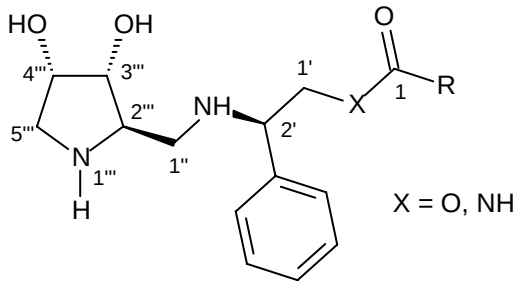

(2*R*)-2-({[(2*R*,3*R*,4*S*)-3,4-Dihydroxypyrrolidin-2-yl]methyl}amino)-2-phenylethyl acetate ((-)-123)

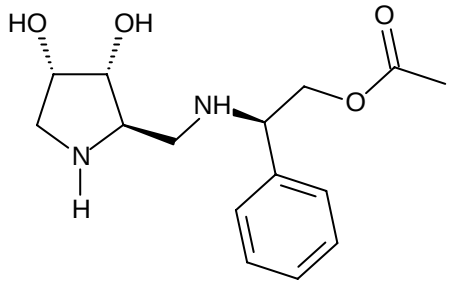

Procedure 1. Amine **112** (147 mg, 0.82 mmol, 1.5 eq), **87** (150 mg, 0.55 mmol, 1.0 eq), $NaBH(OAc)_3$ (164 mg, 0.77 mmol, 1.4 eq), $Cl(CH_2)_2Cl$ (6 ml). Flash chromatography (pentane/EtOAc 3/2) afforded 133 mg (0.31 mmol, 55 %, colourless oil) of the fully protected compound which was directly engaged in **procedure 2b**. Purification by flash chromatography ($MeCN/NH_4OH$ 7/1) afforded **123** (84 mg, 94 %) as a white foam.

For atom numbering, see page 162.

$[\alpha]_{589}^{25}$ = -5, $[\alpha]_{435}^{25}$ = -9, $[\alpha]_{405}^{25}$ = -10 (c = 0.50, MeOH).

UV (MeCN): 260 (250), 228 (250), 213 (150).

IR (film): 3015, 1680, 1435, 1210, 840, 760, 670 cm^{-1}.

^{1}H-NMR (400 MHz, MeOD):
7.51-7.36 (m, $4H_{arom}$); **7.31** (m, $1H_{arom}$); **4.24** (m, 1H, H-C(3’’’)); **4.19** (m, 1H, H-C(4’’’)); **4.09** (m, 1H, H-C(2’)); **3.85** (m, 2H, 2H-C(1’)); **3.75** (m, 1H, ^3J(H-C(2’’’), H-C(1’’)) = 9.0, H-C(2’’’)); **3.48** (dd, 1H, ^3J(H-C(5’’’), H-C(4’’’)) = 3.9, $^2J_{gem}$ = 12.9, H-C(5’’’)); **3.30** (m, 1H, H-C(5’’’)); **3.24** (m, 2H, H-C(1’’)); **2.35** (s, 3H, H-C(2)).

^{13}C-NMR (101 MHz, MeOD):
176.7 (s, C=O); **137.8** (s, $1C_{arom}$); **130.2** (d, ^1J(C,H) = 161, $2C_{arom}$); **129.4** (d, ^1J(C,H) = 161, $1C_{arom}$); **128.1** (d, ^1J(C,H) = 157, $2C_{arom}$); **75.2** (d, ^1J(C,H) = 146, C(4’’’)); **70.0** (d, ^1J(C,H) = 153, C(3’’’)); **64.6** (d, ^1J(C,H) =141, C(2’)); **63.6** (d, ^1J(C,H) =149, C(2’’’)); **61.7** (t, ^1J(C,H) =143, C(1’)); **51.3** (t, ^1J(C,H) =145, C(5’’’)); **44.3** (t, ^1J(C,H) =138, C(1’’)); **22.0** (q, ^1J(C,H) =129, C(2)).

MALDI-TOF: 295.51 $(M+H)^+$.
HRMS ($C_{15}H_{22}N_2O_4$ + H): calc. 295.1658; found 295.1660.

(2*R*)-2-({[(2*R*,3*R*,4*S*)-3,4-Dihydroxypyrrolidin-2-yl]methyl}amino)-2-phenylethyl propionate (124)

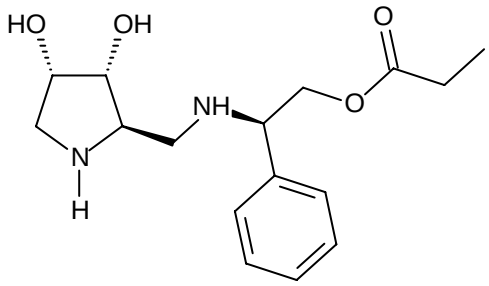

Procedure 1. Amine **113** (149 mg, 0.77 mmol, 1.4 eq), **87** (150 mg, 0.55 mmol, 1.0 eq), $NaBH(OAc)_3$ (164 mg, 0.77 mmol, 1.4 eq), $Cl(CH_2)_2Cl$ (6 ml). Flash chromatography (pentane/EtOAc 4/1) afforded 103 mg (0.23 mmol, 42 %, brown oil) of the fully protected compound which was directly engaged in **procedure 2b**. Purification by flash chromatography ($MeCN/NH_4OH$ 7/1) afforded **124** (22 mg, 31 %) as a brown oil.

For atom numbering, see page 162.

^{1}H-NMR (400 MHz, MeOD):
7.44-7.37 (m, 4H$_{arom}$); **7.32** (m, 1H$_{arom}$); **4.26-4.23** (m, 3H, H-C(4’’’) and 2H-C(1’)); **3.99** (t, 1H, ^3J(H-C(2’), H-C(1’)) = 6.2, H-C(2’)); **3.94** (dd, 1H, ^3J(H-C(3’’’), H-C(4’’’)) = 8.4, ^3J(H-C(3’’’), H-C(2’’’)) = 4.1, H-C(3’’’)); **3.45** (ddd ,1H, ^3J(H-C(2’’’), H-C(3’’’)) = 4.1, ^3J(H-C(2’’’), H-C(1’’)) = 4.3, ^3J(H-C(2’’’), H-C(1’’)) = 8.8, H-C(2’’’)); **3.42** (dd, 1H, ^3J(H-C(5’’’), H-C(4’’’)) = 4.1, $^2J_{gem}$ = 12.5, H-C(5’’’)); **3.22** (dd, 1H, ^3J(H-C(5’’’), H-C(4’’’)) = 2.1, $^2J_{gem}$ = 12.5, H-C(5’’’)); **2.92** (dd, 1H, ^3J(H-C(1’’), H-C(2’’’)) = 4.3, $^2J_{gem}$ = 13.2, H-C(1’’)); **2.71** (dd, 1H, ^3J(H-C(1’’), H-C(2’’’)) = 8.8, $^2J_{gem}$ = 13.2, H-C(1’’)); **2.34** (q, 2H, ^3J(H-C(2), H-C(3)) = 7.6, H-C(2)); **1.09** (t, 3H, ^3J(H-C(3), H-C(2)) = 7.6, H-C(3)).

^{13}C-NMR (101 MHz, MeOD):
175.9 (s, C=O); **141.3** (s, 1C$_{arom}$); **129.8** (d, ^1J(C,H) = 160, 2C$_{arom}$); **129.0** (d, ^1J(C,H) = 161, 1C$_{arom}$); **128.6** (d, ^1J(C,H) = 157, 2C$_{arom}$); **74.9** (d, ^1J(C,H) = 143, C(4’’’)); **71.2** (d, ^1J(C,H) = 148, C(3’’’)); **68.9** (t, ^1J(C,H) =151, C(1’)); **63.3** (d, ^1J(C,H) =138, C(2’)); **62.6** (d, ^1J(C,H) =146, C(2’’’)); **50.7** (t, ^1J(C,H) =145, C(5’’’)); **47.7** (t, ^1J(C,H) =139, C(1’’)); **28.2** (t, ^1J(C,H) =128, C(2)); **9.3** (q, ^1J(C,H) =128, C(3)).

MALDI-TOF: 309.45 $(M+H)^+$
HRMS ($C_{16}H_{24}N_2O_4$ + H): calc. 309.1814; found 309.1817.

^{1}H-NMR spectrum of **123**

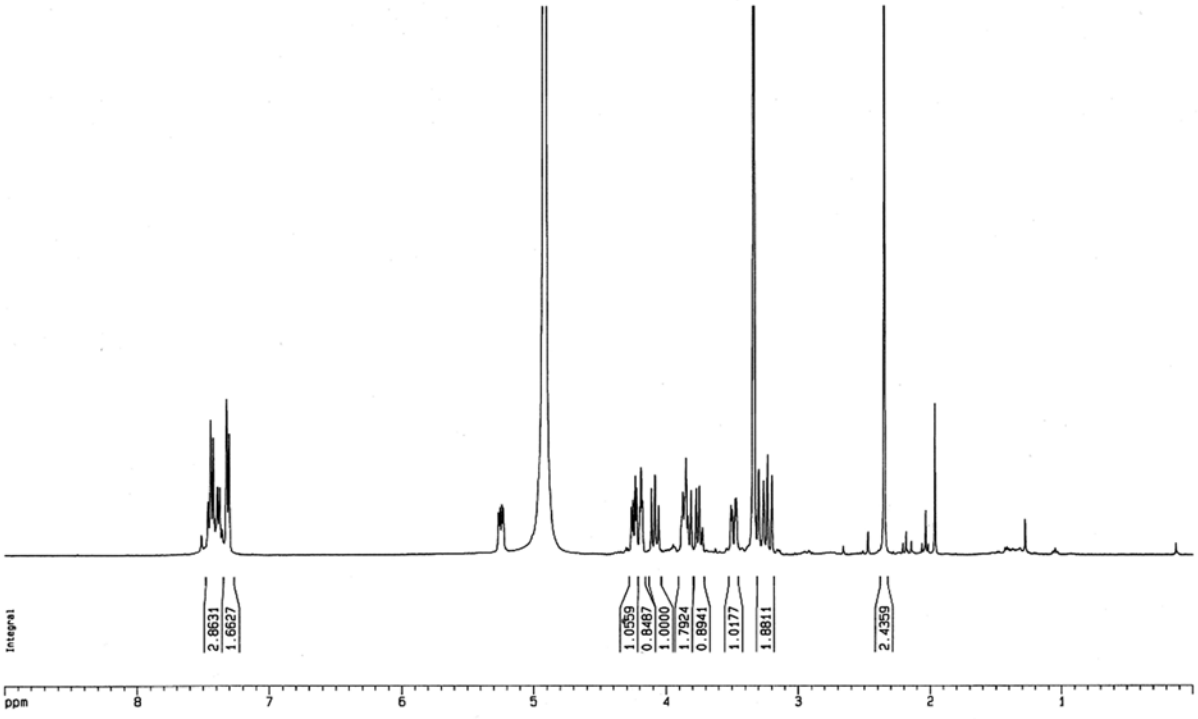

^{1}H-NMR spectrum of **124**

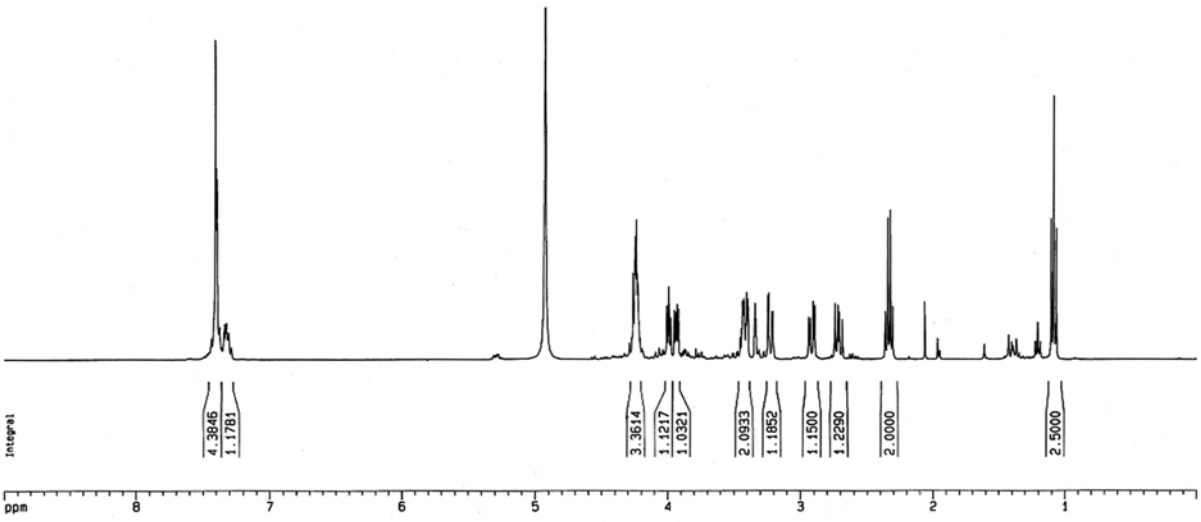

(2*R*)-2-({[(2*R*,3*R*,4*S*)-3,4-Dihydroxypyrrolidin-2-yl]methyl}amino)-2-phenylethyl butyrate ((-)-125)

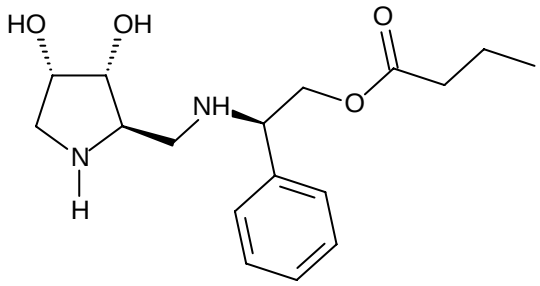

Procedure 1. Amine **114** (118 mg, 0.57 mmol, 1.0 eq), **87** (155 mg, 0.57 mmol, 1.0 eq), $NaBH(OAc)_3$ (169 mg, 0.80 mmol, 1.4 eq), $Cl(CH_2)_2Cl$ (6 ml). Flash chromatography (pentane/EtOAc 7/3) afforded 112 mg (0.24 mmol, 42 %, yellow oil) of the fully protected compound which was directly engaged in **procedure 2b**. Purification by flash chromatography (MeCN/NH_4OH 8/1) afforded **125** (99 mg, 95 %) as a brown oil after lyophilisation.

For atom numbering, see page 162.

$[\alpha]_{589}^{25} = 0$, $[\alpha]_{577}^{25} = -1$, $[\alpha]_{435}^{25} = -3$, $[\alpha]_{405}^{25} = -5$ (c = 0.56, MeOH).

UV (MeCN): 213 (4500).

IR (film): 3410, 1680, 1455, 1205, 1140, 840, 800, 725 cm^{-1}.

^{1}H-NMR (400 MHz, MeOD):
7.44-7.39 (m, $4H_{arom}$); **7.33** (m, $1H_{arom}$); **4.26** (m, 3H, H-C(4’’’) and 2H-C(1’)); **4.07** (t, 1H, ^3J(H-C(2’), H-C(1’)) = 6.1, H-C(2’)); **3.98** (dd, 1H, ^3J(H-C(3’’’), H-C(4’’’)) = 8.3, ^3J(H-C(3’’’), H-C(2’’’)) = 4.1, H-C(3’’’)); **3.52** (ddd ,1H, ^3J(H-C(2’’’), H-C(3’’’)) = 4.1, ^3J(H-C(2’’’), H-C(1’’)) = 4.2, ^3J(H-C(2’’’), H-C(1’’)) = 9.0, H-C(2’’’)); **3.47** (dd, 1H, ^3J(H-C(5’’’), H-C(4’’’)) = 4.2, $^2J_{gem}$ = 12.6, H-C(5’’’)); **3.27** (dd, 1H, ^3J(H-C(5’’’), H-C(4’’’)) = 2.0, $^2J_{gem}$ = 12.6, H-C(5’’’)); **2.97** (dd, 1H, ^3J(H-C(1’’), H-C(2’’’)) = 4.2, $^2J_{gem}$ = 13.3, H-C(1’’)); **2.84** (dd, 1H, ^3J(H-C(1’’), H-C(2’’’)) = 9.0, $^2J_{gem}$ = 13.3, H-C(1’’)); **2.29** (t, 2H, ^3J(H-C(2), H-C(3)) = 7.4, H-C(2)); **1.58** (m, 2H, ^3J(H-C(3), H-C(2)) = 7.4, ^3J(H-C(3), H-C(4)) = 7.4, H-C(3)); **0.89** (t, 3H, ^3J(H-C(4), H-C(3)) = 7.4, H-C(4)).

^{13}C-NMR (101 MHz, MeOD):
175.0 (s, C=O); **140.4** (s, $1C_{arom}$); **129.8** (d, ^1J(C,H) = 160, $2C_{arom}$); **129.2** (d, ^1J(C,H) = 160, $1C_{arom}$); **128.7** (d, ^1J(C,H) = 158, $2C_{arom}$); **74.7** (d, ^1J(C,H) = 145, C(3’’’)); **70.9** (d, ^1J(C,H) = 153, C(4’’’)); **68.4** (t, ^1J(C,H) =147, C(1’)); **63.2** (d, ^1J(C,H) =137, C(2’)); **62.2** (d, ^1J(C,H) =146, C(2’’’)); **50.7** (t, ^1J(C,H) =149, C(5’’’)); **47.3** (t, ^1J(C,H) =134, C(1’’)); **36.7** (t, ^1J(C,H) =130, C(2)); **19.3** (t, ^1J(C,H) =126, C(3)); **13.8** (q, ^1J(C,H) =125, C(4)).

MALDI-TOF: 323.40 $(M+H)^+$.
HRMS ($C_{17}H_{26}N_2O_4$ + H): calc. 323.1971; found 323.1972.

(2*R*)-2-({[(2*R*,3*R*,4*S*)-3,4-Dihydroxypyrrolidin-2-yl]methyl}amino)-2-phenylethyl pentanoate ((-)-126)

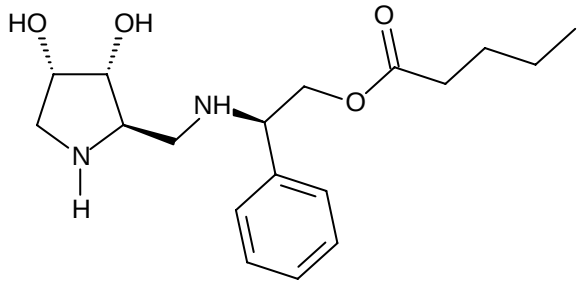

Procedure 1. Amine **115** (170 mg, 0.77 mmol, 1.4 eq), **87** (150 mg, 0.55 mmol, 1.0 eq), $NaBH(OAc)_3$ (164 mg, 0.77 mmol, 1.4 eq), $Cl(CH_2)_2Cl$ (7 ml). Flash chromatography (pentane/EtOAc 4/1) afforded 130 mg (0.27 mmol, 35 %, colourless oil) of the fully protected compound which was directly engaged in **procedure 2b**. Purification by flash chromatography ($MeCN/NH_4OH$ 6/1) afforded **126** (83 mg, 91 %) as a brown oil after lyophilisation.

For atom numbering, see page 162.

$[\alpha]_{589}^{25}$ = -3, $[\alpha]_{577}^{25}$ = -4, $[\alpha]_{435}^{25}$ = -11, $[\alpha]_{405}^{25}$ = -15 (c = 0.32, MeOH).

UV (MeCN): 210 (5500).

IR (film): 3020, 1670, 1455, 1215, 1140, 840, 800, 765 cm^{-1}.

^{1}H-NMR (400 MHz, MeOD):
7.36-7.30 (m, $5H_{arom}$); **4.33-4.12** (m, 3H, H-C(4’’’) and 2H-C(1’)); **4.02** (t, 1H, ^3J(H-C(2’), H-C(1’)) = 6.3, H-C(2’)); **3.95** (dd, 1H, ^3J(H-C(3’’’), H-C(4’’’)) = 8.1, ^3J(H-C(3’’’), H-C(2’’’)) = 4.0, H-C(3’’’)); **3.45** (m , 1H, H-C(2’’’)); **3.42** (dd, 1H, ^3J(H-C(5’’’), H-C(4’’’)) = 4.1, $^2J_{gem}$ = 12.6, H-C(5’’’)); **3.27** (dd, 1H, ^3J(H-C(5’’’), H-C(4’’’)) = 2.1, $^2J_{gem}$ = 12.6, H-C(5’’’)); **2.96** (dd, 1H, ^3J(H-C(1’’), H-C(2’’’)) = 4.3, $^2J_{gem}$ = 13.3, H-C(1’’)); **2.72** (dd, 1H, ^3J(H-C(1’’), H-C(2’’’)) = 9.0, $^2J_{gem}$ = 13.3, H-C(1’’)); **2.31** (t, 2H, ^3J(H-C(2), H-C(3)) = 7.4, H-C(2)); **1.54** (tt, 2H, ^3J(H-C(3), H-C(2)) = 7.4, ^3J(H-C(3), H-C(4)) = 7.4, H-C(3)); **1.29** (qt, 2H, ^3J(H-C(4), H-C(3)) = 7.4, ^3J(H-C(4), H-C(5)) = 7.4, H-C(4)); **0.89** (t, 3H, ^3J(H-C(5), H-C(4)) = 7.4, H-C(5)).

^{13}C-NMR (101 MHz, MeOD):
174.9 (s, C=O); **130.1** (d, ^1J(C,H) = 161, $2C_{arom}$); **129.8** (d, ^1J(C,H) = 158, $1C_{arom}$); **129.0** (d, ^1J(C,H) = 161, $2C_{arom}$); **128.0** (s, $1C_{arom}$); **75.0** (d, ^1J(C,H) = 145, C(3’’’)); **70.7** (d, ^1J(C,H) = 154, C(4’’’)); **67.3** (t, ^1J(C,H) =148, C(1’)); **63.2** (d, ^1J(C,H) =141, C(2’)); **61.0** (d, ^1J(C,H) =148, C(2’’’)); **51.0** (t, ^1J(C,H) =145, C(5’’’)); **47.2** (t, ^1J(C,H) =138, C(1’’)); **34.5** (t, ^1J(C,H) =128, C(2)); **27.9** (t, ^1J(C,H) =127, C(3)); **23.1** (t, ^1J(C,H) =127, C(4)); **14.0** (q, ^1J(C,H) =124, C(5)).

MALDI-TOF: 337.46 $(M+H)^+$.
HRMS ($C_{18}H_{28}N_2O_4$ + H): calc. 337.2127; found 337.2129.

^{1}H-NMR spectrum of **125**

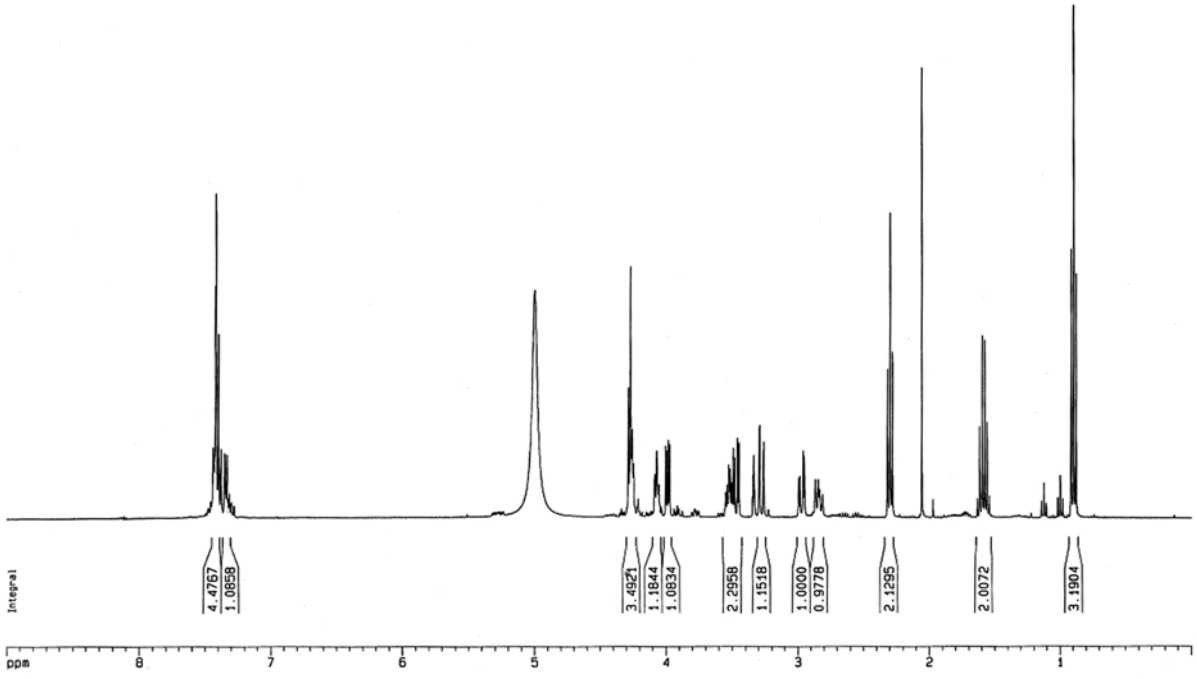

^{1}H-NMR spectrum of **126**

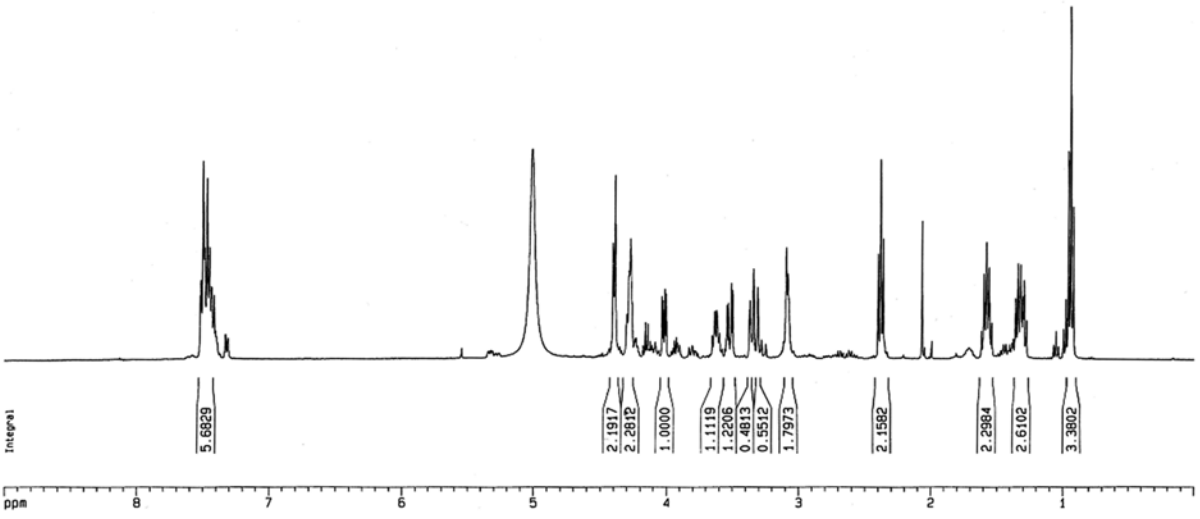

(2*R*)-2-({[(2*R*,3*R*,4*S*)-3,4-Dihydroxypyrrolidin-2-yl]methyl}amino)-2-phenylethyl 2-methylpropanoate ((+)-127)

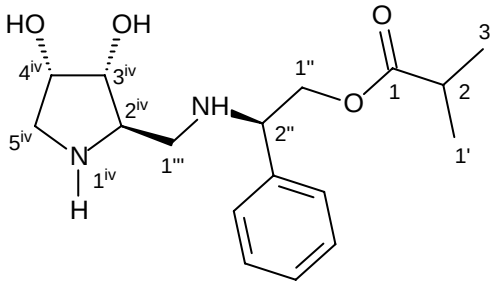

Procedure 1. Amine **116** (131 mg, 0.63 mmol, 1.0 eq), **87** (172 mg, 0.63 mmol, 1.0 eq), $NaBH(OAc)_3$ (188 mg, 0.89 mmol, 1.4 eq), $Cl(CH_2)_2Cl$ (7 ml). Flash chromatography (pentane/EtOAc 7/3) afforded 60 mg (0.13 mmol, 20 %, brown oil) of the fully protected compound which was directly engaged in **procedure 2b**. Purification by flash chromatography ($MeCN/NH_4OH$ 10/1) afforded **127** (39 mg, 94 %) as a brown oil.

$[\alpha]_{589}^{25} = +11$, $[\alpha]_{577}^{25} = +18$, $[\alpha]_{405}^{25} = +25$ (c = 0.26, MeOH).

UV (MeCN): 209 (5500).

IR (film): 3315, 2975, 1675, 1455, 1390, 1345, 1200, 1140, 840, 800, 760, 700 cm^{-1}.

^{1}H-NMR (400 MHz, MeOD):
7.46-7.37 (m, $4H_{arom}$); **7.35** (m, $1H_{arom}$); **4.31** (m, 2H, 2H-C(1'')); **4.24** (ddd, 1H, ^3J(H-C(4^{iv}), H-C(5^{iv})) = 1.9, ^3J(H-C(4^{iv}), H-C(5^{iv})) = 4.1, ^3J(H-C(4^{iv}), H-C(3^{iv})) = 8.3 , H-C(4^{iv})); **4.11** (dd, 1H, ^3J(H-C(2''), H-C(1'')) = 5.8, ^3J(H-C(2''), H-C(1'')) = 6.5, H-C(2'')); **3.97** (dd, 1H, ^3J(H-C(3^{iv}), H-C(2^{iv})) = 4.0, ^3J(H-C(3^{iv}), H-C(4^{iv})) = 8.3, H-C(3^{iv})); **3.52** (ddd, 1H, ^3J(H-C(2^{iv}), H-C(3^{iv})) = 4.0, ^3J(H-C(2^{iv}), H-C(1''')) = 4.2, ^3J(H-C(2^{iv}), H-C(1''')) = 9.1, H-C(2^{iv})); **3.46** (dd, 1H, ^3J(H-C(5^{iv}), H-C(4^{iv})) = 4.1, $^2J_{gem}$ = 12.5, H-C(5^{iv})); **3.27** (dd, 1H, ^3J(H-C(5^{iv}), H-C(4^{iv})) = 1.9, $^2J_{gem}$ = 12.5, H-C(5^{iv})); **3.00** (dd, 1H, ^3J(H-C(1'''), H-C(2^{iv})) = 4.2, $^2J_{gem}$ = 13.3, H-C(1''');; **2.87** (dd, 1H, ^3J(H-C(1'''), H-C(2^{iv})) = 9.1, $^2J_{gem}$ = 13.3, H-C(1''')); **2.55** (qq, 1H, ^3J(H-C(2), H-C(3)) = 7.0, ^3J(H-C(2), H-C(1')) = 7.0, H-C(2)); **1.10** (d, 3H, ^3J(H-C(3), H-C(2)) = 7.0, H-C(3)); **1.09** (d, 3H, ^3J(H-C(1'), H-C(2)) = 7.0, H-C(1')).

^{13}C-NMR (101 MHz, MeOD):
178.3 (s, C=O); **140.1** (s, $1C_{arom}$); **129.9** (d, ^1J(C,H) = 160, $2C_{arom}$); **129.3** (d, ^1J(C,H) = 161, $1C_{arom}$); **128.8** (d, ^1J(C,H) = 158, $2C_{arom}$); **74.8** (d, ^1J(C,H) = 145, C(3^{iv})); **70.9** (d, ^1J(C,H) = 153, C(4^{iv})); **68.1** (t, ^1J(C,H) =147, C(1'')); **63.2** (d, ^1J(C,H) =135, C(2'')); **61.9** (d, ^1J(C,H) =139, C(2^{iv})); **50.8** (t, ^1J(C,H) =145, C(5^{iv})); **47.4** (t, ^1J(C,H) =137, C(1''')); **35.0** (d, ^1J(C,H) =130, C(2)); **19.2** (q, ^1J(C,H) =128, C(3)); **19.1** (q, ^1J(C,H) =128, C(1')).

MALDI-TOF: 323.44 $(M+H)^+$.
HRMS ($C_{17}H_{26}N_2O_4$ + H): calc. 323.1971; found 323.1973.

(2*R*)-2-({[(2*R*,3*R*,4*S*)-3,4-Dihydroxypyrrolidin-2-yl]methyl}amino)-2-phenylethyl 3-methylbutanoate ((+)-128)

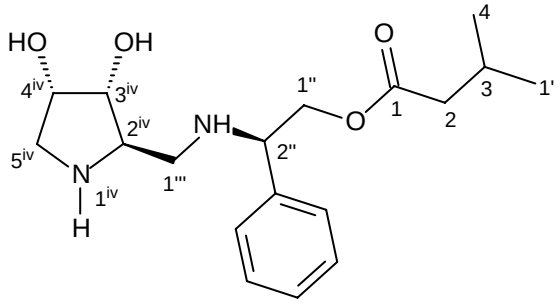

Procedure 1. Amine **117** (170 mg, 0.77 mmol, 1.4 eq), **87** (150 mg, 0.55 mmol, 1.0 eq), $NaBH(OAc)_3$ (164 mg, 0.77 mmol, 1.4 eq), $Cl(CH_2)_2Cl$ (6 ml). Flash chromatography (pentane/EtOAc 7/3) afforded 95 mg (0.20 mmol, 36 %, colourless oil) of the fully protected compound which was directly engaged in **procedure 2b**. Purification by flash chromatography ($MeCN/NH_4OH$ 12/1) afforded **128** (66 mg, 99 %) as a brown oil.

$[\alpha]_{589}^{25} = +6$, $[\alpha]_{577}^{25} = +9$, $[\alpha]_{435}^{25} = +11$, $[\alpha]_{405}^{25} = +12$ (c = 0.57, MeOH).

UV (MeCN): 260 (500), 229 (500), 208 (250).

IR (film): 2960, 1680, 1455, 1200, 835, 800, 720, 700 cm^{-1}.

^{1}H-NMR (400 MHz, MeOD):
7.41 (m, $4H_{arom}$); **7.33** (m, $1H_{arom}$); **4.30-4.23** (m, 3H, 2H-C(1'') and H-C(4^{iv})); **3.99** (t, 1H, ^3J(H-C(2''), H-C(1'')) = 6.2, H-C(2'')); **3.94** (dd, 1H, ^3J(H-C(3^{iv}), H-C(4^{iv})) = 8.0, ^3J(H-C(3^{iv}), H-C(2^{iv})) = 4.0, H-C(3^{iv})); **3.46-3.39** (dd and m, 2H, ^3J(H-C(5^{iv}), H-C(4^{iv})) = 4.0, $^2J_{gem}$ = 12.4, H-C(5^{iv}) and H-C(2^{iv})); **3.23** (dd, 1H, ^3J(H-C(5^{iv}), H-C(4^{iv})) = 2.1, $^2J_{gem}$ = 12.4, H-C(5^{iv})); **2.91** (dd, 1H, ^3J(H-C(1'''), H-C(2^{iv})) = 4.3, $^2J_{gem}$ = 13.2, H-C(1''')); **2.70** (dd, 1H, ^3J(H-C(1'''), H-C(2^{iv})) = 9.0, $^2J_{gem}$ = 13.2, H-C(1''')); **2.18** (d, 2H, ^3J(H-C(2), H-C(3)) = 7.1, H-C(2)); **2.00** (m, 1H, H-C(3)); **0.90** (d, 6H, ^3J= 6.7, 3H-C(4) and 3H-C(1')).

^{13}C-NMR (101 MHz, MeOD):
174.4 (s, C=O); **141.3** (s, $1C_{arom}$); **129.7** (d, ^1J(C,H) = 160, $2C_{arom}$); **128.9** (d, ^1J(C,H) = 160, $1C_{arom}$); **128.6** (d, ^1J(C,H) = 153, $2C_{arom}$); **74.7** (d, ^1J(C,H) = 145, C(3^{iv})); **71.1** (d, ^1J(C,H) = 153, C(4^{iv})); **68.7** (t, ^1J(C,H) =148, C(1'')); **63.2** (d, ^1J(C,H) =137, C(2'')); **62.6** (d, ^1J(C,H) =147, C(2^{iv})); **50.7** (t, ^1J(C,H) =145, C(5^{iv})); **47.5** (t, ^1J(C,H) =135, C(1''')); **44.0** (t, ^1J(C,H) =124, C(2)); **26.7** (d, ^1J(C,H) =126, C(3)); **22.6** (q, ^1J(C,H) =125, 2x*Me*(^{i}Pr)).

MALDI-TOF: 337.60 $(M+H)^+$.
HRMS ($C_{18}H_{28}N_2O_4$ + H): calc. 337.2127; found 337.2129.

^{1}H-NMR spectrum of **127**

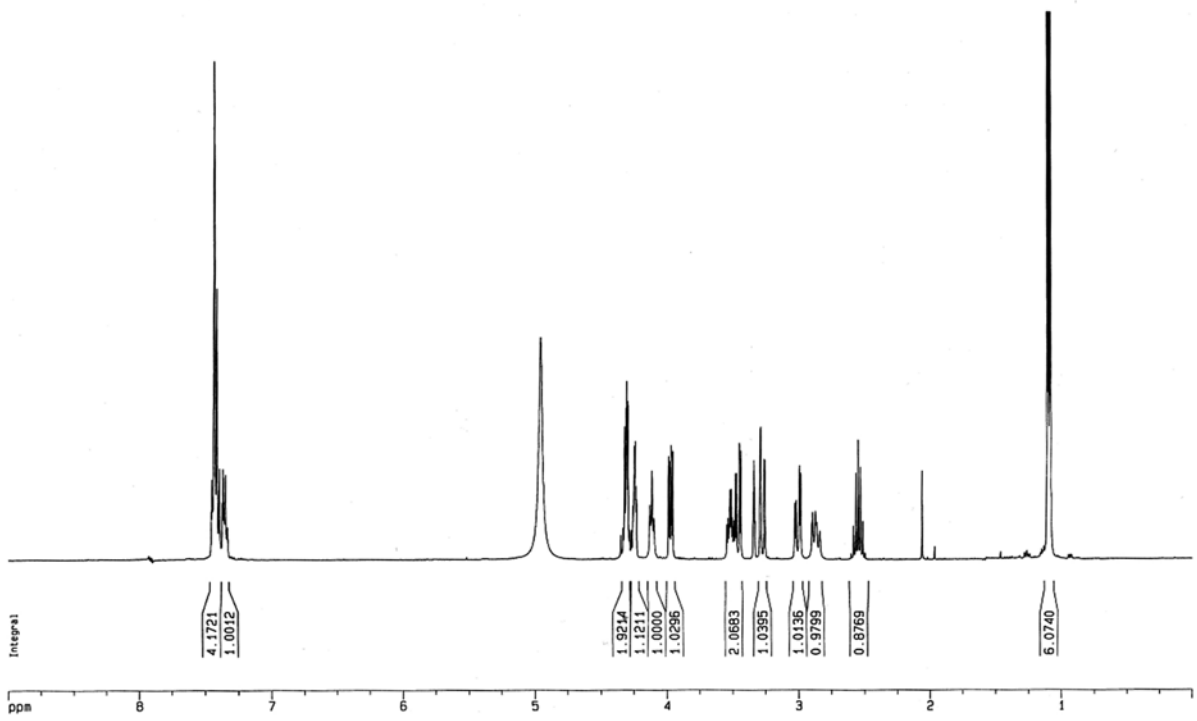

^{1}H-NMR spectrum of **128**

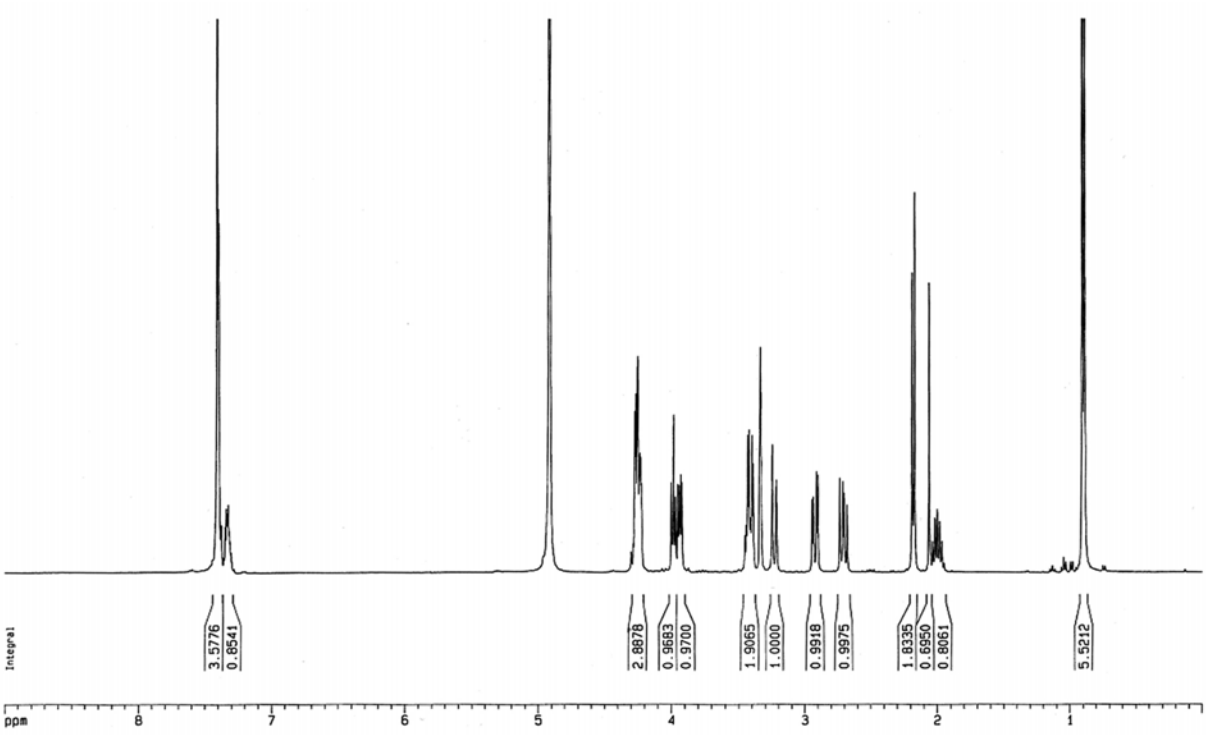

(2*R*)-2-({[(2*R*,3*S*,4*S*)-3,4-Dihydroxypyrrolidin-2-yl]methyl}amino)-2-phenylethyl 2-fluorobenzoate ((-)-129)

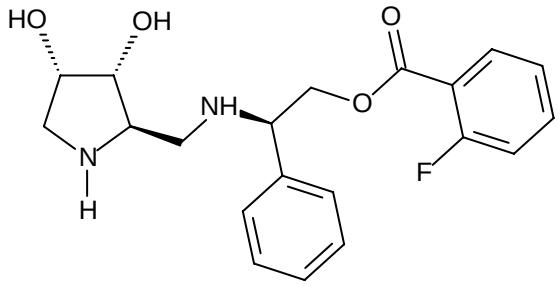

Procedure 1. Amine **118** (191 mg, 0.74 mmol, 1.0 eq), **87** (200 mg, 0.74 mmol, 1.0 eq), $NaBH(OAc)_3$ (219 mg, 1.03 mmol, 1.4 eq), $Cl(CH_2)_2Cl$ (7.5 ml). Flash chromatography (pentane/EtOAc 4/1) afforded 186 mg (0.36 mmol, 49 %, pale yellow solid) of the fully protected compound which was directly engaged in **procedure 2b**. Purification by flash chromatography (CH_2Cl_2/MeOH 8/1) afforded **129** (100 mg, 74 %) as a brown solid after lyophilisation.

For atom numbering, see page 162.

$[\alpha]_{589}^{25}$ = -5, $[\alpha]_{435}^{25}$ = -9, $[\alpha]_{405}^{25}$ = -14 (*c* = 0.45, MeOH).

UV (MeCN): 225 (6000), 210 (5000), 206 (5500), 203 (6000).

IR (film): 3390, 2360, 2340, 1680, 1455, 1210, 1140, 845, 800, 755, 725 cm^{-1}.

^{1}H-NMR (400 MHz, MeOD):
7.88 (m, 1H$_{arom}$); **7.66-7.62** (m, 1H$_{arom}$); **7.48-7.22** (m, 7H$_{arom}$); **4.50** (m, 2H, 2H-C(1'); **4.22** (ddd, 1H, ^3J(H-C(4'''), H-C(5''')) = 2.1, ^3J(H-C(4'''), H-C(5''')) = 4.2, ^3J(H-C(4'''), H-C(3''')) = 4.0, H-C(4''')); **4.14** (t, 1H, ^3J(H-C(2'), H-C(1')) = 6.1, H-C(2')); **3.96** (dd, 1H, ^3J(H-C(3'''), H-C(4''')) = 4.0, ^3J(H-C(3'''), H-C(2''')) = 8.0, H-C(3''')); **3.48-3.38** (m and dd, 2H, ^3J(H-C(5'''), H-C(4''')) = 4.2, $^2J_{gem}$ = 12.5, H-C(5''') and H-C(2''')); **3.23** (dd, 1H, ^3J(H-C(5'''), H-C(4''')) = 2.1, $^2J_{gem}$ = 12.5, H-C(5''')); **2.98** (dd, 1H, ^3J(H-C(1''), H-C(2''')) = 4.2, $^2J_{gem}$ = 13.3, H-C(1'')); **2.75** (dd, 1H, ^3J(H-C(1''), H-C(2''')) = 8.75, $^2J_{gem}$ = 13.3, H-C(1'')).

^{13}C-NMR (101 MHz, MeOD):
167.1 (s, O*C*(O)Ar); **141.2** (s, 1C$_{arom}$); **136.3**, **136.2**, **133.1**, **129.8**, **129.1**, **128.6**, **125.4**, **118.1**, **117.9** (11C$_{arom}$); **74.8** (d, ^1J(C,H) = 146, C(3''')); **71.2** (d, ^1J(C,H) = 158, C(4''')); **69.7** (t, ^1J(C,H) = 150, C(1')); **63.3** (d, ^1J(C,H) = 134, C(2')); **62.7** (d, ^1J(C,H) = 145, C(2''')); **50.8** (t, ^1J(C,H) = 147, C(5''')); **47.5** (t, ^1J(C,H) = 138, C(1'')).

MALDI-TOF: 374.99 $(M+H)^+$.
HRMS ($C_{20}H_{23}FN_2O_4$ + H): calc. 375.1720; found 375.1716.
Purity measured by HPLC (C_{18}, C_4 columns): 100%, 100%.
M.P: 99-103°C.

(2*R*)-2-({[(2*R*,3*S*,4*S*)-3,4-Dihydroxypyrrolidin-2-yl]methyl}amino)-2-phenylethyl 4-fluorobenzoate ((+)-130)

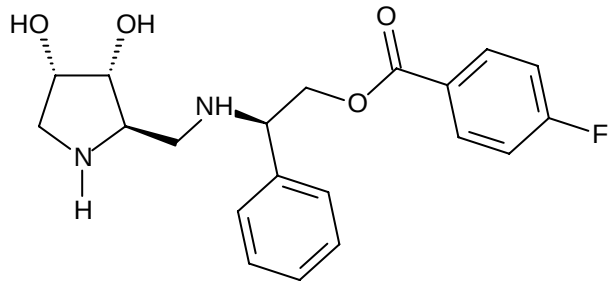

Procedure 1. Amine **119** (185 mg, 0.72 mmol, 1.0 eq), **87** (194 mg, 0.72 mmol, 1.0 eq), $NaBH(OAc)_3$ (212 mg, 1.0 mmol, 1.4 eq), $Cl(CH_2)_2Cl$ (10 ml). Flash chromatography (pentane/EtOAc 7/3) afforded 218 mg (0.42 mmol, 60 %, white foam) of the fully protected compound which was directly engaged in **procedure 2b**. Purification by flash chromatography (CH_2Cl_2/MeOH 9/1) afforded **130** (131 mg, 83 %) as a pale yellow solid after lyophilisation.

For atom numbering, see page 162.

$[\alpha]_{589}^{25}$ = +2 (*c* = 0.37, MeOH).

UV (MeCN): 230 (7500), 205 (7000), 196 (2500).

IR (film): 3415, 2360, 2340, 1680, 1280, 1205, 1140, 845, 800, 725, 670 cm^{-1}.

^{1}H-NMR (400 MHz, MeOD):
8.05 (m, $2H_{arom}$); **7.48-7.33** (m, $5H_{arom}$); **7.22** (m, $2H_{arom}$); **4.53** (dd, 1H, ^3J(H-C(1'), H-C(2')) = 6.8, $^2J_{gem}$ = 10.9, H-C(1')); **4.45** (dd, 1H, ^3J(H-C(1'), H-C(2')) = 5.6, $^2J_{gem}$ = 10.9, H-C(1')); **4.22** (m, 1H, H-C(4''')); **4.15** (dd, 1H, ^3J(H-C(2'), H-C(1')) = 5.6, ^3J(H-C(2'), H-C(1')) = 6.8, H-C(2')); **3.95** (dd, 1H, ^3J(H-C(3'''), H-C(4''')) = 4.0, ^3J(H-C(3'''), H-C(2''')) = 8.1, H-C(3''')); **3.48** (ddd, 1H, ^3J(H-C(2'''), H-C(1'')) = 4.2, ^3J(H-C(2'''), H-C(3''')) = 8.1, ^3J(H-C(2'''), H-C(1'')) = 9.0, H-C(2''')); **3.41** (dd, 1H, ^3J(H-C(5'''), H-C(4''')) = 4.1, $^2J_{gem}$ = 12.5, H-C(5''')); **3.24** (dd, 1H, ^3J(H-C(5'''), H-C(4''')) = 2.1, $^2J_{gem}$ = 12.5, H-C(5''')); **2.99** (dd, 1H, ^3J(H-C(1''), H-C(2''')) = 4.2, $^2J_{gem}$ = 13.2, H-C(1'')); **2.74** (dd, 1H, ^3J(H-C(1''), H-C(2''')) = 9.0, $^2J_{gem}$ = 13.2, H-C(1'')).

^{13}C-NMR (101 MHz, MeOD):
173.0 (s, O*C*(O)Ar); **141.3** (s, $1C_{arom}$); **133.4** (d, ^1J(C,H) = 166, $2C_{arom}$); **130.0** (s, $1C_{arom}$); **129.8** (d, ^1J(C,H) = 160, $2C_{arom}$); **129.4** (s, $1C_{arom}$); **129.0** (d, ^1J(C,H) = 161, $1C_{arom}$); **128.6** (d, ^1J(C,H) = 162, $2C_{arom}$); **116.7** (d, ^1J(C,H) = 166, $2C_{arom}$); **74.8** (d, ^1J(C,H) = 145, C(3''')); **71.1** (d, ^1J(C,H) = 148, C(4''')); **69.5** (t, ^1J(C,H) = 147, C(1')); **63.4** (d, ^1J(C,H) = 136, C(2')); **62.7** (d, ^1J(C,H) = 146, C(2''')); **50.7** (t, ^1J(C,H) = 145 , C(5''')); **47.6** (t, ^1J(C,H) = 132, C(1'')).

MALDI-TOF: 375.08 $(M+H)^+$.
HRMS ($C_{20}H_{23}FN_2O_4$ + H): calc. 375.1720; found 375.1716.
Purity measured by HPLC (C_{18}, C_8 columns): 100%, 100%.
M.P: 85-90°C.

^{1}H-NMR spectrum of **129**

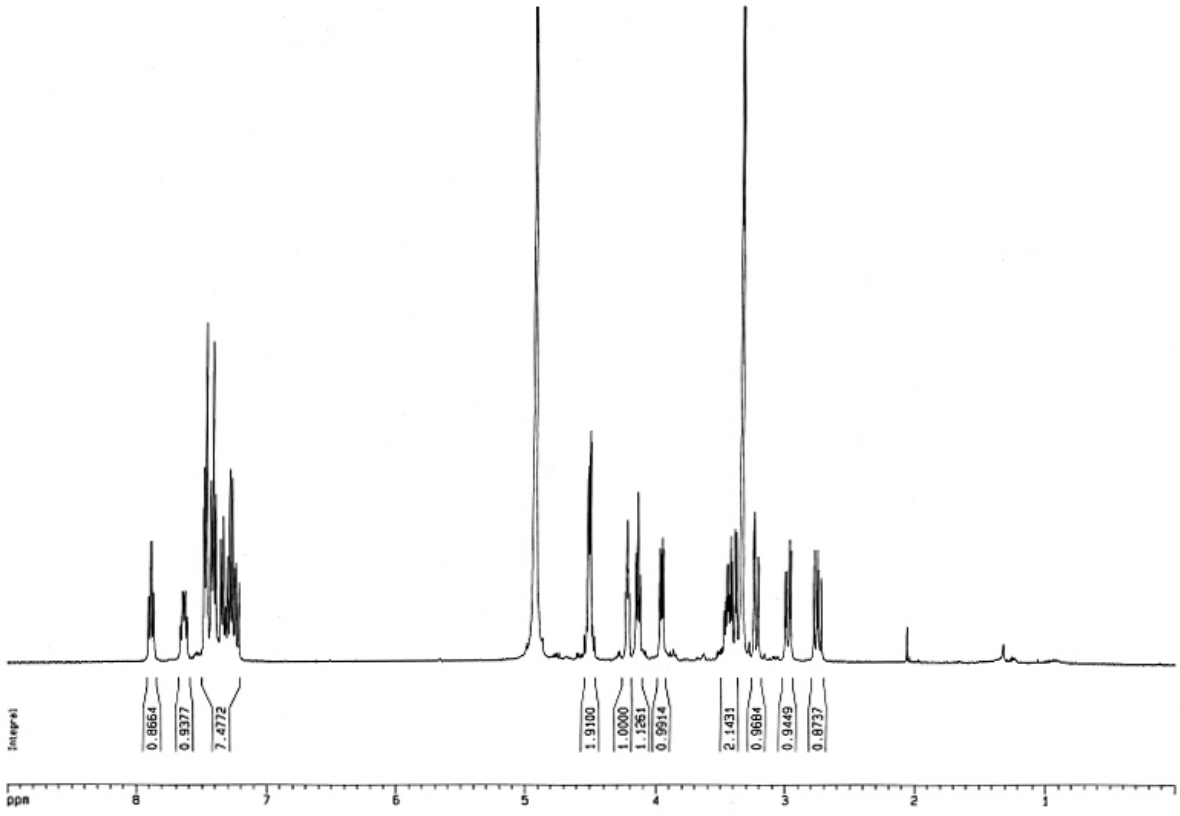

^{1}H-NMR spectrum of **130**

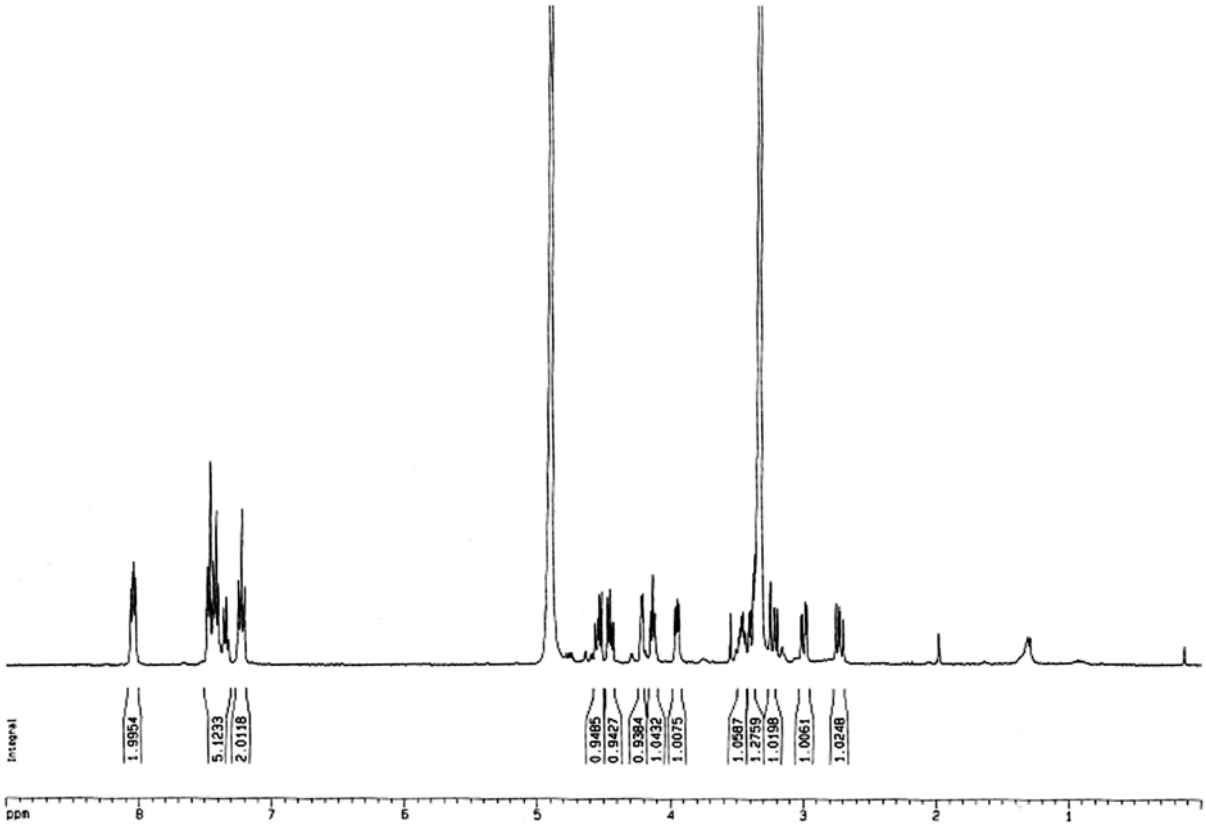

(2*R*)-2-({[(2*R*,3*S*,4*S*)-3,4-Dihydroxypyrrolidin-2-yl]methyl}amino)-2-phenylethyl 3-bromobenzoate ((-)-131)

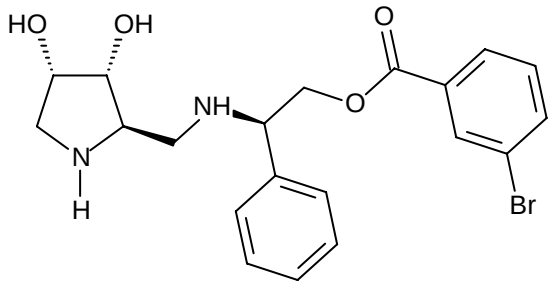

Procedure 1. Amine **120** (180 mg, 0.56 mmol, 1.0 eq), **87** (152 mg, 0.56 mmol, 1.0 eq), $NaBH(OAc)_3$ (166 mg, 0.78 mmol, 1.4 eq), $Cl(CH_2)_2Cl$ (8 ml). Flash chromatography (pentane/EtOAc 4/1) afforded 118 mg (0.21 mmol, 37 %, colourless oil) of the fully protected compound which was directly engaged in **procedure 2b**. Purification by flash chromatography (CH_2Cl_2/MeOH 9/1) afforded **131** (70 mg, 78 %) as a pale yellow solid after lyophilisation.

For atom numbering, see page 162.

$[\alpha]_{589}^{25} = 0$, $[\alpha]_{435}^{25} = -16$, $[\alpha]_{405}^{25} = -28$ (*c* = 0.21, MeOH).

UV (MeCN): 229 (2500), 205 (7000), 194 (1000).

IR (film): 3415, 2350, 1435, 1205, 1140, 840, 800, 725, 670 cm^{-1}.

^{1}H-NMR (400 MHz, MeOD):
8.11 (s, 1H$_{arom}$); **7.97** (d, ^3J = 7.8, 1H$_{arom}$); **7.80** (d, ^3J = 7.9, 1H$_{arom}$); **7.49-7.41** (m, 5H$_{arom}$); **7.35** (d, ^3J = 7.1, 1H$_{arom}$); **4.55** (dd, 1H, ^3J(H-C(1'), H-C(2')) = 6.8, $^2J_{gem}$ = 11.0, H-C(1')); **4.46** (dd, 1H, ^3J(H-C(1'), H-C(2')) = 5.6, $^2J_{gem}$ = 11.0, H-C(1')); **4.21** (ddd, 1H, ^3J(H-C(4'''), H-C(5''')) = 2.1, ^3J(H-C(4'''), H-C(5''')) = 4.0, ^3J(H-C(4'''), H-C(3''')) = 4.1, H-C(4''')); **4.14** (dd, 1H, ^3J(H-C(2'), H-C(1')) = 5.6, ^3J(H-C(2'), H-C(1')) = 6.8, H-C(2')); **3.95** (dd, 1H, ^3J(H-C(3'''), H-C(4''')) = 4.1, ^3J(H-C(3'''), H-C(2''')) = 8.0, H-C(3''')); **3.48-3.42** (ddd, 1H, ^3J(H-C(2'''), H-C(1'')) = 4.2, ^3J(H-C(2'''), H-C(3''')) = 8.0, ^3J(H-C(2'''), H-C(1'')) = 8.9, H-C(2''')); **3.41-3.34** (m, 1H, H-C(5''')); **3.22** (dd, 1H, ^3J(H-C(5'''), H-C(4''')) = 2.1, $^2J_{gem}$ = 12.5, H-C(5''')); **2.98** (dd, 1H, ^3J(H-C(1''), H-C(2''')) = 4.2, $^2J_{gem}$ = 13.2, H-C(1'')); **2.72** (dd, 1H, ^3J(H-C(1''), H-C(2''')) = 8.9, $^2J_{gem}$ = 13.2, H-C(1'')).

^{13}C-NMR (101 MHz, MeOD):
163.3 (s, O*C*(O)Ar); **144.4**, **141.3**, **138.8** (3s, 3C$_{arom}$); **137.2**, **133.4**, **131.5**, **129.9**, **129.3**, **129.1**, **128.6** (7d, 9C$_{arom}$); **74.9** (d, ^1J(C,H) = 142, C(3''')); **71.2** (d, ^1J(C,H) = 153, C(4''')); **69.7** (t, ^1J(C,H) = 145, C(1')); **63.4** (d, ^1J(C,H) = 137, C(2')); **62.7** (d, ^1J(C,H) = 150, C(2''')); **50.8** (t, C(5)); **47.7** (t, C(1'')).

MALDI-TOF: 437.07 $(M+2)^+$, 435.07 $(M)^+$.
HRMS ($C_{20}H_{23}BrN_2O_4$ + H): calc. 435.0919; found 435.0919.
Purity measured by HPLC (C_{18}, C_8 columns): 94%, 100%.
M.P: 114-117°C.

(2*R*)-2-({[(2*R*,3*R*,4*S*)-3,4-Dihydroxypyrrolidin-2-yl]methyl}amino)-2-phenylethyl 4-bromobenzoate ((-)-132)

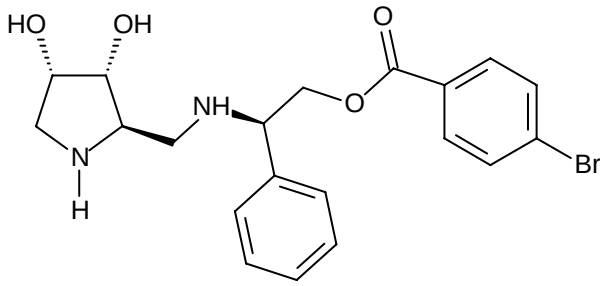

Procedure 1. Amine **121** (132 mg, 0.41 mmol, 1.0 eq), **87** (112 mg, 0.41 mmol, 1.0 eq), $NaBH(OAc)_3$ (122 mg, 0.58 mmol, 1.4 eq), $Cl(CH_2)_2Cl$ (5 ml). Flash chromatography (pentane/EtOAc 7/3) afforded 109 mg (0.25 mmol, 61 %, white foam) of the fully protected compound which was directly engaged in **procedure 2b**. Purification by flash chromatography (CH_2Cl_2/MeOH 9/1) afforded **132** (109 mg, quantitative) as a brown solid after lyophilisation.

For atom numbering, see page 162.

$[\alpha]_{589}^{25}$ = -3, $[\alpha]_{435}^{25}$ = -7, (c = 0.35, MeOH).

UV (MeCN): 244 (12500), 211 (8000), 203 (7000), 193 (1500), 189 (1500).

IR (film): 3265, 2355, 2340, 1680, 1455, 1205, 1140, 1010, 845, 800, 755, 725, 670 cm^{-1}.

^{1}H-NMR (400 MHz, MeOD):
7.90 (d, ^3J = 8.5 , $2H_{arom}$); **7.68** (d, ^3J = 8.5 , $2H_{arom}$); **7.48-7.40** (m, $4H_{arom}$); **7.34** (dd, ^3J = 7.2, $1H_{arom}$); **4.54** (dd, 1H, ^3J(H-C(1'), H-C(2')) = 6.8, $^2J_{gem}$ = 11.0, H-C(1')); **4.46** (dd, 1H, ^3J(H-C(1'), H-C(2')) = 5.6, $^2J_{gem}$ = 11.0, H-C(1')); **4.22** (m, 1H, H-C(4''')); **4.14** (dd, 1H, ^3J(H-C(2'), H-C(1')) = 5.6, ^3J(H-C(2'), H-C(1')) = 6.8, H-C(2')); **3.95** (dd, 1H, ^3J(H-C(3'''), H-C(4''')) = 8.0, ^3J(H-C(3'''), H-C(2''')) = 4.0, H-C(3''')); **3.46** (ddd, 1H, ^3J(H-C(2'''), H-C(1'')) = 4.2, ^3J(H-C(2'''), H-C(3''')) = 4.0, ^3J(H-C(2'''), H-C(1'')) = 8.9, H-C(2''')); **3.41** (m, 1H, H-C(5''')); **3.23** (dd, 1H, ^3J(H-C(5'''), H-C(4''')) = 1.9, $^2J_{gem}$ = 12.5, H-C(5''')); **2.99** (dd, 1H, ^3J(H-C(1''), H-C(2''')) = 4.2, $^2J_{gem}$ = 13.2, H-C(1'')); **2.73** (dd, 1H, ^3J(H-C(1''), H-C(2''')) = 8.9, $^2J_{gem}$ = 13.2, H-C(1'')).

^{13}C-NMR (101 MHz, MeOD):
170.0 (s, O*C*(O)Ar); **141.3** (s, $1C_{arom}$); **133.0** (d, ^1J(C,H) = 169, $2C_{arom}$); **132.3** (d, ^1J(C,H) = 164, $2C_{arom}$); **130.3** (s, $1C_{arom}$); **129.9** (d, ^1J(C,H) = 160, $2C_{arom}$); **129.2** (s, $1C_{arom}$); **129.1** (d, ^1J(C,H) = 161, $1C_{arom}$); **128.6** (d, ^1J(C,H) = 157, $2C_{arom}$); **74.8** (d, ^1J(C,H) = 145, C(3''')); **71.1** (d, ^1J(C,H) = 153, C(4''')); **69.6** (t, ^1J(C,H) = 147, C(1')); **63.4** (d, ^1J(C,H) = 136, C(2')); **62.7** (d, ^1J(C,H) = 146, C(2''')); **50.7** (t, ^1J(C,H) = 148, C(5''')); **47.7** (t, ^1J(C,H) = 137, C(1'')).

MALDI-TOF: 437.18 $(M+2)^+$, 435.18 $(M)^+$.
MALDI-HRMS ($C_{20}H_{23}BrN_2O_4$ + H): calc. 435.0919; found 435.0919.
Purity measured by HPLC (C_{18}, C_8 columns): 100%, 100%.
M.P: 125-130°C.

^{1}H-NMR spectrum of **131**

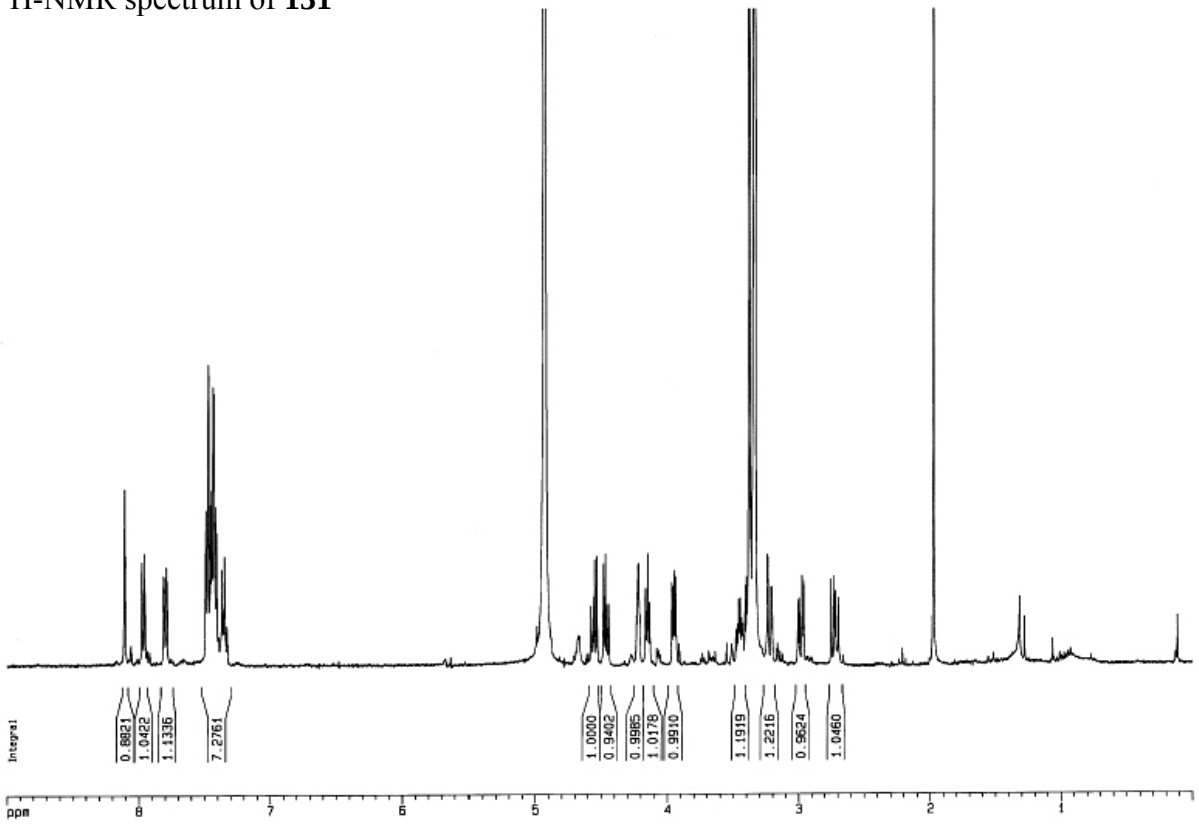

^{1}H-NMR spectrum of **132**

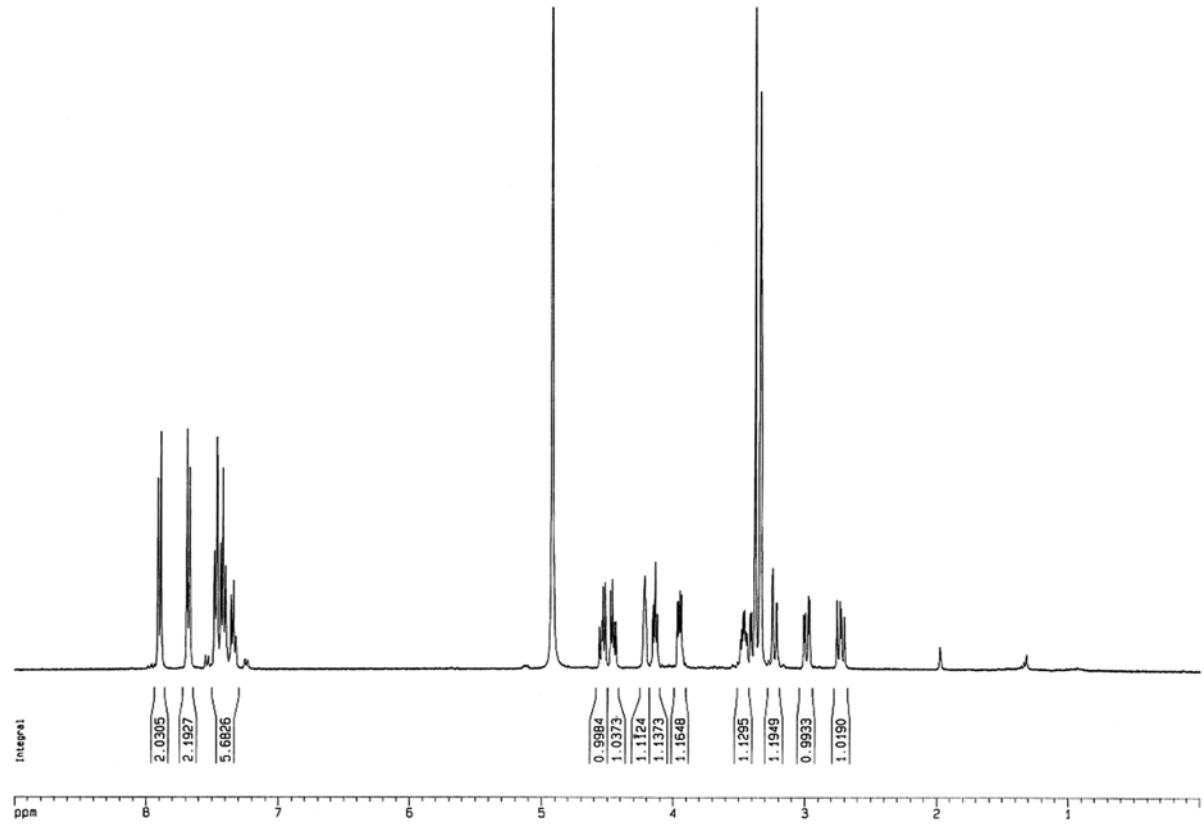

(2*R*)-2-({[(2*R*,3*R*,4*S*)-3,4-Dihydroxypyrrolidin-2-yl]methyl}amino)-2-phenylethyl 4-trifluoromethylbenzoate ((+)-133)

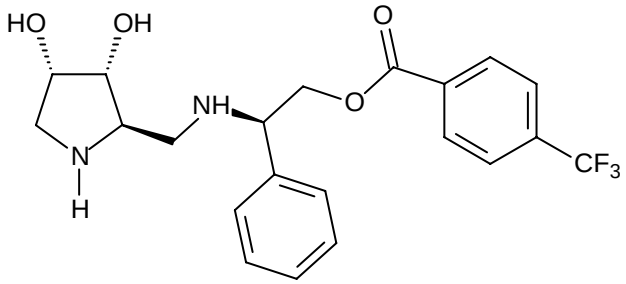

Procedure 1. Amine **122** (200 mg, 0.65 mmol, 1.0 eq), **87** (175 mg, 0.65 mmol, 1.0 eq), $NaBH(OAc)_3$ (192 mg, 0.91 mmol, 1.4 eq), $Cl(CH_2)_2Cl$ (9 ml). Flash chromatography (pentane/EtOAc 7/3) afforded 206 mg (0.36 mmol, 56 %, white foam) of the fully protected compound which was directly engaged in **procedure 2b**. Purification by flash chromatography (CH_2Cl_2/MeOH 9/1) afforded **133** (155 mg, quantitative) as a pale yellow solid after lyophilisation.

For atom numbering, see page 162.

$[\alpha]_{589}^{25} = 0$, $[\alpha]_{577}^{25} = +3$, $[\alpha]_{435}^{25} = +9$, $[\alpha]_{405}^{25} = +11$ (c = 0.39, MeOH).

UV (MeCN): 230 (1000), 206 (500), 187 (500).

IR (film): 3395, 1675, 1280, 1205, 1140, 760 cm^{-1}.

^{1}H-NMR (400 MHz, MeOD):
8.17 (d, ^3J = 8.0, $2H_{arom}$); **7.82** (d, ^3J = 8.0, $2H_{arom}$); **7.49-7.40** (m, $4H_{arom}$); **7.34** (m, $1H_{arom}$); **4.58** (dd, 1H, ^3J(H-C(1'), H-C(2')) = 6.7, $^2J_{gem}$ = 11.0, H-C(1')); **4.50** (dd, 1H, ^3J(H-C(1'), H-C(2')) = 5.7, $^2J_{gem}$ = 11.0, H-C(1')); **4.23** (m, 1H, H-C(4''')); **4.17** (dd, 1H, ^3J(H-C(2'), H-C(1')) = 5.7, ^3J(H-C(2'), H-C(1')) = 6.7, H-C(2')); **3.97** (dd, 1H, ^3J(H-C(3'''), H-C(4''')) = 8.1, ^3J(H-C(3'''), H-C(2''')) = 4.0, H-C(3''')); **3.48** (ddd, 1H, ^3J(H-C(2'''), H-C(1'')) = 4.2, ^3J(H-C(2'''), H-C(3''')) = 4.0, ^3J(H-C(2'''), H-C(1'')) = 9.0, H-C(2''')); **3.42** (dd, 1H, ^3J(H-C(5'''), H-C(4''')) = 4.2, $^2J_{gem}$ = 12.5, H-C(5''')); **3.23** (dd, 1H, ^3J(H-C(5'''), H-C(4''')) = 1.7, $^2J_{gem}$ = 12.5, H-C(5''')); **3.00** (dd, 1H, ^3J(H-C(1''), H-C(2''')) = 4.2, $^2J_{gem}$ = 13.2, H-C(1'')); **2.74** (dd, 1H, ^3J(H-C(1''), H-C(2''')) = 9.0, $^2J_{gem}$ = 13.2, H-C(1'')).

^{13}C-NMR (101 MHz, MeOD):
163.6 (s, O*C*(O)Ar); **141.2** (s, $1C_{arom}$); **131.3** (d, ^1J(C,H) = 166, $2C_{arom}$); **129.9** (d, ^1J(C,H) = 159, $2C_{arom}$); **129.5** (s, $1C_{arom}$); **129.1** (d, ^1J(C,H) = 161, $1C_{arom}$); **128.7** (s, $1C_{arom}$); **128.9** (d, ^1J(C,H) = 159, $2C_{arom}$); **126.6** (d, ^1J(C,H) = 163, $2C_{arom}$); **74.8** (d, ^1J(C,H) = 138, C(3''')); **71.1** (d, ^1J(C,H) = 153, C(4''')); **69.9** (t, ^1J(C,H) = 150, C(1')); **63.3** (d, ^1J(C,H) = 139, C(2')); **62.7** (d, ^1J(C,H) = 144, C(2''')); **50.7** (t, ^1J(C,H) = 149 , C(5''')); **47.6** (t, ^1J(C,H) = 138, C(1'')).

MALDI-TOF: 425.60 $(M+H)^+$.
HRMS ($C_{21}H_{23}F_3N_2O_4$ + H): calc. 425.1688; found 425.1684.
M.P: 125-130°C.

^{1}H-NMR spectrum of **133**

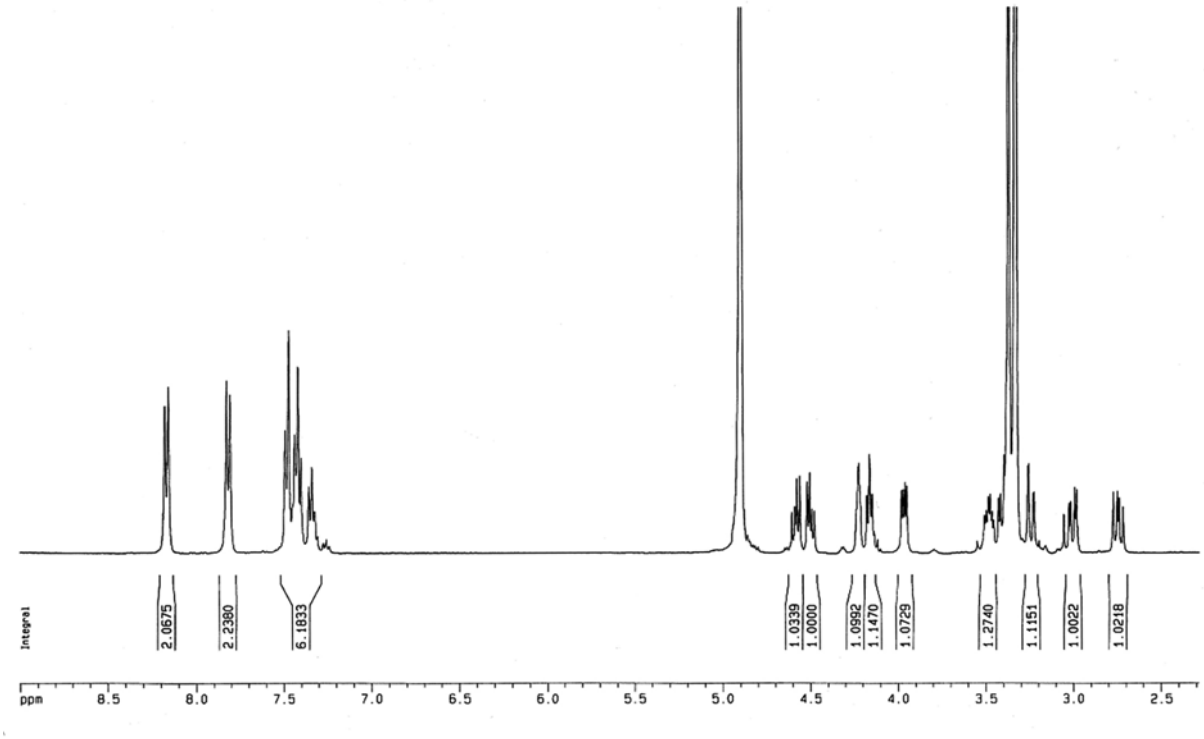

(2*S*)-2-({[(2*R*,3*R*,4*S*)-3,4-Dihydroxypyrrolidin-2-yl]methyl}amino)-2-phenylethyl 4-bromobenzoate ((+)-134)

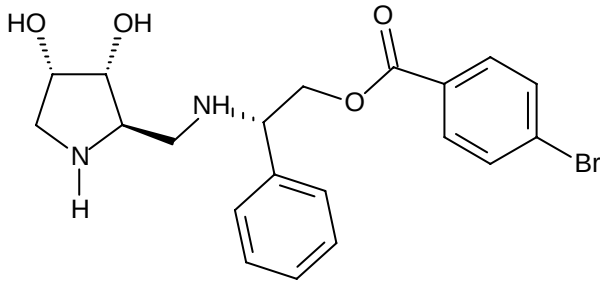

To a solution of **L-(+)-α-phenylglycinol** (5.0 g, 36.5 mmol, 1.0 eq) in anhydrous CH_2Cl_2 (350 ml) were added pyridine (5.9 ml, 73 mmol, 2.0 eq), $(Boc)_2O$ (8.0 g, 36.5 mmol, 1.0 eq) and a catalytic amount of DMAP. The mixture was stirred at 0°C for 2 hours and poured into a saturated aqueous solution of $NaHCO_3$ (150 ml). The aqueous layer was extracted with CH_2Cl_2 (80 ml, 2 times). The combined organic extracts were dried over $MgSO_4$ and evaporated *in vacuo*. The residue was purified by flash chromatography (CH_2Cl_2/MeOH 20/1) to afford the corresponding carbamate (7.3 g, 86 %) as a pale yellow solid.

To a solution of this carbamate (300 mg, 1.26 mmol, 1.0 eq) in anhydrous CH_2Cl_2 (4 ml), at 0°C, were added NEt_3 (705 µl, 5.06 mmol, 4.0 eq), 4-bromobenzoyl chloride (388 mg, 1.77 mmol, 1.4 eq) and a catalytic amount of DMAP. The mixture was allowed to warm up to 25°C and was stirred for 3 hours. The resulting mixture was poured into a saturated aqueous solution of $NaHCO_3$ (10 ml). The aqueous layer was extracted with EtOAc (15 ml, 3 times). The combined organic extracts were washed with a saturated aqueous solution of NH_4Cl (5 ml) and brine (5 ml), dried over $MgSO_4$, filtered and concentrated *in vacuo*. Purification by flash chromatography on silica gel (Pentane/EtOAc 7/3) afforded 505 mg of a pale yellow solid (1.20 mmol, 95 %) which was directly engaged in **Procedure 2b** to afford the corresponding amine (365 mg, 95 %) as a white solid.

Procedure 1. Amine (365 mg, 0.11 mmol, 1.1 eq), **87** (281 mg, 1.04 mmol, 1.0 eq), $NaBH(OAc)_3$ (309 mg, 1.46 mmol, 1.4 eq), $Cl(CH_2)_2Cl$ (11 ml). Flash chromatography (pentane/EtOAc 7/3) afforded 420 mg (0.72 mmol, 70 %, white foam) of the fully protected compound which was directly engaged in **procedure 2b**. Purification by flash chromatography (CH_2Cl_2/MeOH 9/1) afforded **134** (234 mg, 74 %) as a pale yellow solid.

For atom numbering, see page 162.

$[\alpha]_{589}^{25}$ = +25, $[\alpha]_{577}^{25}$ = +26, $[\alpha]_{435}^{25}$ = +50, $[\alpha]_{405}^{25}$ = +58 (c = 0.38, MeOH).

IR (film): 3270, 2345, 1680, 1460, 1210, 1145, 1010, 840, 795, 755, 725 cm^{-1}.

^{1}H-NMR (400 MHz, MeOD):
7.94 (d, ^3J = 8.4 , $2H_{arom}$); **7.64** (d, ^3J = 8.6 , $2H_{arom}$); **7.55** (d, ^3J = 7.0 , $2H_{arom}$); **7.43** (m, $3H_{arom}$); **4.68** (m, 2H, 2H-C(1')); **4.60** (m, 1H, H-C(2')); **4.20** (m, 1H, H-C(4''')); **3.97** (dd, 1H, ^3J(H-C(3'''), H-C(2''')) = 3.8, ^3J(H-C(3'''), H-C(4''')) = 9.2, H-C(3''')); **3.78** (ddd, 1H, ^3J(H-C(2'''), H-C(1'')) = 3.2, ^3J(H-C(2'''), H-C(3''')) = 3.8, ^3J(H-C(2'''), H-C(1'')) = 8.9, H-C(2''')); **3.44** (dd, 1H, ^3J(H-C(5'''), H-C(4''')) = 3.8, $^2J_{gem}$ = 12.7, H-C(5''')); **3.28** (m, 2H, H-C(5'''), H-C(1'')); **3.14** (dd, 1H, ^3J(H-C(1''), H-C(2''')) = 8.9, $^2J_{gem}$ = 13.2, H-C(1'')).

^{13}C-NMR (101 MHz, MeOD):
166.7 (s, O*C*(O)Ar); **135.7** (s, $1C_{arom}$); **133.0** (d, ^1J(C,H) = 168, $2C_{arom}$); **132.5** (d, ^1J(C,H) = 166, $2C_{arom}$); **130.5** (s, $1C_{arom}$); **130.4** (d, ^1J(C,H) = 161, $2C_{arom}$); **129.8** (s, $1C_{arom}$); **129.4** (d, ^1J(C,H) = 160, $1C_{arom}$); **129.3** (d, ^1J(C,H) = 158, $2C_{arom}$); **75.2** (d, ^1J(C,H) = 140, C(3''')); **70.3** (d, ^1J(C,H) = 154, C(4''')); **67.2** (t, ^1J(C,H) = 151, C(1')); **63.0** (d, ^1J(C,H) = 143, C(2')); **59.4** (d, ^1J(C,H) = 145, C(2''')); **51.4** (t, ^1J(C,H) = 147, C(5''')); **46.9** (t, ^1J(C,H) = 141, C(1'')).

MALDI-TOF: 437.57 $(M+2)^+$, 435.57 $(M)^+$.
MALDI-HRMS ($C_{20}H_{23}BrN_2O_4$ + H): calc. 435.0919; found 435.0920.
M.P: 70-75°C.

^{1}H-NMR spectrum of **134**

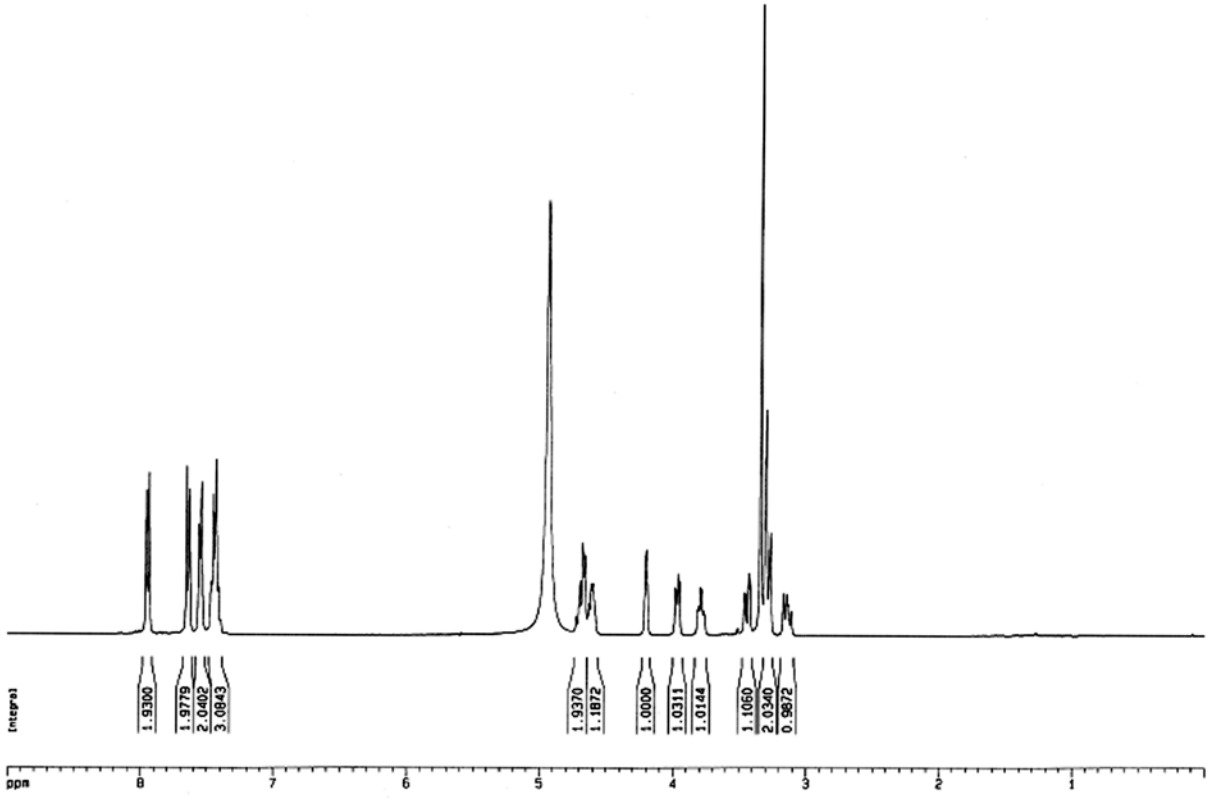

Tert-butyl ((1*R*)-2-amino-1-phenylethyl) carbamate ((-)-135)

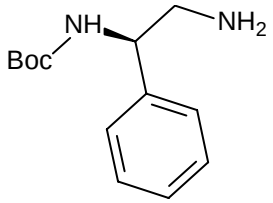

To a solution of primary alcohol **111** (5.7 g, 24 mmol, 1.0 eq) in anhydrous CH_2Cl_2 (200 ml) was added NEt_3 (8.4 ml, 60 mmol, 2.5 eq) and methanesulfonyl chloride (2.3 ml, 28.8 mmol, 1.2 eq). The mixture was stirred at 0°C for 3 hours and then poured into water (200 ml). The aqueous layer was extracted with CH_2Cl_2 (100 ml, 3 times). The combined organic extracts were washed with a saturated aqueous solution of NH_4Cl (150 ml) dried over $MgSO_4$ and evaporated *in vacuo*.

To a solution of crude (2*R*)-2-[(*Tert*-butoxycarbonyl)amino]-2-phenylethyl methanesulfonate (7.3 g, 23.2 mmol, 1.0 eq) in anhydrous THF (200 ml) was added sodium azide (7.6 g, 116 mmol, 5.0 eq). The mixture was warmed at 60°C and stirred for 14 hours. The mixture was poured into a saturated aqueous solution of $NaHCO_3$ (60 ml) and the aqueous layer was extracted with EtOAc (40 ml, 3 times). The combined organic extracts were dried over $MgSO_4$ and evaporated *in vacuo*. The yellow residue was purified by flash chromatography (pentane/EtOAc 8/1) to afford a white solid (4.4g, 71 %, 2 steps).

A solution of *Tert*-butyl [(1*R*)-2-azido-1-phenylethyl]carbamate (2.0 g, 7,7 mmol, 1.0 eq) in anhydrous methanol (50 ml) was stirred vigorously at 25°C under one atmosphere of hydrogen in the presence of a catalytic amount of 10 % $Pd(OH)_2/C$ for 7 hours. The mixture was filtered through a pad of Celite and concentrated *in vacuo*. The yellow residue was purified by flash chromatography (CH_2Cl_2/MeOH 9/1) to afford amine **135** (1.1 g, 60 %) as a waxy solid.

$[\alpha]_{589}^{25}$ = -50, $[\alpha]_{435}^{25}$ = -109, $[\alpha]_{405}^{25}$ = -137 (*c* = 0.43, CH_2Cl_2).

UV (MeCN): 216 (3000).

IR (film): 3580, 3430, 3055, 2980, 2530, 1705, 1495, 1455, 1390, 1265, 1170, 825 cm^{-1}.

^{1}H-NMR (400 MHz, $CDCl_3$):
7.34-7.23 (m, $5H_{arom}$); **4.67** (m, 1H, H-C(1)); **2.98** (m, 2H, H-C(2)); **2.22** (s, 2H, N*H*$_2$); **1.41** (s, 9H, *Me*$_3$C).

^{13}C-NMR (101 MHz, $CDCl_3$):
155.6 (s, N*C*(O)O); **140.5** (s, $1C_{arom}$); **128.6** (d, ^1J(C,H) = 160, $2C_{arom}$); **127.3** (d, ^1J(C,H) = 161, $1C_{arom}$); **126.3** (d, ^1J(C,H) = 157, $2C_{arom}$); **79.5** (s, O*C*Me$_3$); **56.3** (d, ^1J(C,H) = 144, C(1)); **46.8** (t, ^1J(C,H) = 137, C(2)); **28.3** (q, ^1J(C,H) = 127, *Me*$_3$C).

MALDI-TOF: 275.42 $(M+K)^+$, 259.45 $(M+Na)^+$, 237.52 $(M+H)^+$.
HRMS ($C_{13}H_{20}N_2O_2$ + H): calc. 237.1603; found 237.1604.

_N_-((2_R_)-2-Amino-2-phenylethyl)-3-bromobenzamide ((-)-136)

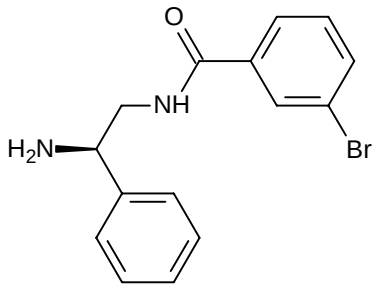

To a solution of amine **135** (100 mg, 0.42 mmol, 1.0 eq) in anhydrous CH_2Cl_2 (4 ml) at 0°C were added NEt_3 (236 µl, 1.69 mmol, 4.0 eq), 3-bromobenzoyl chloride (111 µl, 0.85 mmol, 1.2 eq) and a catalytic amount of DMAP. The mixture was allowed to warm up to 25°C and was stirred for 2 hours. The resulting mixture was poured into a saturated aqueous solution of $NaHCO_3$ (10 ml). The aqueous layer was extracted with EtOAc (5 ml, 3 times). The combined organic extracts were washed with a saturated aqueous solution of NH_4Cl (5 ml) and brine (5 ml), dried over $MgSO_4$, filtered and concentrated *in vacuo*. Purification by flash chromatography on silica gel (CH_2Cl_2/MeOH 9/1) afforded 180 mg of a yellow solid (0.40 mmol, 95 %) which was directly engaged in **Procedure 2b** to afford **136** (140 mg, quantitative) as a pale yellow solid.

$[\alpha]_{589}^{25}$ = -30, $[\alpha]_{577}^{25}$ = -42, $[\alpha]_{435}^{25}$ = -78, $[\alpha]_{405}^{25}$ = -85 (*c* = 0.2, CH_2Cl_2).

^{1}H-NMR (400 MHz, $CDCl_3$):
7.70-7.48 (m, $3H_{arom}$); **7.28** (m, $6H_{arom}$); **4.58** (dd, 1H, H-C(2')); **3.93** (dd, 1H, H-C(1')); **3.70** (dd, 1H, H-C(1')).

^{13}C-NMR (101 MHz, $CDCl_3$):
168.9 (s, N*C*(O)Ar); **135.9** (s, $1C_{arom}$); **135.5** (s, $1C_{arom}$); **134.2**, **133.3**, **132.6**, **129.5**, **128.1**, **126.6**, **125.5** (7d, $9C_{arom}$); **122.8** (s, $1C_{arom}$); **55.9** (d, ^1J(C,H) = 147, C(2')); **43.9** (t, ^1J(C,H) = 143, C(1')).

MALDI-TOF: 321.14 $(M+2)^+$, 319.13 $(M)^+$.
HRMS ($C_{15}H_{15}BrN_2O$ + H): calc. 319.0446; found 319.0453.

_N_-[(2_R_)-2-({[(2_R_,3_R_,4_S_)-3,4-Dihydroxypyrrolidin-2-yl]methyl}amino)-2-phenylethyl]-3-bromobenzamide ((+)-137)

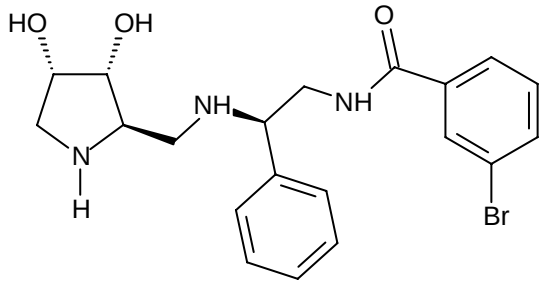

Procedure 1. Amine **136** (100 mg, 0.31 mmol, 1.0 eq), **87** (85 mg, 0.31 mmol, 1.0 eq), $NaBH(OAc)_3$ (93 mg, 0.44 mmol, 1.4 eq), $Cl(CH_2)_2Cl$ (5 ml). Flash chromatography (pentane/EtOAc 3/7) afforded 135 mg (0.23 mmol, 75 %, yellow oil) of the fully protected compound which was directly engaged in **procedure 2b**. Purification by flash chromatography (CH_2Cl_2/MeOH 9/1) afforded **137** (101 mg, 99 %) as a pale yellow solid after lyophilisation.

For atom numbering, see page 162.

$[\alpha]_{589}^{25}$ = +5, $[\alpha]_{435}^{25}$ = +15, $[\alpha]_{405}^{25}$ = +16 (*c* = 0.31, MeOH).

UV (MeCN): 260 (1500), 213 (8500), 187 (1000).

IR (film): 3615, 3580, 3425, 3055, 2360, 1675, 1465, 1265, 1190, 1140, 845, 815, 730 cm^{-1}.

^{1}H-NMR (400 MHz, MeOD):
7.93 (s, 1H$_{arom}$); **7.72** (dd, ^3J = 8.0, ^3J = 15.2 , 2H$_{arom}$); **7.41-7.31** (m, 6H$_{arom}$); **4.25** (m, 1H, H-C(4’’’)); **3.99** (m, 2H, H-C(2’), H-C(3’’’)); **3.67** (dd, 1H, ^3J(H-C(1’), H-C(2’)) = 7.1, $^2J_{gem}$ = 13.5, H-C(1’)); **3.59** (dd, 1H, ^3J(H-C(1’), H-C(2’)) = 7.1, $^2J_{gem}$ = 13.5, H-C(1’)); **3.51-3.43** (m, 2H, H-C(2’’’), H-C(5’’’)); **3.28** (dd, 1H, ^3J(H-C(5’’’), H-C(4’’’)) = 2.1, $^2J_{gem}$ = 12.5, H-C(5’’’)); **2.96** (dd, 1H, ^3J(H-C(1’’), H-C(2’’’)) = 4.1, $^2J_{gem}$ = 13.2, H-C(1’’)); **2.73** (dd, 1H, ^3J(H-C(1’’), H-C(2’’’)) = 9.1, $^2J_{gem}$ = 13.2, H-C(1’’)).

^{13}C-NMR (101 MHz, MeOD):
169.0 (s, N*C*(O)Ar); **142.4** (s, 1C$_{arom}$); **137.7** (s, 1C$_{arom}$); **135.6**, **131.4**, **129.8**, **128.9**, **128.4**, **127.1** (6d, 9C$_{arom}$); **123.5** (s, 1C$_{arom}$); **74.7** (d, ^1J(C,H) = 145, C(3’’’)); **71.1** (d, ^1J(C,H) = 148, C(4’’’)); **64.1** (d, ^1J(C,H) = 135, C(2’)); **62.7** (d, ^1J(C,H) = 147, C(2’’’)); **50.6** (t, ^1J(C,H) = 146, C(1’)); **47.4** (t, ^1J(C,H) = 132 , C(1’’)); **46.8** (t, ^1J(C,H) = 144, C(5’’’)).

MALDI-TOF: 436.24 $(M+2)^+$, 434.23 $(M)^+$.
MALDI-HRMS ($C_{20}H_{25}BrN_3O_3$ + H): calc. 434.1080, found 434.1078.
Purity measured by HPLC (C_{18}, C_8 columns): 100%, 100%.

M.P: 162-164°C.

^{1}H-NMR spectrum of **137**

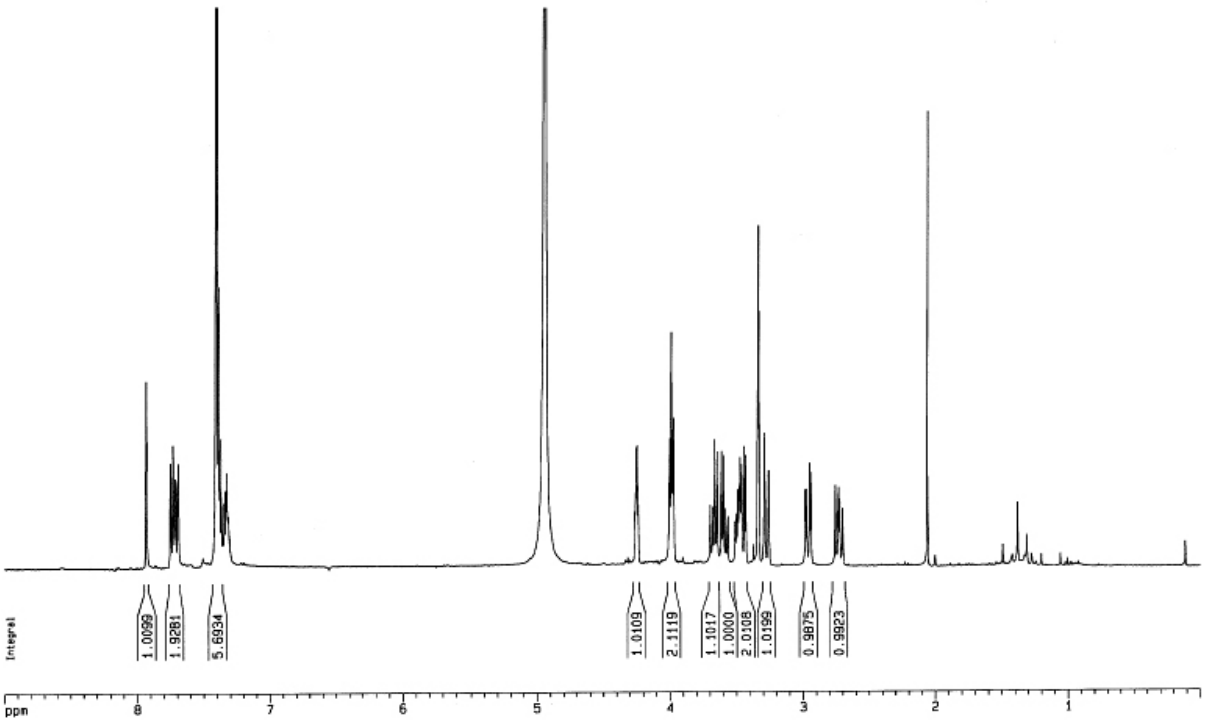

(2*R*)-2-({[(2*R*,3*R*,4*R*)-3,4-Dihydroxy-5-oxopyrrolidin-2-yl]methyl}amino)-2- phenylethyl 4-bromobenzoate ((+)-138)

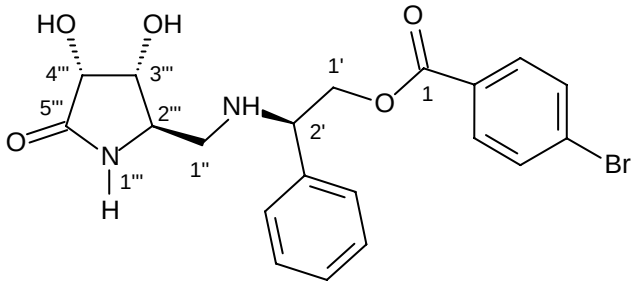

Procedure 1. Amine **121** (115 mg, 0.36 mmol, 1.0 eq), aldehyde **79** (102 mg, 0.36 mmol, 1.0 eq), $NaBH(OAc)_3$ (107 mg, 0.50 mmol, 1.4 eq), $Cl(CH_2)_2Cl$ (4 ml). Flash chromatography (pentane/AcOEt 7/3) afforded 70 mg (0.12 mmol, 33 %, 2 steps, brown oil) of the fully protected compound which was directly engaged in **procedure 2b**. Purification by flash chromatography ($MeCN/NH_4OH$ 9/1) afforded **138** (34 mg, 78 %) as a brown oil.

$[\alpha]_{589}^{25} = 3$, $[\alpha]_{577}^{25} = 5$, $[\alpha]_{435}^{25} = 10$, $[\alpha]_{405}^{25} = 11$ (c = 0.50, MeOH).

IR (film): 3395, 1695, 1590, 1450, 1275, 1200, 1135, 1110, 845, 755, 700 cm^{-1}.

^{1}H-NMR (400 MHz, MeOD):
7.91 (d, ^3J=8.6, $2H_{arom}$); **7.68** (d, ^3J=8.6, $2H_{arom}$); **7.50-7.35** (m, $5H_{arom}$); **4.53** (m, 2H, 2H-C(1)); **4.26-4.23** (m and d, 2H, ^3J(H-C(4'''), H-C(3''')) = 5.4, H-C(2') and H-C(4''')); **4.24** (dd, 1H, ^3J(H-C(3'''), H-C(2''')) = 1.6, ^3J(H-C(3'''), H-C(4''')) = 5.4, H-C(3''')); **3.58** (m, 1H, H-C(2''')); **2.76** (m, 2H, 2H-C(1'')).

^{13}C-NMR (101 MHz, MeOD):
177.9 (s, C(5''')); **166.9** (s, O*C*(O)Ar); **133.0** (d, ^1J(C,H) = 167, $2C_{arom}$); **132.3** (d, ^1J(C,H) = 164, $2C_{arom}$); **132.2** (s, $1C_{arom}$); **130.2** (s, $1C_{arom}$); **130.0** (d, ^1J(C,H) = 160, $2C_{arom}$); **129.5** (d, ^1J(C,H) = 161, $1C_{arom}$); **129.3** (s, $1C_{arom}$); **128.9** (d, ^1J(C,H) = 157, $2C_{arom}$); **72.3** (d, ^1J(C,H) = 153, C(3''')); **71.2** (d, ^1J(C,H) = 145, C(4''')); **68.8** (t, ^1J(C,H) = 147, C(1')); **63.2** (d, ^1J(C,H) = 137, C(2')); **60.8** (d, ^1J(C,H) = 142, C(2''')); **50.3** (t, ^1J(C,H) = 137, C(1'')).

ESI-MS: 451.29 $(M+2)^+$, 449.31 $(M)^+$.
HRMS ($C_{20}H_{21}BrN_2O_5$ + H): calc. 449.0712; found 449.0713.

(2*R*)-2-({[(2*R*,3*R*,4*R*)-3,4-Dihydroxy-1-methyl-5-oxopyrrolidin-2-yl]methyl}amino)-2-phenylethyl 4-bromobenzoate ((-)-139)

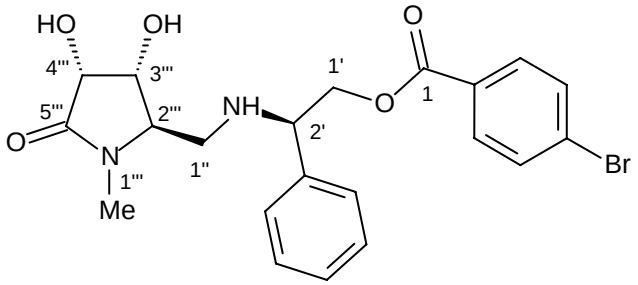

Procedure 1. Amine **121** (160 mg, 0.50 mmol, 1.0 eq), aldehyde **85** (100 mg, 0.50 mmol, 1.0 eq), $NaBH(OAc)_3$ (148 mg, 0.70 mmol, 1.4 eq), $Cl(CH_2)_2Cl$ (5 ml). Flash chromatography (CH_2Cl_2/MeOH 97/3) afforded 226 mg (0.45 mmol, 89 %, 2 steps) of the fully protected compound which was directly engaged in **procedure 2b**. Purification by flash chromatography (MeCN/NH_4OH 15/1) afforded **139** (88 mg, 42 %) as a white foam.

$[\alpha]_{589}^{25}$ = -11 (c = 0.38, MeOH).

IR (film): 3290, 2930, 1715, 1590, 1545, 1450, 1400, 1270, 1120, 1110, 845, 755, 695 cm^{-1}.

^{1}H-NMR (400 MHz, MeOD):
7.89 (d, ^3J=8.5, $2H_{arom}$); **7.66** (d, ^3J=8.5, $2H_{arom}$); **7.44-7.31** (m, $5H_{arom}$); **4.48** (dd, 1H, ^3J(H-C(1'), H-C(2')) = 7.5, $^2J_{gem}$ = 11.2, H-C(1')); **4.42** (dd, 1H, ^3J(H-C(1'), H-C(2')) = 5.4, $^2J_{gem}$ = 11.2, H-C(1')); **4.40** (d, 1H, , ^3J(H-C(4'''), H-C(3''')) = 5.4, H-C(4''')); **4.25** (d, 1H, , ^3J(H-C(3'''), H-C(4''')) = 5.4, H-C(3''')); **4.13** (dd, 1H, , ^3J(H-C(2'), H-C(1')) = 5.4, ^3J(H-C(2'), H-C(1')) = 7.5, H-C(2')); **3.41** (dd, 1H, ^3J(H-C(2'''), H-C(1'')) = 3.4, ^3J(H-C(2'''), H-C(1'')) = 6.1, H-C(2''')); **2.84** (dd, 1H, ^3J(H-C(1''), H-C(2''')) = 3.4, $^2J_{gem}$ = 12.9, H-C(1'')); **2.71** (s, 3H, Me-N);. **2.65** (dd, 1H, ^3J(H-C(1''), H-C(2''')) = 6.1, $^2J_{gem}$ = 12.9, H-C(1'')).

^{13}C-NMR (101 MHz, MeOD):
175.4 (s, C(5''')); **167.0** (s, O*C*(O)Ar); **133.0** (d, ^1J(C,H) = 166, $2C_{arom}$); **132.3** (d, ^1J(C,H) = 163, $2C_{arom}$); **130.3** (s, $1C_{arom}$); **129.8** (d, ^1J(C,H) = 160, $2C_{arom}$); **129.5** (s, $1C_{arom}$); **129.2** (s, $1C_{arom}$); **129.1** (d, ^1J(C,H) = 161, $1C_{arom}$); **128.8** (d, ^1J(C,H) = 158, $2C_{arom}$); **71.6** (d, ^1J(C,H) = 145, C(4''')); **71.0** (d, ^1J(C,H) = 154, C(3''')); **69.4** (t, ^1J(C,H) = 149, C(1')); **68.0** (d, ^1J(C,H) = 145, C(2')); **63.3** (d, ^1J(C,H) = 135, C(2''')); **46.6** (t, ^1J(C,H) = 135, C(1'')); **28.8** (q, ^1J(C,H) = 138, Me-N).

ESI-MS: 465.30 $(M+2)^+$; 463.30 $(M)^+$.
HRMS ($C_{21}H_{23}BrN_2O_5$ + H): calc. 463.0869; found 463.0872.

^{1}H-NMR spectrum of **138**

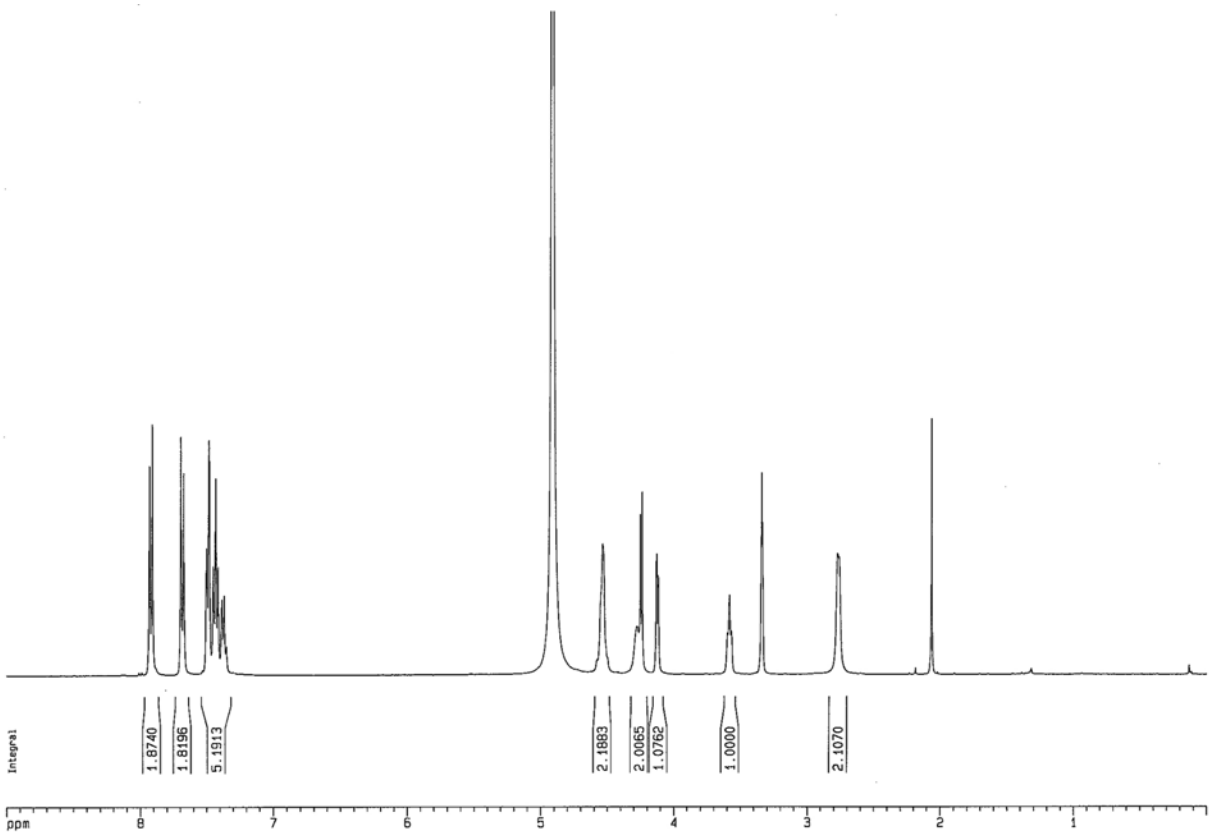

^{1}H-NMR spectrum of **139**

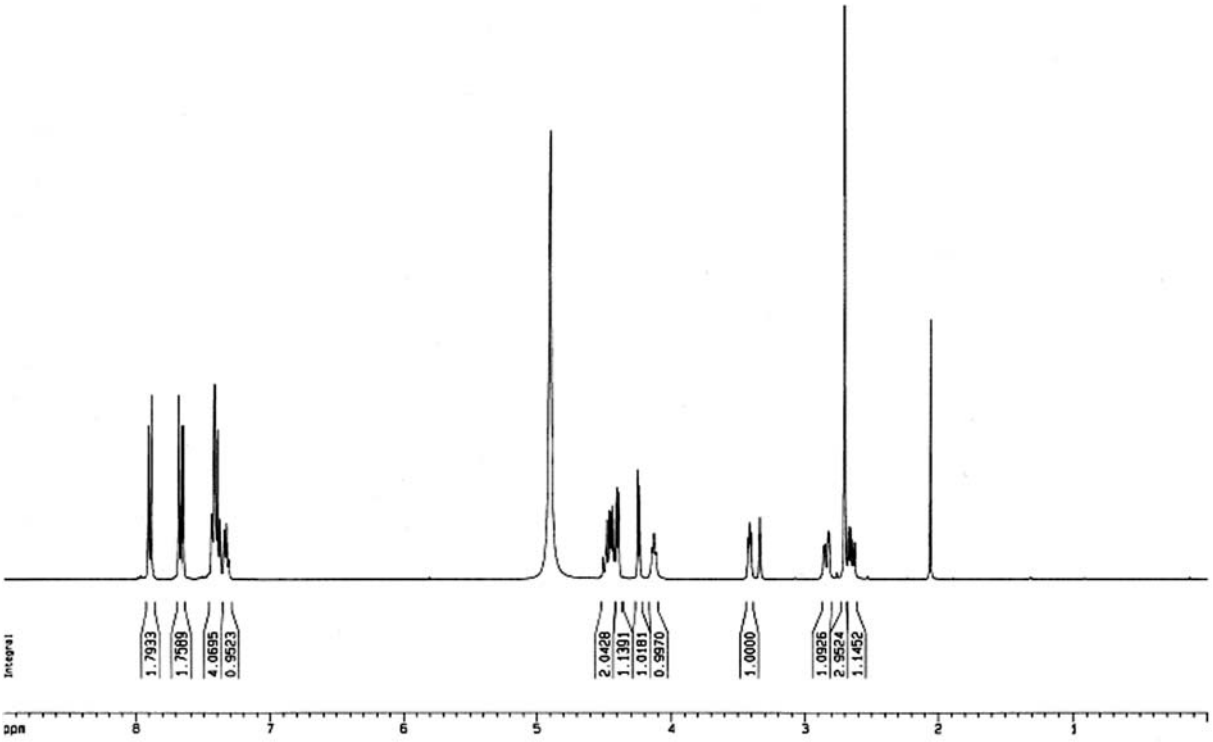

Hélène FIAUX
Ch. Guiguer-de-Prangins 6
CH-1004 Lausanne

Tel: +41/ 21 647 31 45
Mobile: +41/ 78 623 65 24
E-mail: helene.fiaux@epfl.ch

08.03.1976
Swiss, single

EDUCATION:

Since oct. 2003 Candidate for **PhD** in the laboratory of Glycochemistry and Asymmetric Synthesis (LGSA) at the Institute of Chemical Sciences and Engineering (ISIC), Swiss Institute of Technology of Lausanne (EPFL).

2004 **DEA** multinational de chimie moléculaire, Ecole Polytechnique, Palaiseau (France)

2001 - 2002 **Licence ès Science en Chimie** (eq. Bachelor in Chemistry), University of Lausanne (UNIL)

1995 - 2001 **Diplôme en Biologie** (eq. Master in Biology), UNIL
- Certificate in cellular and molecular biology
- Certificate in pharmacology and toxicology
- Certificate in pharmaceutical sciences (I and II)

1991 - 1995 Scientific Matura, Gymnasium CESSOUEST, Nyon (CH)

PROFESSIONAL ACTIVITES:

2003 - **EPFL**, Lausanne (CH):
- Synthesis of organic compounds and their evaluation on cancer cells
- Supervision of advanced practical work and diploma projects
- Exercises and corrections of exams in organic chemistry (1st year)

2005 (4 months) **University McGill**, Montreal (Canada), Department of Chemistry:
- Programmation and Docking Studies on Unix Software (sgi)

2003 (8 months) **NOVARTIS**, Basel (CH), Department of Research and Development:
- Physicochemistry profiling, laboratory robotics and data analysis

2002 (1 month) **Hôpital Cantonal Fribourg** (CH), Pharmacy:
- Development and validation of two systems of steril tests
- Control analyses and preparation of medicine

2001 (1-2months) **Collège du Château d'Aubonne** (CH):
- Teaching

1999 (2 months) **Ares SERONO**, Aubonne (CH), Department of metrology:
- Development of statistic calculations

1995 - 1998 (4x 2months) **Ares SERONO**, Aubonne (CH), Department of Quality Control:
- Various Quality Control analyses
- Biochemistry, Immunology and Microbiology assays

PRIZES AND DISTINCTIONS:

- Prize Metler Toledo for the **Best oral presentation in Medicinal Chemistry**, Fall Meeting of the Swiss Chemical Society (SCS), **2005**
- **Grant of Excellence** for the first year of PhD, EPFL, **2004**
- **Prize of Faculty of Sciences** for results obtained during the Licence ès Science en Chimie, UNIL, **2002**